Neuroimaging correlates of progressive cognitive decline and clinical symptoms in prodromal Lewy body disease. A multimodal imaging study.

Rory Thomas Durcan

Translational and Clinical Research Institute

October 2020

A thesis submitted to Newcastle University for the Degree of Doctor of Philosophy

Abstract

Introduction

There has been an interest in earlier diagnosis of cognitive impairment at the prodromal stage. Mild cognitive impairment (MCI) is a prodromal cognitive phenotype of dementia. Differentiating MCI with Lewy bodies (MCI-LB) and MCI due to AD (MCI-AD) using clinical features alone is challenging and biomarkers are likely to aid diagnosis.

This thesis investigated whether cross-sectional structural magnetic resonance imaging (MRI) or repeat ^{123}I-FP-CIT single photon emission tomography (SPECT) could be utilised to differentiate between MCI-LB and MCI-AD.

Methods

Prospective repeat ^{133}I-FP-CIT SPECT study: 85 subjects were included in this analysis, consisting of; healthy controls (HC) (n=29), MCI-AD (n=19), possible MCI-LB (n=10), probable MCI-LB (n=27). All subjects underwent comprehensive clinical and neuropsychological assessment as well as repeat ^{123}I-FP-CIT SPECT and baseline cardiac ^{123}I-MIBG scintigraphy.

Cross- sectional MRI study: 97 subjects were included in this analysis, consisting of; HC (n=31), MCI-AD (n=32), probable MCI-LB (n=34). All subjects underwent comprehensive clinical and neuropsychological assessment as well as baseline ^{123}I-FP-CIT SPECT, cardiac ^{123}I-MIBG scintigraphy and structural magnetic resonance imaging.

Results

Progressive dopaminergic loss was detected in MCI-LB in excess of HC, with mean annual striatal decline of 6% in the MCI-LB cohorts. MCI-AD had no difference in longitudinal striatal uptake when compared to HC. Structural MRI data found: (1) grey matter volume loss in the frontal and temporal lobes in MCI-LB compared to HC, (2) bilateral cerebellar volume reduction in MCI-LB compared to

MCI-AD, (3) no relative preservation of the medical temporal lobe in MCI-LB compared to MCI-AD, (4) no cortical thickness difference between MCI-LB and MCI-AD (5) thalamic volume loss and relative preservation of the amygdala in MCI-LB compared to MCI-AD.

Conclusion

Sequential ^{123}I-FP-CIT SPECT imaging is a promising biomarker for identifying MCI-LB. Structural MRI showed no difference in cortical indexes but some differences in subcortical and cerebellar measures between MCI-LB and MCI-AD.

Acknowledgements

I would like to thank my supervisors Professor Alan Thomas, Professor Nicola Pavese and Professor David Brooks. In particular, I am very grateful to Professor Alan Thomas and Professor David Burn whose support enabled me to undertake and complete a PhD. I am indebted to the invaluable advice, support and guidance provided to me by Professor Alan Thomas at our weekly supervision sessions.

I would like to acknowledge and thank the whole SUPErB study team in Newcastle University, led by Professor Thomas – in particular Sally Barker, Helen Kain, Nicola Barnett, Denise Golden, Dr Sarah Lawley, Dr Paul Donaghy, Dr Gemma Roberts, Calum Hamilton, Joanna Ciafone. I am very thankful for the help and support of all the staff in the Clinical Ageing Research Unit.

I would like to recognise that recruitment to the SUPErB study would not have been successful without the support provided by the staff of the North East Dementia and Neurodegenerative Diseases Research Network (DeNDRoN). The recruitment efforts of Dr Barbara Wilson and Bryony Storey were greatly appreciated and their contribution since the inception of the study enabled an efficient recruitment process. Many of the participants were recruited from memory clinics throughout the North East of England and I would like to acknowledge the commitment of consultants and support staff in these clinics to enable this research study to be completed.

I would like to thank all the staff at the nuclear medicine department in the Newcastle upon Tyne Hospitals NHS Foundation Trust - in particular, Elizabeth Jefferson, Andrew Curry, Dr Jim Lloyd, Kim Howe and Dr George Petrides.

My thanks also to Dr Gemma Roberts for her help, time and expertise in teaching me to undertake the semi-quantitative analysis of ^{123}I-FP-CIT SPECT. I am also grateful to Dr Sean Colloby and Dr Michael Firbank who patiently guided me through the imaging analysis.

I would like to thank the research participants, their family and friends who generously gave up their time and energy to take part in these studies for the benefit of others. Their dedication and willingness to involved in this study was a constant source of inspiration and vital to the success of this study.

Finally, I would like to thank my wife Marie and son James for their support and patience, without their encouragement this thesis would not have been possible.

Declaration

No portion of the work in this thesis has been submitted in support of an application for another degree or qualification at this or any other university or institute of learning. I confirm this thesis is my own work, and any assistance from others is acknowledged. The author was responsible for the writing of the thesis. Author contributions are acknowledged, clearly listed and permission obtained for all data included in this thesis.

Professor Thomas was the principal investigator responsible for the original applications for grant funding to Alzheimer's Research UK and ethical approval for these studies which were in place prior to my joining of the study. Professor Thomas was also the principal investigator on the LewyPro study which was a pilot study which proceeded the SUPErB study. The LewyPro study was funded by Newcastle NIHR biomedical research centre. Dr Michael Firbank and Dr George Petrides designed the SUPErB and LewPRO study's imaging protocols which were operational prior to my commencing the project. GE Healthcare provided funding for the ^{123}I-FP-CIT imaging and provided the DaTQUANT software.

I was directly responsible for the recruitment and clinical assessment of SUPErB study subjects. All study participants gave written informed consent prior to enrolling in the study. Study participants expressly consented to their data being used in other Newcastle studies. I used some data from the LewyPro study for chapter 6 for this thesis as some of the subjects recruited to be part of that study also consented to be part of the SUPErB study. I was responsible for formulating the hypotheses for this thesis and carrying out statistical analyses. Statistical analysis using mixed linear effects modelling was assisted by Mr Calum Hamilton.

Neuropsychological assessment and carer questionnaires were carried out by Joanna Ciafone, Calum Hamilton, Nicola Barnett, Sally Barker and the author. Data entry and management was carried out by Dr Sarah Lawley, Helen Kain, Sally Barker and Nicola Barnett. Final clinical diagnosis was carried out by Professor Thomas, Dr Paul Donaghy and Professor John-Paul Taylor.

The MRI data was acquired at the Newcastle Magnetic Resonance centre and was performed by Mr Tim Hodgson. I performed the pre-processing of the MRI data and all image analyses presented in this thesis with the support of Dr Sean Colloby and Dr Michael Firbank.

Dr Jim Lloyd, Dr George Petrides, Dr Gemma Roberts, Prof Alan Thomas and Dr Paul Donaghy performed the visual rating of the ^{123}I-FP-CIT SPECT scans. I performed semi-quantitative analysis of ^{123}I-FP-CIT SPECT using DaTQUANT software.

Throughout my PhD I have been involved in the publication of number of first author manuscripts in peer reviewed journals. The data from these manuscripts are not contained within this PhD thesis and were based on data from other studies. These papers are listed below:

My role in the SUPErB study has enabled me to contribute significantly to the work of my colleagues who I have assisted with data collection, data analysis, writing and reviewing manuscripts. These papers have been published in peer reviewed journal or have been submitted to journals for considerations for publication. These papers are listed below:

I have also presented preliminary results from my thesis at the International Lewy Body Dementia meeting in Las Vegas in 2019. These are listed below alongside those that I have been involved as a co-author.

Publications

The following first-author papers have been published during my PhD; a number of papers are part of my background reading for this PhD. These publications do not contain any data from this thesis.

Durcan R, Thomas AJ. Translating progress in neuroimaging in clinical practice. Int Psychogeriatr 2018 May; 30(5):607-609.

Durcan R, Donaghy P, Osborne C, Taylor JP, Thomas AJ. Imaging in prodromal dementia with Lewy bodies: Where do we stand? Int J Geriatr Psychiatry. 2019 May; 34(5):635-646

Durcan R, Donaghy PC, Barnett NA, Olsen K, Yarnall AJ, Taylor JP, McKeith I, O'Brien JT, Thomas AJ. Prevalence and severity of symptoms suggestive of gastroparesis in prodromal dementia with Lewy bodies. Int J Geriatric Psychiatry 2019 Jul; 34(7):990-998

Durcan R, Wiblin L, Lawson RA, Khoo TK, Yarnall AJ, Duncan GW, Brooks DJ, Pavese N, Burn DJ. Prevalence and duration of non-motor symptoms in prodromal Parkinson's disease. Eur J Neurol. 2019 Jul:36(7):979-985

*Pasquini J, ***Durcan R**, Wiblin L, Gersel Stokholm M, Rochester L, Brooks DJ, Burn DJ, Pavese N. Clinical implications of early caudate dysfunction in Parkinson's disease. J Neurol Neurosurg Psychiatry. 2019 Oct; 90(10):1098-1104. * Joint first-authors

The following publications are work that I have contributed to during my PhD but the data are not contained within this thesis.

Roberts G, Lloyd JJ, Petrides GS, Donaghy PC, Kane JPM, **Durcan R,** Lawley S, Howe K, Sims AJ, Taylor JP, O'Brien JT, Thomas AJ. ^{123}i-FP-CIT striatal binding ratios do not decrease significantly with age in older adults. Ann Nucl Med. 2019 Jun; 33(6):434-443

Wiblin L, **Durcan R**, Galna B, Lee M, Burn D. Clinical Milestones Preceding the Diagnosis of Multiple System Atrophy and Progressive Supranuclear Palsy: A Retrospective Cohort Study, J Mov Disord 2019 Sept:12(3):177-183

Wiblin L, **Durcan R**, Lee M, Brittain K. The Importance of Connections to Others in QoL in MSA and PSP. Parkinsons Dis 2017;2017:5283259

Roberts G, Lloyd JJ, Jefferson E, Kane JPM, **Durcan R**, Lawley S, Petrides GS, Howe K, Haq I, O'Brien JT, Thomas AJ. Uniformity of cardiac ^{123}I-MIBG uptake on SPECT images in older adults with normal cognition and patients with dementia. J Nucl Cardiol 2019 Dec 9 online ahead of print

Roberts G, Lloyd JJ, Kane JPM, **Durcan R**, Lawley S, Howe K, Petrides GS, O'Brien JT, Thomas AJ. Cardiac ^{123}I-MIBG normal uptake values are population-specific: Results from a cohort of controls over 60 years of age. J Nucl Cardiol 2019 Sept 16. Online ahead of print.

Abbreviations

Aβ	Amyloid beta
Aβ	Amyloid-β 1-38
Aβ40	Amyloid-β 1-40
Aβ42	Amyloid-β 1-42
ABLE	Australian Imaging, Biomarkers and Lifestyle study
ABCA7	ATP binding cassette subfamily A member 7 gene
ACE-R	Addenbrooke's Cognitive Examination Revised
AD	Alzheimer's disease
ADNI	Alzheimer's Disease Neuroimaging Initiative
ANCOVA	Analysis of covariance
ANOVA	One-way analysis of variance
ApoE	Apolipoprotein E
aMCI	Amnestic mild cognitive impairment
APP	Amyloid precursor protein
AVLT	Rey Auditory Verbal Learning Test
CAF	Clinician Assessment of Fluctuation
CBD	Corticobasal degeneration
CDR	Clinical Dementia Rating Scale
CERAD	Consortium to Establish a Registry for Alzheimer's Disease
CI	Confidence Interval
CIRS-G	Cumulative Illness Rating Scale for Geriatrics
CSF	Cerebrospinal Fluid
DARTEL	Diffeomorphic anatomical registration through exponential Lie algebra

DAT	Dopamine transporter
DaTQUANT	Software for performing SBR analysis, manufactured by GE Healthcare
DCFS	Dementia Cognitive Fluctuations Scale
DeNDRON	Dementia and Neurodegenerative Diseases Research Network
DICOM	Digital Imaging and Communications in Medicine
DLB	Dementia with Lewy bodies
DSM-5	Diagnostic and Statistical Manual of Mental Disorders fifth edition
DTI	Diffusion tensor imaging
EEG	Electroencephalogram
ESS	Epworth Sleepiness Scale
FAS	FAS verbal fluency test
FDG-PET	(^{18}F) Fluorodeoxyglucose positron emission tomography
FLAIR	Fluid-attenuated inversion recovery
FTD	Frontotemporal dementia
FTLD	Fronto-temporal-lobar-degeneration
FWE	Family-wise error
FWHM	Full-width half maximum
FreeSurfer	Software for processing structural MRI data
GBA	Glucocerebrosidase
GDS	Geriatric Depression Scale
GM	Grey matter
HC	Healthy Control
HRV	Heart rate variability
IADL	Instrumental Activities of Daily Living Scale

IRBD	Idiopathic rapid eye movement sleep behaviour disorder
IWG-2	International working group
LB	Lewy body
LBD	Lewy body dementia (DLB and PDD)
LBSQ	Lewy Body Symptom Questionnaire
LewyPro	Pilot study preceding SUPErB study investigating ^{123}I-FP-CIT SPECT in MCI
LID	Levodopa induced dyskinesia
LN	Lewy neurite
LRRK2	Leucine-rich repeat kinase 2
MAPT	Microtubule associated protein tau
MBq	Megabecquerel
MCI	Mild cognitive impairment
MCI-AD	Mild cognitive impairment due to Alzheimer's Disease
MCI-LB	Mild cognitive impairment with Lewy bodies
Md-MCI+a	Multi-domain, amnesic mild cognitive impairment
Md-MCI+na	Multi-domain, non-amnestic mild cognitive impairment
MDS	International Parkinson and Movement Disorder Society
MDS-UPDRS	Movement Disorder Society-Unified Parkinson's Disease Rating Scale
MIBG	^{123}I-metaiodobenzylguanidine (used to refer to the cardiac sympathetic imaging technique using ^{123}I-MIBG myocardial scintigraphy)
MMSE	Mini Mental State Examination
MNI	Montreal Neuroimaging Initiative
MOCA	Montreal Cognitive Assessment
MRI	Magnetic resonance imaging

MSA	Multiple System Atrophy
MSQ	Mayo Sleep Questionnaire
MTL	Medial temporal lobe
NA	Not applicable
NART	National Adult Reading Test
naMCI	Non-amnestic MCI
NCD	Neurocognitive disorder
NCDLB	Neurocognitive disorder with Lewy bodies
NEVHI	North-East Visual Hallucinations Interview
NFT	Neurofibrillary tangles
NHS	National Health Service – public funded healthcare provider in the UK
NIHR	National Institute for Health Research
NICE	National Institute for Health and Care Excellence
NuTH	Newcastle upon Tyne Hospitals NHS Foundation Trust
NIA-AA	National Institute on Ageing/Alzheimer's Association
NMDA	N-Methyl-D-aspartate
NPI	Neuropsychiatric Inventory
OR	Odds ratio
PD	Parkinson's disease
PDD	Parkinson's disease dementia
PD-MCI	Parkinson's disease with mild cognitive impairment
PET	Positron emission tomography, a radionuclide imaging technique
PiB	^{11}C-Pittsburgh Compound B
PSENI	Presenilin 1

PSEN2	Presenilin 2
PSP	Progressive Supranuclear Palsy
p-tau	Hyperphosphorylated tau
P-value	Probability value
RBD	Rapid Eye Movement Sleep Behaviour Disorder
REM	Rapid Eye Movement
ROI	Region of Interest
RVI	Royal Victoria Infirmary; NuTH site and location of nuclear medicine department where study patients were scanned.
SBR	Specific binding ratio; striatal to background ratio
SD	Standard deviation
Sd-MCI+a	Single domain, amnestic mild cognitive impairment
Sd-MCI+na	Single domain, non-amnestic mild cognitive impairment
SNCA	α-synuclein gene
SORL1	Sortilin related receptor 1 gene
SPECT	Single photon emission computed tomography
SPM	Statistical Parametric Mapping
SPSS	Statistical Package for Social Sciences software
SRT	Simple reaction time
SUPErB	^{123}I-MIBG Scintigraphy Utility as a biomarker for Prodromal DEmentia with Lewy Bodies (SUPErB) study – Research study into the development of biomarkers in prodromal DLB
t-tau	Total tau
T1	Spin-lattice relaxation time
T2	Spin-spin relaxation time

TIV	Total intracranial volume
TREM2	Triggering receptor expressed on myeloid cells 2 gene
UPDRS	Unified Parkinson's Disease Rating Scale
VaD	Vascular dementia
VBM	Voxel-based morphometry
VOI	Volume of interest
WM	White matter
WMH	White matter hyperintensities
Yrs	Years
^{123}I-FP-CIT	^{123}I-N-ω-fluoropropl-2β-carbomethoxy-3β-(4-iodophenyl) nortropane; ioflupane

Table of Contents

List of Tables

List of Figures

Chapter 1. Introduction

Dementia is defined as an irreversible and progressive cognitive decline that interferes with an individual's level of social or occupational function [1]. The illness is a major challenge to health and social services with an annual estimated cost to the UK economy of £26 billion [2]. Approximately, 850,000 people in the UK have dementia and the numbers are expected to rise over the coming decades due to the ageing population both in the UK and around the world [2]. Worldwide estimation of the prevalence of dementia in the population over 60 years of age is 5-7% which is approximately 46.8 million people but that figure is expected to increase to 74.7 million in 2030 and 131.5 million in 2050 [3, 4]. Moreover, the impact of dementia is felt not only by the affected individual, but also by families and carers. It has profound psychological sequelae for families and carers with 40% suffering with mood disorders such as anxiety and depression [1]. Unsurprisingly, improving accuracy of diagnosis and earlier diagnosis of dementia are strategic aims of the UK government and the National Health Service, as described in the National Dementia Strategy [3].

Dementia is an acquired clinical syndrome of heterogeneous aetiology which can be classified into neurodegenerative and non-neurodegenerative origins. In terms of causes of neurodegenerative dementia, Alzheimer's disease (AD), dementia with Lewy bodies (DLB), Parkinson's disease dementia (PDD) and frontotemporal dementia (FTD) account for the great majority of these. Dementia with Lewy bodies (DLB) is the second commonest cause of neurodegenerative dementia representing 4.6-7.5% of all dementia cases by clinical diagnosis [5, 6]. DLB and PDD represent a spectrum of Lewy body (LB) disease and are also referred to as Lewy body dementias (LBD). PDD occurs in the setting of an established diagnosis of idiopathic Parkinson's disease (PD). Both PDD and DLB share many clinical characteristics but differ in temporal onset of motor and cognitive symptoms, with extrapyramidal features in PDD normally occurring years in advance of dementia [7].

DLB manifests as progressive cognitive decline with accompanying core features; parkinsonism, visual hallucinations, REM sleep behaviour disorder and fluctuating levels of alertness and attention, and indicative imaging biomarkers displaying reduced striatal dopaminergic uptake and reduced postganglionic cardiac sympathetic innervation [7]. While the diagnostic criteria for DLB are highly specific for DLB compared with autopsy findings, their sensitivity for identifying DLB are low. Hence,

DLB is often misdiagnosed as AD and only one in three cases of DLB clinically identified when compared with autopsy findings [8].

The neurodegenerative process in DLB begins in advance of dementia. In the pre-symptomatic or preclinical phase of DLB, the pathological process occurs in advance of the manifestation of obvious symptoms. The next phase of neurodegeneration is the prodromal phase characterised by the manifestation of clinical symptoms which are insufficient to diagnosis DLB but suggestive that DLB will eventually develop (Figure 1.1).

There has been shift towards trying to identify DLB in the prodromal period before irreversible widespread neuronal damage has already occurred. Recently, diagnostic criteria for prodromal DLB have been published which outlines three phenotypes for the presentation of prodromal DLB [9]. Mild cognitive impairment with Lewy bodies (MCI-LB) is the commonest prodromal phenotype of DLB and its clinical characteristics are outlined in chapter 2 of this thesis. Imaging biomarkers have been incorporated into the research criteria for the diagnosis of probable and possible MCI-LB due to their ability to identify early neurodegeneration consistent with an underlying α-synucleinopathy pathological process, (e.g. striatal dopamine transporter reduction or cardiac sympathetic denervation in DLB) [9]. The application of imaging biomarkers in MCI-LB, namely ^{123}I-FP-CIT single photon emission tomography (SPECT) and magnetic resonance imaging (MRI), to identify structural and functional differences between MCI-LB and mild cognitive impairment due to AD (MCI-AD) and elderly healthy controls (HC), is the underlying rationale for this thesis.

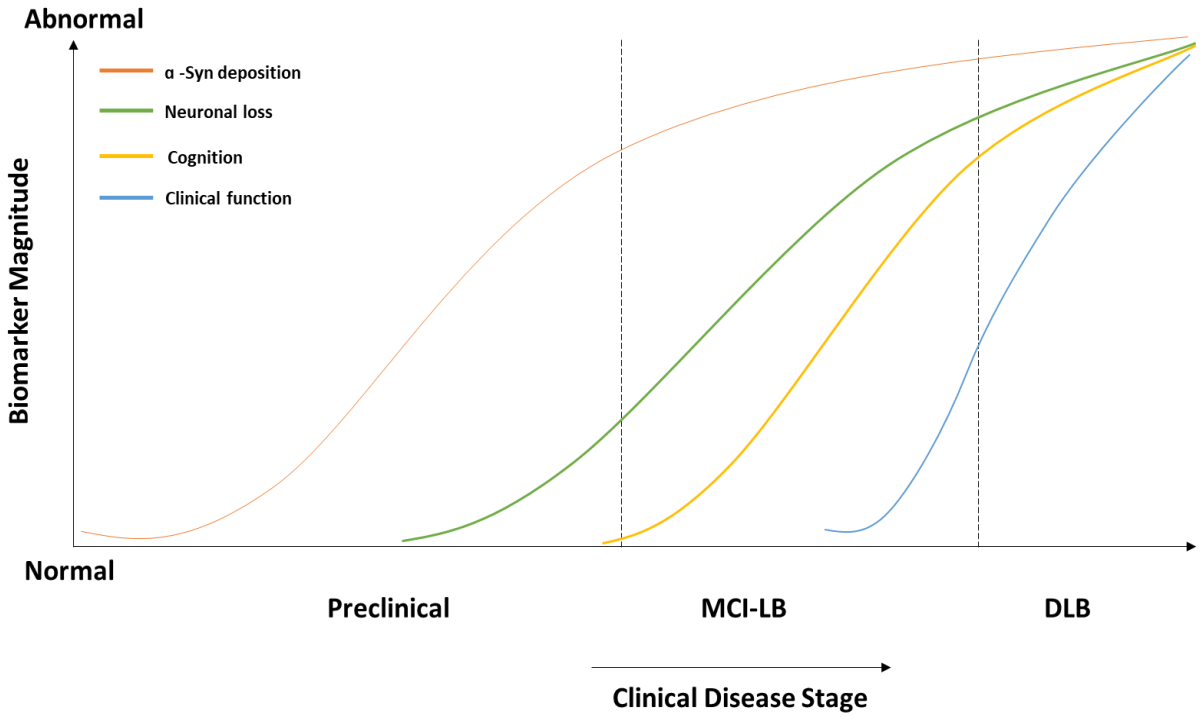

Figure 1. 1 The relationship of clinical disease stage to biomarker potential.

1.1 Mild cognitive impairment

Mild cognitive impairment (MCI) is a cognitive state which is intermediate between normal cognitive ageing and dementia. It is recognised as a pre-dementia stage which is associated with a high risk of future progression to dementia. MCI patients report cognitive decline in excess of that expected with normal ageing. In contrast with dementia, MCI subjects have relative preservation of functional independence and normal social and occupational functioning. MCI is a heterogeneous condition which originally was defined as precursor state (MCI-AD) of AD dementia but the concept has been broadened to recognise that MCI is the prodromal stage of other dementia subtypes.

Recently, research criteria for the diagnosis of prodromal DLB have been published which detail the necessary requirements for the diagnosis of possible or probable MCI-LB [9]. Two other prototypic prodromal DLB syndromes are also recognised; (1) delirium-onset, and (2) psychiatric-onset [9]. MCI-LB is best considered as a pre-dementia stage with signs or symptoms indicating that DLB will develop in the future. The proposed MCI-LB research criteria outlined in prodromal DLB are based on the National Institute on Aging and Alzheimer's Association (NIA-AA) criteria for MCI [10, 11] but also require concurrent Lewy body (LB) features (parkinsonism, rapid eye movement sleep

behaviour disorder (RBD), visual hallucinations and cognitive fluctuations). Neuropsychological cognitive scoring in MCI-LB should be between 1- to- 1.5 standard deviations below age and education matched control measures. Furthermore, biomarkers have been incorporated into the research criteria for MCI-LB and these include; (1) ^{123}I-FP-CIT SPECT or positron emission tomography (PET) showing reduced dopamine transporter uptake in the basal ganglia, (2) ^{123}I-metaiodobenzylguanidine myocardial scintigraphy (MIBG) showing reduced uptake, (3) polysomnographic confirmation of REM sleep without atonia. MCI-LB as a concept will be discussed in more detail in chapter 2.

1.2 Dementia with Lewy bodies

1.2.1 Epidemiology

Dementia with Lewy bodies (DLB) is increasingly recognised as a common type of neurodegenerative dementia in older people but the true prevalence of the condition in routine clinical practice remains unclear. It has been reported as being the second most common dementia after AD [12, 13] and becomes more common with increasing age [14, 15]. One of the main difficulties in ascertaining it's true prevalence is that more than 50% of cases are undetected [5, 16]. One recent UK study showed that overall DLB accounted for 4.6% (95% CI: 4.0-5.2%) of all dementia cases but prevalence varied between geographical regions in the UK with a higher prevalence in the North East of the UK (5.6%) than in East Anglia (3.3%). A recent meta-analysis found that DLB accounted for 4.2% of dementia cases in community samples and 7.5% of cases in secondary care, with an incidence of 0.87 per 1000 person-years [6]. Meanwhile, neuropathological studies in community-based cohorts with and without dementia has shown that significant Lewy body (LB) pathology is prevalent. A Japanese study investigating the prevalence of LB pathology found it in 22.5% (n=23/102) of all autopsy cases and 41.4% (n=12/29) of dementia cases [14]. A Finnish population-based study consisting of individuals at least 85 years old of which 64% were demented, found LB pathology in 36% of the whole cohort (3% brainstem-predominant, 14% limbic, 15% neocortical, 4% uncategorisable) [17]. Among the 36% non-demented subjects in the study, 20% had LB pathology while the corresponding figure for dementia patients was 38%. A study by Schneider et al. reported the prevalence of significant LB pathology in dementia patients was similar in a community (24.7%) and clinic based cohorts (21.4%) [18].

1.2.2 Clinical presentation and consensus diagnostic criteria

DLB is a disorder of cognition characterised by an insidious progressive decline over years eventually leading to interference with normal social or occupational function and accompanied by other characteristic symptoms which will be discussed below [7].

Cognitive symptoms and presentation

Patients frequently report early difficulties with short-term memory deficits including difficulty with multitasking and losing thread of conversations. However, in the early stages of DLB, memory loss tends to be less affected than other cognitive domains but memory deficits become more evident with disease progression. Non-amnestic neuropsychological deficits are more common than memory impairment in DLB; these include deficits in attention, visuo-perceptual abilities and fronto-executive function [19].

Cognitive impairment in DLB is associated with fluctuations in the level of a patient's attention, arousal and level of function. Although fluctuations may occur in other dementia subtypes, it is the qualitative features of the cognitive fluctuations in DLB which are generally regarded as their distinguishing feature, with fluctuations in DLB having greater prevalence and severity. Carers' report patients having episodes of "blank staring", non-logical flow of ideas, or frequent daytime drowsiness and naps [20]. Cognitive fluctuations may result in varying performance on cognitive testing with scoring varying from day-to-day or even within a day.

Neuropsychiatric symptoms

Neuropsychiatric symptoms are more common in DLB in comparison to AD and typically occur earlier in the disease trajectory. Hallucinations are usually visual without accompanying sound, smell or touch [21, 22]. Visual hallucinations are characteristically recurrent, complex and well-formed and animate and include small children, deceased family members and small animals, whereas in AD they are usually simple flashes and shadows.

Other neuropsychiatric features occur in DLB such as paranoid delusions and aggressive behaviour. Delusions tend to arise later in the disease course [23]. The content of delusions usually relates to

infidelity, house intruders, and theft, the last often occurring as patients misplace items around the home [23]. Capgras syndrome may develop as cognition progressively deteriorates and DLB patients may believe that their caregiver has been replaced by an imposter [23]. Anxiety, apathy, depression and sleep disturbance may also be present with varying degrees of severity and these neuropsychiatric symptoms are present at the earliest stages of DLB [11, 24, 25]. MCI-LB subjects are more likely to have two or more neuropsychiatric features (non-visual hallucinations, delusions, anxiety, depression and apathy) compared to MCI-AD, with a likelihood ratio of between 4.2 and 6.5 [11, 26]. Furthermore, neuropsychiatric symptoms are more severe and result in greater carer distress in LB disease than in AD [11].

Extrapyramidal features of DLB

Extrapyramidal features are common in the earliest stages of DLB. At the MCI-LB stage, 40-50% of subjects have extrapyramidal features [27] and eventually 70-80% of DLB patient develop at least one feature of spontaneous parkinsonism [7, 28]. The diagnostic criteria for DLB supports the "1-year rule" between the onset of dementia and parkinsonism to define the boundary between a PDD and DLB diagnosis [7]. The "1-year rule" states that DLB may be diagnosed based on the presence of parkinsonism which occurs less than 1-year before the onset of dementia. Motor dysfunction is common in DLB but symptoms are milder than in PD [7, 29]. Consequently, many patients with DLB may fall short of the definition of parkinsonism in PD, which is bradykinesia in combination with rest tremor and/or rigidity and/or postural instability [7, 30]. In DLB, only one parkinsonian feature suffices to meet the core feature criterion of parkinsonism [7]. Not all DLB patients have clinically detectable parkinsonism; 70-80% of DLB patients have parkinsonism on clinical assessment while 90% have evidence of nigrostriatal dysfunction on ^{123}I-FP-CIT imaging [28].

In terms of individual parkinsonian features, there are some differences between DLB and PD. Tremor occurs less frequently in DLB than in PD and tends to be a bilateral symmetric postural tremor rather than the classic asymmetric pill-rolling tremor of PD. Gait impediments are similar to that found in PD, with short stepping, shuffling, en-bloc turning and reduced arm swing [31]. There are more falls in DLB and PDD patients than in AD patients [32]. Falls may be related to dysautonomia, cognitive impairment, motor symptoms, or a combination of these factors [32].

The clinical features of DLB and PDD overlap significantly and include dementia in the setting of cognitive fluctuations, RBD and visual hallucinations. However, some clinical differences exist between the two entities. In terms of extra-pyramidal symptoms, parkinsonism is always present in PDD and often proceeds PDD by several years and is very levodopa responsive early in the disease trajectory [7]. In contrast, while parkinsonism is highly prevalent in DLB and becomes more common with disease progression, there still remains approximately 10-15% of DLB patients who never develop extrapyramidal symptoms [28]. Furthermore, the parkinsonism in DLB develops in close temporal association to the dementia in DLB as outlined in the "1-year rule" in prior paragraphs. Furthermore, the parkinsonism in DLB is much less levodopa responsive than in PDD and more likely to result in worsening of psychotic symptoms [33]. In terms of cognitive fluctuations while similar in character between DLB and PDD, occur much less frequently in PDD (29%) compared to DLB (42%) [34]. Hallucinations in DLB occur spontaneously but in PDD are typically related to dopaminergic therapy [35]. The rate of cognitive decline in DLB is much faster than in PDD [34].

Neuroleptic sensitivity

Neuroleptic sensitivity is seen in 30-50% of DLB cases and is thought to be related to blockade of striatal dopamine D2 receptors [36]. Neuroleptic sensitivity may be observed despite using low doses of typical neuroleptics and even with the use of atypical antipsychotic medications. Presentation of this condition is characterised by worsening of parkinsonism, acute confusion, psychosis, and rarely neuroleptic malignant system which can lead to death within several days.

Fortunately, neuroleptic sensitivity is encountered less frequently in recent years due to a decrease in the prescription of neuroleptic medication [37]. This has resulted in this feature being downgraded to a supportive feature in the latest fourth consensus criteria for the diagnosis of DLB [7] whereas it had been previously listed as a suggestive feature in the third consensus criteria [38].

Sleep disorders/ Rapid eye movement behaviour disorder

Parasomnias are common in DLB and rapid eye movement (REM) sleep behaviour disorder (RBD) is the most common parasomnia in DLB. RBD is a core clinical feature of DLB but also occurs in other α-synucleinopathies [7]. RBD can precede the diagnosis of DLB by several years or occur early within the disease [39]. RBD is diagnosed by polysomnography which reveals a lack of normal muscle atonia

during REM sleep which results in abnormal violent motor activity (kicking, punching and failing limbs) or vocalisations due to dream enactment [40]. RBD may also be diagnosed on the basis of clinical interview. The Mayo Sleep Questionnaire (MSQ) is used to screen for RBD by asking a patient's bed partner about their nocturnal sleep patterns [41]. The MSQ has a sensitivity of 98% and specificity of 74% for the diagnosis of RBD when compared with polysomnography [41]. The MSQ is used frequently to identify the presence of RBD in DLB due to polysomnography not being feasible in dementia patients [42].

Autonomic Dysfunction

Autonomic impairment is common in DLB. DLB patients frequently experience neurogenic urinary frequency/incontinence, orthostatic hypotension, constipation and sialorrhoea [43]. Autonomic symptoms may exacerbate other features in DLB such as fluctuating cognition and repeated falls. Symptomatic orthostatic hypotension occurs in 15% of patients with DLB [44].

1.2.3 Diagnostic criteria

The consensus diagnostic criteria for DLB are the agreed international standard for clinical and pathological diagnosis of DLB. The original consensus criteria were first established in 1996 and have been revised on three subsequent occasions, in 1999, 2005 and more recently in 2017. The diagnostic criteria for DLB are outlined in Table 1 and based on the most recent iteration of the fourth consensus report from McKeith et al. [7]. In brief, a definite diagnosis of DLB requires pathological assessment and confirmation at post-mortem. Ante-mortem, a diagnosis of 'probable' or 'possible' DLB can be assigned to a patient based on clinical features and imaging biomarkers. The consensus criteria recognise four 'core clinical features': fluctuating cognition with pronounced variations in attention and alertness; well-formed and detailed, recurrent visual hallucinations; RBD which may precede cognitive decline; and one or more spontaneous cardinal features of parkinsonism. There are also three indicative biomarkers; reduced dopamine transporter binding in the basal ganglia on SPECT or PET, low myocardial uptake of MIBG and polysomnographic confirmation of RBD. There are also 'supportive clinical features' of a DLB diagnosis and these are detailed in Table 1.1. In brief, the diagnosis of 'probable DLB' can be made clinically in the presence of dementia syndrome if two or more core clinical features of DLB are present regardless of the presence or absence of indicative biomarkers. If only one core clinical feature is present, one or

more indicative biomarkers are required to assign a diagnosis of 'probable DLB'. A diagnosis of 'possible DLB' requires the presence of dementia alongside either one core clinical feature with no indicative biomarker or one or more indicative biomarker in the absence of any core clinical features.

A significant overlap exists between the clinical features occurring in DLB and those occurring in PDD. In order to categorise patients into either of these two diagnoses, knowledge of the temporal onset of the motor dysfunction relative to the development of dementia is a prerequisite. DLB may be diagnosed based on the presence of parkinsonism which occurs less than 1-year before the onset of dementia. The consensus criteria recognises that this distinction can be difficult and that in clinical practice the term LBD may be preferred.

Dementia is the essential hallmark symptom of DLB. Dementia by definition must be severe enough to interfere with a patient's day-to-day functioning, often interfering with occupational and social activities. Screening tests such as the Mini-Mental State Examination (MMSE) and Montreal Cognitive Assessment (MOCA) have utility for rating a patient's overall mentation and impairment. These tests alone may not be adequate for establishing the full spectrum of neurocognitive deficits in DLB patients. A thorough assessment for DLB involves in depth testing of the most commonly affected domains of cognition including visual processing, attention, and executive function.

- **Essential**

Dementia: defined as a progressive cognitive decline of sufficient magnitude to interfere with normal social or occupational functions, or with usual daily activities. Prominent or persistent memory impairment may not necessarily occur in the early stages but is usually evident with progression. Deficits on tests of attention, executive function, and visuo-perceptual ability may be especially prominent and occur early.

- **Core clinical features (The first 3 typically occur early and may persist throughout the course.)**

1. Fluctuating cognition with pronounced variations in attention and alertness
2. Recurrent visual hallucinations that are typically well formed and detailed
3. REM sleep behaviour disorder, which may precede cognitive decline
4. One or more spontaneous cardinal features of parkinsonism: these are bradykinesia (defined as slowness of movement and decrement in amplitude or speed), rest tremor, or rigidity.

- **Supportive clinical features**

Severe sensitivity to antipsychotic agents; postural instability; repeated falls; syncope or other transient episodes of unresponsiveness; severe autonomic dysfunction, e.g. constipation, orthostatic hypotension, urinary incontinence; hypersomnia; hyposmia; hallucinations in other modalities; systematized delusions; apathy, anxiety and depression.

- **Indicative biomarkers**

Reduced dopamine transporter uptake in basal ganglia demonstrated by SPECT or PET

Abnormal (low uptake) on MIBG

Polysomnographic confirmation of REM sleep without atonia

- **Supportive biomarkers**

Relative preservation of medial temporal lobe structures on MRI scan.

Generalised low uptake on SPECT/PET perfusion/metabolism scan with reduced occipital activity ± the cingulate island sign on fluorodeoxyglucose positron emission tomography (FDG-PET) imaging.

Prominent posterior slow-wave activity on electroencephalogram (EEG) with periodic fluctuations in the pre-alpha/theta range

- **Probable DLB can be diagnosed if:**

A Two or more core clinical features of DLB are present, with or without the presence of indicative biomarkers, or

B Only one core clinical feature is present, but with one or more indicative biomarkers.

Probable DLB should not be diagnosed on the basis of biomarkers alone.

- **Possible DLB can be diagnosed if:**

A Only one core clinical feature of DLB is present, with no indicative biomarker evidence, or

B One or more indicative biomarkers is present but there are no clinical features

- **DLB is less likely:**

A. In the presence of any other physical illness or brain disorder including cerebrovascular disease, sufficient to account in part or in total for the clinical picture although these do not exclude a DLB diagnosis and may serve to indicate mixed or multiple pathologies contributing to the clinical presentation or
B. If parkinsonian features are the only core clinical feature and appear for the first time at a stage of severe dementia

DLB should be diagnosed when dementia occurs before or concurrently with parkinsonism. The term Parkinson disease dementia (PDD) should be used to describe dementia that occurs in the context of well-established Parkinson disease. In a practice setting the term that is most appropriate to the clinical situation should be used and generic terms such as Lewy body disease are often helpful. In research studies in which distinction needs to be made between DLB and PDD, the existing 1-year rule between the onset of dementia and parkinsonism continues to be recommended.

Table 1. 1 Revised criteria for the clinical diagnosis of probable and possible dementia with Lewy bodies (DLB) (from McKeith et al. 2017 [7]).

1.2.4 Prognosis

Despite DLB being a common form of neurodegenerative dementia, there is a relative paucity of studies detailing prognostic outcomes in the condition. The limited evidence available indicates that outcomes are poorer in DLB in contrast to AD, particularly with regard to early mortality, increased healthcare utilisation, long-term care needs/placement, accelerated cognitive decline, adverse drug reactions [45, 46]. Life expectancy in DLB is difficult to predict as at the time of diagnosis many patients are elderly and will have significant other co-morbidities. A number of studies in DLB have reported survival of 5.5-7.7 years from disease onset and 1.9-.6.3 years from diagnosis [45]. Prognosis appears to be worse in males, with survival being poorer in males than females [46]. Median survival in DLB appears to be approximately half that in AD, with survival in DLB being 3.72 years and 6.95 years in AD [46]. Cognitive decline is accelerated in DLB in comparison to AD, a 5 year prospective study showed an annual decline in MMSE of 4.4 points in DLB vs 3.2 points in AD, with DLB patients reaching a severe dementia state 5 months earlier than AD patients [47]. Carer stress is also more pronounced in DLB than other dementias' and in turn higher carer stress is associated with higher levels of psychosis, worsened mood and cognitive fluctuations in DLB patients [48]. Overall quality of life measures have been reported to be low in DLB due to the

accompanying neuropsychiatric features, high dependency level and loss of personal autonomy [45].

1.2.5 Genetics

There is an incomplete understanding of the core genes involved in the disease process and genetic research in DLB is still in its infancy. In addition to the clinical and pathological overlap, there appears to a substantial overlap in the genetic architecture of DLB with both PD and AD. Mutations in genes associated with PD, such as α-synuclein (SNCA) [49, 50], leucine-rich repeat kinase 2 (LRRK2) [51] and glucocerebrosidase (GBA) [52] have been associated with DLB. Similarly, mutations in genes associated with AD such as presenilin 1 (PSEN 1), presenilin 2 (PSEN 2), amyloid precursor protein (APP) [53], apolipoprotein E (ApoE) [54] and microtubule associated protein tau (MAPT) [55] have also been associated with DLB.

1.2.6 Neuropathology

The pathologic hallmark of DLB is the progressive accumulation of the protein α-synuclein into proteinaceous intracellular aggregates within neuronal cell bodies referred to as Lewy bodies (LB) or within neuronal processes referred to as Lewy neurites (LN) (Figure 1.2). Transmission of α-synuclein between neurons in the progression of disease may occur in a prion-like propagation [56].

LBs and LNs are widely distributed throughout the central and peripheral nervous system in DLB. The consensus criteria describe three patterns of central LB/LN deposition: (1) brainstem predominant, (2) limbic (also called transitional), and (3) neocortical [7]. Brainstem lesions affect the substantia nigra, nuclei of the vagus and glossopharyngeal nerves, reticular nuclei, and locus coeruleus. Limbic or transitional pathology occurs in the amygdala, transentorhinal cortex and cingulate. Limbic and neocortical α-synuclein lesions are associated with clinical features characteristic of DLB. Neuropathological studies also demonstrate that a proportion of dementia cases will have mixed LB and AD pathology (amyloid-beta (Aβ) plaques and neurofibrillary triangles (NFT)) and these patients have a varying degree of core and suggestive features of DLB [8]. Table 1.2 shows the likelihood that the pathologic findings will be associated with a typical DLB clinical syndrome. Therefore, the diversity of clinical phenotypes associated with DLB is likely to reflect the

timing and different combinations of one or more pathologies within different brain regions. The temporal progression of LB pathology will be discussed in chapter 2.

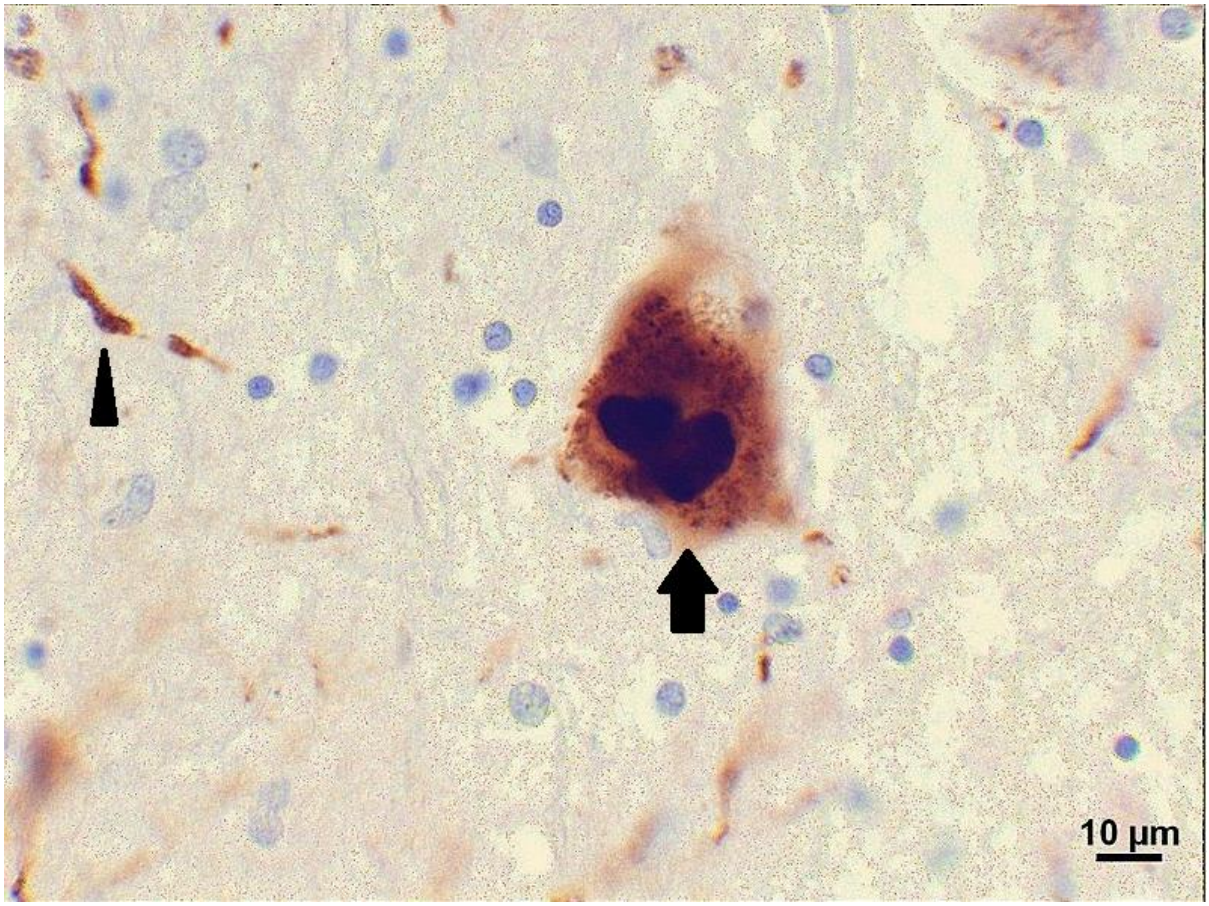

Figure 1. 2 Lewy body and Lewy neurite pathology: Photomicrograph of Lewy body (arrow) and Lewy neurite (arrow head) in the substantia nigra stained with alpha-synuclein antibody (made available by Suraj Rajan under creative Commons licence https://commons.wikimedia.org/wiki/File:Lewy_bodies_(alpha_synuclein_inclusions).svg).

Alzheimer's disease neuropathologic change	NIA-AA None/low (Braak stage 0-II)	NIA-AA Intermediate (Braak stage III-IV)	NIA-AA high (Braak stage V-VI)
Lewy-related pathology			
Diffuse neocortical	High	High	Intermediate
Limbic (transitional)	High	Intermediate	Low
Brainstem-predominant	Low	Low	Low
Amygdala-predominant	Low	Low	Low
Olfactory bulb only	Low	Low	Low
Substantia nigra neuronal loss to be assessed as none, mild, moderate, and severe) [57] in order to subclassify cases into those likely or not to have parkinsonism			
Abbreviations: NIA-AA = National Institute on Aging-Alzheimer's Association guidelines for the neuropathological assessment of Alzheimer disease [58].			

Table 1. 2 Assessment of the likelihood that the pathologic findings are associated with typical, dementia with Lewy bodies, clinical syndrome (from McKeith et al. 2017 [7]).

1.2.7 Clinico-pathologic correlations

Whilst AD is the most common cause of dementia, LB disease, cerebrovascular disease and frontotemporal lobar degeneration are other important causes and it's now evident from autopsy studies that in older people, who form the great majority of those with dementia, most have multiple underling pathologies [59]. Multiple pathology is usual even in those with clinically diagnosed AD. For example, two population based studies reported that more than 75% of people

with dementia had AD pathology insufficient alone to cause dementia (Braak stage <IV) with additional pathologies, especially LB pathology, causing the dementia [60]. Similarly, the major US study ADNI (Alzheimer's Disease Neuroimaging Initiative) reported about 75% of subjects at autopsy had other significant pathologies, with 45.5% having LB pathology [61]. Such findings are consistent with the high prevalence of LB pathology in brain bank studies. For example, Schneider et al. reported that 24.7% of 194 community subjects and 21.4% of a clinic cohort with a clinical diagnosis of probable AD had underlying LB pathology [18]. The Vantaa 85+ study found 36% of older people had LB pathology [17] and a population study in Japan found LB pathology in 22.5% of all subjects and in 41.4% of those who had developed dementia [14]. It is likely that different misfolded proteins interact along the course of neurodegenerative diseases, and synergies between Aβ, tau and α-synuclein can accelerate neurodegeneration and cognitive decline [62].

DLB is a type of dementia which shares clinical and pathological features with other dementia subtypes such as AD, PDD and vascular dementia. The relationship between LBs and the evolution of clinical phenotype in DLB remains unclear. A correlation between cortical LB burden and clinical dementia severity has yet to be established, although the pattern of distribution of LBs may be responsible for distinct clinical characteristics [7] [63, 64]. Loss of dopaminergic neurons in the nigrostriatal pathway is a common finding in DLB and other LB disorders and correlates with motor deficits. Although individuals may have cortical and striatal LB pathology without significant nigrostriatal neuronal loss. Visual hallucinations may be associated with LB pathology in the amygdala and parahippocampal cortex, while early hallucinations may be associated with LB pathology in the parahippocampal and inferior temporal cortices [65].

1.2.8 Striatal dopaminergic and cardiac sympathetic imaging in DLB

Pathological underpinning for striatal dopaminergic imaging

Neuropathologically, DLB patients display varying degrees of dopaminergic neuronal loss in the nigrostriatal pathway. Clinically, progressive nigrostriatal dysfunction manifests as extrapyramidal motor features of DLB. However, nigrostriatal pathway abnormalities occur before clinical manifestations of parkinsonism as 50% of dopaminergic terminals and 80% of striatal dopamine are required to be lost before motor symptoms are manifest [66, 67]. *In vivo*, functional imaging, such as ^{123}I-FP-CIT SPECT, of the dopaminergic nigrostriatal pathway provides information about the

integrity of dopamine terminals. ^{123}I-FP-CIT SPECT imaging acts as a marker of dopaminergic nigrostriatal integrity by binding to the presynaptic dopamine transporter receptors, any loss of nigrostriatal projections will result in a deficit of striatal ^{123}I-FP-CIT in binding. ^{123}I-FP-CIT binding to pre-synaptic dopamine transporter in the striatum has been shown to correlate with nigral dopaminergic neuronal density at post-mortem [68]. A pooled analysis of four clinical trials assessing the sensitivity and specificity of ^{123}I-FP-CIT, found that visual assessment of ^{123}I-FP-CIT images had a sensitivity 88.7% and a specificity 91.2% to detect a striatal dopaminergic deficit when clinical diagnosis was used as the reference standard [69]. Dopaminergic imaging with ^{123}I-FP-CIT identified DLB with a sensitivity of 80% and a specificity of 92% relative to AD dementia when compared with autopsy diagnosis [28].

Clinical utility of ^{123}I-FP-CIT SPECT

^{123}I-FP-CIT imaging enhances the accuracy of the diagnosis of DLB compared with clinical criteria alone and is particularly useful in differentiating between DLB from non-DLB. An abnormal ^{123}I-FP-CIT SPECT is highly predictive of DLB rather than AD in the setting of dementia, as significant nigrostriatal degeneration does not occur in AD [7, 28]. An abnormal scan is more likely to instigate a clinician to revise a clinical diagnose and thereby improve diagnostic certainty of DLB [70]. However, care must be taken to differentiate DLB from other α-synucleinopathies such as PD, PDD and multiple system atrophy (MSA), which also have abnormal ^{123}I-FP-CIT imaging, as can AD dementia with extensive small vessel disease. An abnormal ^{123}I-FP-CIT SPECT it the setting of a dementia but with the absence of core or suggestive features is sufficient to classify patients as possible DLB [7]. Meanwhile, a normal ^{123}I-FP-CIT SPECT in the early phases of dementia does not exclude the diagnosis of possible or probable DLB if subjects meet the clinical criteria. A proportion of DLB patients with a normal ^{123}I-FP-CIT SPECT will eventually develop an abnormal scan if it is repeated in the future [71]. However, the optimal timing to repeat the ^{123}I-FP-CIT SPECT imaging as DLB develops remains unknown. The ^{123}I-FP-CIT SPECT remains normal in approximately 10% of DLB with autopsy proven LB pathology [28]. The likely explanation for this is the involvement of cortical tissue with LBs, with relative sparing of the brainstem. A more in depth discussion of the Braak hypothesis of LB spread in the central nervous system is outlined in chapter 2 [72].

Clinical Correlations

The relationship between ^{123}I-FP-CIT binding and clinical characteristics in DLB has been explored in a relatively small number of studies with some conflicting results. Motor deficits, as measured by unified Parkinson's disease rating scale (UPDRS) have been shown to be negatively correlated with putaminal dopaminergic deficits in one study [73]. However, no association between dopaminergic deficits and motor dysfunction has been found in other studies [74, 75]. There has been no association found between the general level of cognitive impairment as assessed by MMSE and striatal ^{123}I-FP-CIT binding, implying neurological pathways other than nigro-striatal dopaminergic pathways are of more importance in cognitive decline [75, 76].

In terms of the relationship between hallucinations and ^{123}I-FP-CIT uptake in DLB, significant correlations were found between the severity and frequency of visual hallucinations and reduced ^{123} I-FP-CIT uptake in both caudate and putamen [73]. In terms of the relationship between other neuropsychiatric features and ^{123}I-FP-CIT uptake, caudate uptake alone has been shown to correlate with the Neuropsychiatric Inventory (NPI) depression, apathy and delusion scores, particularly in the right caudate [73]. Another study found a more limited correlation between neuropsychiatric features and ^{123}I-FP-CIT uptake, with the only correlation found between reduced right putaminal uptake and apathy [77].

Cardiac sympathetic degeneration: MIBG imaging

Cardiac sympathetic denervation is an early feature of DLB, in contrast with AD in which there is relative preservation of the cardiac sympathetic architecture [78]. Non-invasive *in vivo* assessment of cardiac sympathetic nervous system can be undertaken by MIBG scintigraphy. MIBG uptake is substantially reduced in DLB in comparison to HC and AD subjects as assessed by the heart-to-mediastinum ratio [79, 80]. In 2010, a meta-analysis of several studies including a total of 346 dementias patients, consisting of 152 DLB patients and 194 other dementia patients found a pooled sensitivity 98% and pooled specificity of 98% in MIBG discriminating DLB from other dementias [81]. This study also evaluated the usefulness of ^{123}I-FP-CIT SPECT relative to MIBG scintigraphy. The authors reported that imaging with ^{123}I-FP-CIT appeared to detect DLB better than with MIBG due to its high sensitivity (93% vs 83%). However, MIBG excluded DLB better than ^{123}I-FP-CIT imaging due to its higher specificity (79% vs 41%), suggesting that they may have a complementary role. A

more recent longitudinal study by Tiraboschi et al. showed that sensitivity was similar between MIBG (93%) and ^{123}I-FP-CIT (90%) imaging but MIBG was more specific (100%) than ^{123}I-FP-CIT (76%) for DLB [82]. Meanwhile, the combination of MIBG and ^{123}I-FP-CIT SPECT has been shown to have a diagnostic accuracy of 90% in distinguishing DLB from other dementia subtypes, with a sensitivity of 90% and a specificity of 91% [83]. The utility of MIBG scintigraphy as a biomarker for DLB is highly influenced by the cut-off values of the heart-to- mediastinum ratio used to determine a normal from abnormal scan. There is evidence to suggest cut-off ratios may need to be adjusted to account for differing ethnic backgrounds which may affect sensitivity and specificity is certain populations such as the Caucasian population who appear to have lower cut-off values [79, 84].

1.2.9 Other biomarkers

Amyloid imaging

Post-mortem studies in DLB patients have found multiple pathologies that may contribute to cognitive impairment. A common finding in DLB is concomitant AD pathology (Aβ plaques and tau NFTs) [8, 28, 85-87]. Visually positive amyloid PET imaging occurs commonly in DLB (54%) and 80% are positive on quantitation (Gomperts 2008). This is higher than the prevalence in elderly HCs (20%) but lower than can be seen in AD (85%) [88, 89]. In DLB patients compared with HC, Aβ has been shown to be widespread throughout the frontal and temporoparietal cortices [90]. Aβ deposition was associated with more pronounced hippocampal and subiculum atrophy in DLB, highlighting the important role mixed pathology plays in many DLB patients. [90].

EEG

EEG features consistent with DLB are the presence of posterior (temporal) transient slow or sharp waves and this has been incorporated into the diagnostic criteria for DLB as a supportive feature of the condition [7, 91]. The slow-wave activity has been found to positively correlate with the presence and severity of cognitive fluctuations and these may be seen at the MCI stage [92, 93]. Also, EEG microstate analysis, which measures brain dynamic change on a sub-second scale by segmenting the ECG signal into short, non-overlapping quasi-stable topographies known as microstates, has shown differences between LBD and both AD and HC [94]. LBD have increased microstate duration compared with AD and HC and the number of distinct microstates per second

is reduced in LBD compared to AD and HC [94]. Microstate duration was also found to be related to the severity of cognitive fluctuations in DLB [94].

Cerebrospinal fluid biomarkers

Quantification of several cerebrospinal fluid (CSF) biomarkers for DLB has been proposed but there is much debate about their utility. At present, there are no established CSF biomarkers for DLB. Caution must be applied in interpretation of results from CSF biomarker studies as studies are plagued by high variability and poor reproducibility [95-97].

CSF levels of α-synuclein have been investigated as a biomarker for DLB. The results of studies to date are conflicting with α-synuclein levels having been shown to be lower in DLB, PD and MSA than in patients without an α-synucleinopathy in some studies but in other studies α-synuclein levels were unable to discriminate α-synucleinopathies from other conditions [97]. At the present moment, no definite cut-off level of α-synuclein in the CSF has been established to identify patients with α-synucleinopathy [97]. A recent study found that total α-synuclein had a sensitivity of 40% and specificity of 78.9% in differentiating DLB from AD and differentiated DLB from HC with a sensitivity of 80% and specificity of 56.3% [96].

The role of CSF in DLB is largely confined to determining the presence of concomitant AD pathology. CSF biomarkers for the diagnosis of AD are: amyloid-β 1-38 (Aβ38), amyloid-β 1-40 (Aβ40), amyloid-β 1-42 (Aβ42), total tau (t-tau), and hyperphosphorylated tau (p-tau) [97]. Aβ42 is a predominant component of amyloid plaques; t-tau and p-tau, which are associated with neuronal damage and intracellular neurofibrillary tangles. Approximately, 25% of DLB patients have a CSF profile consistent with AD [97]. The majority of studies show no statistical difference between DLB and AD in terms of CSF Aβ42 levels. Comparison between AD and DLB patients showed that Aβ42 had a sensitivity of 48% and specificity of 94% for AD [97]. P-tau levels are higher in AD than in DLB, with a sensitivity 75-94% and specificity 61-94% but has a large variability due the assays used according to a recent review [97]. In DLB, the majority of studies show an overlap between DLB and AD with regard to levels of CSF AD biomarkers limiting their utility in differentiating between the two conditions [97-99].

1.2.10 Management

There are no disease modifying therapies which slow down or halt the progression of the cognitive decline associated with the neurodegenerative process in DLB. In the absence of disease modifying therapies, management of the condition is focused on amelioration of symptoms. The initial approach is to rationalise the amount of medication the patient is taking and thereby reduce the risk of drug interaction. This is of particular importance in DLB as patients are frequently sensitive to medications.

Cognitive impairment

There is a marked loss of acetylcholine neurons in DLB due to LB pathology affecting the nucleus basalis of Meynert which leads to a cholinergic deficit [100]. Cholinesterase inhibitors have been utilised to treat both cognitive and neuropsychiatric features of DLB [35]. Both rivastigmine and donepezil have been shown to have a therapeutic benefit in randomised controlled trials and demonstrated an improvement in cognitive function and behavioural symptoms [101-103]. Donepezil has been shown to be beneficial to decrease the neuropsychiatric features such visual hallucinations, agitation, apathy and reduce caregiver burden [102, 104-106]. Rivastigmine similarly has been shown to reduce visual hallucinations, delusions, agitation, and apathy and improve sleep [101, 107, 108]. An alternative medication to treat DLB is memantine, a NMDA- receptor antagonist, but findings from clinical trials are inconsistent for the use of memantine in DLB and it has not been shown to improve cognitive function [35].

Non-cognitive symptoms

Motor symptoms must be treated judiciously with levodopa through careful up-titration to avoid worsening cognitive, neuropsychiatric and orthostatic symptoms. At present, no double-blind randomised controlled trials have investigated the use of levodopa in DLB. However, open-label studies have indicated the beneficial effect of levodopa on motor function in DLB by improving the bradykinesia and tremor in 30-50% of subjects taking the medication [35]. However, the improvement in motor function must be balanced with the potential to worsen the neuropsychiatric features of DLB. Approximately, 30% of DLB patients treated with levodopa will experience a worsening in hallucinations and delusions [33]. Furthermore, improvement in motor function without exacerbation of neuropsychiatric features will occur in 20% of DLB patients treated with

levodopa [33]. In clinic, other dopaminergic agents are avoided such as dopamine agonists, monoamine oxidase b-inhibitors and amantadine, as they adversely affect cognition and neuropsychiatric symptoms. Motor symptoms and mobility may be improved by physical therapy input with focus on improving gait impairment and limiting falls.

Antipsychotic agents, either typical or atypical neuroleptics, are not routinely used for the treatment of the neuropsychiatric features of DLB as patients may be quite sensitive to these medications. In the short-term, 50% of DLB patients will experience a severe sensitivity reaction to antipsychotics and long-term use may increase the morality risk for patients [35]. Antipsychotic agents are only considered for use in DLB if non-pharmacological strategies have not succeeded and cholinesterase inhibitors have been tried but the psychotic symptoms remain. There are no randomised controlled trials to guide the use of any particular individual antipsychotic agent in DLB [35]. Among the atypical antipsychotics, quetiapine appears to be better tolerated and may have a role in very carefully selected individual patients [20]. Both quetiapine and clozapine have been found to be less likely to exacerbate parkinsonism or to cause neuroleptic malignant syndrome [109].

RBD does not necessarily require pharmaceutical treatment if the patient is not harming himself/herself or bed-partner. Simple non-pharmaceutical approaches may be taken that include removing sharp objects from the sleep environment, adding soft bedding to the floor next to the patient, and using separate beds. RBD may be treated with benzodiazepines (clonazepam) but being cognisant that it could worsen cognition and affect alertness [7]. There are retrospective case series supporting the use of clonazepam in RBD [35]. Melatonin may also be useful for the treatment of RBD and is well tolerated [7]. There is clinical data supporting the use of melatonin in RBD, with a therapeutic dose between 3-12mg well tolerated by patients [35]. Enquiry must be undertaken into the presence of concomitant obstructive sleep apnoea in anyone suspected of having RBD as the two often co-exist, and these patients will require positive airway pressure.

Only a few studies have focused on the management of autonomic symptoms in LBD [35]. Orthostatic hypotension can be treated with hydration, salt tablets, compression stockings, avoidance of exacerbating medications, and in resistant cases, with fludrocortisone and midodrine [35].

1.2.11 Summary

DLB is a common form of neurodegenerative dementia whose clinical hallmark is the presence of visual hallucinations, parkinsonism, fluctuating attention, and RBD. Clinical differentiation from other forms of dementia, particularly AD and PDD can be challenging but can be assisted by the clinical course as well as ancillary testing. Cognitive testing reveals impairments in multiple cognitive domains which are predominately non-amnestic in nature and affects visuospatial function, attention and executive abilities. The pathological hallmark changes in DLB are the progressive accumulation of α-synuclein in intracellular LBs'. However, a significant proportion of DLB subjects will have mixed DLB/AD pathology. Imaging biomarkers are helpful in delineating DLB from other dementia subtypes and improving correlation between clinical diagnosis and pathologic findings. Symptomatic control is the mainstay of treatment and therapeutic interventions need to be carefully selected to avoid worsening cognitive and behavioural symptomology.

1.3 Alzheimer's Disease

1.3.1 Overview of Alzheimer's disease

AD is a progressive neurodegenerative brain condition which causes dementia. Individuals with AD report a decline in memory, language, problem-solving and other cognitive abilities which interfere with their ability to perform everyday activities. Post-mortem examination of patients shows that AD-related pathological changes often co-exist with other pathological changes consistent with vascular-ischaemic cerebral injury and diffuse Lewy body disease.

1.3.2 Epidemiology

AD is the most common cause of dementia and is primarily a condition of increasing age, with the incidence at the highest in the 7^{th} and 8^{th} decade of life. The prevalence of dementia is highest in North America and Western Europe and around 50-70% of all cases are attributable to AD [110]. AD is a leading cause of reduced lifespan and accounts for 11.6% of all deaths registered [111].

1.3.3 Clinical features and diagnostic guidelines

The classical presentation of AD is insidious and progressive episodic memory decline with patients reporting difficulty in remembering conversations, recent events and word finding [112]. Impairment of memory is the phenotype most typically observed first as an isolated short-term

recall problem without any other major functional disability. The progressive neurodegeneration eventually becomes more widespread leading to interference in the activities of daily living; at this stage a patient can be diagnosed with Alzheimer's dementia. Neuropsychological testing reveals the cognitive domains most prominently affected in AD are; memory, language, executive and visuospatial function. Early neuropsychiatric features include apathy and depression. Later in the disease trajectory behavioural change, hallucination and seizure can emerge which lead to a significant level of care dependency. Death is on average 8.5 years from presentation which is approximately double the life expectancy observed in DLB post-diagnosis [46, 111].

There are a number of rarer atypical clinical presentations of AD which do not encompass a memory deficit early in their disease trajectory; these include posterior cortical atrophy, logopenic aphasia and the frontal variant of AD. In posterior cortical atrophy, patients initially present with visuospatial and visuoperceptual deficits and dyspraxia with relatively preserved memory. In logopenic aphasia, patients have problems in word finding, anomia and impairments in working memory. The frontal variant of AD is very similar to the behavioural variant of frontotemporal dementia.

Whilst a definitive diagnosis of AD requires pathological confirmation, clinical criteria for a diagnosis of 'probable AD' has been established and are outlined in Table 1.3. However, the pathological process underlying AD occurs years prior to symptom manifestation and the advent of modern imaging techniques incorporating biomarkers for Aβ and tau pathology, and MRI structural imaging, have meant that diagnostic criteria have evolved and allow the diagnosis to be made earlier in the disease trajectory. The Australian Imaging, Biomarkers and Lifestyle (AIBLE) study of aging, in which participants were healthy, aged over 60 years and had no objective cognitive impairment, demonstrated that 33% of subjects had a positive amyloid PET imaging. Those with high amyloid burden on baseline imaging showed longitudinal cognitive decline [113, 114]. The most recent diagnostic criteria from both the National Institute of Aging and the International working Group (IWG-2) now incorporate one or more preclinical AD phases, where biomarker evidence of AD pathology exists in the absence of symptoms [112, 115-117]. Therefore, biomarker information allows MCI to be classified as being attributable to AD with high, intermediate or low likelihood.

	NIA-AA Criteria [10, 112, 117]	IWG-2 Criteria [115]	Proposed preclinical AD criteria by Dubois et al. [116]
Asymptomatic individuals			
Evidence of Aβ pathology only	Stage 1 preclinical AD	Asymptomatic at risk for AD	Asymptomatic at risk for AD (asymptomatic A+)
Evidence of tau pathology only			Asymptomatic at risk for AD (asymptomatic T+)
Evidence of both Aβ and tau pathology	Stage 2 preclinical AD Stage 3 preclinical AD (when additional subtle cognitive changes exist which do not meet criteria for mild cognitive impairment)	Asymptomatic at risk of AD	Preclinical AD
Symptomatic Individuals			
Symptoms that do not meet criteria for dementia	Mild cognitive impairment due to AD High likelihood (requires positive Aβ and neuronal injury biomarkers) Intermediate likelihood (requires either positive Aβ or neuronal injury biomarker, where other biomarker not tested or unavailable) Unlikely (negative Aβ and neuronal injury biomarkers) Uninformative (biomarkers ambiguous or conflict with each other)	Prodromal AD (typical or atypical) Requires consistent History plus Biomarker evidence (CSF Aβ and tau or amyloid PET)	

Symptoms that meet criteria for dementia (both typical and atypical phenotypes)	Dementia due to AD Probable (no biomarker evidence required, based on clinical picture) Possible (no biomarker evidence required based on clinical picture) Probable or possible with evidence of AD pathophysiological process (Aβ and/or neuronal injury biomarker evidence – high likelihood, intermediate likelihood, unlikely and uninformative)	Typical or atypical AD Requires consistent history plus biomarker evidence (CSF Aβ and tau or amyloid PET)	

Table 1. 3 An overview of the different clinical and research diagnostic criteria for AD, and terminology used, from the preclinical through the symptomatic stages

1.3.4 Genetics

The vast majority of AD occurs sporadically and an autosomal dominant genetic aetiology occurs in only approximately 1% of cases [118]. Although, genetic susceptibility plays a role in 60-80% of sporadic cases of AD, many of the underlying genetic mechanism remain to be established [118]. Therefore, routine genetic testing for genetic risk factors / mutations is not recommended.

Autosomal dominant AD is caused predominantly by three genetic mutations. These are mutations in PSEN1 accounting for 80% of autosomal dominant cases [118]. Mutations in the PSEN2 account for 5% of cases [118]. About 15% of autosomal dominant cases are due to mutations in the APP gene [119].

The ApoE gene is a susceptibility gene for AD. ApoE is a polymorphic lipoprotein which is involved in the transport and delivery of cholesterol and other lipids through the cell surface ApoE receptor. There are three common ApoE alleles (ε2, ε3, and ε4), ε4 is associated with an increased risk of AD in a dose dependent manner, as well as lowering the age of onset. The relative risk for ε4

heterozygotes is 3-fold and for homozygotes it is about 15 fold [118]. ApoE ε4 allele is the strongest genetic risk factor for AD and the ApoE ε2 allele is the strongest genetic protective factor.

Genome-wide association studies and whole-exome sequencing studies have uncovered additional moderate risk genes. The majority of genes identified by genome-wide association studies cluster into three pathways: cholesterol metabolism, inflammation response and endocytosis/intracellular trafficking. An autosomal dominant mutation in ABCA7 (ATP binding cassette subfamily A member 7 gene) was found in a Belgian late-onset family, but ABCA7 variants have also been associated with an increased risk in African Americans that equals the risk of ApoE [118]. ABCA7 functions in the apolipoprotein-mediated phospholipid and cholesterol efflux from cells. TREM2 (triggering receptor expressed on myeloid cells 2 gene) variants increase the risk of AD significantly [118]. TREM2 is a receptor which is part of the immune system and located on immune cells such as microglia, macrophages and dendritic cells. The SORL1 (sortilin related receptor 1 gene) has a role in both lipid transport/metabolism as well as endocytosis [118].

1.3.5 Neuropathology

The cardinal features of AD pathology are cerebral accumulation of insoluble Aβ plaques and NFTs and subsequent neuronal loss [120]. Aβ plaques are extracellular aggregates of abnormally folded Aβ-peptide - both Aβ40 and Aβ42 [111]. NFTs are primarily composed of hyperphosphorylated tau. Aβ deposition is specific for AD whereas tau accumulation occurs in several other neurodegenerative diseases, known as tauopathies, including PSP, Pick disease and corticobasal degeneration (CBD).

NFTs undergo a typical topographical pattern of progression, commencing in the medial entorhinal cortex, progressing to the hippocampal area and spreading to the associated isocortex [121]. Unlike NFTs, Aβ plaques initially target the cingulate and inferior frontal cortex rather than the entorhinal cortex and hippocampal formation and then spread dorsally and laterally to the isocortex before affecting the subcortical structures.

A number of different criteria have been proposed to stage pathology in AD, including Braak [122], and the Thal criteria [123] and the Consortium to Establish a Registry for Alzheimer Disease (CERAD) [124]. However, the application of an individual staging system is hindered by low specificity or sensitivity [125]. An AD diagnosis is made if there is clinico-pathologic correlation between a diagnosis of dementia with evidence of high or intermediate likelihood of AD pathology on the NIA-AA neuropathological guideline [120]. Table 1.4 show how levels of neuropathological change are classified into one of four levels of AD neuropathological changes: Not, Low, Intermediate or High.

		B: NFT score (Braak stage)		
A: Aβ amyloid plaque score (Thal phases)	**C: Neuritic plaque score (CERAD)**	**B0 or B1 (None or I/II)**	**B2 (III/IV)**	**B3 (V/VI)**
A0 (0)	C0 (none)	Not	Not	Not
A1 (1/2)	C0 or C1 (none to sparse)	Low	Low	Low
A2 (3)	C2 or C3 (mod to freq)	Low	Intermediate	Intermediate
A3 (4/5)	Any C	Low	Intermediate	Intermediate
	C0 or C1 (none to sparse)	Low	Intermediate	Intermediate
	C2 or C3 (mod to freq)	Low	Intermediate	High
The combination of A, B, and C scores receive a descriptor "Not", "Low", "Intermediate" or "High" AD neuropathologic change. **CERAD= Consortium to Establish a Registry for Alzheimer Disease**				

Table 1. 4 Evaluation of AD neuropathological change using an "ABC" score that derives from three separate scales: Aβ amyloid plaques (A) by the method of Thal phases, NFT Stage by the method of Braak (B), and neuritic plaque score by the method of CERAD (C) [120]

1.3.6 Imaging and other biomarkers

Research focusing on the ability to detect *in vivo* biomarkers of AD pathology has added greatly to understanding at identifying disease onset and progression. The A/T/N method of classification is utilised to divide *in vivo* AD biomarkers into 3 distinct categories; "A" refers to amyloid biomarkers

(amyloid PET or CSF Aβ42); "T" refers to tau biomarkers (tau PET or CSF p-tau); "N" refers to biomarkers of neurodegeneration ([^{18}F]-fluorodeoxyglucose PET (FDG-PET), structural MRI or CSF t-tau) [126].

Structural MRI Imaging

Structural MRI imaging is a clinically useful tool for differentiating AD from vascular and non-AD neurodegenerative pathologies. A characteristic pattern of atrophy is seen in early AD, with the medial temporal lobes (MTL) being affected initially (i.e., hippocampal volume and entorhinal cortex thickness) [127]. As AD progresses, there is more global cerebral atrophy affecting the frontal, parietal and occipital lobes [127]. MRI studies have shown that the rate of hippocampal atrophy is associated with conversion from MCI to AD dementia [128]. The atrophy on MRI is correlated with cognitive decline in AD [129]. MRI studies comparing AD and DLB will be considered later (See chapter 4).

FDG PET

A decreased FDG PET signal is as a marker of neurodegeneration reflecting synaptic depletion. In patients with AD, a characteristic pattern of glucose hypometabolism is observed affecting the posterior cingulate and precuneus cortex first, followed by the posterior and lateral temporoparietal glucose hypometabolism and finally progressing to frontal hypometabolism [130]. FDG PET has shown high sensitivity (>90%) but lower specificity for discriminating AD from DLB and FTD, 71% and 65% respectively [131]. DLB shows greater involvement of occipital cortex than AD while FTD targets inferior temporal and frontal cortex. FDG PET has limited utility to predict outcome in early neurodegenerative disease. FDG PET predicted conversion from MCI to AD dementia with 25-100% sensitivity and 15%-100% specificity [132]. The high variability observed in FDG PET might be reflective of technical issues with imaging and the lack of adequate biomarker verification [132].

Amyloid PET Imaging

Three amyloid PET tracers are approved by the European Medicines Agency and the US Food and Drug Administration. These amyloid PET tracers are all fluorine-18 (^{18}F) ligands with a 110 minute half-life and are ^{18}F-flutemetamol, ^{18}F-florbetapir and ^{18}F-florbetaben. They all bind to fibrillary Aβ and ante-mortem uptake closely correlates with Aβ burden at post-mortem [133, 134].

The first PET ligand to be commonly used in research was ^{11}C-Pittsburgh Compound B (PiB), a neutral analogue of the stain thioflavine -T. However, one of the main limitations of PiB-PET imaging is the short radioactive half-life of carbon-11 (~20 min), which limits the distribution of PiB to PET imaging centres with on-site cyclotrons. Numerous studies using PIB PET have shown that the global Aβ plaque load in AD dementia patients leads to a 50-70% increase in tracer uptake compared to levels seen in cognitively normal older individuals [130]. Around 60% of amnestic MCI cases show Aβ positivity while 20-30% of elderly cognitively normal individuals show incidental amyloid [130].

Tau PET

Tau PET imaging is a more recent imaging technique which complements amyloid imaging. The general applicability of tau ligands is limited by the different ultrastructural and isoform composition of tau deposits and most bind to paired helical tau. There are a number of "first generation" tracers, including ^{18}F-THK5317 and ^{18}F-THK5351, which were also MAOB ligands, and ^{18}F-floratucipir (also known as ^{18}F-AV-1451, ^{18}F-T807), which is licenced as Tauvid by the FDA. Elevated levels of ^{18}F-floratucipir uptake have been reported in AD and also in MCI compared to HC [130] but off target binding is also seen in the nigra and striatum. Comparative studies between different ligands shows differing sensitivity and specificity toward tau pathology found in AD and second generation tracers are being developed to capture the complete range of the tauopathies [130].

Fluid biomarkers

The Alzheimer's Biomarker Standardisation Initiative has stated that the utility of CSF biomarkers is limited by the validity and comparability of CSF results across different laboratories due to differences in the assays [135] The core CSF biomarkers used in both research and clinical setting are derived from enzymatic cleavage of the APP resulting in residues of different length (Aβ38, Aβ40, Aβ42), as well as t-tau, and p-tau. The typical CSF pattern in AD is low Aβ42 and elevated levels of both t-tau and p-tau [136]. This pattern has been shown to be present also at the MCI stage and predict future conversion to AD dementia [136]. The deposition of Aβ42 peptide in Aβ plaques is thought to be responsible for the decreased levels detected of CSF Aβ42 in AD and higher CSF tau levels are indicative of neuronal injury during AD progression.

CSF AD biomarkers can discriminate accurately between AD and HC. The sensitivity and specificity for decreased CSF Aβ42 ranges from 63-97% and 67-92%, respectively across different studies for AD versus HC [137]. The sensitivity and specificity for t-tau is between 61-91% and 53-97% and for p-tau sensitivity is between 61-89% and specificity between 37-92% compared with HC [137]. The levels of Aβ38 and Aβ40 are unaffected in AD and may be useful for the normalization of inter-individual differences in Aβ-production in the form of ratios (Aβ42/Aβ38), though some studies have failed to show increased diagnostic accuracy using these biomarkers. Importantly, the CSF AD biomarkers have lower sensitivities and specificities when trying to differentiate between AD and other dementia subtypes. One study indicated that sensitivity and specificity for CSF biomarkers for discriminating between AD and non-AD dementia were was follows; Aβ42 (83% and 54%), p-tau (80% and 64%), t-tau (78% and 57%) [138]. The low specificity of CSF biomarkers for AD in this study and others, would suggest a limited role for CSF to discriminate between AD and other dementia subtypes. There are no replicated blood based biomarkers at present in use in the diagnosis of AD though SIMOA ELISA technology may now make that possible. .

1.3.7 Management

There are no disease-modifying treatments available for AD. Instead, management is directed towards individualised symptomatic needs and may need to adapt as the disease progresses. The 2018 National Institute for Health and Care Excellence (NICE) guidelines for the management of dementia highlight both non-pharmacological and pharmacological approaches [139]. In terms of non-pharmacological interventions, the NICE guidelines recommends cognitive stimulation therapy and cognitive rehabilitation [140].

The mainstay of early pharmacologic management of AD are the acetylcholinesterase inhibitors; donepezil, galantamine and rivastigmine [111, 141]. In moderate to severe AD, memantine is an option. Its mechanism of action is thought to be the reduction of L-glutamate excitatory neurotoxicity by having low affinity for the N-methyl-D-aspartate receptor antagonist.

1.3.8 Summary

Clinically, AD is characterised by insidious onset and slowly progressive cognitive decline and neuropsychological testing most commonly demonstrates amnestic memory impairment.

Neuropathologically, it is characterised by the extracellular accumulation of Aβ plaques and intracellular aggregation of hyperphosphorylated tau. AD is associated with cortical atrophy on structural imaging, particularly in the MTL; cerebral hypometabolism on PET imaging and amyloid deposition on PET imaging. CSF Aβ, tau and phosphorylated tau levels can be used to differentiate AD from HC, but are less useful in differentiating between AD and other dementias. Cholinesterase inhibitors and memantine are used to improve cognitive function in AD, but no disease modifying agents are yet available.

Chapter 2. Clinical characterisation of MCI-LB

2.1 Introduction

Increasingly, clinical research has focused on earlier detection of neurodegenerative conditions. The justification for this shift to earlier disease detection is to study disease modifying agents in brains without substantial pathological damage. In the last decade, criteria have been established to identify the phenotypes of AD and PD in the prodromal phase, which is defined as the period between the onset of earliest symptoms but before full clinical syndrome manifestation [10, 115, 117, 142]. Recently, research criteria have been published for the diagnosis of prodromal DLB which outline three prodromal phenotypes of DLB; (1) MCI, (2) delirium-onset and (3) psychiatric-onset [7]. At present, there is a lack of evidence to support formal criteria for the diagnosis of both delirium-onset and psychiatric-onset phenotypes [9]. However, the proposed criteria for the diagnosis of MCI-LB still require validation in longitudinal studies before adoption into clinical practice.

Evidence indicates that LB disorders have a long prodromal phase before the onset of dementia [25, 143]. During the prodromal phase, there is progressive accumulation of LB pathology throughout the central, peripheral and autonomic nervous system. Clinically, the progressive neuropathological accumulation of LB pathology manifests early with distinct symptoms complexes such as olfactory dysfunction, sleep disorders, autonomic dysfunction and cognitive impairment insufficient to be classified as a dementia. Therefore, these symptoms, in isolation or in combination with each other could be indicative of an evolving LB process prior to the development of a dementia.

Prodromal DLB as a concept is a relatively understudied topic, only a limited number of studies have focused on its clinical characteristics. An issue limiting research in this field was the lack of diagnostic criteria for prodromal DLB until the recent publication of diagnostic criteria for MCI-LB. Although, the diagnostic utility of the MCI-LB criteria remain to be validated by longitudinal studies with pathological verification. Retrospective studies in established DLB have consistently demonstrated that onset of cognitive and non-cognitive symptoms precedes dementia by several years in some cases [144, 145]. In prospective studies, clinical phenotypes such as MCI and idiopathic RBD (IRBD) has been shown to convert to DLB in a substantial proportion of patients if

followed-up over time [146-148]. Furthermore, cross-sectional studies have shown that biomarker abnormalities indicative of DLB have been demonstrated to be present in MCI-LB and IRBD before the onset of a dementia syndrome [27, 149].

This chapter will focus on clinical presentations of MCI-LB as a prodromal phenotype of DLB and the biological underpinning of such symptomatic manifestations. Dopaminergic imaging biomarkers in prodromal DLB will be examined in more detail in chapter 3.

2.2 Neuropathological underpinnings of Lewy body disorders

Conceptuality, the disease evolution in DLB can be considered as abnormal protein deposition resulting in cell damage which manifests symptomatically as impaired function. The accumulation of abnormal protein in different regions of the peripheral and central nervous system occur at different time points. A conceptual framework for the spatial and temporal progression of LB pathology in PD was developed by Braak and colleagues [72]. The Braak staging system in PD classifies LB progression into six stages of sequential ascending spread through the central nervous system. In stage 1, LB pathology is found in the olfactory bulb and the dorsal motor nucleus of the glossopharyngeal and vagal nerve. In stage 2, the LB pathology ascends to the brainstem before reaching the medulla oblongata and pontine tegmentum. In stage 3, the amygdala and substantia nigra become involved. In stage 4, the forebrain and cerebral cortex become involved and in stage 5 and 6, the pathology appears initially in the anterior association and prefrontal areas of the prefrontal cortex and spreads towards the posterior association areas. This spread of LB pathology can take several years to complete.

There is some debate whether the Braak staging model is representative of the spread of LB pathology in DLB. Autopsy findings in subjects with incidental LB disease have shown that it is possible to have widespread LB pathology in the peripheral and central nervous system without symptomatic manifestations [150]. Evidence that undermines the Braak staging model in DLB relates to findings from imaging studies as well as from post-mortem brains. Kane et al. reported that in 17.6% (n=3/17) of DLB subjects, there was no evidence of sympathetic cardiac denervation as assessed by MIBG but evidence of dopaminergic deficits on ^{123}I-FP-CIT SPECT, which would indicate LB pathology in these subjects did not spread from the peripheral to the central nervous

system [151]. Thomas et al. also reported that 10% of DLB subjects had no dopaminergic deficit on ante-mortem ^{123}I-FP-CIT SPECT but at post-mortem had evidence of neocortical and limbic LB pathology, consistent with a "top-to-bottom" spread of LB pathology rather than a "bottom-to-top" spread". Furthermore, in approximately 10% of DLB patients at autopsy, there is a pattern of cortical involvement with LB pathology consistent with an advanced Braak Stage but with relative sparing of the subcortical structures from LB pathology [28, 150, 152]. These autopsy findings indicate that at least in some DLB patients the sequential ascent of LB pathology via the brainstem into the substantia nigra is not an accurate representation of the spread of LB pathology. These pathological findings correlate with clinical manifestations in early DLB, as a substantial proportion of patient who despite having dementia do not display parkinsonism indicating that early DLB pathology may affect cortical structures without the substantia nigra pars compacta experiencing significant neuronal loss [27, 28]. However, as time progresses and the disease progresses cortical to subcortical spread may occur with the substantia nigra eventually becoming affected by LB pathology.

Although LB pathology is the pathological hallmark of DLB, caution must be taken in attributing all the clinical manifestations to LB pathology alone. Co-existing AD and LB pathology is frequently found at post-mortem [153]. The exact interplay between AD and LB pathology remains to be determined in DLB. Interestingly, cortical LB pathology alone does not account for dementia severity [154].

2.3 Overview of MCI

2.3.1 Evolution of MCI as a concept

MCI is considered an intermediate stage between age-related cognitive changes and dementia. The key distinguishing feature separating MCI from dementia is the preservation of functional independence and normal social or occupational functioning. Although, the clinical criteria for MCI have undergone a number of iterations over the last twenty years, the core clinical characteristics have remained largely unaltered. The original clinical criteria for MCI were developed by Petersen et al. (referred to as the original Mayo Clinic criteria) and focused primarily on episodic memory deficits [155]. The criteria was revised in 2003 (referred to as the revised Mayo clinic criteria) to recognise that the cognitive disability in MCI is heterogeneous and can incorporate cognitive

domains other than memory impairment [156, 157]. The revised criteria classified patients with MCI into those with amnestic MCI (aMCI), evidenced by deficits in episodic memory on neuropsychological testing or non-amnestic MCI (naMCI) based on deficits in non-memory cognitive domains. Impairment in cognition could be limited to one domain (MCI single domain) or encompass multiple domains (MCI multiple domain). Therefore, there are four proposed subtypes for MCI; single domain amnesic MCI (sd-MCI+a), multi-domain amnesic MCI (md-MCI+a), single domain non-amnestic MCI (sd-MCI+na) and multi-domain non-amnestic MCI (md-MCI+na) [158]. Each MCI subtype is associated with a differential risk of progression to a future subtype of dementia. Amnestic MCI subtype is associated with a higher risk of developing AD dementia in the future and non-amnestic MCI is more likely to progress to one of the other main subtypes of neurodegenerative dementia including DLB [159]. Implementation of the MCI criteria require the utilisation of clinical judgement in conjunction with neuropsychological tests as cut-off levels on neuropsychological testing alone are insufficient to make the diagnosis.

In 2011, the NIA-AA proposed criteria for the diagnosis of MCI-AD for use in clinical and research settings [10]. The purpose of the criteria is to identify subjects in the "symptomatic, pre-dementia phase" whose biological underpinning for their cognitive decline is related to AD pathology. The core clinical features outlined in the NIA-AA are nearly identical to the revised Mayo clinic criteria but differ in their incorporation of AD biomarkers. Biomarkers of AD can be divided into two types: 1) biomarkers of Aβ deposition and tau including CSF evidence of; decreased Aβ42, increased t-tau and p-tau levels or evidence of amyloid deposition using amyloid PET imaging 2) biomarkers of neuronal injury such as hippocampal atrophy on structural MRI and glucose hypometabolism on FDG –PET [10] [115].

In 2013, the American Psychiatric Association published the fifth edition of the *Diagnostic and Statistical Manual for Mental Disorders* (DSM-5), which details a group of disorders, 'neurocognitive disorders', characterised by a decline in cognition from prior level of cognitive functioning [160]. Application of the DSM-5 criteria is a two-step process, with the first step separating subjects into normal neurocognitive function, mild neurocognitive disorder (NCD) and major NCD (equivalent to dementia). The second step in the process attributes the cognitive decline to an underlying

pathological substrate (e.g. FTD, DLB, AD, vascular). The criteria for mild NCD overlap with the revised Mayo clinic core criteria and the NIA-AA criteria.

	Peterson et al. **(Original Mayo clinic criteria)[155]**	**Revised Mayo clinic criteria [156, 161]**	**NIA-AA 2011 [10]**	**DSM-5: Mild neurocognitive disorder [160]**
Subjective memory problem	Yes	Yes	Yes	Yes
Objective cognitive impairment	Memory deficit >1.5 SD below normal population	≥1 cognitive domain; no recommended cut-off	≥1 cognitive domain; 1-1.5 SD below average	≥1 cognitive domain; 1-2 SD below age and education adjusted norms
Preserved general cognitive function	Yes	Yes	Yes	Yes
Functional independence	Yes	Yes	Yes	Yes
Role for biomarkers	NA	NA	Incorporated into research criteria.	NA
Abbreviations: SD= Standard Deviation; NIA-AA= National Institute on Aging and Alzheimer's Association DSM-5= Diagnostic and Statistical Manual of Mental Disorders, fifth edition; NA= Not applicable				

Table 2. 1 Diagnostic criteria for mild cognitive impairment.

2.3.2 MCI-AD

MCI-AD is characterised by gradual onset and progressive course of episodic memory deficits, with a neuropsychological test profile consistent with a sd-MCI+a [162]. The progression of MCI-AD into AD dementia results in more cognitive domains being impaired such as; language, attention/executive and visuospatial dysfunction. Atypical AD may occur which tend to have "hippocampal sparing" pathology. Clinically patients present with focal syndromes such as progressive aphasia, corticobasal syndrome, or posterior cortical atrophy with relative preservation of memory. Atypical AD tend to have a naMCI, in which attention/executive, language, and/or

visuospatial impairment occur before memory problems. In general, the amnestic subtypes of MCI likely represent evolving AD, and the non-amnestic subtypes are more likely a non-AD disorder. The NIA-AA criteria for the diagnosis of MCI-AD requires a deficit in one or more cognitive domains (not necessarily memory) plus findings on biomarkers to increase or decrease the likelihood of underlying AD pathology.

2.4 Clinical presentations of prodromal DLB

2.4.1 Proposed diagnostic criteria for MCI-LB

The research criteria for the diagnosis of MCI-LB are based on the NIA-AA [10] criteria for MCI. Subjects are required to have cognitive decline in excess of that expected for normal ageing. The cognitive impairment may result in subjects being slower and less proficient at completing tasks but does not represent sufficient severity to interfere with dally social or occupational functioning.

Neuropsychological cognitive scoring would typically be 1- to- 1.5 standard deviations below age and education matched healthy control performance on standardised assessments. However, this neuropsychological cut-off measures are not absolute and clinical context must be taken into consideration.

Neuropsychological testing may allow for further subdivision of cognitive impairment based on affected cognitive domain. Cognitive deficits may be subdivided into single or multiple domain, as well as amnestic or non-amnestic. The cognitive deficits observed in MCI-LB are similar to those in DLB, with early deficits affecting attention/executive function as well as relatively preserved memory [163]. MCI-LB is best characterised as sd-MCI+na or md-MCI+na [9]. In comparison, MCI-AD is characterised by sd-MCI+a [10]. However, sd-MCI+a, md-MCI+a, sd-MCI+na, and sd-MCI+na may all progress to DLB [164, 165].

Clinical diagnostic criteria for probable and possible MCI-LB are outlined in Table 2.2. These are similar to the diagnostic criteria for DLB but require subjects to have MCI as defined by NIA-AA criteria instead of dementia [10]. Core clinical features at the MCI-LB stage may be of less pronounced severity and less frequent than in DLB, thus potentially limiting their diagnostic

specificity. The “1-year rule” is applied to parkinsonism features in a similar manner to separate a DLB from a PDD diagnosis although it is recognised that a degree of uncertainty may exist in classifying MCI with parkinsonism due to the potential conflict with a PD with mild cognitive impairment (PD-MCI) diagnosis. Most PD-MCI subjects have had extrapyramidal symptoms for over a year before the development of cognitive complaints, especially the younger cases.

It is important to note that these research diagnostic criteria for probable/possible MCI-LB are not validated yet and will require longitudinal follow-up studies with pathological verification of final neurodegenerative diagnosis. This process will allow sensitivity and specificity for the diagnostic criteria and the individual clinical features and biomarker components that identify early LB disease to be determined.

Essential Requirement: MCI defined by the presence of each of the following;

- Concern by the patient, informant, or clinician regarding cognitive decline.
- Objective impairment in 1 or more cognitive domains.
- Preserved/minimally impaired activities of daily living, insufficient to meet the criteria for dementia

Core clinical features;

- Fluctuating cognition with variations in attention and alertness
- Recurrent visual hallucinations
- RBD
- One or more spontaneous cardinal features of parkinsonism; these are bradykinesia, rest tremor or rigidity

Proposed biomarkers

- Reduced dopamine transporter uptake in the basal ganglia demonstrated on SPECT or PET
- Polysomnographic confirmation of REM sleep without atonia
- Reduced MIBG uptake

Probable MCI-LB can be diagnosed if:

- Two or more core clinical features are present, with or without the presence of a proposed biomarker.

Or

- Only 1 core clinical feature is present but with 1 or more proposed biomarkers

Probable MCI-LB should not be diagnosed based on biomarkers alone.

Possible MCI-LB can be diagnosed if:

- Only 1 core clinical feature is present, with not proposed biomarkers.

Or

- One or more of the proposed biomarkers is present, but there are no core clinical features.

Supportive clinical features:

- Severe sensitivity to antipsychotic agents; postural instability; repeated falls; syncope or other transient episodes of unresponsiveness; prolonged or recurrent delirium; autonomic dysfunction, e.g. constipation, orthostatic hypotension, urinary incontinence, hypersomnia, hyposmia, hallucinations in other modalities including passage, and sense of presence phenomena, systematised delusions, apathy, anxiety and depression

Potential biomarkers of MCI-LB

- Relative preservation of the medial temporal lobe on structural imaging
- Insular thinning and grey matter volume loss on MRI
- Quantitative EEG showing slowing and dominant frequency variability
- Low occipital uptake on perfusion/metabolism scan

Abbreviations: MCI= mild cognitive impairment; MCI-LB= MCI with Lewy bodies; RBD= Rapid eye movement sleep behaviour disorder; SPECT= single photon emission computer tomography; PET=Positron emission tomography; MRI= Magnetic resonance imaging; EEG= electroencephalogram; MIBG=123I-metaiodobenzylguanidine myocardial scintigraphy

Table 2. 2 Research criteria for the clinical diagnosis of probable and possible MCI-LB [9].

2.4.2 Biomarkers in MCI-LB

Imaging biomarkers are important elements of the research criteria of MCI-LB. Of the three proposed biomarkers of MCI-LB, two are imaging biomarkers; (1) reduced dopamine transporter uptake in basal ganglia demonstrated by SPECT or PET, (2) reduced cardiac MIBG uptake [9]. The role of ^{123}I-FP-CIT SPECT as an imaging biomarker for DLB/MCI-LB is discussed in more detail in chapter 3. The utilisation of ^{123}I-FP-CIT SPECT to distinguish between MCI-LB and MCI-AD has been reported to have a sensitivity of 54% and specificity 89% [27]. Imaging using MIBG at the MCI stage is relatively understudied but reduced cardiac MIBG is an indicative biomarker in the DLB diagnostic criteria. Sakakibara et al. reported decreased MIBG uptake in 30% (n=13/44) of amnestic MCI patients, with 7/13 MCI patients reporting visual hallucinations and/or RBD [166]. Fujishiro et al. reported on nine patients with a clinical diagnosis of RBD and no dementia (only one had MCI) and found reduced cardiac MIBG levels in all subjects [167]. In 2 cases of amnestic MCI reported by Fujishiro et al., both had decreased MIBG uptake and one of these subjects developed DLB 2 years later [168]. However, longitudinal follow-up of MCI-LB subjects until conversion to dementia and subsequent pathological verification of the diagnosis are still needed to determine the utility of ^{123}I-FP-CIT and MIBG in early LB disease. DLB patients have a high prevalence of RBD and one polysomnography study in DLB has shown that 83% of patients have confirmation of REM sleep without atonia with or without dream enactment during polysomnography [169]. Polysomnography in idiopathic RBD has been shown to predict cognitive decline (the development of MCI) and parkinsonism, particularly in older patients with high amounts of REM sleep without atonia [170].

Other biomarkers for MCI-LB which are not part of the research criteria diagnostic algorithm for MCI-LB but are mentioned as potential biomarkers include EEG, structural MRI and FDG-PET [9]. A quantitative EEG pattern showing slowing and dominant frequency variability at the MCI stage has demonstrated that 83% of MCI patients with this pattern will convert to DLB in 3 years [171].

Structural MRI changes in MCI-LB will be discussed in more detail in chapter 4. However, relative preservation of hippocampal volumes, grey matter (GM) volume loss and insular thinning at the MCI stage are potential structural MRI biomarkers for differentiating MCI-LB from MCI-AD [172, 173]. Occipital hypometabolism and relative preservation of posterior cingulate metabolism on FDG-PET has been associated with DLB but no studies have examined whether it can distinguish MCI-LB from MCI-AD [9].

Features	MCI-AD	MCI-LB
Core early features	Absence of core DLB features	Presence of one of more of: parkinsonism, REM sleep behaviour disorder, visual hallucinations and cognitive fluctuations.
Cognitive domains affected on neuropsychological testing	Memory effected earliest with subsequent language, attention/executive, visuospatial domains affected later	Relative preservation of memory domain, with more pronounced deficits in attention/executive and/or visuospatial and language domains.
Most common MCI subtypes	aMCI , md-MCI+a	Sd-MCI+na, md-MCI+na
Ancillary clinical features		Anosmia Autonomic dysfunction -Orthostatic hypotension -Erectile dysfunction -Urinary dysfunction -Constipation -Sialorrhoea Mood problems -Depression -Anxiety -Apathy Sleep disorders -Excessive daytime sleepiness -Restless legs syndrome -Insomnia
Proposed biomarkers distinguishing MCI-LB from MCI-AD		
Dopaminergic system imaging	Normal striatonigral uptake	Decreased striatonigral uptake
Cardiac sympathetic denervation on MIBG	Normal cardiac uptake	Reduced cardiac uptake

Polysomnography	No REM sleep without atonia ± dream enactment	REM sleep without atonia ± dream enactment
Potential Biomarkers distinguishing MCI-LB from MCI-AD		
EEG		
Magnetic Resonance imaging	Hippocampal atrophy	Normal hippocampal volume
Positron emission tomography **-Fluorodeoxyglucose** **-Amyloid radiotracer**	Decreased metabolism in temporoparietal cortex Increased uptake in neocortex	Decreased metabolism in occipital cortex. Preservation of posterior cingulate metabolism. No increased uptake
Cerebrospinal fluid (CSF)	Low beta-amyloid High tau	Normal to high beta-amyloid Normal to low tau
Abbreviations: REM= Rapid eye movement; aMCI= amnestic mild cognitive impairment; sd-MCI+na= single domain, non-amnestic mild cognitive impairment; md-MCI+a= multidomain amnestic mild cognitive impairment; naMCI= non-amnestic mild cognitive impairment; md-MCI+na= multidomain, non-amnestic mild cognitive impairment; EEG= Electroencephalogram; MCI-LB= mild cognitive impairment with Lewy body disease; MCI-AD= mild cognitive impairment due to AD.		

Table 2. 3 Clinical, neuropsychological and biomarkers finds in MCI-AD versus MCI-LB.

2.4.3 Delirium-onset phenotype of prodromal DLB

The research criteria for prodromal DLB also extended the phenotypic presentation for prodromal DLB to include both delirium-onset and psychiatric-onset [9]. The delirium-onset subtype of prodromal DLB consists of subjects with no underlying cognitive impairment, presenting with an episode of delirium in advance of subsequent progression to DLB months or years later [174]. Typically, these patients have recurrent episodes of delirium which may be provoked or unprovoked and the episodes of delirium may be prolonged. Provoked delirium occurs in the context of a physiological stress such systemic illness due to sepsis, fever, surgery, medication alternation etc. Unprovoked episodes of delirium refer to a situation where the precipitating factor causing the delirium cannot be identified. Evidence supporting the delirium-onset of prodromal DLB is limited

and confined to case reports in the literature [9]. One study which examined post-operative delirium among patients following gastrectomy found that alpha-synuclein pathology was more common in the myenteric plexus in those who developed post-operative delirium compared with those who did not (44% vs 6%) [175]. Furthermore, more patients with DLB (25%) had a preceding episode of delirium compared with AD (7%) [176]. At present, there is insufficient evidence to support diagnostic criteria for the delirium-onset phenotype of DLB [9].

2.4.4 Psychiatric-onset phenotype of prodromal DLB

The last proposed subtype of prodromal DLB is the psychiatric onset subtype which is characterised by a late onset affective disorder or psychosis [9]. One of the challenges with psychiatric-onset DLB is differentiating it from non-LB late onset psychosis as there is a significant overlap in neuropsychiatric features and motor symptoms such as bradykinesia may be attributable to psychomotor retardation. At present, there is insufficient evidence to support diagnostic criteria for the psychiatric-onset phenotype of DLB [9].

2.4.5 Mild neurocognitive disorder with Lewy bodies

There are also other published diagnostic criteria for the identification of the earliest neurodegenerative features of DLB. The latest revision of the Diagnostic and Statistical Manual of Mental Disorders, fifth edition (DSM-5), has incorporated a prodromal phase to DLB into their criteria in the form of mild neurocognitive disorder with Lewy bodies (NCDLB) which approximately corresponds to MCI criteria based on the NIA-AA criteria with the addition of subjects having either one (possible NCDLB) or two (probable NCDLB) of the core clinical features of DLB used in the previous 2005 consensus DLB criteria [160]. The key difference between DSM-5 mild NCDLB criteria and the McKeith probable/possible MCI-LB criteria discussed previously is that the former criteria does not use biomarkers of LB pathology.

2.4.6 Idiopathic REM sleep behaviour disorder as a prodrome to DLB

IRBD is a high risk prodromal condition for the development of α-synucleinopathies such as DLB, PD, and MSA. It is characterised by a lack of motor inhibition during REM sleep resulting in dream-enactment behaviours with complex motor activity such as punching, kicking, arm flailing and shouting but without evidence of cognitive impairment or parkinsonism [177]. IRBD may develop at any time during the α-synucleinopathic neurodegenerative process. Symptoms of RBD may proceed

the manifestation of motor, cognitive or autonomic dysfunctions by years or even decades in some cases [148]. In one study on subsequently autopsy-confirmed DLB patients, 60% of patients had RBD, as assessed by the Mayo Sleep Questionnaire, before or during the year of estimated dementia onset [42]. The importance of RBD in predicting/delineating DLB has been recognised by its recent incorporation as one of the core features of the condition in the DLB diagnostic criteria as well as its incorporation into the MCI-LB diagnostic criteria [7, 9]. RBD accompanying other core features has been shown to improve the diagnostic accuracy of autopsy-confirmed DLB [178]. However, one limitation of using IRBD as a prodrome for DLB, is that there is an equal risk of phenoconversion into either PD or DLB and occasionally MSA on longitudinal follow-up studies [39, 148]. Analysis of pooled prospective follow-up data from 24 centres of the International RBD study group found that significant predictors of conversion from IRBD to a neurodegenerative disorder included; olfactory deficit (HR=2.62), MCI (HR=1.91-2.37), motor symptoms (HR=2.11), and abnormal ^{123}I-FP-CIT SPECT (HR=1.98), age (HR=1.54), constipation (HR=1.67), and colour vision (HR=1.69) [179].

The cognitive deficits in early RBD are similar to the deficits encountered in DLB. MCI occurs in 33%-50% of RBD subjects formally assessed in sleep clinic studies [180, 181] [182] [180]. The cognitive deficits observed in RBD are predominantly naMCI rather than aMCI which is consistent with the deficits seen in DLB, with deficits in attention, executive and visuospatial domains [180, 181]. In a longitudinal study followed by Marchand et al. [181], those subjects who had both RBD and MCI at baseline were at greater risk of developing dementia first (93% developed dementia) compared with the parkinsonism first group (42% developed dementia) [181]. Moreover, deficits of attention and execution function reliably predicted dementia (area under curve ≥0.85) compared with the parkinsonism first group. Another study by Terzaghi et al. demonstrated that visuospatial dysfunction is the most commonly affected cognitive domain in RBD [182]. MCI was found to be more prevalent in the RBD cohort who converted to dementia first versus those who converted to parkinsonism first (84% vs 25%, $p<0.001$) in a pooled analysis of data from 24 centres of the International RBD study group [179].

Prodromal development and progression of parkinsonism has been studied in RBD [183]. Postuma et al. investigated the evolution of parkinsonism in IRBD and reported that motor changes were present for 6 years preceding the diagnosis of DLB but the extrapyramidal signs progressed slowly

(UPDRS increase: 2 points per year) [183]. This implies that motor dysfunction in prodromal DLB has a more indolent course and progresses more slowly than in PD. The authors of this study suggested that extrapyramidal signs in DLB may be in part due to degeneration of extra-nigral structures.

The prevalence and temporal onset of autonomic dysfunction has been investigated in one study of IRBD subjects [184]. In a prospective study by Postuma et al., there was clear evidence of autonomic dysfunction several years before a neurodegenerative diagnosis. This study examined 73 subjects with IRBD and followed them up over an average duration of 3.3 ± 2.3 years [184]. During follow-up 32 patients developed a neurodegenerative disease, 17 developed parkinsonism, 15 developed dementia (all met possible DLB criteria and 11 met probable DLB criteria). Autonomic symptoms progressed slowly over the prodromal period with estimated onset of autonomic symptoms ranging from 11 to 20 years prior to a neurodegenerative diagnosis, with alterations in systolic blood pressure (20.4 years prior) and constipation (15.3 years prior) being the earliest estimated autonomic systems. Systolic drop in blood pressure, erectile dysfunction and constipation could identify disease up to 5 years before diagnosis with sensitivity ranging from 50 to 90%. However, pooled prospective follow-up data from 24 centres of the International RBD study group did not find any predictive value for orthostatic symptoms or urinary dysfunction on the rate of phenoconversion from RBD to a neurodegenerative syndrome [179].

2.5 Clinical studies in prodromal DLB

Research into prodromal DLB is still in its infancy and relatively few studies have explored the pre-dementia stage of DLB. The following paragraphs will detail the cross-sectional, prospective and retrospective studies conducted to date investigating symptom prevalence and clinical progression in the pre-dementia stage of DLB.

2.5.1 Retrospective studies

Retrospective studies of patients with DLB are helpful in assessing symptom development, but these may be susceptible to recall bias. Findings from these studies confirm that some core features of DLB are already present before dementia onset. Retrospective studies based on symptom questionnaires have shown that visual hallucinations, gait problems, tremor/stiffness, falls and

sleep symptoms including RBD, are prevalent in early DLB and can precede dementia by several years. Chiba et al. investigated the prevalence and time of onset of non-motor symptoms relative to the onset of memory loss in early DLB compared with early AD using a standardised worksheet of 15 non-motor symptoms which occur in PD [144]. This study showed that a number of non-motor symptoms preceded the onset of memory loss in a significant proportion of DLB patients, these were; constipation (53%), increased sweating (29%), crying/shouting during sleep (77%), depression (32%), limb movement during sleep (47.1%), anosmia/hyposmia, nightmares (65%), sleep rhythm change (82%). The time to onset of RBD when constipation and olfactory dysfunction preceded memory loss, ranged from 2.5 to 9.4 years. One limitation of this study was the lack of enquiry about core features such as parkinsonism, visual hallucinations or cognitive fluctuations. Another retrospective study has shown that the presence of mild parkinsonism at the pre-dementia stage of DLB (UPDRS motor score ≤ 5), was a sensitive predictor of future DLB [157].

A retrospective study by Fujishiro et al. [145] found that LB related symptoms were present in 87.8% (79/90) patients with probable DLB before or at the time of memory loss onset. These symptoms preceded the onset of memory loss between 1.2 and 9.3 years. LB symptoms which preceded memory impairment were constipation (57.7%) (-9.3 ± 13.8 years), anosmia/hyposmia (37.8%) (-8.7 ± 11.9 years), depression (18.9%) (-4.8 ± 11.4 years), REM sleep behaviour disorder (45.5%) (-4.5 ±10.5 years), and orthostatic dizziness (17.7%) (-1.2 ± 6.5 years). Visual hallucinations were present in 31.1% and parkinsonism in 31.1%. The prevalence of autonomic symptoms was not very high, orthostatic dizziness 17.7% and syncope 6.7%.

In a study by Cagnin et al. [157], a retrospective evaluation of patient charts (n=25) at the MCI stage who were eventually diagnosed with dementia (DLB vs AD), indicated the best clinical predictor of the developing DLB was presence of soft extrapyramidal signs, detected in 72% of DLB patients, followed by presence of RBD (60%) and fluctuations (60%) [157]. This study supports the view that temporal development of some core features of DLB occurs before the onset of dementia. Moreover, 52% of MCI-DLB patients presented at the first assessment with 2 core features (fluctuations and extrapyramidal involvement).

In a retrospective study by Kim et al. [185] who examined heart rate variability (HRV) data in MCI subjects who subsequently developed probable DLB (n=23) compared with MCI subjects who developed AD dementia (n=46), there was significantly lower levels of almost all HRV parameters in MCI progressing to DLB compared with the MCI progressing to AD dementia. Furthermore, there was no significant correlation between the HRV data and nigrostriatal dopaminergic depletion in the 19 MCI subjects who eventually progressed to probable DLB and also had undertaken nigrostriatal dopaminergic imaging. The lack of correlation between HRV data and striatal dopaminergic deficiency would likely indicate the presence of extra-nigral LB pathology. However, the interpretation of this study is limited by the lack of post-mortem confirmation of the neurodegenerative diagnosis. Therefore, the extent of autopsy proven LB pathology was not established.

2.5.2 Prospective and cross-sectional studies in prodromal DLB

Prospective and cross-sectional clinical studies have reported that the diagnostic symptoms of DLB may already be present in the MCI phase of the disease. The intent of these studies was to differentiate MCI into different clinical subtypes based on clinical symptoms, neuropsychological profiles and biomarkers, with the aim of potentially predicting future progression to either DLB or AD.

In a prospective study by Sadiq et al. [186], a clear difference in clinical features was found in a memory clinic setting across 429 patients with MCI who subsequently eventually developed either DLB, AD dementia or remained stable. The MCI subjects who progressed to DLB (n=21, 5% of cohort) were more likely to have parkinsonism, fluctuating cognition and RBD. There was a trend towards higher visual hallucinations in this group. Cognitive assessment in MCI subjects whom progressed to DLB had significantly worse visuospatial function and letter fluency than MCI due to AD and stable MCI, as well as relatively preserved episodic memory.

In a prospective study, Yoon et al. [187] studied olfactory and neuropsychological tests at the MCI stage with the aim of differentiation MCI due to DLB from MCI due to AD at an early stage. In total 122 MCI subjects were followed-up over a mean period of 4.9 years (range: 3.9-6.2 years), 32 developed AD dementia, 18 developed DLB, 35 remained with MCI and 8 developed non-AD/DLB

dementia. The mean scores on olfactory testing were significantly lower in MCI-LB compared with MCI-AD and MCI-Stable patients. Subjects with MCI-LB had worse performance on frontal executive and visuospatial function compared to MCI-stable and MCI-AD. The MCI-LB patients had higher UPDRS motor scores than MCI-AD patients (4.5 vs 1.3, respectively $p<0.005$) as well as more frequent RBD (RBD; 66.7% vs 6.2%, respectively; $p<0.05$). The MCI-LB had more frequent parkinsonism (77.7% vs 12.5%, respectively; $p<0.05$), visual hallucinations (38.9% vs 6.2%, respectively; $p<0.05$) and more fluctuating cognition (22.2% vs 3.1%, respectively; $p=0.032$).

Donaghy et al. explored the presence of symptoms associated with LB disease in MCI-LB compared to MCI-AD, as well as in DLB and AD dementia, using an interview-based questionnaire [188]. Symptoms that were significantly more common in both MCI-LB than MCI-AD, and in DLB than AD dementia, were fluctuating attention and concentration (39% vs 10%), unexplained episodes of confusion (28% vs 0%), rigidity or stiffness in muscles (28% vs 0%), shuffling walk (53% vs 19%), change in handwriting (75% vs 38%), drooling (53% vs 10%), frequent falls 43% vs 11%), change in posture (67% vs 29%), weak voice (41% vs 11%), and symptoms of RBD (35% vs 0%). The earliest symptoms reported for MCI-LB was loss of sense of smell and RBD. Apathy (47% vs 19%, $p=0.03$) and excessive daytime sleepiness (56% vs 29%, $P=0.048$) were more common in MCI-LB than MCI-AD but not in DLB vs AD. A 10 symptom scale was developed by identifying symptoms that were specific (>80%) and relatively sensitive (>50%) to identify DLB compared with AD. This scale was applied to MCI groups and was found to accurately discriminate between MCI-LB and MCI-AD. The mean score of LB symptoms were higher at 4.1 ± 1.9 compared with 0.7 ± 0.7 in MCI-AD. The symptoms largely reflected cognitive fluctuations, motor parkinsonism and RBD. This study did not show that hyposmia, constipation and dizziness differentiated between MCI-LB and MCI-AD in contrast to a study by Chiba et al. [144]. However, the symptoms of 'dizziness or fainting' was different to the 'orthostatic dizziness' reported in that study. The rates of hyposmia and constipation were similar to the Chiba et al. study but the prevalence of these in MCI-AD was higher among the Donaghy et al. cohort.

The findings of these studies indicate that clinical discrimination between MCI subtypes (MCI-LB and MCI-AD) is possible at an early stage of the disease process. The exact time of onset and sequence of evolution of core features of DLB in the prodromal MCI-LB stage remains to be determined.

Furthermore, the longitudinal follow-up studies of MCI-LB will confirm rates of conversion to DLB and facilitate pathological validation of the clinical criteria used.

2.5.3 Post-mortem studies of prodromal symptoms of DLB

A number of post-mortem studies have assessed the prevalence and time of onset of core and suggestive symptoms in relation to cognitive symptoms. Jicha et al. found that neuropathologically confirmed cases of MCI-LB and MCI-AD differed clinically in their expression of LB features [189]. In this study, cognitively normal individuals aged 65 years and older were enrolled and followed up annually with cognitive testing and physical examination, as well as having agreed to brain donation. Clinical features were compared between subjects who met neuropathological criteria for neocortical DLB (n=9) versus those who met neuropathological criteria for AD (n=12). The retrospective identification of clinical features was then undertaken based on review of cases, with the presence or absence of both cognitive and non-cognitive features recorded prospectively. A total of 21 subjects were identified who progressed to a MCI stage during follow-up. Among the MCI-LB cohort (n=9), five met criteria for dementia and 4 had a diagnosis of MCI-LB at death. Among the MCI-AD group (n=12), 7 had a diagnosis of dementia and 5 MCI at death. None of the MCI-AD cases had evidence of LB pathology in any brain region examined. Parkinsonism (p=0.012) and provoked hallucinations/delirium (p=0.042) at the MCI stage were more common among the MCI-LB than the MCI-AD group. In fact, none of the pathologically confirmed MCI-AD group reported the presence of core features. In terms of cognitive dysfunction, MCI-LB cohort performed worse on phonemic fluency test and trail making tasks. In 8/9 patients with MCI developing brain pathology changes supportive of DLB had at least 1 symptom among the core features of DLB versus none of the MCI subjects developing later AD dementia.

Molano et al. reported on prospectively followed-up cases of MCI (n=8) who subsequently had autopsy confirmed DLB [190]. The MCI subtypes consisted of two with sd-MCI+na, three with md-MCI+na, and three with md-MCI+a. The cognitive domains most frequently affected were attention/executive (n=6) functioning and visuospatial (n=6) function. All four core features of DLB were present in five subjects. Visual hallucination were present in six patients, with 5/6 occurring 3 years after the onset of cognitive symptoms (range: 1-4 years). RBD was present in 6/8 subjects, with features preceding the onset of cognitive symptoms in six patients by a median of 10 years

(range: 2-47 years) and mild cognitive impairment diagnosis by 12 years (range: 2-48 years). Parkinsonism was present in 7/8; in 5 of these subjects, parkinsonism occurred at median of 3 years after onset of cognitive symptoms (range: 2-5 years). This study underscores the importance of investigating symptoms beyond cognition in prodromal DLB and suggests that RBD may be the most sensitive predictor of developing DLB. Probable DLB is usually diagnosed when dementia appears in conjunction with more than two core features and that this usually occurs 2-to-6 years after MCI is diagnosed.

Ferman et al. explored ante-mortem symptomatic differences between DLB cases with a pathological diagnosis. The DLB cases were divided into intermediate-high likelihood of DLB and no-low likelihood of DLB groups. RBD preceded the onset of dementia by an average of 6 years [191]. Parkinsonism and visual hallucinations preceded MCI by an average of 1.8 years and 2.6 years. The use of 2 of 3 core features to diagnose probable DLB had a sensitivity 85% and specificity 73%. The addition of RBD increased the sensitivity of 88% without any loss of specificity.

2.6 Neuropsychological profiles of MCI-LB

Numerous studies have reported on the neuropsychological profile of DLB. Many studies are based on later stages of the disease and some at the early stages. Various neuropsychological deficits predict conversion into defined neurodegenerative dementia syndromes. Studies to date have revealed that patients with prodromal DLB have more visuospatial and letter fluency deficits and less memory deficits [164, 192]. These findings are in line with the suggestion that impairment in non-memory domains (e.g. executive function, visuospatial abilities) is more likely to progress to DLB than sd-MCI+a cognitive impairment.

Kemp et al. explored the difference in cognitive profile between prodromal DLB and HC [164]. It found prodromal DLB had lower scores than HC in visual recognition memory, free recall, short-term memory and working memory. There was also a difference in visuoconstruction and visuoperceptual abilities. The results indicate executive, visual memory and visuoconstructive deficits occur in the very early stages of the disease. Praxis differences between prodromal DLB and HC for pantomime of tool use ($p=0.002$) or for imitation of meaningless gestures ($p=0.005$) were also found. In total, 27% of the patients had sd-MCI+na, 24.32% with md-MCI+na, 48.65% with md-

MCI+a, none had sd-MCI+a. The impairment in praxis in this study could have resulted from the visuoconstructive impairment [193].

Belden et el reported a case series of ten prodromal DLB patients consisting of patients with MCI and core features of DLB [192]. Neuropsychological evaluation showed that 6/10 had aMCI and 4/10 had naMCI. Of the 4 non-amnestic cases, 2 had single domain, 2 were multidomain. All 6 amnestic cases were multidomain. In total, executive and visuospatial impairment was noted in 9 of 10 cases. Six of the ten had progressed to DLB, both amnestic and non-amnestic MCI subtype. In terms of other core features of DLB, the following prevalence was reported; hallucinations 5/10, fluctuations 8/10, parkinsonism 9/10, RBD 4/10. Three core features were present in 5/10, 4 core features were present in 2/10, 10/10 had 2 or more core symptoms.

Visuoconstructional impairment may serve as an early marker of DLB, a reduced ability to determine the number of angles on the MMSE pentagon copy could be a marker of prodromal DLB with a specificity of 91% in the discrimination from prodromal AD [194]. However, the sensitivity for MMSE pentagon angle scoring was low at 41%, meaning that a normal performance on the test still leaves the possibility of patients developing either DLB or AD. Furthermore, the study was not prospective but retrospective - subjects were selected on the basis that they had converted to either DLB or AD after 3 years of follow-up. It is likely that the sensitivity and specificity of this method for the diagnosis of MCI-LB would be significantly reduced in a prospective study as many MCI subjects have outcomes other than developing DLB or AD. In another study which was also retrospective [157], aimed at identifying the clinical and cognitive characteristics of MCI subjects evolving to DLB (n=25) and MCI evolving to AD dementia (n=28), found that an impaired recognition of the number of angles (angle item score <4) was present in 44% of prodromal DLB patients compared with 3.7% of prodromal AD ($p<0.001$). Prodromal DLB patients had more impairment than prodromal AD patients in their speed of visual attention (Trial Making Test A, $p=0.03$), working memory (digit span backword, $p=0.001$) and executive functions (verbal fluency, $p=0.002$). Visuospatial abilities as assessed by Visual Object and Space Perception battery showed more significant visuoconstructional deficits (cube analysis subtest) and visual-attentional deficits (number location subtest) than prodromal AD patients. The sensitivity of the number of pentagon angles was low at 42% but had high specificity at 96% and a good positive predictive value at 91% and negative

predictive value of 63%. Prodromal AD showed a disproportionate involvement of long-term episodic memory, while prodromal DLB manifested a poorer verbal working memory (digit span backward) and a prominent difficulty in the speed and ease of verbal production (verbal fluency), as a consequence of more frontal/dysexecutive function. Prodromal DLB patients with a reduced number of angles on the pentagon copy task, an index of altered visuoconstructional ability, had better verbal memory immediate recall scores than DLB patients with preserved number of angles.

In a longitudinal study previously mentioned, Yoon et al. studied olfactory and neuropsychological tests at the MCI stage with the aim of differentiating MCI-LB with from MCI-AD at an early stage [187]. Subjects with MCI--LB had worse performance on frontal executive and visuospatial function compared to stable MCI and MCI-AD.

2.7 Discussion

The symptoms in DLB are likely to arise from dysfunction of a number of interacting neuronal networks. Parkinsonism is strongly associated with progressive degeneration of the nigrostriatal system which also affects frontal lobe control of executive tasks. Cognitive impairment will also arise from loss of cholinergic projections from the nucleus basalis of Meynert to the basal forebrain/limbic and neocortex. Dysfunction of attentional circuity secondary to: (1) loss of cholinergic and dopaminergic innervation (2) atrophy in the right anterior cingulate cortex and bilateral insular regions, (3) dysfunction in the default mode network, (4) thalamic cholinergic denervation [195] may contribute to cognitive fluctuations. Visual hallucinations may be related to neuronal loss in the subcortical visual structures such as the superior colliculus and pulvinar [196]. The RBD seen in DLB is likely due to LB pathology affecting cortical and brainstem sleep control structures, as DLB patients with RBD were found to be just as likely to have brainstem and limbic LBs as they were to have brainstem, limbic and neocortical LBs [42]. However, RBD was associated with lower Braak neurofibrillary tangle stage and lower neuritic plaque score among DLB subjects [42]. The presence of RBD is associated with early visual hallucinations, early parkinsonism and more cognitive decline in DLB [42]. The evolution of clinical features must reflect the topography of degeneration in neurons over time due to the presence of LB pathology on its own or with co-existent AD ((Aβ) and tau) pathology.

From the studies outlined above, there is an increasing evidence of the existence of a clinically identifiable prodromal stage of DLB where the progressive neuronal dysfunction leading to the presence of symptoms/signs is of insufficient severity to meet the diagnosis of dementia. As discussed in previous sections, the "bottom-to-top" spread of LB pathology in the Braak staging system does not explain the clinical phenotypes and evolution of symptoms/signs in DLB. In fact, Toledo et al. has shown neuropathological spread of LB pathology can be impacted upon by the presence of concomitant AD pathology [197]. In dementia subjects with both AD and LB pathology, there is a different distribution of LB pathology compared to PD subjects, with these dementia subjects having little LB pathology in the brainstem [197]. The presence of coincident AD pathology has been reported to be associated with increased LB pathology in PD [197].

A "top-to-bottom" spread of LB pathology from the neocortex/limbic system to the nigrostriatal system may better explain the onset of cognitive impairment prior to parkinsonism in many DLB cases [28]. Indeed a number of cross-sectional and retrospective studies have shown that core features of DLB are present before or at the time of memory difficulty onset and the latency between core symptom onset to probable DLB diagnosis could be up to 10 years [145]. The reported prevalence rates of core symptoms vary significantly between studies which is likely due to the heterogeneous methodology used to identify patient cohorts. However, the reported prevalence of core symptoms occurring before dementia onset, in descending order are; RBD (range 45-80%), parkinsonism (range 31-75 %), cognitive fluctuation (range 22-60 %) and visual hallucinations (range 32-39%). Two or more core symptoms are reported to occur in approximately 50% of people before developing DLB [157]. Furthermore, in a cross-sectional study by Donaghy et al. exploring the range of LB symptoms present at the MCI stage, only symptoms consistent with core features of DLB (parkinsonism, RBD and fluctuating cognition) differentiated MCI-LB from MCI-AD and not those symptoms considered to be suggestive of LB disease such as autonomic symptoms, constipation and hyposmia. A number of explanations may exist for why suggestive LB symptoms did not differ between MCI-LB and MCI-AD. Firstly, the study was undertaken in an elderly population (78.5 ± 7.6 years) who likely had co-morbidities and were taking polypharmacy which could increase the symptom prevalence in the MCI-AD group. Secondly, even some of the core symptoms are subtle and much less pronounced at the MCI stage [157], it is entirely possible that many of the suggestive features of LB become more severe and those patients become aware of them later in the disease trajectory.

At present, the medical literature is lacking prospective studies investigating the risk of progression to DLB in cohorts of MCI patients with associated LB symptoms. Prospective studies have investigated MCI cohorts progressing to dementia which were not selected based on the presence of co-existent LB symptoms [186, 187]. Another limitation of these studies is that a non-enriched MCI cohort may progress onto a number of neurodegenerative conditions such as AD, frontotemporal dementia, primary progressive aphasia, posterior cortical atrophy and corticobasal syndrome. This limitation may be ameliorated by sub-categorisation of MCI patients on the basis of neuropsychological testing impairments into amnestic and non-amnestic subtypes, with naMCI subtype more likely to have a higher rate of progressing to DLB. However, in reality any MCI subtype regardless of it being amnestic or non-amnestic, can progress on to any dementia subtype. Based on the available accumulated evidence to date one can hypothesise that 1) MCI plus RBD and/or parkinsonism is likely to reflect evolving DLB, and 2) impairments of the attention/executive and visuospatial cognitive domains on neuropsychological testing is most likely to reflect evolving DLB. Molano et al. demonstrated on neuropathological examination that all patients that had MCI (having impairments in the attention/executive, and/or visuospatial functioning domains) plus RBD had evidence reflective of LB disease throughout the brainstem and cerebrum [190]. This caused the authors to conclude that the naMCI subtype plus RBD has the potential to evolve to DLB. Clearly, large prospective case series of clinical, neuropsychological and neuropathological findings are needed to confirm this hypothesis.

2.7.1 Future directions and challenges in prodromal DLB

A number of questions need to be answered about the prodromal period in DLB. It is critical to understand when core symptoms of DLB emerge and how they evolve over the prodromal period. It is also important to know the sensitivity/specificity and positive predictive value of individual and combined numbers of core symptoms at different time points. It will be important to obtain estimations of conversion rates of MCI-LB to DLB and the latency period between symptom onset and DLB diagnosis.

In order to answer these questions, MCI-LB subjects will have to be followed-up longitudinally with a spectrum of clinical tests and potential biomarkers to assess the natural history of the disease

state. This will provide challenges in order to recruit adequate numbers so future phenoconversion will occur in sufficient numbers after accounting for drop-outs, to be able to draw statistically powerful conclusion. A sufficient latency period from symptom onset until dementia diagnosis is necessary as too long a latency until disease imposes practical challenges in the design of such study and increase rate of loss to follow-ups.

2.7.2 Limitations

A number of limitations are inherent in studies examining the pre-dementia stage of DLB and identifying the prevalence of LB symptoms. Firstly, despite the increasing number of studies in the field, the majority of the data is derived from retrospective studies and therefore may be subject to participant recall bias. Secondly, the lack of validated criteria for prodromal DLB has resulted in a heterogeneity of in enrolment criteria to studies purporting to examine the prodromal period of DLB. While the recent publication of criteria for MCI-LB should standardise research in the area, these criteria remain to be validated. Another major limitation of current research in the field of prodromal DLB is the lack of post-mortem verification of longitudinally follow-up prodromal DLB cohorts. Therefore, it is difficult to establish sensitivity, specificity, positive and negative predictive value of individual LB symptoms at the MCI stage to discriminate cognitive impairment due to underlying LB disease from other causes and to accurately predict progression to an eventual DLB diagnosis.

2.8 Conclusions

The evidence suggests that DLB has a clinically identifiable prodromal phase. The prodromal phase of DLB has distinct phenotypes and these include; (1) MCI-LB, (2), Delirium-onset, (3) psychiatric-onset. Recently, research criteria for the diagnosis of MCI-LB have been published which are similar in nature to established DLB diagnostic criteria. Probable/possible MCI-LB can be diagnosed on clinical symptoms alone or by incorporation of biomarkers in conjunction with clinical symptoms. These diagnostic criteria for MCI-LB remain to be validated by longitudinal clinical studies demonstrating phenoconversion to dementia and ultimate pathological confirmation of the diagnosis. Therefore, the sensitivity and specificity of proposed criteria for MCI-LB remains unknown. Relatively few studies have examined the ability of biomarkers to differentiate MCI-LB

from MCI-AD, in particular those listed as proposed and potential biomarkers in the MCI-LB diagnostic criteria

Chapter 3. Striatal dopaminergic imaging in DLB

3.1 Introduction

DLB is a neurodegenerative disorder in which dopaminergic nigrostriatal pathway degeneration is a key component. Early clinical diagnosis is challenging as many individuals with DLB will manifest some but not all of the core features of the condition, and many of symptoms/signs are only subtly present at the early stages resulting in difficulty in distinguishing the condition from other causes of dementia, especially AD. The ultimate determination of the aetiology of a dementia can only be established by neuropathological findings at post-mortem. Unfortunately, poor clinico-pathological correlation has been shown [8] suggesting that while core clinical features of DLB are specific for the condition they are not sensitive and cases of DLB are often misdiagnosed early on or missed altogether [5]. Comparisons of pathological and clinical findings suggest that the typical DLB clinical syndrome is seen most clearly in people with 'pure' DLB pathology. In contrast, DLB subjects who also have significant AD pathology, in particular tau pathology, are found to have an attenuated clinical syndrome that is harder to recognise ante-mortem [198]. Moreover, core features such as visual hallucinations and parkinsonian motor symptoms, may occur in a subtle form in the early stages and may also occur in other forms of dementia at the moderate to severe stages. This means that there is some considerable difficulty in distinguishing between dementia subtypes in their early stages on the basis of clinical criteria alone and to accurately attribute LB pathology as the aetiological agent for the cognitive decline.

The inherent limitations of clinical diagnosis means that an in-vivo biomarker for DLB would be extremely useful to support the diagnosis as well as potentially improve future clinical prognoses. The characteristics of an ideal biomarker are an ability to objectively measure and evaluate *in vivo* biological processes that can serve as "an indicator of normal biological processes, pathogenic processes or pharmacological response to a therapeutic intervention" [199]. Imaging the degeneration or loss of function of the dopaminergic nigrostriatal pathway differentiates parkinsonian syndromes (DLB, PD, MSA and PSP) from other degenerative syndromes without dopamine deficiency such as AD provides a strong biomarker target for LB disorders. The *in-vivo* functional integrity of the dopaminergic nigrostriatal pathway can be studied with ^{123}I-FP-CIT SPECT a marker of pre-synaptic dopamine transporter protein (DAT) availability in part of the brain known as the striatum. PET markers of dopamine storage capacity (^{18}F-dopa) and vesicle monoamine

transporter binding ($^{11}C/^{18}F$-DTBZ) and dopamine transporter binding (^{18}F-FP-CIT) also exist. The majority of research to date has utilised ^{123}I-FP-CIT SPECT to investigate dopaminergic nigrostriatal integrity as an indirect measure of underlying LB pathology rather that PET imaging as it is widely available. Importantly, ^{123}I-FP-CIT is also the only imaging technique clinically licensed for use in differentiating between AD and DLB [200, 201]. A reduction of ligand binding to striatal DAT ante-mortem is associated with loss of nigral neurones at post mortem in DLB and animal lesion models of PD. Reduced DAT uptake in the basal ganglia as demonstrated by SPECT or PET is an indicative biomarker supporting the diagnosis of DLB in the fourth consensus criteria, as well as being a proposed biomarker for MCI-LB diagnosis in the recently published research criteria of MCI-LB [7, 9].

The aim of this chapter is to summarise the findings of studies utilising presynaptic dopaminergic imaging, predominately ^{123}I-FP-CIT SPECT imaging, to differentiate DLB from other dementia subtypes and that examine the correlation between imaging findings and clinical symptomology. This chapter will also review the limited literature on dopaminergic imaging in prodromal DLB.

3.2 The nigrostriatal pathway and dopaminergic system evaluation

The core pathway underlying dopaminergic neurotransmission deficits in DLB is the pathway of projections from the substantia nigra pars compacta, a midbrain nucleus with melanin pigmented dopaminergic neurons, which synapse with GABA spiny neurons in the striatum. This pathway is known as nigrostriatal pathway, stretching from the midbrain into the striatum. The presynaptic nigrostriatal dopaminergic neuron terminals highly express the dopamine transporter protein (DAT) which is a sodium chloride-dependent transmembrane protein [202]. DAT plays a critical role in controlling the regulation of synaptic dopamine levels by removing dopamine from the synaptic cleft and into the presynaptic nerve ending [203]. DAT concentration closely relates to striatal dopamine levels [204]. DAT density can be measured *in vivo* by using tropane radioligands which bind with nanomolar affinity but also bind less tightly to noradrenergic and seronergic transporters in the brainstem [201]. Degeneration of dopaminergic nigrostriatal neurons leads to reduced binding of striatal ^{123}I-FP-CIT and the decreased uptake of ^{123}I-FP-CIT correlates with DAT density [205]. By the time, patients with parkinsonism are diagnosed clinically, dopaminergic imaging indicates 30-60% of dopamine terminal transporters are lost [206]. There is also evidence that striatal dopaminergic

deficits can be detected in many cases of the prodromal α-synucleinopathy RBD ahead of development of clinical parkinsonism, but the dopaminergic deficit is less pronounced than in overt parkinsonism [146, 207]. In RBD, the extent of baseline dopaminergic deficit predicts risk of conversion to DLB/PD, a 25% reduction in ^{123}I-FP-CIT uptake in the putamen at baseline predicting conversion to DLB/PD/MSA within a 3 year follow-up [149]. The precise time interval between the onset of substantia nigra neuronal loss and development of parkinsonism is not known.

3.3 Functional Imaging of the nigrostriatal dopaminergic pathway

In vivo assessment of the nigrostriatal dopaminergic system can be conducted by molecular imaging techniques investigating the availability of pre-synaptic DAT using either PET or SPECT. The PET and SPECT radioligands currently available for measuring the availability of DAT binding are relatively non-selective also binding to noradrenaline, and serotonin transporters with a similar or lower nanomolar affinity [208]. SPECT is more advantageous to use than PET in a clinical setting as it does not require complex and expensive infrastructure and has commercially available radioligands and ^{123}I-FP-CIT SPECT is available generally in the UK. The majority of the reported molecular imaging studies in DLB have been SPECT studies, hence the main focus of this chapter will be based around SPECT imaging.

Several radioligands have been developed for use in SPECT imaging to bind to the striatal presynaptic DAT. These include [^{123}I]-2β-carbomethoxy-3β-(4-iodophenyl) tropane (^{123}I-β-CIT), ^{123}I-altropane, [^{123}I] N-w-flouropropyl-2β-carbomethoxy-3β-(4-iodophenyl) nortropane (^{123}I-FP-CIT) and the technectium based tropane tracer, ^{99m}Tc-TRODAT-1. ^{123}I-FP-CIT is the most widely used radioligand to assess the integrity of presynaptic dopaminergic nigrostriatal neurons as it possesses characteristics which make it ideal for clinical use [209]. ^{123}I FP-CIT is a ^{123}I-labeled tracer that binds with high affinity to DAT. It also has high specific binding to the striatum relative to the cerebellum which is used as a reference tissue for non-specific uptake. Diagnostic imaging can be performed after an interval of 3-4 hours following intravenous injection of ^{123}I-FP-CIT. The tracer ^{123}I-β-CIT takes up to 24 hours to equilibrate throughout the brain following its intravenous injection while ^{99m}Tc-TRODAT-1 and ^{123}I-altropane give low specific signals. ^{123}I-FP-CIT was first approved for use in the European Union in 2000 and in the United States of America by the Food and Drug Administration in 2011 under the trade name DaTscan. In 2005, imaging of the DAT with SPECT was

added to the diagnostic criteria for DLB as a suggestive feature, with diagnostic weight [38]. The latest consensus criteria include ^{123}I-FP-CIT SPECT among the indicative biomarkers of DLB as well MCI-LB, thereby giving presynaptic dopaminergic imaging a high level of importance in guiding diagnosis of DLB and MCI-LB [7, 9]. It's important to note that availability of ^{123}I-FP-CIT varies internationally, with some countries having no access such as Korea and Australia where ^{18}F-FP-CIT PET is used. Moreover, in countries where there is availability, the utilisation of ^{123}I-FP-CIT SPECT varies with some services being more likely to refer for imaging in order to support a diagnosis and this may be a contributing factor to the variation in diagnostic prevalence of DLB within countries [5].

3.4 Assessment of ^{123}I-FP-CIT images

3.4.1 Visual assessment

Visual assessment of ^{123}FP-CIT SPECT by a nuclear medicine expert is the generally accepted method of determining the extent of *in vivo* nigrostriatal dopaminergic denervation. Interpretation of imaging relies on assessment of striatal distribution of activity and comparing of both left and right striatal uptake to ascertain whether there is asymmetric radioligand uptake. The ^{123}I-FP-CIT uptake gradient between the caudate and the putamen, and the degree of reduction needs to be taken into account with the clinical context as well. In normal controls, striatal uptake should appear as "comma-shaped" indicative of similar radioligand uptake in both the dorsal putamen and head of caudate. In contrast parkinsonian conditions are characterised by more pronounced anterior-posterior asymmetry, the putamen shows greater signal reduction than the head of caudate nucleus, and visually this is noted by progressive loss of the comma shaped tail. The ^{123}I-FP-CIT SPECT can be then classified broadly as normal or abnormal by visual interpretation based on the striatal activity. The side with relatively lower uptake is contralateral to the clinically more affected limb. Clinical reporting of ^{123}I-FP-CIT SPECT scans in DLB are conducted using visual assessment though semi-quantification is increasingly used as an adjunct as it is more accurate where doubt exists. Visual rating is primarily conducted using a scale introduced by Benamer which has been validated in PD [210]. The application of the Benamer scale to the ^{123}I-FP-CIT scans of DLB results in a number of shortcomings, particularly the lack of a category for symmetrical global reduction which is more common in DLB [211, 212].

Visual assessment is limited by a number of factors related to the observer interpretation of the images and the patient's positioning within the scanner. Observer interpretation of the scan depends on their level of expertise and shows inter- and intra-observer variability. Furthermore, subtle anatomical variation and head tilt may result in slight asymmetry being misinterpreted as pathologically reduced uptake. Patient positioning and motion within the scanner may result in variability in the recorded images. Therefore, in "borderline cases" when visually it is difficult to differentiate between normal and abnormal scans, quantitative assessment is essential to increase diagnostic confidence and provide an objective numerical value in addition to the visual interpretation.

3.4.2 Semi-quantitative assessment

Semi-quantitative SPECT analysis provides an estimate of tracer uptake by the dopaminergic transporters in the nigrostriatal pathway terminals which may be performed *in vivo* using a ratio approach whereas absolute quantification is a direct determination of dopaminergic neurons in the striatum which is very difficult to achieve *in vivo* but may be conducted at post-mortem. The ratio of striatal:cerebellar ^{123}I-FP-CIT uptake at 3-4 hours is not an accurate determination of dopaminergic neurons in the nigra which may only be conducted at post-mortem but correlates well with this measure. There are a number of semi-quantitative methods available to allow for unbiased assessment of uptake in the striatum and these have been incorporated into commercially available software packages. In the UK, semi-quantitative methods are being used in conjunction with visual ratings in the clinical assessment of ^{123}I-FP-CIT SPECT [213]. Semi-quantification of ^{123}I-FP-CIT SPECT images as an adjunct to visual assessment can improve sensitivity and diagnostic accuracy [214]. The analytical approach calculates striatal binding ratios (SBR) from regions of interest applied to the SPECT volume after automated registration to a chosen template and calculates the ratio of specific and non-specific uptake in the striatum to the nonspecific binding in the cerebellum or occipital lobe as the reference region. The patient's results are then compared with a group of 'normal' patients, which should be age-matched according to the European Association of Nuclear Medicine guidelines [215]. Z scores are then generated to determine the number of standard deviations a subject's SBR is different from an HC mean SBR. Abnormal Z scores are usually greater than two standard deviations below the mean SBR for HC. However, striatal uptake is thought to decline with age [216]. Therefore, it is necessary to compare patient's SBRs against age-matched HC and the means by which commercial quantitative software achieves this age correction varies, with

controls over 60 years of age being underrepresented [84]. In order to better determine changes in SBRs with age, some institutions have been able to put together small local databases to extrapolate for what constitutes age-matched uptake. The advantages of semi-quantitative methods include lower inter- and intra-observer variability thus improving reporting performance and improved diagnostic confidence with a reduction in the reporting of equivocal scans. Furthermore, semi-quantification software offers the possibility of monitoring disease progression by measuring change over time. Several studies have suggested that the addition of semi-quantification can improve reporting performance, particularly in terms of reduced equivocal reporting rates and improved inter-observer variability [217, 218].

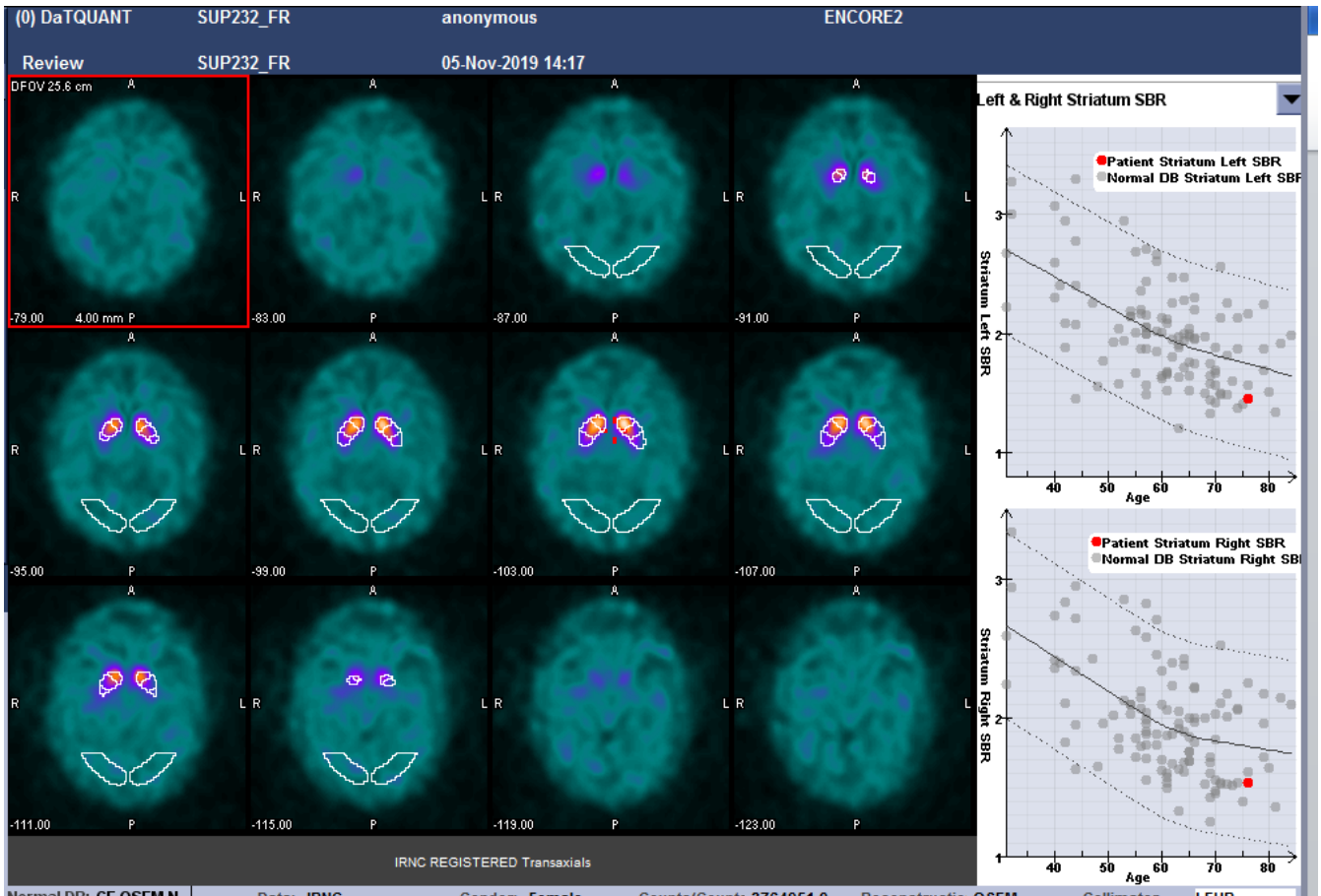

	Striatum Right SBR	Striatum Left SBR	Putamen Right SBR	Putamen Left SBR	Caudatus Right SBR	Caudatus Left SBR
Measured	+1.53	+1.46	+1.32	+1.17	+2.02	+2.03
Mean (±1 SD)	+1.80 (±0.33)	+1.75 (±0.35)	+1.70 (±0.33)	+1.64 (±0.35)	+2.02 (±0.40)	+1.96 (±0.42)
Deviation	-15%	-17%	-23%	-29%	+0%	+4%
Z-Score	-0.80	-0.82	-1.18	-1.37	+0.02	+0.18

Figure 3. 1 Results screen for semi-quantitative ^{123}I-FP-CIT analysis using the commercial software package DaTQUANT.

3.5 Patterns of dopaminergic loss in DLB on ^{123}I-FP-CIT SPECT

Dopaminergic deficits are commonly demonstrated on ^{123}I-FP-CIT SPECT imaging in DLB but the pattern of decreased binding is variable in the striatum. Indeed, it is possible to have a normal ^{123}I-FP-CIT SPECT but still fulfill diagnostic criteria for DLB [7]. It is well established in AD that degeneration of the nigrostriatal pathway does not occur and therefore an abnormal ^{123}I-FP-CIT SPECT scan regardless of any pattern of dopaminergic loss is useful for differentiating DLB from AD. It must be remembered that there are other dementia syndromes associated with parkinsonism

(PDD, CBD and PSP) that also have abnormal ^{123}I-FP-CIT SPECT and therefore cannot be differentiated from each other on the basis of SPECT imaging alone but instead require careful clinical phenotyping and MRI sequences such as diffusion tensor imaging to help distinguish them. Although, all these parkinsonian conditions have significant overlap in terms of patterns of dopaminergic loss on ^{123}I-FP-CIT SPECT imaging, DLB does display some difference on a group level in the predilection for diminished DAT availability in the striatum in comparison with PD. In PD, there tends to be an asymmetric pattern of dopaminergic loss targeting putamen tracer uptake, particularly affecting the posterior subregion, on the side contralateral to clinical motor signs. There is also a rostro-caudal (caudate-to-putamen) gradient of dopaminergic loss in the early stages of PD diagnosis. Eventually, dopaminergic nigrostriatal denervation progresses to involve both putamina and with time leads to a decline in the rostro-caudal gradient. In contrast, if there is a dopaminergic deficit present at the early stages in DLB, it tends to be more symmetrical and have a flatter rostro-caudal gradient, with a reduced caudate-to-putamen ratio [75, 211, 212, 219]. This would be in keeping with the clinical phenotype observed among patients with DLB of a predominantly symmetrical parkinsonian syndrome in DLB compared to PD. A study by O'Brien et al. [212], examining the amount and pattern of DAT loss in DLB (n=23) compared with PD (n=38) and other dementias (AD n=34, PDD=36), showed that DLB had a similar extent of dopaminergic loss to that seen in PD but also had a flatter caudate-to-putamen gradient than PD (P=0.001). The regional difference in DAT uptake between DLB and PD therefore indicates that DLB has a trend towards lower DAT uptake in the caudate and may display dopaminergic deficits in both the caudate and putamen. The exact clinical significance of early reduced caudate uptake on ^{123}I-FP-CIT SPECT imaging remains unknown. Furthermore, the progression of dopaminergic loss appears to be more severe in DLB than PD, with more rapid and more severe loss of striatal DAT in DLB compared to PD [220]. The results of these studies indicate that basal ganglia pathology has a different distribution in DLB and PD patients. In DLB, the complex and poorly understood interactions between multifactorial pathology could affect the nigrostriatal connections without affecting DAT binding. Other factors may impact on the degree of dopaminergic loss, a subgroup of DLB patients with RBD may have lower DAT binding in the striatum, putamen and caudate nucleus [74]. Longitudinal studies of early cases of DLB are needed for better understanding of the course of loss of striatal DAT function in DLB and will help to elucidate the significance of dopaminergic deficits in the evolution of clinical phenotypes.

3.6 Monitoring nigrostriatal pathway degeneration with DAT imaging

Striatal DAT imaging is a potential biomarker to objectively monitor progressive dopaminergic loss and predict clinical disease evolution *in-vivo*. Previous studies have indicated the ability of dopaminergic SPECT imaging to detect nigrostriatal degeneration in advance of manifestation of clinical features. Subjects who have a positive ^{123}I-FP-CIT SPECT but do not have clinical DLB features, tend to develop clinical DLB features overtime - in particular parkinsonism and cognitive fluctuations - and, therefore, represent a clinically undetectable early stage of DLB [221]. Siepel et al. longitudinally followed-up 7 subjects who had evidence of an abnormal ^{123}I-FP-CIT imaging but absent core features for between 2-5 years [221]. All of these subjects developed Parkinsonism and cognitive fluctuations consistent with a diagnosis of DLB. The findings of this study is consistent with other published work which would indicate a potential role of ^{123}I-FP-CIT SPECT imaging to detect clinical disease progression in DLB. A study by O'Brien et al., examining the outcomes of patients with a diagnosis of "possible DLB", but not fulfilling criteria for probable DLB, showed that ^{123}I-FP-CIT SPECT differentiated between those who developed probable DLB from those who did not after 1 year [222]. A similar picture has been seen in other LB disorders such as PD where at-risk asymptomatic subjects with GBA and LRRK2 mutations have shown reduced striatal signal with (^{123}I) FP-CIT SPECT ahead of the onset of motor signs and this mismatch can be seen present years beforehand [223]. The clinical threshold of approximately 50-80% of striatal dopaminergic neurons needs to be lost before the onset of motor dysfunction in PD [224].

Despite a number of studies indicating that abnormal DAT imaging can predict future development of LB symptoms, there has been relatively limited number of studies exploring the utility of serial ^{123}I-FP-CIT SPECT imaging. Specifically, whether the annual percentage decline in DAT uptake is greater in DLB and can be used as a diagnostic or prognostic biomarker for the development of LB features. In the following sections, the findings from studies using serial DAT imaging in PD, DLB and RBD are discussed and Table 3.1 summarises the results of these studies.

3.6.1 Healthy controls

Age is an important factor to take into consideration when evaluating the utility of ^{123}I-FP-CIT SPECT imaging to monitor progressive decrease in DAT binding in the striatum. Studies in HC have consistently demonstrated that striatal uptake levels decrease with age [216]. The exact annual

percentage decline in SBR and whether it's a linear decline across all age ranges is still a matter of debate. Based on the best available evidence, it would indicate that there is decline per decade in SBR of between 4-8% [225-228]. However, most of these studies recruited healthy adults of varying age ranges, for instance the ENC-DAT study, a large European study examining this question recruited 139 adults ranged between 20-83 years [227]. When older healthy adults only are examined, there appears to be a tailing off in older age [229]. Further published work by my colleague Roberts et al. in Newcastle, would also indicate any decrease in SBR in older healthy adults between 70-80 years appears to very small and ranges between -7 to +3% [84]. This work highlights the need to ensure that any longitudinal assessment of ^{123}I-FP-CIT in a followed-up dementia cohort also requires an appropriately age-matched heathy control group for longitudinal follow-up as well.

3.6.2 DLB cohorts

In early clinically probable DLB, initial imaging may indicate a negative or intermediate ^{123}I-FP-CIT SPECT and on subsequent future repeat imaging the ^{123}I-FP-CT SPECT becomes abnormal [71]. There is a lack of knowledge about the optimal time to wait in order to repeat the ^{123}I-FP-CIT SPECT imaging. If the imaging is repeated too early, the repeat DAT imaging may remain negative and the clinician is left with the dilemma of suspecting an evolving LB disorder but having repeated the imaging too soon for any detectable meaningful decline in DAT uptake to have occurred. Unfortunately, there is a paucity of research into the rate of decline in uptake of ^{123}I-FP-CIT in DLB and whether the rate of decline in DAT uptake can be utilised as a biomarker to distinguish DLB from AD at the early stages. A study by Colloby et al. [68], examined the rate of progression of nigrostriatal dopaminergic loss in subjects with DLB (n=20 (17 probable DLB and 3 possible DLB), PD (n=20), PDD (n=15) and HC (n=22) using serial ^{123}I-FP-CIT SPECT, with subjects undergoing a baseline and one repeat scan. Images were analysed using the semi-automated region of interest. The mean interval between scans were; HC: 1.04 years (SD 0.07), DLB: 1.06 years (SD 0.10), PD: 1.05 years (SD 0.12), PDD: 1.06 years (SD 0.009). The mean annual percentage decline in ^{123}I-FP-CIT imaging in DLB was; caudate -12.7% (SD 28.1), anterior putamen -13.0% (SD 17.8), posterior putamen -9.1% (SD 28.3). Although, the differences were significant between patients and HC, there was no difference in the rate of decline between DLB, PD and PDD.

Approximately 5-10% of patients with clinical dementia have an intermediate ^{123}I-FP-CIT SPECT scans, that is abnormal DAT binding but not as low as typical of DLB [221]. There has been only one study to date which has examined the question of the outcomes of normal ^{123}I-FP-CIT imaging in a DLB cohort. This was a longitudinal study by Van der Zande et al., who found at baseline 7/67 (10.4%) of patients had clinically probable DLB but normal ^{123}I-FP-CIT SPECT imaging [71]. A further repeat ^{123}I-FP-CIT SPECT was conducted in 5/7 of these subjects on average 1.5 years later (range: 9-38 months), and all of these were abnormal. The results of this study demonstrate that striatal DAT imaging can be normal in some DLB patients, who may develop a significant nigrostriatal dopaminergic deficit later in the course of the disease. The authors of this study concluded that those patients with clinically probable DLB, an initial normal ^{123}I-FP-CIT SPECT may represent a distinct DLB subtype ("neocortical predominant subtype") suggestive of a "top-to-bottom" spread of α-synuclein. The results of this study indicate that ^{123}I-FP-CIT SPECT imaging would become abnormal in a proportion of clinically probable DLB with an initial normal imaging after an interval between scans. However, it remains to be determined the optimal time point to repeat ^{123}I-FP-CIT SPECT imaging. The fate of patients with a clinically possible or probable DLB diagnosis but an initial negative ^{123}I-FP-CIT SPECT remains unclear. The best clinical course of action in such a context is unsupported by evidence at present and the diagnostic yield from repeating ^{123}I-FP-CIT SPECT at 1 or 2 years post initial scan is still not known.

3.6.3 PD cohorts

A number of studies have used serial SPECT or PET as an objective biomarker to monitor the rate of decline in tracer uptake over time. These have been predominately clinical trials in PD which used the difference in the rate of change of striatal DAT uptake as an outcome measure to investigate the possible neuroprotective effects of various agents. In general, the PET studies were largely conducted around the turn of this century and showed variable rates of annual percentage decline with the putamen experiencing a greater annual decline than the caudate, the reported range is as follows; -3.5% to -12.5% in caudate and -8.9% to -13.1% in putamen [230-233] and -5.3% in the whole striatum [230]. Similar annual percentage rates of decline have been observed using SPECT, with the range of annual percentage decline in the caudate ranging from -4.6% to -11.0% and in the putamen -6.0% to 10.0% [234-236]. There is suggestion from some of the clinical trials in PD that levodopa ingestion may result in a greater percentage decline in DAT uptake over the long term

[234, 236]. The following paragraphs detail the findings from the main studies investigating the rate of striatal DAT uptake in PD over time.

The CALM-PD study was a large study assessing if the percentage loss of striatal ^{123}I-β-CIT differed between PD patients treated with levodopa or the dopamine agonist pramipexole [236]. Eighty-two PD patients were recruited and had serial ^{123}I-β-CIT at baseline, 22 months, 34 months and 46 months. The mean percentage loss from baseline of ^{123}I-β-CIT uptake to 46 months, in the whole 82 patients, was greater in the putamen 22.5% (19.5) than in the caudate 19.6% (13.6), which is approximately equivalent to whole striatum decline of 5.2% per year. Although the PD patients demonstrated a greater baseline reduction in the side contralateral to initial motors symptoms, the progressive loss of ^{123}I-β-CIT uptake in each hemi-striatum did not differ between the affected and unaffected side. Those treated initially with levodopa showed a significantly greater decline in striatal ^{123}I-β-CIT uptake from baseline compared to the group treated initially with pramipexole despite the initial ^{123}I-β-CIT uptake being similar between the two groups and random allocation to either of the two treatment groups. The mean (SD) percentage loss from baseline of ^{123}I-β-CIT striatal uptake in the pramipexole vs levodopa groups was 16.0% (13.3) vs 25.5% (14.1) at 46 months (P=0.01). Another study also showed increase loss of striatal ^{123}I-β-CIT uptake between baseline and week 40 with increasing dose of levodopa. This study showed percentage loss in striatal uptake from baseline to re-imaging at 40 weeks to be less among the group taking placebo -2.6% (SD: 11.3) and to progressively worsen with increasing doses of levodopa (150mg/day: -4.7% (SD: 10.8), 300mg/day: -3.7% (SD: 9.1), 600mg/day -6.9% (SD: 8.1)) [234]. The larger loss of DAT binding with levodopa has never been adequately explained and could be reflective of an adaptive neurobiological response leading to a downregulation of the presynaptic DAT resulting from chronic exposure to levodopa or indicator of levodopa toxicity. However, it is unlikely to be levodopa toxicity as the UPDRS scores were better in the levodopa group than the pramipexole group in the CALM-PD. The reason for the discordance between imaging and clinical findings remains unexplained.

There is evidence to suggest that the lower baseline DAT uptake in PD and the rate of decline in DAT uptake in PD affects the phenotype of the disease. Jeong et al. investigated whether the changes in ^{123}I-FP-CIT uptake at baseline, 1 year, 2 years and 4 years had an impact on the development of levodopa-induced dyskinesia (LID) in PD [235]. The percentage change in putaminal SBRs from

baseline was significantly greater at 24 months (PD with LID 36.4% vs 27% PD without LID, $p<0.05$) and 48 months (PD with LID 50.4% vs 38.4% PD without LID, $p<0.01$) in PD patients with LID compared to those without LID despite having similar symptom duration. There was no difference between the PD with LID compared to those without LID at 12 months (PD with LID 23.6% vs 22.2% PD without LID, $p=0.65$). The results of this study indicate a greater deterioration rate in nigrostriatal dopaminergic innervation can have an impact of the motor phenotype in PD, with more aggressive dopaminergic denervation associated with LID. The other interesting thing to note from this study, is that there appears to be a thresholding affect to the percentage reduction in putaminal uptake, with approximately 50% of the total percentage decline in both PD with LID and without LID occurring within 12 months. This is not the only study to suggest that the reduction in striatal DAT uptake may be more severe in the early rather than late stage of PD. Pirker et al. showed that the rates of decline in the striatum on repeat ^{123}I-β-CIT imaging are greater in short duration PD (-7.1% decline) (mean disease duration 2.4 ± 1.5 yrs, mean age 58 yrs) compared with long duration PD (-2.4% decline) (mean disease duration 9.2 ± 2.6 yrs, mean age 65yrs) [237]. This study also examined the rates of decline in atypical parkinsonian syndromes and showed more rapid decline of striatal ^{123}I-β-CIT binding in atypical parkinsonian syndromes (mean disease duration 2.1 ± 1.5 yrs, mean age 62 yrs) (-14.9% ± 7.0) compared to PD (9.6% ± 5.1), again this would accord with the faster clinical deterioration in atypical parkinsonian syndromes. Pirker et al. then followed up the PD patients of short duration since diagnosis (mean disease duration 2.4 ± 1.5 yrs) and had them undertake a further imaging, so that difference from baseline to first repeat imaging was, 26 ± 11 months and from first repeat scan to second repeat scan was 38 ± 15 months [238]. The annual rate of decline of striatal ^{123}I-β-CIT binding did not differ between baseline and first repeat scan and first and second repeat scan; mean striatum yearly decline between baseline and first repeat was -7.5% (± 7.5%) vs -5.6 (± 4.6%) per year from first to second repeat scan. Therefore there is some conflicting evidence on longitudinal DAT imaging studies, some of which suggest a relatively rapid decline of dopaminergic function in early PD, followed by a slowing in the rate of DAT uptake loss in later stages of the disease. Meanwhile, other studies showing a consistent rate of decline in DAT uptake over time regardless of the stage of PD diagnosis. Whether the rate of decline in DAT uptake predicts clinical phenotype in DLB remains unknown and no studies have study have addressed this hypothesis yet.

3.6.4 Prodromal synucleinopathies (IRBD & Hyposmia)

There are number of studies which indicate that reduced striatal uptake on baseline imaging in IBD is predictive of quicker phenoconversion to an overt synucleinopathy [149, 207, 239]. A study by Iranzo et al. [149], in 87 polysomnography-confirmed IRBD patients demonstrated that an abnormal ^{123}I-FP-CIT SPECT was present in 59% (n=51) and 28.7% (n=25) IRBD patients developed an α-synucleinopathy (PD in 11, DLB in 13, MSA in 1) in 3.2 ± 1.9 years from imaging. Receiver operating characteristics curve revealed that a reduction of ^{123}I-FP-CIT uptake in putamen greater than 25% from the mean of normal control value discriminated patients with DAT deficit who developed an α-synucleinopathy from those who did not.

Serial ^{123}I-FP-CIT SPECT imaging has only been used to monitor changes over time in striatal tracer binding in one IRBD study [240]. In this prospective study Iranzo et al. [240], examined serial DAT imaging in 20 IRBD patients (mean age 71 years) at baseline, 1.5 years and 3 years as well as in 20 age matched HC at baseline and 3 years. They found the mean reduction in ^{123}I-FP-CIT binding from baseline to 3 years was substantially greater in IRBD patients than in age-matched HC across all striatal regions except the right caudate. The change in striatal ^{123}I-FP-CIT uptake from baseline to 3 years between IRBD patients and HC were as follows; left putamen (IRBD 19.36% vs 9.6% HC), left putamen (IRBD 15.57% vs 10.13% HC), left caudate (IRBD 10.81% vs 2.74% HC), right caudate (IRBD 7.14% vs 11.31% HC). This is roughly equivalent to a 6% decline in putaminal binding per year in the IRBD cohort. Interestingly, in the 3/20 IRBD subjects who converted to PD within 3 years, the rate of decline in $^{123-}$I-FP-CIT uptake in the putamen was greater in these patients at approximately 10% per year. The other important finding from this study was the percentage change from baseline to 3 years did not differ in any striatal region between the IRBD patients with normal ^{123}I-FP-CIT uptake at baseline versus those IRBD patients with reduced ^{123}I-FP-CIT uptake at baseline. It should be noted that the rate of decline of striatal tracer uptake in HC was quite high - approximately 8% over 3 years - in excess of the previously reported 4-8% per decade. In summary, the overall value of this study is in demonstrating that there is a progressive decline in striatal tracer uptake consistent with progressive neurodegeneration affecting the nigrostriatal pathway in this prodromal α-synucleinopathy phenotype.

Serial DAT imaging has also been conducted on other prodromal PD cohorts recruited on the basis of having hyposmia and dopamine deficiency. Jennings et al., in the Parkinson Associated Risk Study [241], examined the decline of DAT uptake over a 4 year period by scanning a hyposmic cohort with ^{123}I-β-CIT SPECT at baseline, 2 years and 4 years. In total, 185 hyposmic individuals were recruited (mean age 64.5 years) and 11.4% (n=21) had abnormal DAT imaging at baseline (defined as 65% or less of age-expected lowest putamen binding ratio). Over 4 years of follow-up 14/21 (67%) prodromal PD cases with baseline abnormal DAT imaging converted to PD, compared with 2/22 (9%) cases with indeterminate range DAT at baseline and 3/109 (2.8%) with no DAT deficit. They found that hyposmic individuals with a baseline DAT deficit experienced a 4 year decline of 20.2% (SD 15.0%) in DAT uptake from baseline, so approximately 5% decline per year. Interestingly, the 5% yearly decline in DAT imaging is similar to the yearly percentage decline in IRBD [240]. Meanwhile, the indeterminate DAT and no baseline DAT deficit group experienced a 3.7% (SD 18.4%) and 5.5% (SD 13.6%) decline over a 4 year period. Of note in this study, parkinsonian syndromes (i.e., PSP, MSA, CBD, and DLB) were included in the definition of conversion to PD due to the difficulty in distinguishing them apart at the early stage. However, when clinically characterised the conversion was largely to idiopathic PD, with only 1 individual diagnosed as having dementia with Lewy bodies of the 19 who converted, moreover only 4 (21% of converters) had any cognitive impairment.

Study	Year	Ligand (PET/SPECT)	Group	Findings of annual rate of decline
Chouker et al. *[242]*	2001	123I-IPT SPECT	PD (n=8) Repeat 123I-IPT at baseline, 1 and 2 years	Specific striatal IPT binding decreased by a mean of 6.6% in the first year and another 5.3% in the second year. Similar changes over time in both caudate and putamen
Marek et al. *[243]*	2001	123I-β-CIT SPECT	Early PD (n=32) underwent repeat imaging during 1- to 4-year period.	Annual percentage decline of 11.2%, 11% and 10% in striatum, caudate and putamen respectively. Annual decline did not correlate with the annual loss in measures of clinical function.
Morrish et al. *[230]*	1998	18F-FDOPA	PD (n=32) repeat imaging at a mean of 18 months apart	Annual rate of decline in 18F-FDOPA up was 5.3%, 3.5% and 8.9% in striatum, caudate and putamen respectively
Nurmi et al. *[232]*	2000	18F-CFT	Early PD (n=8) HC (n=7)	Annual decline in caudate was 12.5% and in the putamen was 13.1% compared with controls who had a decline of 2.9% in the caudate and 2.1% the putamen
Nurmi et al. *[233]*	2001	18F-FDOPA	PD (n=21)	5.9%, 8.3% and 10.3% in caudate and anterior and posterior putamen respectively
Nurmi et al. *[231]*	2003	18F-CFT	Early PD (n=12)	8.0% in caudate, 11.9% and 12.1% in anterior and posterior putamen
Pirker et al. *[237]*	2002	123I-β-CIT SPECT	Early PD (n=24) Late PD (n=12)	Early stage PD annual decline was 7.1% in the striatum compared with 2.4% in striatum for early and last stage PD respectively atypical parkinsonism 14.9%
Pirker et al. *[238]*	2003	123I-β-CIT SPECT	Early PD (n=24)	Striatal uptake decline measured over a 5-year period was on average 6.6% per year
Staffen et al. *[244]*	2000	123I-β-CIT SPECT	PD (n=15) HC (n=11) Mean interval between imaging 15 months.	Decrease in DAT binding dependent on the initial clinical stage. 6.8%, 6.1% and 1.25% for Hoehn and Yahr stages I, II and III respectively
Winogrodzka et al. *[245]*	2003	123I-β-CIT SPECT	Early PD (n=50) Imaging completed 12 months apart	Annual % decline of 8% in the striatum, 8% in the putamen and 4% in the caudate.

Colloby et al. *[68]*	2003	123I-FP-CIT SPECT	HC (n=22) DLB (n= 20) PD (n=20) PDD (n=15)	Rates of decline were similar between DLB, PD and PDD. DLB annual decline in caudate was 12.7%, anterior putamen 13%, posterior putamen 9.1%. PDs annual rate of decline in the caudate 11.4%, anterior putamen 5.2%, posterior putamen 12.9% PDD annual rate of decline in caudate 40.7%, anterior putamen 17.1%, posterior putamen 7.1%.
Van der Zande et al. *[71]*	2016	123I-FP-CIT SPECT	DLB with normal baseline 123I-FP-CIT (n=6) DLB with abnormal baseline 123I-FP-CIT (n=8)	In 5 DLB subjects with a normal baseline scan a repeat 123I-FP-CIT was repeated after an average of 1.5 years (range 9-38 months), and these scans were abnormal.
CALM-PD study *[236]*	2002	123I-β-CIT SPECT	PD group treated with pramipexole (n=42) PD group treated with Levodopa (n=40)	% decline in 123I-β-CIT uptake to 46 months, in the whole 82 patients, was greater in the putamen 22.5% than in the caudate 19.6%.
Fahn et al. *[234]*	2004	123I-β-CIT SPECT	RCT with 361 early PD patients assigned to the following groups: Placebo (n=90) Levodopa 150mg (n=92) Levodopa 300mg (n=88) Levodopa 600mg (n=91)	% loss in striatal uptake from baseline to reimaging at 40 weeks found to be less among the group taking placebo 2.6% and to progressively worsen with increasing doses of levodopa (150mg/day: 4.7% , 300mg/day: 3.7% , 600mg/day -6.9%)
Jeong et al. *[235]*	2008	123I-FP-CIT SPECT	Early drug naïve PD patients (n=290) underwent sequential imaging at baseline, 12, 24, 48 months.	% decline in putaminal SBRs from baseline was significantly greater at 24 months (PD with LID 36.4% vs 27% PD without LID, $p<0.05$) and 48 months (PD with LID 50.4% vs 38.4% PD without LID, $p<0.01$) in PD patients with LID compared to those without LID despite having similar symptom duration.

Iranzo et al. *[149]*	2017	123I-FP-CIT SPECT	Idiopathic RBD (n=20)	The change in striatal 123I-FP-CIT uptake from baseline to 3 years between IRBD patient and controls were; left putamen (IRBD 19.36% vs 9.6% controls), left putamen (IRBD 15.57% vs 10.13% controls), left caudate (IRBD 10.81% vs 2.74% controls), right caudate (IRBD 7.14% vs 11.31% controls). This is roughly equivalent to a 6% decline in putaminal binding per year in IRBD cohort
Jennings et al. *[241]*	2017	123I-β-CIT SPECT	185 hyposmic individuals underwent repeat 123I-β-CIT SPECT at baseline, 2 and 4 years follow-up	Abnormal DAT uptake present in 11.4% (n=21) at baseline with 14/21 (67%) converted to PD at 4 years. Hyposmic individuals with a baseline DAT deficit experienced a 4 year decline of 20.23% (SD 15.04%) in DAT uptake from baseline, so approximately 5% decline per year
Abbreviations: 123I-IPT = N-(3-iodopropen-2-yl)-2beta-carbomethoxy-3beta-(4-chlorophenyl) tropane (IPT), SPECT= single photon emission computed tomography, 123I-β-CIT= 123-labelled (123 I)-β-carboxymethoxy-3-β-(4-iodophenyl) tropane (CIT) SPECT, PD= Parkinson's disease, PDD= PD dementia, DLB = Dementia with Lewy bodies, HC=Healthy controls, RBD= Rapid eye movement behaviour disorder, IRBD= idiopathic RBD, PDD= Parkinson's disease dementia, RCT= Randomised controlled trial, DAT=Dopamine transporter, (18)F-FDOPA= 3,4-dihydroxy-6-(18)F-fluoro-l-phenylalanine, PET= Positron Emission Tomography, 18F-CFT= 8F-radiolabelling synthesis (18F; T(1/2) = 109.8 min) of 2-beta-carbomethoxy-3 beta-(4-fluorophenyl)tropane, SBR= Striatal binding ratio, LID=Levodopa induced dyskinesia's, RCT= Randomised control trial				

Table 3. 1 Studies measuring dopaminergic degeneration in DLB, PD and prodromal α-synucleinopathies using repeat SPECT and PET

3.7 Clinical utility of ^{123}I-FP-CIT in the diagnosis of DLB

The majority of patients with clinically probable DLB do not require ^{123}I-FP-CIT SPECT imaging. The added value of ^{123}I-FP-CIT imaging is predominately in those dementia cases in whom the subtype diagnosis is uncertain which is equivalent to a possible DLB diagnosis (i.e. those patients with dementia plus one core feature). It may also be of assistance at the earliest stages of the condition when symptoms/signs are present but are not florid and so their presence cannot be determined with as much confidence and so the use of a biomarker as an adjunct to increase diagnostic confidence may be of merit. It may also help in those patients who have conditions or who are on medications which can induce signs/symptoms clinically indistinguishable from a neurodegenerative condition such as medications with extrapyramidal side effect or vascular Parkinsonism.

3.7.1 Neuropathological correlation of ^{123}I-FP-CIT SPECT with DLB pathology

The gold standard of neurodegenerative disease is post-mortem confirmation of the condition. Four studies to date have evaluated ^{123}I-FP-CIT SPECT against post-mortem confirmation of DLB. Jung et al. scanned 18 subjects with dementia with subsequent pathological confirmation of LB dementia in 12. They found that the sensitivity and specificity of an abnormal ^{123}I-FP-CIT scan to identify LB disease by visual inspection was 92% and 83%, respectively [246]. Five of the six non LB dementia cases had normal ^{123}I-FP-CIT SPECT. The application of semi-quantitative analysis confirmed that in subjects with LB dementia the mean putamen-to-occipital ratio was significantly reduced compared to non-LB dementia cases [246]. Colloby et al. examined substantia nigra neuronal loss in 23 cases (7 with DLB, 4 AD, 12 PDD), reporting an association between neuronal density in the substantia nigra and reduced uptake on ^{123}I-FP-CIT SPECT with mean interval of 3.7 years between ante-mortem imaging and post-mortem examination [247]. Interestingly, there was no association between ^{123}I-FP-CIT uptake in the striatal region with α-synuclein burden ($p \geq 0.46$). In the largest study assessing the sensitivity and specificity of ^{123}I-FP-CIT with pathological confirmation, Thomas et al. validated the diagnostic accuracy of ^{123}I-FP-CIT against 33 autopsy-confirmed DLB cases and 22 AD cases [28]. This study demonstrated that ^{123}I-FP-CIT SPECT had a good diagnostic accuracy of 86%, sensitivity of 80% and specificity of 92% for distinguishing DLB from AD. ^{123}I-FP-CIT imaging had a 20% higher specificity for the diagnosis of DLB compared to clinical diagnosis. Approximately 10% of pathologically confirmed DLB cases had visually normal ^{123}I-FP-CIT SPECT and an absence of brainstem pathology though had α-synucleinopathy pathology in limbic and neocortical regions. An

earlier study from 2007 by Walker et al. investigated whether semi-quantitative ^{123}I-FP-CIT SPECT analysis improved the accuracy of diagnosis when compared with clinical DLB criteria and with pathological diagnosis. They showed semi-quantitation yielded both a higher sensitivity and specificity than visual assessment, 88% and 100%, respectively [248]. Visual assessment of images resulted in the same sensitivity 88% and a lower specificity 88%. Notably, clinical diagnosis had a lower sensitivity of 75% and a low specificity of 42% than the imaging biomarker and was poor compared to the rates published elsewhere. The mean time from clinical diagnosis and ^{123}I-FP-CIT SPECT to autopsy was 34 months (range 6-94). However, this series had only a small number of DLB cases (n=8) included (non-DLB n=12) and clinical diagnosis was not carried out by a panel but by one rater.

Based on the evidence available ^{123}I-FP-CIT SPECT is a valid biomarker of dopamine deficiency in DLB with a high sensitivity and specificity when compared with pathologically diagnosis. Therefore, an abnormal ^{123}I-FP-CIT SPECT in the setting of an early dementia is supportive of an underlying LB disorder. In cases where the ^{123}I-FP-CIT SPECT is borderline visually abnormal, semi-quantitative analysis of striatal regions may aid diagnostic certainty in clarifying the scan as abnormal, particularly if the uptake is greater than two standards deviations below age-matched HC. The studies examining the correlation between DAT imaging and neuropathological as well as clinical diagnosis are summarised in Table 3.2.

3.7.2 Sensitivity and specificity of ^{123}I-FP-CIT SPECT in comparison with clinical diagnosis

Based on the pooled data analysis of 9 clinico-pathological studies including 135 DLB patients and 350 non-LBDs, clinical criteria for detecting DLB have good specificity, with the average specificity being 92% (range 79-100%) [249]. However, the sensitivity of clinical diagnosis is highly variable with the average sensitivity of clinical diagnosis being 49% (range: 0-83%). The low sensitivity is consistent with mis-match between the lower reported prevalence of DLB diagnosed clinically compared with the high rate of LB pathology found at post-mortem. The clinico-pathological confirmation of a clinical diagnosis of possible DLB is less specific than probable DLB, with a specificity of 28% at autopsy [250]. In order to improve the diagnostic accuracy (sensitivity and specificity) for the detection of DLB the 4th international consensus criteria was published in 2017 which allows the assignment of a possible or probable DLB diagnosis on the base of a biomarker abnormality (^{123}I-FP-CIT SPECT, MIBG or polysomnography confirmed RBD). The sensitivity and

specificity of the new diagnostic criteria as yet are not available. It's hoped that the inclusion of *in-vivo* biomarkers of LB pathology alongside clinical feature into the criteria may improve the sensitivity of DLB diagnosis as the specificity is already very high. The inclusion of RBD as a core clinical feature has already been shown to increase the odds of post-mortem confirmed DLB by 6-fold while each of the other 3 core features increase the odds of post-mortem confirmed DLB by 2-fold [178]. Below, the evidence for the sensitivity and specificity of ^{123}I-FP-CIT SPECT is compared with clinical diagnosis of DLB.

A number of both single- and multi-centre studies have assessed the ability of DAT imaging to differentiate between DLB and AD [200, 212, 222, 248, 251-254]. In 2007 a large European Phase III multicentre study, involving 40 different sites and enrolling 326 DLB patients, using a consensus panel clinical diagnosis of probable DLB, possible DLB and non-DLB, an ^{123}I-FP-CIT SPECT scan had 78% sensitivity and 90% specificity for DLB vs non-DLB dementia [200]. It has a PPV 82.4 % (68.1-91.7%), it has NPV 87.5% (79.4 -93.4%). This study highlights the valuable nature of ^{123}I-FP-CIT SPECT in supporting the clinical diagnosis of DLB, particularly considering that the mean sensitivity of clinical diagnosis is 49% (range 0-83%)[249], there is a potential gain in diagnostic sensitivity from a mean of 49% to 77.7% reported in this study. In 2014, O'Brien et al. conducted a pooled analysis of four clinical trials assessing the sensitivity and specificity of ^{123}I-FP-CIT SPECT, found that visual assessment of ^{123}I-FP-CIT images had a sensitivity 88.7% and a specificity 91.2% to detect a striatal dopaminergic deficit when clinical diagnosis was used as the reference standard [69]. The results of the pooled analysis reported similar findings in terms of diagnostic accuracy as the aforementioned European multicentre study in 2007, finding that ^{123}I-FP-SPECT had a high diagnostic accuracy in differentiation DLB from non-LBD with a pooled sensitivity of 86.6% (95% confidence interval: 72%-94%) and a pooled specificity of 93.6% (95% CI: 88.5%-96.6%) [255]. A further Cochrane review of the data in 2015 concluded that ^{123}I-FP-CIT SPECT was more accurate than clinical diagnosis for separating DLB from AD [201].

The application of ^{123}I-FP-CIT SPECT in the setting of a clinical diagnosis of possible DLB should lead to improved diagnostic confidence of underlying DLB. A study by O'Brien et al., examined the merits of ^{123}I-FP-CIT SPECT imaging in patients with clinically possible DLB followed-up for 12 months [222]. Among the 44 patients with possible DLB at baseline, 43% (n=19) were diagnosed with probable

DLB, 7 people with diagnosed with non-Lewy body dementia (16%) and 18 individuals the diagnosis remained possible DLB (41%). Of the 19 (43% of possible DLB at baseline) who at follow-up were diagnosed with probable DLB, 12 had abnormal scans at baseline (sensitivity 63%, specificity 100%); all 7 individuals with possible diagnosis who were diagnosed as having AD at follow-up had normal scans. The authors concluded that an abnormal ^{123}I-FP-CIT SPECT imaging in possible DLB is highly predictive of progression to probable DLB. In most individuals diagnosed with possible DLB who did actually have DLB this became apparent within 1 year. However, a limitation of this study was the relatively short follow-up of 1 year and indeed possible DLB subjects with normal scans given a longer follow-up period may well develop additional features of DLB. A further study by Walker et al., investigated whether ^{123}I-FP-CIT SPECT would lead to a more certain diagnosis in those patients with possible DLB [70]. 187 possible DLB subjects were randomised to receive a ^{123}I-FP-SPECT or not. In total 114 subjects had a ^{123}I-FP-CIT SPECT and 56 did not (controls), and an abnormal ^{123}I-FP-CIT SPECT was recorded in 43% of patients. This led to a significantly greater change in diagnosis compared with controls at 8 and 24 weeks (61% (n=70) imaged with ^{123}I-FP-CIT v 4% (n=2) not imaged and 71% (n=77) imaged with ^{123}I-FP-CIT v 16% (n=9) not imaged; both P<0.0001).

The diagnostic accuracy of ^{123}I-FP-CIT SPECT may be of greatest utility at the earlier stage of disease where the clinical symptoms are not as pronounced, especially in DLB [248, 256]. An abnormal ^{123}I-FP-CIT SPECT can occur in advance of extrapyramidal signs. In a study by Walker et al. an abnormal ^{123}I-FP-CIT SPECT occurred in 43% of possible DLB patients but only 26% of patients had clinical parkinsonism [70]. A similar pattern was shown in PD with not only the striatal uptake being reduced on the side contralateral to unilateral symptom onset (by 53%) but also the ipsilateral side (by 38%) to a less extent [257]. However, false-positive results, as well as false negative results, do occur with ^{123}I-FP-CIT SPECT and this is likely to be more problematic with early stage scanning. In particular, non-DLB forms of dementia such as PSP, MSA and CBD, FTD and Creutzfeldt-Jakob disease, can give rise to an abnormal ^{123}I-FP-CIT SPECT, so thorough clinical phenotyping is required to differentiate these conditions. Notably in clinic-pathological cohorts of DLB such as the Thomas et al. study [28], the reason recorded for the two false positives (approximately 10% (2/24) of abnormal ^{123}I-FP-CIT SPECT results in total) was fronto-temporal-lobar-degeneration (FTLD) with no LBD or AD pathology in the first patient and AD pathology in the second case . In the Walker et al. neuropathology paper, a false positive rate on visual assessment alone was 22.2% (2/9) but this was improved to 0% when combined with semi-quantitative assessment [248]. The first false positive ^{123}I-FP-CIT SPECT turned

out to be AD with cerebrovascular disease and careful correlation with structural MRI may have avoided the misinterpretation. The second false positive was due to FTLD.

A subset of DLB patients appear to have false negative ^{123}I-FP-SPECT imaging. In the Thomas et al. paper, 10% (3/33) of clinical probable DLB patients had a false negative ^{123}I-FP-CIT SPECT [28]. Similarly, in the Walker et al. paper 12.5% (1/8) with DLB pathology had negative ante-mortem dopaminergic imaging [248]. The explanation for a false negative scan maybe due to number of factors: (A) early-stage disease that spares the midbrain initially but eventually on repeat imaging becomes abnormal, (B) a significant proportion of DLB patients who have cortical DLB pathology without involvement of the nigrostriatal pathway leading to a false negative ^{123}I-FP-CIT SPECT, (C) a flatter posterior-anterior gradient in DLB leading to difficulty in identifying an abnormal scan. The reduced posterior-to-anterior gradient in DLB is recognised, with relatively early involvement of the caudate leading to a “balanced loss” which is visually more difficult to recognise. Therefore, the Cochrane review of DAT imaging in DLB concluded that semi-quantitative analysis seemed to be more accurate than visual rating in DLB [201].

Study	Ligand	Clinical Diagnosis	Reference diagnostic standard	Cut-off point adopted	Methods used to judge SPECT	Independent Comparison blind to reference diagnostic standard	Findings
Donnemiller et al. *[258]*	123I-β-CIT	7 DLB, 6 AD	Clinical diagnosis	Not reported	Semi-quantitative assessment	Not reported	Striatal binding lower in DLB than AD
Ransmayr et al. *[220]*	123I-β-CIT	20 DLB, 24 PD, 10 HC	Clinical diagnosis	Not reported	Semi-quantitative region of interest analysis	Not reported	Striatal binding lower in DLB and PD than HC; asymmetry more marked in PD than DLB
Walker et al. *[259]*	123I-FP-CIT	27 DLB, 17 AD, 19 PD, 16 HC	Clinical diagnosis	Visual ratings (0 normal uptake in all four striatal regions, 1 slight reduction of striatal uptake in all four regions, 2 significant reduction in uptake in all four striatal regions)	Visual assessment	Yes	Striatal binding lower in DLB and PD than AD and HC
Ceravolo et al. *[251]*	123I-FP-CIT 99mTc-ECD	20 DLB, 24 AD	Clinical diagnosis	Not reported	Semi-quantitative region of interest analysis	Not reported	Striatal binding lower in DLB than AD
Ceravolo et al. *[260]*	123I-FP-CIT	15 DLB, 13 AD , 20 PD, 8 HC	Clinical diagnosis	Not reported	Semi-quantitative region of interest analysis	Yes, single observer blind to the diagnosis	Reduce striatal binding in DLB and PD

O'Brien et al. *[212]*	123I-FP-CIT	23 DLB, 34 AD, 38 PD, 36 PDD, 33 HC	Clinical Diagnosis	1.5 SDs of control mean being considered normal Visual ratings (0 normal; 1-3 abnormal)	Semi-quantitative region of interest analysis visual qualitative assessment of scans	Yes	Striatal binding reduced in DLB versus AD and HC; DLB and PD similar; greatest loss in PDD Mean, left and right caudate, anterior and posterior putamen
McKeith et al. *[200]* Multicentre, phase III trials	123I-FP-CIT	94 probable DLB, 57 possible DLB, 147 non-DLB dementia	Clinical Diagnosis	Visual rating (0 normal; 1-3 abnormal)	Visual assessment & Semi-quantitative method	Yes	High rate of agreement between abnormal striatal 123I-FP-CIT SPECT image and clinical diagnosis of probable DLB
Walker et al. *[248]* Autopsy study	123I-FP-CIT	13 DLB, 6 AD, 1 CBD	Clinical and Autopsy diagnosis	Semi-quantitative method: more than 2 SDs below the mean of the controls	Semi-quantitative assessment	Yes, single observer blinded to the clinical and autopsy diagnosis	123I-FP-CIT had 88% sensitivity and 100% specificity for DLB diagnosis versus 75% and 42% for initial clinical diagnosis (with reference to autopsy diagnosis).
Walker and Walker *[254]* Follow-up from Walker et al. 2007 *[248]* with additional patients and Walker et al. 2002 *[259]*.	123I-FP-CIT	15 DLB, 7 AD, 1 CBD, (autopsy diagnosis 10 DLB, 9 AD, 4 other)	Clinical diagnosis Autopsy diagnosis (McKeith et al) for 20 patients 3 further cases.	Semi-quantitative method: more than 2 SDs below the mean of the controls (<3.02) Visual ratings: (o, normal uptake: 1 slight reduction; and 2, significant reduction . 0-1 normal; 2 abnormal)	Visual assessment & Semi-quantitative method	Yes	123I-FP-CIT had 100% sensitivity and 92% specificity for DLB diagnosis

Colloby et al. *[261]*	123I-FP-CIT & perfusion 99mTc-exametazime SPECT	123I-FP-CIT: 33 AD, 28 DLB, 33 HC, 36 AD, Perfusion 99mTc-exametazime SPECT: 30 DLB, 39 HC	Clinical diagnosis Autopsy diagnosis for 9 patients (neuropathological diagnosis criteria not reported)	Visual ratings (0 normal; 1-3 abnormal)	Visual assessment	Yes	Clinical diagnosis and consensus 123I-FP-CIT assessment matched in 84% of cases for AD versus DLB; diagnostic accuracy with 123I-FP-CIT
Thomas et al. *[28]*	123I-FP-CIT	33 DLB 22 AD	Clinical diagnosis & Autopsy diagnosis	Visual rating	Visual assessment	Yes, neuropathological & clinical diagnosis blind to ^{123}I-FP-CIT imaging	^{123}I-FP-CIT had a diagnostic accuracy 86%, sensitivity 87%, specificity 72%. 10% of pathological proven DLB subjects had a normal ^{123}I-FP-CIT image.
Colloby et al. *[247]*	123I-FP-CIT	4 AD 7 DLB 12 PDD	Clinical Diagnosis	1.5 SDs of control mean being considered normal Visual ratings (0 normal; 1-3 abnormal)	Semi-quantitative region of interest analysis visual qualitative assessment of scans	Yes	An association between neuronal density in the substantia nigra and reduced uptake on 123I-FP-CIT with mean interval 3.7 years between antemortem imaging and post-mortem examination
Kemp et al. *[252]*	123I-FP-CIT	80 patients undergoing 123I-FP-CIT for suspected DLB	Clinical diagnosis	Not reported	Visual assessment	Single observer rated SPECT and has access to the clinical data.	123I-FP-CIT had a marked influence on clinical diagnosis and 123I-FP-CIT result was concordant in 76/80 patients (95%)

Morgan et al. *[262]*	123I-FP-CIT	10 DLB 9 AD 12 FTD	Clinical diagnosis Autopsy diagnosis in 10 DLB, 9 AD and 2 FTD neuropathological diagnostic criteria	Visual ratings: (0, normal uptake; 1 slight reduction; and 2, significant reduction 0-1 normal; 2 abnormal)	Visual qualitative assessment of scans	Yes, blind to the clinical and autopsy diagnoses	9/10 DLB cases has significant reduction of DAT uptake in putamen and caudate. 4/12 FTD cases had and abnormal 123I-FP-CIT 1/9 AD cases had an abnormal scan. Sensitivity and specificity of 123I-FP-CIT in differentiating DLB from AD (90% & 88.9%) and FTD (90% & 66.7%).
O'Brien et al. *[69]* (reporting data from McKeith et al. *[200]* and O'Brien et al. *[222]*	123I-FP-CIT	Total: 351 enrolled, 326 underwent 123I-FP-CIT, 242 efficacy analysis 89 probable DLB, 27 possible DLB 125 AD, 1 other	Clinical diagnosis followed up for 12 months.	Visual ratings (0) normal: 1-3 abnormal)	Visual qualitative assessment of scans Semi-quantification of regional DAT striatal binding.	Yes	Of 44 with possible DLB at 12 month follow-up, 19 (43%) were probable DLB, 7 (16%) non-Lewy body dementia and 18 (41%) remained in possible DLB. Of the 19 who were diagnosed with probable DLB, 12 had baseline abnormal 123I-FP-CIT (sensitivity 63%), all 7 non-Lewy body dementia at follow up had normal baseline scans (specificity 100%)
Treglia et al. *[83]*	123I-FP-CIT 123I-MIBG	20 DLB, 6 AD 3 FTD 2 VD	Clinical Diagnosis	More than 2 SDs below the mean of the controls (cut off 2.60)	Semi-quantitative method	Yes	The diagnostic performance of 123I-FP-CIT SPECT in differentiating

		40 PD 28 Parkinsonism					between DLB & other dementias. Sensitivity 90%, specificity 91%, accuracy 90%, PPV 95% and NPV 83%. No difference with MIBG
Spell et al. *[253]*	123I-FP-CIT F-FDG-PET	13 FTD 12 DLB 9 AD	Clinical diagnosis	Mean values for quantification, as suggested by current European Association of Nuclear Medicine guidelines Scans were categorised as pathological or normal	Semi-quantitative method visual assessment of scans.	Not reported	Semi-quantitative assessment of 123I-FP-CIT differentiated between DLB from AD with high accuracy (AUC 0.94), but also discriminated between DLB and FTD with high accuracy (AUC 0.91).
Siepel et al. *[221]*	123I-FP-CIT	20 DLB 8 Non-DLB	Clinical diagnosis	Visual rating	Visual assessment	Yes, single observer blinded to the clinical data	In 7 subjects whom had evidence of an abnormal 123I-FP-CIT imaging but absent core features. All of these subjects eventually developed parkinsonism and cognitive fluctuations consistent with a diagnosis of DLB
Walker et al. *[70]*	123I-FP-CIT	187 Possible DLB subject divided as follows: 56 possible DLB no scan 114 possible DLB having a scan	Clinical diagnosis	Visual rating (0, normal, 1 abnormal (asymmetric activity with one putamen showing reduced uptake), 2	Visual assessment	Yes	Imaging improved clinical certainty, more patients in the possible DLB with imaging has a change in diagnosis compared with those who did not have imaging (61% vs 4%). Clinicians were

				(absent activity in the putamen of both hemispheres), 3 (absent activity in the putamen of both hemispheres and greatly reduced in one or both caudate nuclei; 4 (other abnormal pattern)			more likely to change the diagnosis if the scan was abnormal (82%) than if it was normal (46%).
Abbreviations: SPECT= single photon emission computed tomography, 123I-β-CIT= 123-labelled (123 I)-β-carboxymethoxy-3-β-(4-iodophenyl) tropane (CIT) SPECT, PD= Parkinson's disease, DLB = Dementia with Lewy bodies, HC=Healthy controls, PDD= Parkinson's disease dementia, FTD= Frontotemporal dementia, AD= Alzheimer's disease, CBD= Corticobasal degeneration, HC= Healthy Controls, DAT=Dopamine transporter, F-FDG PET= Fludeoxyglucose Positron Emission Tomography, 123I-MIBG = ^{123}I-metaiodobenzylguanidine, AUC= Area under curve, PPV=Positive predictive value, NPV=Negative predictive value, SD= Standard Deviation							

Table 3. 2 Summary of dopamine transporter ligand SPECT studies investigating the differentiation of DLB from other dementias.

3.8 Correlation of ^{123}I-FP-CIT SPECT with clinical features

Despite numerous clinical studies evaluating the correlation between clinical features and dopaminergic imaging, the studies are surprisingly inconsistent and variable in their findings. The most consistent finding is the association of motor findings with reduced striatal dopaminergic uptake. However, this finding has not been uniformly observed across all studies. Moreover, studies indicating a correlation between motor findings and dopaminergic imaging only show a weak correlation. In 2017, Shimizu et al. [263] showed a significant correlation between severity of parkinsonism and DAT uptake in entire regions of the striatum in patients with DLB. Those DLB patients with parkinsonism showed a significant lower DAT uptake in the entire striatum compared to those without parkinsonism. Siepel et al. also showed an inverse correlation between the severity of parkinsonism and DAT uptake in the putamen only but not across the whole striatum [264]. On the contrary, Ziebell et al. found no significant difference in DAT binding according to severity of parkinsonism, as assessed with the Hoehn and Yahr scale [75]. Other studies have also failed to identify an association between the severity of Parkinsonism and striatal DAT uptake in DLB patients [211] [265]. Possible explanations for the differences in these studies may be related to age related decline in striatal DAT uptake as the Shimizu et al. had an older study cohort (mean age: 80.6 yrs) than Walker et al. (75.3 yrs) and Ziebell et al. (74.5 yrs) and Shimziu et al. also had a much larger cohort (n=133) than the other two studies (Walker et al., (n= 21); Ziebell et al., (n=51)) [75, 211, 263].

In terms of core clinical features associated with DLB, no study has shown an association between striatal dopamine function and cognitive decline, fluctuation or RBD. Shimizu et al. in 2017 [263], found no correlation between cognitive decline, fluctuations, visual hallucinations, or RBD and the striatal DAT availability, consistent with Ziebell et al. [75]. Roselli et al. did observe a significant inverse correlation between decreased striatal DAT uptake and visual hallucinations but this was not corroborated by other studies [73, 263]. Furthermore, Roselli et al. showed a correlation between DAT uptake in the caudate nucleus and depression, delusions and apathy. In a small study, David et al. showed that higher apathy scores, as assessed by the neuropsychiatric inventory, correlated with lower uptake in striatal DAT values [77]. In terms of symptom evolution over time, a study by Walker et al. examining the evolution of clinical features in possible DLB over a 6 month period based on the presence or absence of abnormal DAT uptake at baseline, showing that the only symptom to evolve in the DLB group was parkinsonism and there was relatively little evolution

of the rest of the DLB features regardless of imaging [37]. There was no difference in the evolution of DLB clinical features over 6 months between cases with normal and abnormal imaging. In fact, fluctuating cognition and visual hallucinations became less common in the possible DLB group at follow-up.

3.9 Striatal dopaminergic imaging in prodromal DLB

The literature reporting the imaging of striatal dopaminergic function is limited in prodromal DLB. Dopaminergic imaging has been studied in two prodromal phenotypes of DLB; idiopathic RBD and MCI-LB. In the following paragraphs, the findings of these studies are discussed and summarised and Table 3.3 outlines the main results from these studies.

A study by Thomas et al., examining the diagnostic accuracy of ^{123}I-FP-CIT SPECT in prodromal DLB, 75 patients with MCI and over the age of 60 years were recruited and underwent ^{123}I-FP-CIT SPECT, alongside detailed clinical, neurological and neuropsychological assessments [266]. A diagnostic panel further classified the MCI patients, based on the presence or absence of core LB symptoms; two or more LB symptoms (probable MCI-LB; n=33), one LB symptom (possible MCI-LB; n=15), no LB symptoms (MCI-AD; n=27). Among the MCI-LB groups 26 (54%) had a visually abnormal ^{123}I-FP-CIT SPECT, with 12 out of this group (46%) having clinical parkinsonism, that is a slight majority of those who had an abnormal ^{123}I-FP-CIT SPECT did not have clinical evidence of parkinsonism. Among the MCI-AD group 3/27 were rated as having abnormal ^{123}I-FP-CIT SPECT. Overall, nigrostriatal dopaminergic imaging rated visually at the MCI-LB stage (combined probable or possible MCI-LB) has a similar high specificity 89% (95% CI 70.8-97.6) but a lower sensitivity 54% (95% CI 39.2 -68.6) than in established DLB [266]. This study suggests that ^{123}I-FP-CIT SPECT may have an important role as a biomarker, detecting disease in advance of parkinsonism and improving accuracy in the early diagnosis of dementia. The mains strengths of this study were the detailed clinical and neuropsychological characterisation of participants, as well as the consensus diagnostic panel approach for determining MCI diagnosis and likely underlying aetiology. However, no longitudinal follow-up data has been reported yet for this cohort so rate of progression from MCI to dementia remains unknown as does whether those with visually abnormal ^{123}I-FP-CIT SPECT will progress to a final diagnosis of DLB.

In a cross-sectional study by Kasanuki et al. [76], the role of ^{123}I-FP-CIT SPECT and its clinical relevance in prodromal DLB (n=20), probable DLB (n=18) and probable AD (n=10) was explored. Prodromal DLB was defined as MCI with FDG-PET showing diffuse hypometabolism in the occipital lobe, and several non-motor symptoms but no core features of DLB other than parkinsonism [156]. Mean striatal ^{123}I-FP-CIT uptake in both prodromal DLB group and probable DLB group was significant lower than in Alzheimer's disease (AD). However, clinical outcome measures such as cognitive function (MMSE) and motor function did not correlate with striatal uptake scores. This study had modest numbers of patients and had no detailed assessment of cognitive function with the only reported cognitive assessment being the MMSE. One PET imaging study assessed striatal dopamine terminal integrity using 11C-dihydrotetrobenazine (DTBZ) in 27 MCI subjects and followed them up for a mean of 3 years [267] . Two of the 27 MCI subjects had markedly reduced striatal [11C] DTBZ-PET binding at baseline. On longitudinal follow-up one developed DLB, the other developed fronto-temporal dementia. In this study a total of four subjects eventually developed DLB but 3 had normal striatal dopamine function at baseline. Therefore, at present there is limited evidence supporting the utility of striatal dopaminergic PET tracers in prodromal DLB.

Three longitudinal studies have reported striatal dopaminergic imaging in polysomnography confirmed IRBD [7, 207, 268]. In one study 87 participants underwent ^{123}I-FP-CIT SPECT, 51 (58.6%) had a baseline dopaminergic deficit on imaging [7]. On follow-up (mean 3.2 ± 1.9 years), 39.2% (n=20) of these subjects had phenoconverted to a parkinsonian syndrome (PD (n=10), DLB (n=9), MSA (n=1)) [7]. Of the 36 (41.4%) who had no dopaminergic deficit on baseline ^{123}I-FP-CIT SPECT, 5 (13.9%) had phenoconverted to a parkinsonian syndrome (1 PD, 2 DLB with parkinsonism and 2 DLB without parkinsonism) at follow-up (mean 3.5 ± 1.3 years). ^{123}I-FP-CIT uptake in the left putamen, right putamen and right caudate was significantly lower in subjects who phenoconverted than those who had an abnormal ^{123}I-FP-CIT SPECT but remained disease free. Furthermore, decreased putamen uptake greater than 25% on baseline imaging predicted phenoconversion within 3 years of follow-up. An earlier study by Iranzo et al. reported both striatal dopamine terminal binding using ^{123}I-FP-CIT SPECT and transcranial echosonography in 43 subjects with IRBD [207]. Eight subjects eventually progressed (by 2.5 years) to a neurodegenerative condition (5 PD, 2 DLB, and 1 MSA). Both IRBD cases who developed DLB displayed substantia nigra hyperechogenicity. However, another study did not find any utility of transcranial ultrasound imaging alone to predict phenoconversion to α-synucleinopathy in an IRBD cohort at five years follow-up [269].

Study	Study Type	Diagnosis	Tracer	Findings
Thomas et al. *[266]*		15 Possible MCI-LB 33 Probable MCI-LB 27 MCI-AD	[123I]FP-CIT	Sensitivity of visually rated [123I]FP-CIT to detect combined possible or probable MCI-LB 54.2%, specificity 89% 26/48 MCI-LB had an abnormal [123I]FP-CIT 3/27 MCI-AD had an abnormal [123I]FP-CIT 41% (n=12) with abnormal [123I]FP-CIT had parkinsonism
Kasanuki et al. *[76]*	Cross-sectional	20 **Pro-DLB 18 DLB 10 AD	[123I]FP-CIT [18F] FDG	Mean striatal uptake reduced in both **Pro-DLB and DLB significantly lower than in AD
†Iranzo et al. [7]	Prospective	87 IRBD 20 HC Follow-up 5.7±2.2 years	[123I]FP-CIT	At follow-up 28.7% (n=25) developed synucleinopathy (PD n=11, DLB n=13, MSA n=1) ROC analyses 25% reduced uptake of FP-CIT at baseline predicts those whom will develop a synucleinopathy over a 3 year period
†Iranzo et al. *[207]*	Prospective	43 IRBD 18 HC Follow-up 2.5 years	[123I]FP-CIT	30% (8) developed synucleinopathy (PD n=5, DLB n=2, MSA n=1) 40% of IRBD subjects had reduced FP-CIT uptake. More pronounced reduction in uptake in putamen than in caudate

Albin et al. *[267]*	Cross-sectional & prospective	27 MCI 11 aMCI 7 mdMCI 9 naMCI Follow-up 3 years	[11C] DTBZ [11C] PiB	2 classified as DLB based on reduced[11C] DTBZ Only 1 of subjects classified as DLB by [11C] DTBZ Converted to DLB

Abbreviations: HC= healthy controls; PD= Parkinson's disease; AD= Alzheimer's disease; MSA= Multisystem atrophy; MCI= Mild cognitive impairment; MCI-LB= mild cognitive impairment with Lewy body disease; MCI-AD= Mild cognitive impairment due to Alzheimer's Disease; aMCI= Amnestic mild cognitive impairment; mdMCI= Multidomain domain mild cognitive impairment; IRBD=idiopathic REM sleep behaviour disorder; PET = positron emission tomography; PET= Positron Emission Tomography; ROC= Receiver Operating characteristic; **prodromal DLB cohort constructed based on Petersen et al. MCI criteria *[156]*, MMSE >26/30, FDG-PET showing diffuse hypometabolism in the occipital lobe, and several non-motor symptoms but no core features of DLB *[156]*;

Tracers:

[^{11}C] DTBZ = 2-Hydroxy-3-isobutyl-9-[^{11}C]methoxy-10-methoxy-1,2,3,4,6,7- hexahydro-11bH-bezo[α]-quinolizine
[^{18}F] FDG = fluoro-2-deoxy-2-D-glucose PET
[^{123}I]FP-CIT = N-(3-fluoropropyl)-2β-carbomethoxy-3β-(4-[^{123}I]iodophenyl)nortropane(=DAT-Scan)

[11C] PiB]= N-Methyl-[11C]-2-(4'-methylaminophenyl)-6-hydroxybenzothiaso Pittsburgh Compound B

Table 3. 3 Nigrostriatal dopaminergic imaging in prodromal DLB.

3.10 Discussion

^{123}I-FP-CIT SPECT is highly sensitive (83%-100%) and specific (88-100%) biomarker for DLB when compared with neuropathological diagnosis. In fact ^{123}I-FP-CIT SPECT improves specificity for the identification of underlying DLB pathology by 20% compared with clinical diagnostic criteria alone [28]. The clinical phenotype should always be considered when interpreting findings from DAT imaging as while it is able to accurately differentiate parkinsonian syndromes from AD, it is unable to discriminate parkinsonian syndromes from each other. Moreover, it must be considered that even a normal ^{123}I-FP-CIT SPECT does not rule out the possibility of underlying DLB pathology as the scan can be normal in 10% of DLB patients with neocortical LB pathology [28]. In clinical practice, DAT imaging is particularly useful for improving diagnostic certainty as subjects referred for the investigation are likely to already to meet some of the clinical features for possible or probable DLB. In order to improve diagnostic accuracy, ^{123}I-FP-CIT SPECT analysis should consist of both visual and semi-quantitative analysis as recommended by a recent Cochrane review [201].

In prodromal DLB, a dopaminergic deficit is present in approximately 50% of subjects at the MCI-LB stage [76, 266]. Moreover, the dopaminergic deficit can precede the onset of clinical parkinsonism [266]. However, some subjects with MCI-LB in these studies did not demonstrate nigrostriatal involvement on ^{123}I-FP-CIT SPECT. This discrepancy between an apparently intact (or minimally affected) nigrostriatal system but with clinical evidence of LB disease elsewhere, may be surprising considering the often assumed Braak staging of LB pathology. In the Braak staging system for LB pathology in PD, six stages of disease development have been proposed [72]: LB pathology beginning in the lower brainstem and olfactory system (Stage 1&2) before progressing through the pons/midbrain, then the subcortical structures (stage 3&4) before finally reaching the neocortex (stage 5 &6). However, this sequential ascent of LB pathology from brainstem to neocortex does not apply in DLB because LB may be found in the neocortex without involvement of the lower brainstem, as demonstrated by prominent visual hallucinations and cognitive fluctuations early in many people with no evidence of striatal involvement, and post mortem evidence that 10-15% patients with DLB have no significant substantia nigra involvement [28, 63, 270]. Furthermore, post mortem studies in DLB patients have also found different combinations of abnormal protein accumulation in individual DLB patients, including α-synuclein, Aβ, and NFT [8, 28, 85-87]. The interaction between variable degrees of AD pathology and LB pathology in DLB remains unclear. The variation in the phenotype of LB disease highlights the need for α-synuclein radiotracer biomarker for better disease delineation and to enable assessment of LB load and brain distribution at different disease stages.

Sequential striatal DAT imaging is an understudied topic in LB disease [70]. Sequential imaging would allow for estimates of annual percentage decline in ^{123}I-FP-CIT uptake in the striatum which is not clearly understood in DLB or in prodromal α-synucleinopathy conditions. A number of studies using SPECT in PD have shown variable rates of annual decline in the caudate (-4.6% to 11.0%) and in the putamen (-6.0% to 10.0%) but the only sequential DAT imaging study in DLB showed a greater annual rate of decline in both the caudate (-12.7%) and the putamen (-13.0%) than in PD. The more rapid decline in neuroimaging biomarkers in DLB would be in keeping with more rapid clinical deterioration in DLB than in PD but this needs to be further evaluated in a larger cohort of DLB patients followed up with sequential imaging over a number of years.

There are some important factors that impact on DAT availability, hence interpretation of serial DAT imaging findings. There is some evidence that dopaminergic and other medications may directly reduce DAT availability over time. Furthermore, there is considerable within-subject and within-group variability which means individual rates of striatal DAT binding are widely dispersed and data is difficult to interpret on an individual basis. The within-group variability is also substantially larger than the average annual decline of striatal binding. Some of the variability can be accounted for by the utilisation of different SPECT cameras, the ligand or the method of data analysis employed. It remains to be determined, given these limitations whether sequential DAT imaging accurately measures disease progression in individual patients and can provide clinically useful information. Finally, progressive dopaminergic denervation of the nigrostriatal pathway is only one facet of the complex disease state that is DLB and it only investigates dopaminergic dysfunction and does not encompass other aspects/neurochemical pathways, such as cholinergic systems, known to be involved in disease evolution.

3.10.1 Limitations of current research and future directions

There are a number of deficiencies in the current literature as there is a scarcity of studies evaluating ^{123}I-FP-CIT SPECT with a neuropathological standard of truth. Instead, most of our data is derived from comparing the diagnosis accuracy of ^{123}I-FP-CIT SPECT to the imperfect standard of clinical diagnosis on follow up. It may well be established that a variety of biomarkers in the correct clinical context are superior to clinical diagnosis alone, particularly at the early stage of disease evolution.

There is evidence to indicate that a subset of early clinically probable DLB may have a negative ^{123}I-FP-CIT SPECT but on repeat imaging the ^{123}I-FP-CIT SPECT becomes abnormal. At the MCI-LB stage, approximately 50% of subjects had a normal ^{123}I-FP-CIT SPECT which implies that 50% of early DLB subjects may benefit from repeat imaging [27]. The optimal timeframe for clinicians to repeat the imaging in order to improve diagnostic certainty remains unknown. Moreover, the rate of decline of DAT uptake may be important in predicting the evolution of core features, such as parkinsonism, before a scan becomes definitely abnormal. Unfortunately, there are only two studies which have reported outcomes of repeat ^{123}I-FP-CIT imaging in DLB, and one of these reported the annual percentage decline in striatal DAT uptake in DLB and this study must be interpreted with a degree of caution as there were only 20 DLB patients involved.

Based on the above limitations, there is a need for a longitudinally follow-up studies in early DLB cohorts who have undergone extensive clinical phenotyping as well a multiple biomarkers which incorporate sequential ^{123}I-FP-CIT imaging. Only this type of study design will be capable of answering key remaining questions posed in relation to the temporal evolution of biomarkers in relation to clinical symptomology.

3.11 Conclusion

^{123}I-FP-CIT SPECT is a well-established imaging modality which is extremely useful in differentiating dementia subtypes, in particular distinguishing between DLB and AD. It targets dopaminergic pathways directly involved in the underlying pathophysiological process. A dopaminergic deficit is evident in the majority of DLB patients and in approximately 50% of MCI-LB subjects. At the DLB stage, there is limited correlation with cognitive decline and neuropsychiatric or sleep symptomatology. While motor dysfunction does appear to correlate with striatal DAT uptake, this has not always been a consistent finding across all studies. Approximately 10% of DLB never develop abnormal DAT imaging as the LB pathology remains confined to the cortical and limbic regions. Interpretation of ^{123}I-FP-SPECT by visual assessment can be challenging in some cases and semi-quantitative measures may be a helpful tool to aid analysis. Determining when a ^{123}I-FP-CIT SPECT becomes abnormal in early DLB and the rate of decline in DAT uptake remain key questions but an understudied topic.

Chapter 4. Structural magnetic resonance imaging in DLB

4.1 Introduction

Neuroimaging biomarkers of underlying brain pathological processes could allow for early diagnosis and insight into disease progression. The ability of neuroimaging biomarkers to detect structural and functional *in vivo* brain alterations depend on the stage of the neurodegenerative process and the proteinopathy responsible for the neurodegeneration. The proposed pathophysiological sequence is based on pathological accumulation of abnormal proteins resulting in neuronal synaptic dysfunction and eventual brain atrophy due to neuronal death. However, the degree and sequential order in which the pathophysiological process occurs is thought to vary markedly between DLB and AD, resulting in differential patterns of early regional brain atrophy and allowing for potential early differentiation of the two conditions based on neuroimaging findings.

MRI is a non-invasive imaging tool capable of providing highly detailed images of structural and functional *in vivo* brain alterations for both clinical and research applications. MRI operates by the principles of nuclear magnetic resonance which cause protons in hydrogen atoms, present in water molecules, to align to a magnetic field. When pulsed radio waves sequences are applied to the protons, they absorb energy and then relax back emitting detectable radiofrequency signals upon returning to their ground state. The signals are then analysed by a computer and converted into an image. The MRI contrast in the brain depends on regional differences in tissue water density (proton density) as well as the tissue effects on proton relaxation times. Conventional structural MRI uses distinct pulse radio waves sequences to obtain longitudinal T1-weighted (T1), transverse T2-weighted (T2), fluid-attenuated inversion recovery (FLAIR) and/or susceptibility-weighted scans.

MRI is an attractive option as a neuroimaging biomarker for a variety of reasons. It is non-invasive, readily available, well-tolerated by patients and relatively inexpensive when compared to other imaging techniques. Moreover, it is a very safe imaging technique which does not require ionising radiation for image acquisition. Some patients may have contra-indications preventing them from undertaking a MRI due to safety concerns related to the implantation of metal containing medical devices such pacemakers, defibrillators, surgical clips etc. Claustrophobia can also prevent patients

from undertaking an MRI. Studies report the prevalence of severe claustrophobia resulting in premature scan termination to be between 2-10% of people undergoing an MRI of their head or neck [271, 272].

Conventional MRI techniques have been increasingly applied in the clinical setting to differentiate patients with cognitive decline due to AD from underlying DLB pathology. MRI is frequently also used clinically to exclude other potential causes of cognitive decline such as cerebrovascular disease, head trauma, normal pressure hydrocephalus etc. Diagnostic criteria have recommended the consideration of regional abnormalities on MRI to assist particularly by identifying the presence or absence of medial temporal lobe (MTL) thinning which is more commonly associated with AD pathology [7, 112]. Furthermore, the proposed research criteria for MCI-LB state that potential structural MRI biomarkers for MCI-LB include; preservation of the MTL, insular thinning and GM volume loss [9]. More advanced MRI techniques have been studied in research settings but have not been established yet in routine clinical practice. They include: diffusion tensor imaging (DTI), arterial spin labelling, magnetic resonance spectroscopy, and functional magnetic resonance imaging.

The aim of this chapter is to provide an overview of the current literature on structural MRI techniques in DLB, highlighting the strengths and limitations of these and suggest areas for future research. This chapter will also highlight the limited structural MRI studies that have been conducted in MCI-LB.

4.2 Structural magnetic resonance imaging assessment

Structural MRI allows for high-resolution static measurement of neuroanatomical structures. Morphometric analysis of MRI brains' has been used to investigate neuroanatomical correlates of cognitive impairment. Several brain morphometry methods are routinely used to analyse MRI data and typically fall into two categories: (1) hypothesis-driven ROI analysis (i.e. visual assessment, automatic, or semi-automatic segmentation) studies of pathologically-affected structures, or (2) more exploratory unbiased voxel-based whole-brain morphometric analysis (i.e. voxel-based morphometry), and surface based approaches (i.e. cortical thickness), which require no *a priori* assumptions. The optimal method for measuring brain tissue loss must be sensitive to small

changes, reproducible and stable over time. The next few sections will outline the details of brain morphometry methods.

4.2.1 Visual assessment of MRI imaging

In the clinical setting, visual assessment of MRI is the primary method of interpretation in order to extract diagnostically useful information. A number of visual rating scales have been developed to rate brain regions associated with atrophy in a range of dementias. An example of a commonly used regional visual rating scale is the Schelten's MTL scale [273]. It is a quick, and clinically useful method for discriminating between AD and normal aging and other causes of dementia. Other evaluation scores for posterior atrophy and global cortical atrophy exist and have been implemented in dementia studies [274, 275]. Similarly, clinical scoring systems exist for measuring how extensive cerebral white matter hyperintensities (WMH) are, for example the Fazekas score [276]. However, visual rating has a number of limitations, in particular rating the degree of global atrophy is limited by poor inter-rater reliability and visual rating methods depend on the appropriate *a priori* choice of structures to be analysed.

4.2.2 Quantitative volumetric MRI analysis

Region-of-Interest analysis

The ROI approach has predominantly been utilised to detect atrophy in discrete neuroanatomical structures according to an *a priori* hypothesis. ROI analysis may be conducted by either a manual method or automatic method. The manual ROI requires the outline of the neuroanatomical structure of interest to be traced and a subsequent calculation of volume. The manual ROI approach has some limitations: firstly, manual methods of ROI analysis are a time-consuming process and require great expertise in neuroanatomy. Secondly, ROI analysis depends on the appropriate *a priori* choice of structures to be analysed. The structures are usually chosen according to an *a priori* hypothesis and so this approach may fail to find new and unexpected cerebral morphological changes. Automated ROI methods are possible as image processing and advanced computational algorithms have enabled automatic extraction of structures from MRI.

Voxel-based morphometry

Voxel-based morphometry (VBM) is a validated operator independent method for comparing volumes of brain structures and gives a whole brain assessment of anatomical differences throughout the brain. It provides an unbiased voxel-by-voxel comparison to assess the whole brain structure. The voxel-wise analysis is possible because all brains can be spatially normalised into a common anatomical space. Thus, each voxel relates to the same anatomical structure across all brains. Spatially normalised brain images can then be segmented into different tissue classes (e.g. GM, white matter (WM), cerebrospinal fluid). The deformation required to normalise brains into standard space gives a measure of atrophy. The smoothed, normalized images can then be statistically interrogated to localise regional volume changes in individual or groups of participants, or correlation analyses between cognitive deficits and volume changes can be performed across participants.

One significant challenge that arises when analysing VBM data is that the statistical tests are performed across many thousands of voxels: if uncontrolled for multiple comparisons, false positives are common. Several approaches have been developed for controlling false positives in neuroimaging at either a voxel or cluster level (a larger group of voxels), including using Gaussian random field theory (Friston et al. 1994), false discovery rate (Chumbley and Friston 2009; Genovese, Lazar, and Nichols 2002), and permutation testing (Nichols and Holmes 2002; Smith and Nichols 2009).

Recently, DARTEL (SPM12; Wellcome Trust Centre for Neuroimaging, London, United Kingdom), a fast diffeomorphic registration algorithm, has been developed for use with VBM [277]. This involves creating a mean image of all those taken, which serves as a subject-specific template. Subsequently, whole-brain images of individual subjects are normalised to the template, modulated, and smoothed. DARTEL was shown to improve registration and provide precise and accurate localisation of structural damage. The DARTEL toolbox is a high-dimensional warping process that increases the registration between individuals and thereby improves localisation and increases sensitivity during analyses.

Surface based analysis

Surface-based morphometry refers to a number of methods used to analyse the cortical surface of the brain while taking into account the individual gyrification of the brain. It attempts to complement VBM analysis by providing measures of cortical thickness, surface area and folding patterns, alongside GM volume. Surface-based analysis is conducted by identifying the borders between tissue subtypes but firstly requires the removal of extra-cerebral voxels using a process called skull stripping. Cortical thickness can be defined by using a number of surface-based measurements and is typically calculated by measuring the distance between the boundary between WM and cortical GM, and GM and the pia mater as determined on the basis of brain segmentation. The variety of means of defining the cortical surface area can limit the ability to reproduce or compare values across studies from different centres.

4.3 Comparison of focal atrophy in DLB and AD

MTL and hippocampal volume differences in DLB and AD

Regional structural changes have an important role in differentiating between DLB and AD (see Table 4.1 and 4.2). MTL or hippocampal atrophy noted on MRI can be used to help distinguish between DLB and AD both in clinically diagnosed patients and in pathologically confirmed cases. Ante-mortem MRI findings in DLB have demonstrated relative preservation of MTL structure, particularly the hippocampus, with more pronounced GM volume loss of the MTL and the hippocampus in AD [278-281]. In patients with a pathologically confirmed diagnosis of DLB and AD, MTL atrophy has been shown to be very specific for AD in comparison with DLB (specificity of 94%) [281]. Therefore, the presence of hippocampal atrophy in DLB is suggestive of co-morbid AD pathology [7]. In clinically diagnosed cohorts, the differences in MTL volume between DLB and AD are based on group studies and do not reliably distinguish DLB from AD on an individual subject level as demonstrated by the low reported sensitivity in some studies. A large European multicentre study with pathological confirmation of the dementia diagnosis found that MTL atrophy on MRI, as assessed by a visual rating scale, had a sensitivity of 64% and specificity of 68% in distinguishing between AD and DLB [282]. These results are not very encouraging for the biomarker potential for MTL volume as assessed by MRI to discriminate between AD and DLB but MTL preservation has been incorporated into the latest consensus criteria for the diagnosis of DLB as a supportive biomarker of DLB and as a potential biomarker for MCI-LB in the research criteria for prodromal DLB [7, 9].

Comparison of hippocampal subfields and extra-hippocampal structures in DLB and AD

The hippocampus and adjacent extra-hippocampal structures are anatomically complex. The hippocampus consists of cytoarchitectonically different subfields, notably the subiculum, cornu ammonis (CA1-CA4), and dentate gyrus (DG). Pathology evidence indicates that the hippocampal subfields are not uniformly affected by AD pathology, with some regions being more vulnerable than others particularly early in the disease trajectory. NFTs begin in the entorhinal area before spreading to the CA1 and subsequently to the CA2 and CA3 areas ahead of affecting the neocortex [283, 284]. This temporal spread of AD pathology results in a distinct pattern of atrophy in the hippocampal subfields and extra-hippocampal structures in DLB and AD.

Relatively few studies have explored the differences in the atrophy patterns of the hippocampal subfields between DLB and AD (see Table 4.2). Mak et al. examined differences between hippocampal subfields in a well characterised clinical cohort of AD (n= 36), DLB (n=35) and HC (n= 35) cases [285]. This study found a global pattern of significant atrophy affecting all hippocampal subfields in AD compared with HC and DLB groups after controlling for age, sex, education and intracranial volume. The only hippocampal subfield found not to have significantly atrophied in AD compared with HC and DLB groups was the fissure. CA1 and fimbria subfields were relatively preserved in DLB compared to HC and AD. Alongside the well characterised clinical cohort, the other major strength of this study was the use of a publicly available automated segmentation technique to delineate the hippocampal subfields. The major limitation of this study was lack of neuropathological confirmation of the AD and DLB diagnosis. Delli Pizzi et al. also examined with structural MRI the differences in hippocampal subfield and adjacent extra-hippocampal structures between AD and DLB [286]. They reported that the CA and subiculum were bilaterally damaged in AD and preserved in DLB. The perirhinal cortex and parahippocampus were damaged in DLB but not in AD. Other studies have also demonstrated that the CA1 hippocampal subfield alongside the fimbria and the fissure is preserved in DLB compared to AD [285, 287].However, some studies have indicated that there was increased atrophy rather than preservation of the CA1 in DLB relative to HC but the results of these studies may be explained by methodological differences in delineating the subfields [280, 288].The clinical utility of hippocampal subfield volumetry to aid in the differential diagnosis of DLB from AD remains unclear due to small number of studies exploring this concept and methodological differences in segmenting out the hippocampal subfields.

Other focal atrophy differences between DLB and AD

Other areas of focal atrophy have been reported in DLB relative to AD. However, there is a substantial overlap between these regions of atrophy in DLB and AD, therefore limiting its clinical utility to allow for differential diagnosis as they are not specific to either condition. An ROI study with 72 patients with a clinical diagnosis of DLB and 72 patients with AD did not find greater atrophy of the striatum in DLB than in AD [278]. Instead, this study found midbrain structures such as dorsal mesopontine GM volume, hypothalamus and the substantia innominate to have increased atrophy in DLB relative to AD [278]. The results of this study are consistent with the idea of greater cholinergic dysfunction in DLB relative to AD as many of these areas are involved in the cholinergic pathways. Regarding striatal atrophy, studies to date would indicate that this is linked to the amount of global atrophy present in the cohort and is not regionally specific. Recent studies would indicate that there is no difference between DLB and AD patients in terms of caudate or putaminal volumes [289, 290].

Study	Year	MR measurement	Group	Diagnosis	Findings in DLB patients
Whitwell et al. *[278]*	2007	Voxel-based morphometry & ROI-based analysis to assess global and regional atrophy	72 DLB 72 AD 72 HC	Clinical Diagnosis (2005 Consensus criteria)	DLB exhibited preservation of the medial temporal lobe, inferior temporal regions as well as hippocampus and temporoparietal cortex compared to AD. Both AD and DLB demonstrated a loss of GM in the substantia innominata, though DLB exhibited a greater loss within the midbrain compared to AD. Substantia innominata was reduced more in AD vs DLB Midbrain reduced in DLB than AD Hippocampus and temporoparietal more greatly reduced in AD than DLB Little cortical loss in DLB. AD has greater GM loss in the MTL bilaterally, the left inferior, middle and superior temporal gyri, and in the left parietal lobe than DLB Compared with DLB hippocampal volumes 16% smaller in AD, Substantia innominata were 4% smaller in AD than DLB
Sabattoli et al. *[280]*	2008	Manual ROI hippocampal and hippocampal subfields segmentation to assess atrophy	14 DLB 28 AD 28 HC	Clinical diagnosis (2005 Consensus criteria)	CA1 loss in AD more than DLB CA2-3 atrophy more distinctive for DLB
Firbank et al. *[287]*	2010	Manual ROI hippocampal and subfields segmentation to assess atrophy	16 DLB 16 AD 16 HC	Clinical diagnosis (2005 Consensus criteria)	CA1 reduced in AD vs DLB Subiculum reduced in AD vs DLB Correlation of the Rey delayed score and hippocampal area and volume.
Goto et al. *[291]*	2010	1.5 MRI to assess GM & WM atrophy SPECT	19 DLB 19 AD	Clinical diagnosis (criteria 2005)	DLB showed significantly lower GM volume in the striatum compared with AD No significant different between hippocampal volumes in DLB and AD

Chow et al. *[288]*	2012	Hippocampal volume assessed by radial distance technique	16 DLB 55 AD 42 HC	Clinical diagnosis (2005 Consensus criteria)	DLB demonstrated atrophy predominately within the left CA1 region and subiculum compared to HC No difference in hippocampal atrophy and subfields between DLB vs AD.
Watson et al. *[292]*	2012	Voxel-based morphometry DARTEL to assess atrophy	35 DLB 36 AD 35 HC	Clinical Diagnosis (2005 Clinical criteria)	DLB appeared to have a relative preservation of the MTL compared to AD. Particularly left hippocampus and parahippocampus (right & left)
Kantarci et al. *[279]*	2012	Multimodal MRI with Voxel-based morphometry & ROI to assess atrophy PiB PET FDG PET	21 DLB 21 AD 42 HC	Clinical diagnosis (Criteria 2005) Five pathological confirmation cases (AD n=2, DLB n=3)	Hippocampal atrophy, global cortical PiB retention and occipital lobe metabolism in combination distinguish DLB from AD better than measurements alone Cortical GM density of patients with DLB was not different from HC. DLB hippocampal preserved relative to AD No correlation between hippocampal volumes and motor, core features.
Mak et al. *[293]*	2015	Cortical thickness and subcortical volumes to assess atrophy	13 DLB, 23 AD 33 HC	Clinical criteria (criteria 2005)	AD exhibited greater hippocampal atrophy compared to DLB. In DLB, cortical thinning in the frontal and parietal regions correlated with a decline in global cognition and motor deterioration.
Delli Pizzi et al. *[286]*	2016	Cortical thickness and subcortical volumes to assess atrophy Hippocampal subfields and extra-hippocampal structures	19 DLB 15 AD 19 HC	Clinical diagnosis (2005 Consensus criteria)	The perirhinal cortex, entorhinal cortex and parahippocampus had more atrophy in DLB vs controls but no difference between DLB vs AD Left but not right hippocampal volumes significantly reduced in AD vs DLB CA1 bilaterally reduced in AD vs DLB Left CA2-3, CA4-DG, and subiculum reduced in AD vs DLB No significant correlations were found between imaging and clinical outcomes

Mak et al. *[294]*	2016	Multimodal study (3T MRI & DTI) Microstructural WM and GM atrophy	23 MCI 17 DLB 14 AD 30 HC	Clinical diagnosis (2005 Consensus criteria)	AD & MCI had smaller hippocampal volumes compared to DLB, mainly affecting CA1 & subiculum subfields. CA1 was smaller in AD and trend-level in MCI compared to DLB. Hippocampal volumes are a strong predictor of memory scores In terms of WM association with GM atrophy, hippocampal mean diffusivity was negatively associated with the total subiculum in DLB.
Mak et al. *[285]*	2016	Automated Hippocampal volumes and subfields using Freesurfer to assess hippocampal atrophy	35 DLB 36 AD 35 HC	Clinical (2005 Consensus criteria)	Relative atrophy rates of hippocampal to controls; AD -29.5%, DLB -10.3%. All hippocampal subfields except fissure atrophied in AD compared to both DLB and HC. Correlation in DLB subjects with CA1 and recent memory score of the CAMCOG and Delayed Recall subscores of the HVLT.
Elder et al. *[295]*	2017	3T MRI Cortical thickness Hippocampal, parahippocampal, entorhinal and temporal pole cortical thickness	65 AD 76 DLB 63 HC	Clinical diagnosis (Criteria 2005)	In DLB, parahippocampal, entorhinal and temporal pole thickness associated with memory scores DLB hipppocampal thickness > than in AD
Shimizu et al. *[296]*	2017	MIBG ^{123}I-FP-CIT 1.5T MRI using ROI Hippocampal z scores	32 AD 32 DLB	Clinical diagnosis (Criteria 2005)	No difference in the z-scores of hippocampal atrophy between DLB & AD

Abbreviations: VBM= Voxel-based morphometry, VBM-Dartel= Voxel-based morphometry Diffeomorphic Anatomical Registration Through Exponentiated Lie Algebra, ROI= Region of Interest, FDG PET= Fluorodeoxyglucose Positron Emission Tomography, PiB PET= Pittsburgh compound B Positron Emission Tomography, SPECT= Single-photon emission computed tomography, MRI= Magnetic Resonance Imaging, MIBG= Metaiodobenzylguanidine, 123I-FP-CIT= (123)I-labelled 2β-carbomethoxy-3β-(4-iodophenyl)-N-(3-fluoropropyl) nortropane, DLB= Dementia Lewy bodies, AD= Alzheimer's disease, HC= healthy controls, PD=Parkinson's disease, PDD=Parkinson's disease dementia, FTD = frontotemporal dementia, FTLD=Frontotemporal lobar degeneration, MCI=Mild cognitive impairment, VaD= Vascular Dementia, FLAIR= Fluid-attenuated inversion recovery, EEG= Electroencephalography, GM=Grey matter, WM= White matter, CA= Cornu Ammonis AUR= Area under receiver operator curve, DG=Dentate gyrus, HVLT= Hopkins verbal learning test, CAMCOG= Cambridge cognition examination, HVLT= Hopkins Verbal Learning Test.

Table 4. 1 Hippocampal atrophy and subfield atrophy studies in DLB

4.4 Global atrophy in DLB and AD

4.4.1 Global atrophy in AD versus healthy controls

Cerebral atrophy is the eventual downstream effect of neurodegeneration and correlates with accompanying neurofibrillary pathology in AD. It may be detectable early in AD and even at pre-symptomatic disease stages. Global atrophy measurements are good discriminators of AD from HC. In AD, increased global atrophy compared to HC is demonstrable several years prior to diagnosis of AD on cross-sectional studies [297] and the accelerated rates of atrophy occurring in AD compared to HC have also been demonstrated at intervals as short as three to six months of follow-up [298, 299]. Reported global atrophy rates of decline in AD range from 1% to 4% per year while atrophy rates in healthy aged individuals range from 0.3% to 0.7% per year [300]. Evans et al. reported a global atrophy rate of 1.5% per year in AD patients compared to 0.5% per year in HC [301]. Furthermore this study showed that MCI subjects had an intermediate rate 1.1% per year and those MCI patients who progressed to AD had a brain atrophy twice that of MCI non-converters. This has resulted in longitudinal global atrophy rates being used as a secondary outcome marker in phase III trials of potentially disease-modifying interventions.

4.4.2 Global atrophy in DLB versus healthy controls

The evidence to date would not support global atrophy being different between DLB and age-matched healthy HC. Mak et al. showed that DLB did not demonstrate any difference in global atrophy rates compared with HC after 12 months despite there being evidence of cognitive decline in the DLB cohort [300]. Similarly, a study by Whitwell et al., in which the eventual diagnosis had pathological verification, showed that global atrophy was similar among DLB patients and HC supporting the idea that early LB pathology resulted in limited neuronal loss and atrophy [302]. However, this study also showed that global atrophy and ventricular expansion were significantly increased in patients with mixed DLB/AD pathology compared to HC [302].

4.4.3 Global atrophy in DLB versus AD

DLB shows less pronounced global atrophy on cross-sectional and longitudinal studies than AD. Generally, the outcome of cross-sectional studies can be summarised to state that among patients with DLB, distinct areas of subcortical atrophy occur involving the midbrain, corpus striatum (caudate, putamen, pallidum) and thalamus, but with sparing of cortical tissue and preservation of the MTL on cross-sectional studies [278, 303]

Longitudinal studies using repeat MRI to investigate differential atrophy rates between DLB and AD have yielded conflicting findings. Global rate of whole brain atrophy has been shown to be significantly less in DLB (1.0%) than AD (1.8%) over 1 year, with DLB atrophy rate being in line with that of HC whole brain atrophy rate (0.9%) [300]. Whitwell et al. showed in a post-mortem confirmed diagnosis cohort that the atrophy rate per year was significantly different between DLB (0.4%) and AD (1.1%) about half the rate reported in the prior study [302]. However, other studies have failed to find a difference between the whole brain atrophy in DLB and AD [304]. In a study by O'Brien et al., the rate of whole brain atrophy was lower in DLB (1.4%) than in AD (2%) but not significantly, the relatively small sample size of the study (10 DLBs and 9 ADs) might have reduced the statistical power to detect a between-group difference. A possible explanation for the conflicting results may be related to mixture of LB and AD pathology found in DLB. Nedelska et al. also showed that mixed DLB/AD pathology had greater rates of whole and focal atrophy than DLB patients without significant AD-type pathology, and global atrophy rates in mixed DLB/AD pathology were similar to AD patients [305].

4.5 Cortical thinning in DLB

Cortical thickness measurement have been shown to be highly accurate in identifying morphological changes arising from underlying neuropathological substrates. Hence, its utilisation in a number of studies to differentiate DLB from AD and HC. Cortical thinning is well established to occur in AD [306]. In DLB, cortical thinning is less diffuse than in AD and affects posterior brain structures and temporal structures [307]. Similar to VBM studies, cortical thickness studies have shown relative sparing of the MTL, particularly the hippocampus and adjacent hippocampal regions [295, 308]. The average reduction in cortical thickness in MTL is less severe in DLB (6-10%) than in AD (15-24%) and with a reduction in cortical thickness observed in other regions including inferior parietal, precuneus, and posterior cingulate (6-9%). In addition, but less consistently, cortical thinning has been reported to be reduced in DLB compared to AD in the temporo-occipital, orbitofrontal, and occipital cortices [173, 307, 308].

In an attempt to explore the role of concomitant AD pathology in DLB, some studies have used Aβ biomarkers in combination with MRI assessment of cortical thickness. Van der Zande measured

cortical thickness between DLB patients with and without AD pathology, AD patients and HC, and found that while there was no significant difference in cortical thickness between the three dementia subgroups, instead there was a stepwise decrease of cortical thickness from HC, DLB, mixed DLB/AD to AD [309]. All dementia groups showed increased atrophy compared to the control group. This includes the "pure DLB" patients who had a less posterior cortical atrophy and lower global cortical atrophy and more diffuse cortical thinning than age-matched HC. Lee et al. compared cortical thinning in Aβ-negative DLB and control group, the Aβ-negative DLB group exhibited cortical thinning in the bilateral insula, entorhinal, basal frontal, and occipito-parietal cortices [310]. Compared to the control group, Aβ-positive DLB group had cortical thinning in almost all brain regions [310]. The findings of this study differ from other studies that showed DLB with negative amyloid biomarkers have cortical thinning that was not different than HC [311].

4.6 Comparison of between DLB and PDD

Structural MRI studies in DLB and PDD have shown GM loss which is more pronounced in DLB compared to PDD, which is in keeping with the greater amyloid burden [312]. However, this has not been a universal finding with Burton et al. being unable to identify distinct cortical atrophy profiles in DLB and PDD [313]. The reason for the differing finding might again be related to the degree of amyloid burden in DLB. Shimada et al. has shown that amyloid-negative DLB/PDD patients had no significant cortical atrophy [311]. In those studies demonstrating a difference in GM loss between DLB and PDD, the localisation of GM loss tended to be in posterior cortical region which would be consistent with presence of early visual hallucinations in DLB. Beyer et al. reported more pronounced cortical atrophy in DLB than in PDD in the temporal, parietal, and occipital lobes [314]. Lee et al. showed a similar pattern of cortical atrophy to Beyer et al. [315]. In terms of MTL atrophy, Tam et al. has shown that on visual rating of the hippocampi, PDD subjects had less hippocampi atrophy that DLB and AD subjects [316].

WM alterations appear to be more pronounced in DLB compared to PDD. The area of WM atrophy in the occipital areas was more extensive than that of GM atrophy in the DLB group compared to PDD [315]. Joki et al. showed that WMH are more prominent in AD, DLB and PDD patients than in PD patients with normal cognition, suggesting that WMH in DLB may reflect mainly AD-related pathology rather than atherosclerotic cerebrovascular changes [317].

Study	Year	MR measurement	Group	Diagnosis	Findings in DLB patients
Barber et al. *[318]*	2000	Cortical thickness	27 DLB 25 AD 24 VaD 26 HC	Clinical diagnosis (1996 Consensus criteria)	DLB patients had larger temporal lobe, amygdala and hippocampal volumes compared to AD, with no volumetric difference compared to VaD. Compared to HC, DLB exhibited relative preservation of whole brain volume.
Barber et al. *[289]*	2002	1T MRI ROI volume analysis of the caudate	26 DLB 21 AD 18 VaD 25 HC	Clinical diagnosis (1996 Consensus criteria)	No correlation between caudate volume and parkinsonism. No difference between dementias in terms of caudate volumes
Burton et al. *[319]*	2002	Voxel-based morphometry	25 DLB 30 AD 25 HC	Clinical diagnosis (1996 Consensus criteria)	Loss of GM volume bilaterally in the temporal and frontal lobes and insular cortex in patients with DLB compared to HC. Preservation of the MTL, hippocampus and amygdala in DLB compared to AD.
Ballmaier et al. *[320]*	2004	Cortical thickness	16 DLB 29 AD 38 HC	Clinical diagnosis (1996 Consensus criteria)	DLB exhibited significantly less GM deficits bilaterally in the temporal lobe compared to AD
Burton et al. *[313]*	2004	Voxel-based morphometry	17 DLB 26 PDD 31 PD 28 AD 26 HC	Clinical diagnosis (1996 Consensus criteria)	PDD exhibited bilateral loss of GM in the occipital lobe compared to PD. AD exhibited temporal lobe atrophy, including parahippocampal gyrus and hippocampus, compared to PDD. No differences found between PDD and DLB
Beyer et al. *[314]*	2007	Voxel-based morphometry	18 DLB 15 PDD 21 AD 20 HC	Clinical diagnosis (2005 Consensus criteria)	DLB exhibited increased cortical atrophy with the temporal, parietal and occipital lobes compared to PDD. AD exhibited greater atrophy within the temporal and frontal lobe compared to DLB
Ishii et al. *[321]*	2007	1.5T MRI VBM FDG-PET	20 DLB 20 AD 20 HC	Clinical diagnosis (1996 Consensus criteria)	Left caudate volume reduced in DLB compared to AD Striatal volume in DLB were significantly smaller than those in AD.

Sanchez-Castaneda et al. *[322]*	2009	Voxel-based morphometry	12 DLB 16 PDD 16 HC	Clinical diagnosis (2005 Consensus criteria)	DLB demonstrated increased GM atrophy in the right inferior frontal lobe, the right superior frontal gyrus and the right premotor area compared to PDD. Within the DLB group, reduced anterior cingulate and prefrontal volume correlated with worse performance on the Continuous Performance Test, whilst right hippocampal and amygdala volume correlated with Visual Memory Test
Lee et al. *[315]*	2010	Voxel-based morphometry	18 DLB 20 PDD	Clinical diagnosis (2005 Consensus criteria)	DLB exhibited greater GM atrophy in the left occipital, parietal and striatal areas compared to PDD, as well as a greater reduction in WM density within the occipital and left occipito-parietal areas
Sanchez – Castaneda et al. *[323]*	2010	Voxel-based morphometry	12 DLB 15 PDD	Clinical diagnosis (2005 Consensus criteria)	DLB with hallucinations exhibited greater loss of GM in the right inferior frontal gryus compared to DLB without hallucinations. Compared to PDD with hallucinations, DLB with hallucinations had a greater reduction of GM in the bilateral premotor area, as well as reduced volume in the left precuneus and inferior frontal lobe correlating with visual hallucination
Takashashi et al. *[324]*	2010	Voxel-based morphometry VBM-Dartel	51 AD 42 DLB 40 HC	Clinical diagnosis (2005 Consensus criteria)	Greater decrease in GM volume in right MTL and left parahippocampal gryus hippocampus in AD than DLB. WM volume was preserved in DLB compared to HC.
Kim et al. *[325]*	2011	3T MRI Manual ROI Substantia innominate volume.	24 HC 45 aMCI 38 PD-MCI 40 AD 31 PDD 22 DLB	Clinical diagnosis (2005 Consensus criteria)	Substantia innominate decreased in all other groups compared to controls. There was significant correlation with substantia innominate and MMSE score in DLB cohorts but not in AD

Hayashi et al. *[284]*	2012	Voxel-based morphometry	60 DLB 210 AD	Clinical diagnosis (2005 Consensus criteria)	DLB exhibited less atrophy in the entorhinal cortex compared to AD
Rodriguez et al. *[326]*	2012	Visual rating of MTL atrophy	30 HC 30 AD 31 DLB	Clinical diagnosis (2005 Consensus criteria)	MTL atrophy is less in DLB compared to AD. MTL atrophy discriminated between DLB and AD
O'Donovan et al. *[327]*	2013	Visual rating 3T MRI	36 AD 35 DLB 35 HC	Clinical diagnosis (2005 Consensus criteria)	MTL visual rating of atrophy higher in AD relative to DLB No difference in posterior atrophy Ventricular enlargement was similar in AD & DLB, but higher that in controls.
Lebedev et al. *[308]*	2013	Cortical thickness	97 DLB 97 AD	Clinical diagnosis (Some 1996 Consensus Criteria 1996, others 2005 Consensus criteria) Pathological confirmation 7 (5 AD and 2 DLB)	DLB and AD were differentiated with a sensitivity of 82.1% and specificity of 85.7%. Cortical thinning, in DLB, was localised to the middle and posterior cingulate, lateral orbito-frontal and superior temporo-occipital regions
Colloby et al. *[328]*	2014	VBM-Dartel 3T MRI	39 HC 47 AD 41 DLB	Clinical diagnosis (2005 Consensus criteria)	No difference in GM and WM atrophy between AD and DLB
Grothe et al. *[329]*	2014	Sub-regional atrophy of basal forebrain ROI automated basal forebrain	11 DLB 11 AD 22 HC	Clinical diagnosis (2005 Consensus criteria)	Similar rates of basal forebrain atrophy in DLB & AD, approximately 20-25% compared to controls.
Watson et al. *[307]*	2015	Cortical thickness	31 DLB 30 AD, 33 HC	Clinical diagnosis (2005 Consensus criteria)	In DLB, cortical atrophy was less diffuse compared to AD, though cortical change was found to predominately affect posterior structures (inferior

					parietal, fusiform gyrus and posterior cingulate). In DLB, the average reduction in MTL cortical thickness was (6-10%) compared to AD (15-24%)
Mak et al. *[300]*	2015	3T MRI Serial MRI baseline and 12 month repeat Whole brain volume change over time	14 DLB 25 AD 33 HC	Clinical criteria (2005 Consensus criteria)	AD rate of atrophy 1.8% per year DLB rate of atrophy 1% per year HC rate of atrophy 0.9% per year AD atrophy significantly greater than DLB and HC No difference between DLB and HC
Tagawa et al. *[330]*	2015	1.5T MRI ROI Entorhinal cortex Hippocampus Amygdala	37 DLB	Clinical diagnosis (2005 Consensus criteria)	MTL atrophy correlated with cognitive impairment in DLB
Watson et al. *[303]*	2016	Cortical thickness and cortical volumes 3T MRI	33 DLB 32 AD 35 HC	Clinical diagnosis (2005 Consensus criteria)	DLB exhibited volumetric loss in the bilateral putamen, left thalamus and total subcortical grey measures compared to controls. AD exhibited a more pronounced loss of GM volumes in the left pallidum, right thalamus and bilateral amydala and hippocampus compared to DLB.
Colloby et al. *[331]*	2015	Visual Rating MTL atrophy Multimodal EEG & MRI	21 HC 30 AD 21 DLB	Clinical diagnosis (2005 Consensus criteria)	MTL atrophy diagnostic accuracy is AUC 0.70 with sensitivity 67% & specificity 57%
Colloby et al. *[332]*	2016	3T MRI	39 HC 47 AD 41 DLB	Clinical diagnosis (2005 Consensus criteria)	Bilateral GM loss in substantia innominata in DLB. No difference between DLB & AD In DLB, GM volume loss in substantia innominata associated with level of cognitive impairment and severity of cognitive fluctuations.
Gazzina et al. *[333]*	2016	1.5T MRI Subcortical atrophy	16 PD 11 PDD 16 DLB	Clinical diagnosis (2005 Consensus criteria)	PDD and DLB showed global subcortical atrophy compared to PD. Greater atrophy in pallidum discriminated DLB from PDD

Sarro et al. *[334]*	2016	3T MRI - VBM-Dartel ^{11}C-PiB PET Association between amyloid deposition and longitudinal rates GM atrophy Longitudinal - MRI preformed 1 to 5 years from baseline	22 DLB	Clinical diagnosis (2005 Consensus criteria)	Significant association between baseline amyloid and GM loss over time in the posterior cingulate gyrus, lateral and MTL, and occipital lobe.
Watson et al. *[335]*	2017	3T MRI Thalamic atrophy	35 DLB 35 HC	Clinical diagnosis (2005 Consensus criteria)	DLB showed bilateral atrophy in the ventral dorsal and pulvinar regions relative to controls

Abbreviations: VBM= Voxel-based morphometry, VBM-Dartel= Voxel-based morphometry Diffeomorphic Anatomical Registration Through Exponentiated Lie Algebra, ROI= Region of Interest, FDG PET= Fluorodeoxyglucose Positron Emission Tomography, PiB PET= Pittsburgh compound B Positron Emission Tomography, SPECT= Single-photon emission computed tomography, MRI= Magnetic Resonance Imaging, MIBG= Metaiodobenzylguanidine, 123I-FP-CIT= (123)I-labelled 2β-carbomethoxy-3β-(4-iodophenyl)-N-(3-fluoropropyl) nortropane, DLB= Dementia Lewy bodies, AD= Alzheimer's disease, HC= healthy controls, PD=Parkinson's disease, PDD=Parkinson's disease dementia, FTD = frontotemporal dementia, FTLD=Frontotemporal lobar degeneration, MCI=Mild cognitive impairment, aMCI= Amnestic mild cognitive impairment, VaD= Vascular Dementia, FLAIR= Fluid-attenuated inversion recovery, EEG= Electroencephalography, WM=White matter, GM=Grey matter, EEG= Electroencephalogram, AUC= Area under the curve, MTL= Medial temporal lobe

Table 4. 2 Structural MRI studies exploring global and regional patterns of atrophy in DLB.

4.7 White matter hyperintensities in DLB

WMH are areas of discrete high signal of varying size and located in WM which are detectable by T2-weighted MRI and are indicative of demyelination and axonal loss of presumed vascular origin [336] [276]. WMH may also be associated with the neurodegenerative process associated with dementia [337]. Assessment of WMH may be carried out using visual rating scales such as; the Fazekas scale [338], age-related WM change scale [339] and the Schelten scale [340]. The utilisation of visual rating scales to quantify WMH is limited by intra-rater and inter-rater variation and a lack of detail relating to the size and location of WMH [341]. A more objective measure of determining WMH burden is semi-automated methods to segment brain volumes into their tissue class based on pre-defined features such as signal intensity. Volumetric studies of WMH are more sensitive and allow for the provision of more anatomical information relating to the location and sizes of WMH [342].

WMH are relatively common in older people and their contribution to dementia is unclear. WM damage can be identified visually on T2-weighted MRI by the presence of focal punctate areas of high intensity signal. Studies have reported no difference in WMH between DLB and AD [318, 343]. A longitudinal study by Burton et al. showed that while baseline WMH was significantly greater in AD compared with HC, no significant difference was found between HC and DLB patients [344]. Significant WMH progression on repeat imaging 1 year later was found not to be significantly different between dementia subtypes but due to the severity of baseline WMH [344]. This is in conflict with other studies which showed WMH are predictive of progression from MCI to AD dementia, an increase of one point in WMH rating associated with a 59% increase risk of conversion [345]. A VBM-DARTEL study by Takahashi et al. revealed no significant decrease in WM in patients with DLB compared with HC. Comparisons between DLB and AD patients revealed more widespread atrophy of WM in AD patients affecting bilateral temporal lobes, right frontal lobe, right temporal lobe and medial parieto-occipital lobe [324]. The more pronounced WM atrophy in the MTL in the AD group is unsurprising given that WMHs correlate with hippocampal atrophy [345]. A post-mortem study by De Reuck et al., using a 7-Tesla MRI reported that DLB had more cerebral micro-infarcts than HC and the smallest lesions were observed more commonly in DLB than in vascular dementia and AD [346]. Ballard et al. showed there was association between orthostatic hypotension and WMH in the basal ganglia and deep WM [347]. WM changes and abnormalities are

relatively understudied in DLB and more work is required to examine in role in DLB and its progression over the disease course.

Study	Year	MR measurement	Assessment	Diagnosis	Group	Findings in DLB patients
Ballard et al. *[347]*	2000	Visual inspection of WM lesions on T2-weighted MR images	WMH	17 DLB 13 AD	Clinical diagnosis (1996 Consensus criteria)	Blood pressure drop >30mm Hg was associated with the severity of hyperintensities in the deep WM and basal ganglia
Barber et al. *[318]*	2000	Ventricular volumes and WM lesions	WMH	27 DLB, 25 AD	Clinical diagnosis (1996 Consensus criteria)	Periventricular hyperintensities correlated with increasing age and ventricular dilation in all subjects. Deep matter hyperintensities were associated with hypertension history
Burton et al. *[344]*	2006	Automated technique using FLAIR image	WM volume	14 DLB, 13 PDD, 23 AD, 33 HC	Clinical diagnosis (2005 Consensus criteria)	AD exhibited increased WM volume compared to HC. No differences were found in WM volume in DLB compared to HC, AD or PDD
Takashashi et al. *[324]*	2010	Voxel-based morphometry VBM-Dartel	Pattern GM atrophy	51 AD 42 DLB 40 HC	Clinical diagnosis (2005 Consensus criteria)	Greater decrease in GM volume in right MTL and left parahippocampal gryus hippocampus in AD than DLB. WM volume was preserved in DLB compared to HC.
Oppedal et al. *[343]*	2012	WM volume Using freesurfer	WMH load	61 AD 16 LBD (12 DLB & 4 PDD) 37 HC	Clinical diagnosis (2005 Consensus criteria) 7 with pathological diagnosis	No significance difference between WMH between AD and DLB No correlation between WMH and cognition in DLB but in AD.
Fukui et al. *[348]*	2013	Visual inspection of T2* weighted MR images	Cerebral microbleeds quantification	59 DLB, 81 AD	Clinically diagnose	DLB exhibited increased microbleeds in all brain areas, apart from occipital lobe, compared to AD. The number of microbleeds was positively correlated with the severity of WM lesion in both DLB and AD
Nakatsuka et al. *[349]*	2013	Voxel-based specific regional analysis for AD (VSRAD) based on SPM8 plus DARTEL T1 Weighted MRI MIBG	WM atrophy	60 DLB 30 AD	Clinical Diagnosis (2005 Clinical criteria)	Midbrain, pons and cerebellum atrophy in DLB patients. Midbrain atrophy has the highest power to discriminate between DLB and AD.

Colloby et al. *[328]*	2014	VBM-Dartel 3T MRI	Cerebellar GM and WM atrophy	39 HC 47 AD 41 DLB	Clinical diagnosis (2005 Consensus criteria)	No difference in GM and WM atrophy between AD and DLB
Hyung-Eun Park et al. *[350]*	2015	3T MRI	Visually rating scale cholinergic pathway hyperintensities scale	20 AD 17 DLB 21 PDD 20 HC	Clinically diagnosed (2005 Consensus criteria)	Mean cholinergic pathway hyperintensities scale score were similar among the three dementia groups with no significant different between the dementia subgroups.
Gungor et al. *[351]*	2015	3T T2* weighted gradient-recalled-echo MRI	Visual rating of cerebral microbleeds	23 DLB 46 AD	Clinical diagnosis (2004 Consensus criteria)	DLB: 30% (7/23) had microbleeds AD: 24% (11/46) had microbleeds Similar frequency of microbleeds between AD and DLB AD had more cerebral microbleeds in temporal and infratentorial regions compared to DLB. No difference in occipital lobes between AD & DLB
Kim et al. *[352]*	2015	T2*-weighted gradient-echo imaging	Visual rating of cerebral microbleeds	42 DLB, 88 PDD, 35 HC	Clinical diagnosis (2005 clinical criteria)	Increased frequency of cerebral microbleeds in DLB (45.2%) compared to PDD (26.1%) Lobar cerebral microbleeds more common in DLB (40.5%) than PDD (17%), HC (8.6%), both deep and infratentorial microbleeds.
Takemoto et al. *[353]*	2016	Visual rating with Fazekas scale	WM	52 PDD 46 DLB	Clinical diagnosis (2005 Consensus criteria)	No difference in WM changes between PDD and DLB groups
Sarro et al. *[354]*	2017	3T MRI	Visual assessment of cortical and subcortical infarcts WMH quantified using a semi-automated algorithm on FLAIR	81 DLB 240 AD 81 HC	Pathology-confirmed	No association between WMH volume and the presence of DLB core features. RBD associated with lower WMH volume in patients with DLB Frequency of infarcts in DLB was not different from the matched HC and AD. WMH volume was higher in the occipital and posterior periventricular regions in DLB, compared to AD. DLB higher WMH volume compared to HC

Abbreviations: VBM= Voxel-based morphometry, VBM-Dartel= Voxel-based morphometry Diffeomorphic Anatomical Registration Through Exponentiated Lie Algebra, ROI= Region of Interest, FDG PET= Fluorodeoxyglucose Positron Emission Tomography, PiB PET= Pittsburgh compound B Positron Emission Tomography, SPECT= Single-photon emission computed tomography, MRI= Magnetic Resonance Imaging, MIBG= Metaiodobenzylguanidine, 123I-FP-CIT= (123)I-labelled 2β-carbomethoxy-3β-(4-iodophenyl)-N-(3-fluoropropyl) nortropane, DLB= Dementia Lewy bodies, AD= Alzheimer's disease, HC= healthy controls, PD=Parkinson's disease, PDD=Parkinson's disease dementia, FTD = frontotemporal dementia, FTLD=Frontotemporal lobar degeneration, LBD= Lewy body dementia, MCI=Mild cognitive impairment, VaD= Vascular Dementia, FLAIR= Fluid-attenuated inversion recovery, EEG= Electroencephalography, WM=White matter, WMH= White matter hyperintensities, RBD= REM sleep behaviour disorder, MTL= Medial temporal lobe .

Table 4. 3 MRI studies assessing WM alternations in DLB.

4.8 Diffusion tensor MRI

DTI is used to assess WM tracts by mapping and characterising the three-dimensional diffusion of water as a function of spatial location. In neurodegeneration, the disintegration of microstructural barriers (i.e. cell membranes, intracellular organelles, and myelin) results in a quantifiable difference in the diffusion of water along WM tracts that could be indexed by various diffusion tensor imaging metrics. Commonly used DTI measures include fractional anisotropy, mean diffusivity, radial diffusivity, and axial diffusivity.

DTI studies in DLB have reported varying extents of WM involvement with loss of posterior WM integrity being a consistent finding across a number of DTI studies when compared to HC [355-358]. Watson et al. revealed that the parieto-occipital WM tracts were preferentially affected in DLB though this appears to be an early phenomenon, as AD demonstrated a greater longitudinal increase in mean diffusivity or fractional anisotropy in DLB relative to HC [359]. There has also been studies that have reported a more widespread alterations in DTI metric such as reduced fractional anisotropy in the corpus callosum, frontal, parietal, occipital and temporal WM [356, 357]. Reduced fractional anisotropy in the occipital WM, specifically in the inferior longitudinal fasciculus, a pathway important for visuo-spatial processing, was a common finding in DLB patients [315, 355, 356, 358]. Comparing patients with DLB against those with PDD, a posterior dominance for reduced fractional anisotropy was found in DLB [357]

4.9 Sensitivity and specificity of structural MRI in pathologically proven DLB

A relatively limited number of studies have examined the role of structural MRI to discriminate between pathologically proven DLB and other neurodegenerative dementias. Burton et al. showed that in pathologically proven cases of AD and DLB, that visually rated MTL atrophy on MRI differentiated AD from DLB and vascular cognitive impairment with a sensitivity of 91% and specificity of 94% [281]. The results of this study indicate that evidence of ante-mortem MTL atrophy on MRI can discriminate AD from DLB with high accuracy. Furthermore, this Burton et al. study demonstrated that MTL atrophy is highly correlated with NFT and Aβ plaques, as opposed to LB pathology. However, another study, using post-mortem MRI to evaluate medical temporal atrophy in those over 85 years of age, showed that while MTL atrophy was highly associated with AD

pathology it had lower sensitivity and specificity (63% and 69%) to discriminate AD [360]. Therefore, MRI may be less able to differentiate between AD and DLB with increasing age due to increasing burdens of both AD and LB pathologies (mixed disease).

Automated approaches for analysing structural MRI data in order to differentiate between DLB and AD are of uncertain additional benefit compared to visual assessment alone. Harper et al. examined structural MRI in 184 post-mortem confirmed dementia subjects and determined the sensitivity and specificity of automated classification based on six visual rated scales (MTL, posterior atrophy, anterior temporal, orbito-frontal, fronto-insula, and anterior cingulate) to distinguish between AD and DLB [282]. Based on automated classification, Harper et al. were able to distinguish AD from DLB with a sensitivity 82% and specificity 64% and diagnostic accuracy of 73%. The lower specificity is likely a reflection of an elevated level of false positives as approximately 50% of DLB cases exhibit significant amyloid burden [361]. Nedelaska et al. reported that mixed DLB/AD subjects had a higher rate of brain atrophy, with areas of brain atrophy being similar to that seen in AD, predominantly affecting the temporoparietal cortices, amygdala and hippocampi [305].

Study	Year	MR measurement	Assessment	Pathological Diagnosis	Findings in DLB patients
Whitwell et al. *[302]*	2007	1.5 T MRI Serial MRI X 2	Rates of brain atrophy in neurodegenerative dementia	25 HC 9 DLB 13 Mixed 12 AD 12 FTLD-U 5 PSP 5 CBD	Atrophy rates in DLB were not different from control rates. In mixed AD/DLB the rates of whole brain atrophy and ventricular expansion were significantly increased compared to controls. AD and mixed AD/DLB showed similar rates of atrophy. DLB: -0.4% per year HC: -0.3% per year AD/DLB: -1.3% per year AD: -1.1% per year
Burton et al. *[281]*	2009	1T MRI	Visual rated MTL atrophy	23 DLB 11 AD 12 VCI	The MTL atrophy was found to serve as a diagnostic marker with high accuracy in differentiating AD from DLB and VCI Sensitivity and specificity DLB vs AD: 91% vs 94%
Vemuri et al. *[362]*	2011	1.5T MRI ROI	Patterns of Atrophy	120 HC 48 AD 20 DLB 47 FTD	DLB had bilateral amygdala, dorsal midbrain, bilateral inferior temporal and left middle temporal lobe atrophy compared to controls.
Kantarci et al. *[363]*	2012	1.5T MRI	Automated ROI Hippocampal Amygdala volumes Dorsal mesopontine	27 HC 25 High likelihood DLB 22 Intermediate DLB 9 Low likelihood DLB 33 AD	Ante-mortem hippocampal and amygdala volumes increase and dorsal mesopontine GM volumes decrease in patients with low to high likelihood DLB
Burton et al. *[364]*	2012	1T or 1.5T MRI	Neuropathological correlates of MTL volume measures on MRI	14 DLB 9 PDD	DLB has significantly smaller amygdala volume when compared with PDD. Negative correlation between amygdala volume and Lewy bodies

De Reuck et al. *[346]*	2014	7T MRI	Visual rating of cerebellar microbleeds and microinfarcts	21 HC 34 AD 15 AD-CAA 38 FTLD 12 ALS 16 Lewy body disease	DLB had more cerebral microinfarcts than HC. Smallest lesions were observed more commonly in DLB than in VaD and AD.
De Reuck et al. *[365]*	2015	7T MRI	Visual rating of cerebellar microbleeds and microinfarcts	29 "Pure" AD 9 AD associated with CAA 10 FTLD 9 ALS 10 Lewy body disease 12 PSP 9 VaD 16 HC	Excellent correlation between the MRI and the neuropathological findings. Cerebellar microbleeds and microinfarcts only significantly increased in the VaD
Nedelska et al. *[305]*	2015	1.5T MRI	Global atrophy and ROI atrophy	20 DLB 22 Mixed DLB/AD 30 AD 15 HC	The DLB group (n=20) without AD pathology lower rates of global & regional rates of atrophy, similar to controls Mixed DLB/AD greater rates in the whole brain, temporo-parietal cortices, hippocampus, amygdala, and ventricle expansion, similar to AD. In DLB and DLB/AD atrophy rates correlated with Braak neurofibrillary tangle stage, cognitive decline, and progression of motor symptoms.
Graff-Radford et al. *[366]*	2016	1.5T or 3T MRI	Survival analysis ROI hippocampal atrophy	167 DLB	Lower hippocampal volumes at diagnosis associated with shorter survival times in DLB
Harper et al. *[282]*	2016	1T/1.5T/3T MRI	VBM Atrophy	28 DLB 101 AD 55 FTLD 55 HC	Visual rating scales classification accuracy demonstrated to be equivalent to or better than expert diagnosis, using six visual rating scales; medial temporal, posterior, anterior temporal, orbito-frontal, anterior cingulate and fronto-insula) Sensitivity and specificity DLB vs AD: 64% & 82%

Abbreviations: VBM= Voxel-based morphometry, VBM-Dartel= Voxel-based morphometry Diffeomorphic Anatomical Registration Through Exponentiated Lie Algebra, ROI= Region of Interest, FDG PET= Fluorodeoxyglucose Positron Emission Tomography, PiB PET= Pittsburgh compound B Positron Emission Tomography, SPECT= Single-photon emission computed tomography, MRI= Magnetic Resonance Imaging, MIBG= Metaiodobenzylguanidine, 123I-FP-CIT= (123)I-labelled 2β-carbomethoxy-3β-(4-iodophenyl)-N-(3-fluoropropyl) nortropane, DLB= Dementia Lewy bodies, AD= Alzheimer's disease, HC= healthy controls, PD=Parkinson's disease, PDD=Parkinson's disease dementia, FTD = frontotemporal dementia, FTLD=Frontotemporal lobar degeneration, GM= Grey matter MCI=Mild cognitive impairment, VaD= Vascular Dementia, FLAIR= Fluid-attenuated inversion recovery, EEG= Electroencephalography, VCI= vascular cognitive impairment, ALS= Amyotrophic lateral sclerosis, CAA= Cerebral amyloid angiopathy, MTL= Medial temporal lobe

Table 4. 4 MRI studies in pathologically proven DLB.

4.10 Structural magnetic resonance imaging in prodromal DLB

Structural MRI has been studied in MCI-LB cohorts in a small number of cross-sectional studies. There is a lack of longitudinal studies in MCI-LB to determine how many do indeed convert to DLB. The studies relevant to structural MRI use in MCI cohorts with suspected underlying LB disease are summarised in Table 4.5 and these studies are discussed in the following paragraphs.

Blanc et al. [172] compared MRI differences between MCI-LB, MCI-AD and HC cases and found that the parietal lobes in MCI-AD participants had more atrophy than in subjects with MCI-LB. This study also suggested that visual hallucinations in the MCI-LB stage were correlated with relative atrophy of the left cuneus [172]. In contrast, a study by Roquet et al. found no difference in GM volume between prodromal AD and DLB groups [367]. One explanation for the lack of structural cortical difference noted between prodromal groups in the Roquet et al. study is that structural change is relatively subtle early on in the neurodegenerative process. It would be reasonable to expect therefore that the patterns of GM atrophy would become more pronounced and diverge as the disease progresses. In a cortical thickness study, which quantifies regional distribution of cortical GM loss, Blanc and colleagues [173] using subjects which overlapped with their previous study [172], showed that there was more right anterior insula thinning in the MCI-LB cohort than in the MCI-AD cohort. Furthermore, the MCI-AD cohort showed more bilateral parietal lobe and left parahippocampal gyri thinning than the MCI-LB cohort [173].

Preservation of hippocampal volumes has been shown to be associated with a greater risk of MCI progression to DLB than AD dementia after a median follow up of 2 years [368]. In this study, 17/20 (85%) of subjects with normal hippocampal volumes eventually developed DLB, while 37/61 (61%) of MCI subjects who had hippocampal atrophy developed AD dementia [368].

There is only study which assessed WM alterations in prodromal DLB. It found no WM volume difference between MCI-LB and MCI-AD cohorts [367]. There are no DTI studies reported to date in prodromal DLB.

Study	**Study Type**	**Diagnosis**	**Findings**
†Roquet et al. *[367]*	Cross-sectional	54 MCI-LB 15 DLB 16 MCI-AD 28 AD 22 HC	***MCI-LB vs MCI-AD,*** No difference in brain atrophy between prodromal groups ***MCI-LB vs HC,*** Decreased GM volume in right medial frontal gyrus, bilateral insula
†Blanc et al. *[172]*	Cross-sectional	28 MCI-LB 27 MCI-AD 33 HC	***MCI-LB vs MCI- AD,*** Increased atrophy in parietal lobes of MCI-AD vs-MCI-LB ***MCI-LB vs HC*** Decreased GM volume bilaterally in insula, precuneus, medial frontal, right anterior cingulate, left middle frontal, right superior & inferior frontal regions ***MCI-LB*** visual hallucinations associated with atrophy left cuneus
†Blanc et al. *[173]*	Cross-sectional	28 MCI-LB 31 DLB 27 MCI-AD 54 AD 33 HC	***MCI-LB vs MCI- AD,*** Increased right anterior insula thinning in MCI-LB More bilateral parietal lobe and left parahippocamal gyri thinning in pro-AD ***MCI-LB vs HC*** Increased right anterior insula thinning in MCI-LB
Kantarci et al. *[368]*	Prospective	160 MCI Median Follow-up 2.0 (0.7-8.1) years 79 MCI stable	***MCI subjects*** 13% of MCI subjects progressed to probable DLB, 38% progressed to AD

		20 DLB progressors 61 AD progressors	Preserved HV associated with increased risk of probable DLB in subjects with MCI.

Abbreviations: HC= healthy controls; DLB= Dementia with Lewy bodies; Pro-DLB= prodromal DLB; Pro-AD= Prodromal AD; MCI-LB = Mild cognitive impairment with Lewy bodies; MCI-AD = Mild cognitive impairment due to AD; MCI= Mild cognitive impairment; AD = Alzheimer's disease; HV= Hippocampal volume; GM= Grey matter

†Reference may represent the same patient cohort

Table 4. 5 MRI studies in prodromal DLB.

4.11 Discussion

Magnetic resonance imaging is one of the most widely used neuroimaging techniques for assisting in the diagnosis of neurodegenerative diseases. MRI modalities harbour great potential as biomarkers because they are non-invasive and have the ability to assess the microstructural properties of the brain and its function. At present, the MRI imaging literature indicates that neuroimaging is playing an increasingly important role in the differential diagnosis of dementia and predicting the underlying pathological entities. In the future, MRI might produce markers to predict the progression of cognitive impairment in defined at risk groups and monitor the response to disease modifying drugs. Structural MRI is already being utilised in a similar manner as indicated previously as an imaging biomarker in clinical trials in AD [369].

In recognition of the collective insights gained from imaging studies, MRI as a biomarker has been incorporated into two dementia diagnostic guidelines, namely for AD and for DLB [7, 112]. It has also included in the research criteria for prodromal DLB as a potential biomarker for MCI-LB [9]. In AD, according to diagnostic guidelines specific patterns of disproportionate global and regional atrophy are identifiable on structural MRI and affect the medial, basal, and lateral temporal lobes, as well as the medial parietal cortex. These patterns of atrophy are a biomarker of neuronal degeneration or injury that occur in AD. In contrast, brain MRI of patients with DLB may not be diagnostically informative, as DLB often have no evidence of cortical atrophy with no distinct regional pattern. The latest diagnostic guidelines of DLB state the absence of or minimal atrophy of the MTL on MRI is a supportive biomarker that is consistent with DLB, but does not have a

sufficiently high sensitivity or specificity for improving diagnostic accuracy. The recently proposed research criteria for MCI-LB states that potential structural MRI biomarkers for MCI-LB include; preservation of the MTL, insular thinning and GM volume loss [9]. However, MCI plus potential structural MRI biomarkers, in the absence of core features or the proposed biomarkers are outlined in chapter 2, are insufficient to make a diagnosis of MCI-LB.

Structural MRI analyses in DLB have yielded inconsistent findings in relation to its sensitivity/specificity to discriminate DLB from AD. Discrepancies are likely to be due to methodological differences in the structural MRI analyses techniques, as well as true heterogeneity in the cohorts studied. Firstly, while no particular structural analysis technique (corticometry or VBM) has been shown to be superior to another, changes in cortical thickness appear to be measurable at earlier stages of the disease than VBM. However, cortical thickness studies in DLB, particularly in the early stage of dementia and MCI-LB are relatively limited. Therefore, there is a need for future cortical thickness studies in the earliest stages of cognitive impairment to ascertain if this might be more beneficial than VBM at detecting the earliest brain changes.

In prodromal DLB, differences in GM atrophy between MCI-LB and HC have been found, with more atrophy among the MCI-LB cohorts in the bilateral insula, precuneus, medial frontal structures, right claustrum, left anterior cingulate, left frontal, right superior and inferior frontal regions and right cingulate cortex [172, 173, 367]. The significance of cortical patterns of atrophy noted on MRI in MCI-LB is unclear. It remains uncertain whether structural brain imaging can differentiate MCI-LB from MCI-AD and no longitudinal studies have assessed the biomarker potential of any such structural differences to predict conversion to DLB. Studies have indicated that predominant insular atrophy may distinguish MCI-LB from MCI-AD but this has not been confirmed in longitudinal studies [173, 367]. One retrospective study has also suggested that hippocampal volume preservation at the MCI stage may predict future conversion to DLB rather than AD [368] but unfortunately as yet no prospective studies have been undertaken to better assess if differential hippocampal volumes exist between MCI-LB cohorts and MCI-AD.

DLB is clinically and pathologically a heterogeneous condition. Clinically, DLB is often underdiagnosed because its symptoms overlap with those of AD and Parkinson's disease [5]. Clinical

diagnosis is less certain with a possible DLB diagnosis compared to a probable DLB diagnosis. Diagnostic certainty in a DLB diagnosis can be improved with the utilisation of biomarkers. Moreover, the prevalence of a DLB diagnosis varies between areas in the UK which may be a reflection of reduced confidence in making the diagnosis in some services in the UK [5]. Imaging biomarkers may be a useful adjunct to help improve diagnostic detection rates of DLB in memory clinics. The complex pathological process which underlies a substantial proportion of DLB patients who have concomitant AD pathology suggest that no single imaging modality will be a reliable biomarker for all patients with DLB. The heterogeneity of pathological findings of clinical DLB cohorts means that multimodal imaging will probably be required to improve ante-mortem diagnostic certainty. Given the clinical availability of magnetic resonance imaging it is likely to form part of such an imaging battery.

4.11.1 Future directions of research

A number of questions needs to be answered by researchers particularly in the earliest pre-dementia stage of the disease, where the neurodegenerative process isn't of such severity to cause global but instead distinct regional atrophy. Atrophy of the MTL is established as being present at MCI stage of those patients who progress onto AD [368]. Prospective longitudinal studies at the MCI stage are needed to determine if preservation of the MTL differentiates MCI-LB from MCI-AD, and could be used a biomarker of subsequent conversion to DLB. Another helpful imaging marker in DLB would be one which gives a better understanding of the rate of yearly atrophy in the condition. Perhaps, the initiation of serial MRI scans at annual or longer intervals to investigate the disease progression will provide insight in predicting the MCI subject that will develop a specific dementia subtype. Furthermore, studies involving multimodal neuroimaging data and larger cohorts are likely to make novel contributions in evaluating the utility of combined biomarkers in DLB. There are also some practical limitation to using MRI as a biomarker in DLB. If multimodal imaging is required it will be expensive and require skilled staff for acquisition and analysis, and will be time consuming.

4.11.2 Limitations

There are some limitations in the current research to date. At present, the evidence base for the use of imaging markers in DLB/MCI-LB is still small, especially when compared with AD, with few large studies evaluating the accuracy of imaging biomarkers in pathologically confirmed DLB. The overwhelming majority of neuroimaging studies in DLB are cross-sectional, relatively small in size,

and in study participants with established stages of the disease. Moreover, there are only two cross-sectional studies examining structural MRI findings in MCI-LB. Therefore, larger prospective longitudinal studies with post-mortem verification are warranted to confirm the utility of structural MRI modalities to monitor disease progression in early disease stages in MCI-LB cohorts.

4.12 Conclusion

In conclusion, magnetic resonance imaging in DLB has provided important advances in terms of understanding the condition's pathophysiology and helping to support the clinical diagnosis. MRI has allowed for substantial progress in delineating the *in vivo* atrophic brain changes associated with cognitive decline allowing for better ante-mortem differentiation of dementia subtypes. However, many early structural brain changes are likely to be subtle and therefore of insufficient sensitivity/specificity to delineate between dementia subtypes. The complex pathological underpinnings of DLB means it is likely to require a multimodal imaging biomarker approach for accurate diagnosis and prognostication.

Chapter 5. ^{123}I-MIBG Scintigraphy Utility as a Biomarker for Prodromal DEmentia with Lewy Bodies (SUPErB) study: Background, Recruitment, Clinical Assessment and Diagnosis

5.1 Introduction

This chapter describes how participants were recruited, the clinical and neuropsychological assessment and imaging undertaking by participants as part of the "^{123}I-MIBG Scintigraphy Utility as a biomarker for Prodromal DEmentia with Lewy Bodies (SUPErB) study". The data in this thesis is a subset of the information collected as part of the SUPErB study.

The SUPErB study is a single centre prospective observational study which recruited older adults with MCI and HC over 60 years of age. The overall aim of the study was to identify biomarkers predictive of cognitive decline and conversion to dementia in subjects with MCI-LB. All subjects underwent detailed clinical and neuropsychological testing at baseline and annual review for up to four years following recruitment. All participants underwent baseline MIBG, ^{123}I-FP-CIT SPECT and structural and functional MRI. All participants were offered the option of undergoing repeat ^{123}I-FP-CIT SPECT between 1-2 years from baseline imaging.

The data in this thesis will examine the utility of imaging biomarkers to discriminate MCI-LB from MCI-AD and structural imaging correlates of cognitive and clinical symptoms in MCI-LB. It will focus on baseline structural MRI data and examine the putative potential of baseline and repeat ^{123}I-FP-CIT SPECT imaging, to identify progressive dopaminergic loss in MCI-LB compared to HC and MCI-AD.

5.2 Methods

5.2.1 Ethical approval

The study received ethical approval from the National Research Ethics Service Committee North East - Newcastle and North Tyneside 2 (Research Ethics Committee Identification Number: 15/NE/0420). All subjects had to have sufficient level of English to complete cognitive testing. All participants gave their written informed consent to take part in the study and were provided with a copy of the signed consent form.

5.2.2 Participant: identification and screening

MCI cohort

Prospective recruitment of participants was undertaken from memory clinics, specialist dementia services, elderly medicine clinics and neurology clinics in the North East of England. Identification of potentially eligible participants was by direct referral from their responsible clinician and through the Dementias and Neurodegenerative Disease Research Network (DeNDRoN) Research Case Register and through screening patient notes based on Mental Health Cluster, an instrument for categorising NHS Mental Health patients based on the type of illness they have and its severity [370]. Patients categorised as 'Cluster 18' were screened. The 'Cluster 18' list is a list of people with 'Cognitive Impairment (low need)' and is the Cluster most likely to be used for people with MCI. Potential volunteers with MCI were also identified from subjects participating in the National Institute for Health Research (NIHR) Biomedical Research Centre LewyPro study. The LewyPro study was a pilot study which led to the funding for the SUPErB study. The inclusion and exclusion criteria for LewyPro are the same as for the SUPERB study but the SUPERB study had a more detailed set of assessments.

Healthy controls

To provide a comparator to control for effects of normal ageing, HC were prospectively recruited from relatives/friends of patients in the MCI group. HC were also recruited from the Control Register held by DeNDRoN and staff working for DeNDRoN also identified suitable volunteers via the NIHR on-line register; "Join Dementia Research".

5.2.3 Inclusion/Exclusion criteria MCI cohort

Subjects were ≥60 years old and had to have the mental capacity to consent to the study. They had to be medically stable, e.g. no delirium or recent changes in prescribed medication (within last month). Subjects fulfilled the NIA-AA clinical criteria for MCI [10] as well as having at least one symptom suggesting they might have LB disease. This included the core and suggestive features of DLB (spontaneous motor parkinsonism, cognitive fluctuations, recurrent visual hallucinations, RBD, severe neuroleptic sensitivity) as well as other symptoms that may be more likely in LB disease, such as auditory hallucinations, falls, hyposmia, etc which also occur in AD. The inclusion criteria were

made as broad as possible in an attempt to capture as many patients with LB disease at the earliest possible stage. MCI subjects were included if they appeared to be developing a core or suggestive feature of DLB.

Subjects were excluded at screening if they had an MMSE score <20; CDR score of > 0.5; if they had developed parkinsonism more than one year prior to cognitive impairment or if they had evidence of clinical stroke or a serious neurological or mental condition that would affect their performance in study assessments. The 'one year rule' was used because patients developing parkinsonism more than one year prior to cognitive impairment would be classified as PDD rather than DLB if they progressed to dementia. Subjects were also excluded if they had contraindications to SPECT or CT scanning, if they could not stop medication which would interfere with MIBG or ^{123}I-FP-CIT SPECT imaging such as tricyclic antidepressants, tramadol or labetalol etc.

5.2.4 Inclusion/Exclusion criteria for healthy controls

HC were ≥ 60 years old and had the mental capacity to consent. They had a MMSE ≥26 and an absence of memory complaints. The reminder of the inclusion and exclusions criteria are the same as for the MCI cohort.

5.2.5 Clinical and cognitive assessments

Participants, both HC and MCI, underwent extensive clinical and neuropsychological assessment to accurately detail LB symptom severity and duration.

Clinical assessment

Suitability for enrolment in the study was determined by a doctor (RD and SL). An expert consensus clinical panel (AT, PD, J-PT) reviewed all the clinical assessment data to confirm that subjects met NIA-AA criteria for MCI without considering aetiology [10]. The consensus panel also rated the presence or absence of each of the four core clinical LB symptoms characteristic of DLB in the fourth consensus report of the DLB consortium [cognitive fluctuations, complex visual hallucinations, clinical parkinsonism, clinical probable RBD] [7]. This consensus panel approach has been validated previously against autopsy diagnoses [200].

Cumulative Illness Rating Scale for Geriatrics

The burden of medical co-morbidity was rated using the Cumulative Illness Rating Scale for Geriatrics (CIRS-G) [371].

North-East Visual Hallucinations Interview

The North-East Visual Hallucinations Interview (NEVHI) is a semi-structured, clinician-administered face-to-face interview designed to assess frequency, intensity and content of visual hallucinations in older patients with cognitive impairment [372].

Epworth Sleepiness Scale

The Epworth sleepiness scale (ESS) is a widely used questionnaire to evaluate daytime sleepiness and asks subjects to grade the likelihood of dozing off or falling asleep in different everyday situations [373]. Subjects grade themselves from 0 (never) to 3 (high chance) of falling asleep in eight different situations.

Geriatric Depression Scale

The 15 item Geriatric Depression Scale (GDS) consists of 15 items assessing the presence or absence symptoms of depression for which patients could answer ‘yes’ or ‘no’ questions [374]. A cut-off of 5/6 gives a sensitivity of 86% and a specificity of 74% when compared with ICD-10 diagnosis [375].

Comprehensive Lewy body Dementia Symptom Checklist

The comprehensive Lewy body dementia symptom checklist (LBSQ) was administered to all subjects on the study [376]. This is a 49-item questionnaire designed to assess cognitive symptoms, Parkinson’s-like symptoms, behaviour and mood changes, sleep symptoms, autonomic symptoms and reactions to medications. In addition, dry/painful eyes, double vision, difficulty reading because words and letters seem to move around the page and misjudging objects were also asked.

Motor assessment

Motor assessment was completed using the Movement Disorder Society- Unified Parkinson's Disease Rating Scale (MDS-UPDRS) part III [377]. The MDS-UPDRS part III is a measure of motor disability in parkinsonism which measures motor ability on a scale of zero (no symptoms) to 132 (very severe).

Hyposmia assessment

Olfactory function was measured using Burghart "Sniffin' Sticks" Identification 16 (blue version) test (Burghart GmBh, Wedel, Germany) which is based on odour-containing felt-tip pens. The pen's cap was removed, and its felt-tip was presented about 2cm in front of both nostrils of the subject for about 3 seconds. The Identification test consists of 16 Sniffin' Sticks with everyday smells which the patients have to identify using a selection card containing four choices.

Autonomic system evaluation

The Composite Autonomic Symptom Scale-31 is a questionnaire which assesses quantitatively the presence of autonomic symptoms. It is a refined abbreviated version of the Autonomic Symptom Profile and the Composite Autonomic System Score and is a set of 31 questions divided into six domains of autonomic systems: orthostatic intolerance, vasomotor, secretomotor, gastrointestinal, bladder, and pupillomotor [378].

- *Valsalva manoeuvre*

Valsalva manoeuvre evaluates the function of baroreceptors. It is a voluntary forced expiration of a subject against a resistance. The manoeuvre is performed with the subject seated, after 15-20 minute rest. The subject then forcefully exhales into a sphygmomanometer with an open glottis at a pressure of 40 mmHg for 15 seconds. ECG is recorded during the resting period. The manoeuvre is generally performed three times and the mean value is calculated.

- *Active standing (orthostatic test)*

Haemodynamic responses to active standing are assessed during this test. In advance of the active stand, the subject remained in the supine position for 10 minutes. After the 10 minute rest period the subject shifted from the supine to the standing position. The subject remained in the standing position for 3 minutes and was requested to inform the examiner of the presence of any symptoms such as dizziness, light-headedness, blurred vision etc. During the rest period and the active stand period blood pressure and ECG was recorded. A decline in systolic blood pressure by more than 20 mmHg and by a more than 10 mmHg for diastolic blood pressure is considered abnormal.

- *Heart Rate Variability*

HRV is a method of evaluating autonomic nervous system. The ECG recordings of all subjects were performed in quiet conditions, and all recordings were done at approximately the same time of day. The subjects were asked to lie on a bed in the supine position, to keep still, to breathe normally, and to stay awake. HRV measurement were recorded for 10 minutes. The subjects were asked to lie on a bed with electrodes placed on their chests and ECG recordings were undertaken. HRV is generally assessed based on time-domain or frequency-domain analysis. Indices of time-domain analysis derive from either direct RR interval measurements or the differences between successive RR intervals.

5.2.6 Neuropsychological assessments

Addenbrooke's Cognitive Examination Revised

The Addenbrooke's Cognitive Examination Revised (ACE-R) is a rapid screening battery consisting of 100-point examination, divided into five sub-scales to explore different cognitive domains: attention/orientation, memory, fluency, language and visuospatial [379].

Verbal fluency

Semantic and phonemic fluency was assessed as part of the study. Semantic fluency was assessed as part of the ACE-R by asking the subjects to name as many animals as they could in one minute.

Phonemic fluency was assessed using the FAS test. The FAS test is probably the best known phonemic fluency test and is a form of the Controlled Oral Word Association Test [380]. Standard administration provides for the listing of three letters. It consists of saying words beginning with the letters F, A and S, one at a time for one minute. The FAS test is related to the frequency of words beginning with each letter.

Trail Making Test

The trail-making test consists of two-part pencil-and-paper test. Part A (TMT-A) assesses visual-search, attention, and motor-speed task and requires an individual to draw lines sequentially connecting 25 encircled numbers distributed on a sheet of paper. Part B (TMT-B) is an assessment of executive function task and the person must alternate between numbers and letters (e.g., 1, A, 2, B, 3, C, etc.).

Graded Naming

The Graded naming test is a cognitive test to assess a subjects object naming ability and is used to detect mild word retrieval difficulties [381]. It requires subjects to recognise and name monochrome drawings of 30 objects.

Rey AVLT

The Rey Auditory Verbal Learning Test (AVLT) is a neuropsychological assessment tool for testing episodic memory, which is commonly used in dementia and pre-dementia stages [382]. The AVLT consists of presenting and assessing the recall of a list of 15 words that are read out at a rate of one per second (List A). The list is read aloud to the participant for five consecutive trials (Trials 1 to 5), after each trial the participant is immediately asked to recall as many of the words from the list as possible. After that, a new list (List B) of 15 new words is read to the participant, who then is immediately asked to recall the words. After the List B trial, the participant is requested to recall the words from List A (Trial 6). After 30-minutes have lapsed from the completion of List B recall), the participant is again asked to recall as many words as possible from List A (delayed recall).

The Mini-Mental State Examination

The MMSE is a widely used screening test of cognitive function [383]. MMSE is a paper based test of cognitive function with a maximum score of 30, with lower scores indicating more severe cognitive problems. A normal MMSE is set at a score of 24 or above, but should be adjusted according to educational level. It encompasses tests of orientation, attention, memory, language and visuso-spatial skills.

The National Adult Reading Test

National Adult Reading Test (NART) is a widely used method for estimating premorbid intelligence in both clinical and research settings in patients with dementia [384]. The test comprises of 50 written words in English.

5.2.7 Carer rating scales

Neuropsychiatric Inventory

NPI is a screening questionnaire and assess 12 behavioural disturbances occurring in dementia patients: delusions, hallucinations, dysphoria, anxiety, agitation/aggression, euphoria, disinhibition, irritability/lability, apathy, aberrant motor, sleep and appetite disturbances. For each positive answer to a behavioural domain, the frequency and severity of neuropsychiatric symptom was determined, as well as the level of carer distress caused by these symptoms [385].

Cognitive Fluctuations Scales

The presence of cognitive fluctuations was assessed using two scales. The dementia cognitive fluctuation scale (DCFS) is a scale based on 4 items from an earlier 17-item scale that were found to best discriminate between patients with and without CFs [386]. Four items enquired about include; the differences in daytime functioning, daytime somnolence, daytime drowsiness, and altered levels of consciousness. Two further symptoms were also rated; staring into space and disorganised speech.

The Clinician Assessment of Fluctuation (CAF) is a 2-item questionnaire, developed to assess fluctuations in attention and alertness [387]. The first question is designed to ascertain the presence of fluctuating level of consciousness. The second question is designed to assess the presence of fluctuating cognitive impairment. A positive 'Yes' answer to either question elicits a further enquiry about their frequency using a scale ranging from 1 to 4, with 4 being the most frequent and their duration of the symptom ranging from 0 to 4. Both the frequency and duration scores are multiplied together to achieve a severity score, ranging from 0 to 16.

Mayo Sleep Questionnaire

The Mayo Sleep Questionnaire (MSQ) is a carer-rated screening questionnaire that consists of 16-items that poses questions about RBD, periodic limb movements during sleep, restless legs syndrome, sleepwalking, obstructive sleep apnoea, sleep related leg cramps [41]. The first question 'Have you ever seen the patient appear to "act out his/her dreams" while sleeping? (punched or flailed arms in the air, shouted or screamed)' on the MSQ had a sensitivity 98% and specificity 74% [41]. It can only be carried out with an informant that lives with the patient.

Assessments of level of function

The Lawton Instrumental Activities of Daily Living (IADL) scale assesses a person's ability to perform tasks such as using a telephone, doing laundry, and handling finances [388]. It measures eight domains and provides an early warning of functional decline or signals the need for further assessment. The maximum score possible is 8, representing full function; the minimum possible score is 0, representing the highest level of functional impairment.

The Clinical Dementia Rating Scale (CDR) [389] is a numeric scale of cognitive function obtained via semi-structured interview and assessing 6 domains of functioning: memory, orientation, judgement and problem solving, community affairs, home and hobbies, and personal care. Each domain is rated on a 5-point scale of functioning to quantify the severity of symptoms of dementia. A score of 1-3 is consistent with dementia; a score of 0.5 is consistent with MCI or dementia. A score of 0 is not consistent with dementia. The global score is calculated by the addition of the score for each of the individual 6 domains sub-scores to give a 'sum of boxes score.

5.2.8 Computerised cognitive tests

Computerised testing was conducted using a laptop computer and patients holding two response buttons, one in either hand. All tests were operated through MATLAB. The tests aim to measure specific cognitive domains that are known to be affected in DLB: visuospatial function and executive functions such as attention, processing speed and decision-making.

Simple reaction time (SRT):

Simple reaction time (SRT) is a basic measure of processing speed and is the minimum time needed to respond to a stimulus. The SRT in this study consisted of one stimulus appearing and the participant responding by clicking one response button on a laptop. The stimulus in our study consisted of a white 'X' on a black background. When a participant saw a white 'X' on a black background, they were instructed to press a response button. The white 'X' was presented to the participant 40 times in varying intervals. The number of correct responses, average response time and standard deviation of response time were recorded.

Choice reaction time (CRT):

Choice reaction time, the time required to discriminate and respond appropriately to different stimuli is a basic measure of attention and processing speed. In this computer test, an arrow-shape is displayed on either the left or the right side of the screen. The participant must select the left-hand button if the stimulus is displayed on the left-hand side of the screen, and the right-hand button if stimulus is displayed on the right-hand side of the screen. The number of correct and incorrect responses are recorded, the average response speed is recorded.

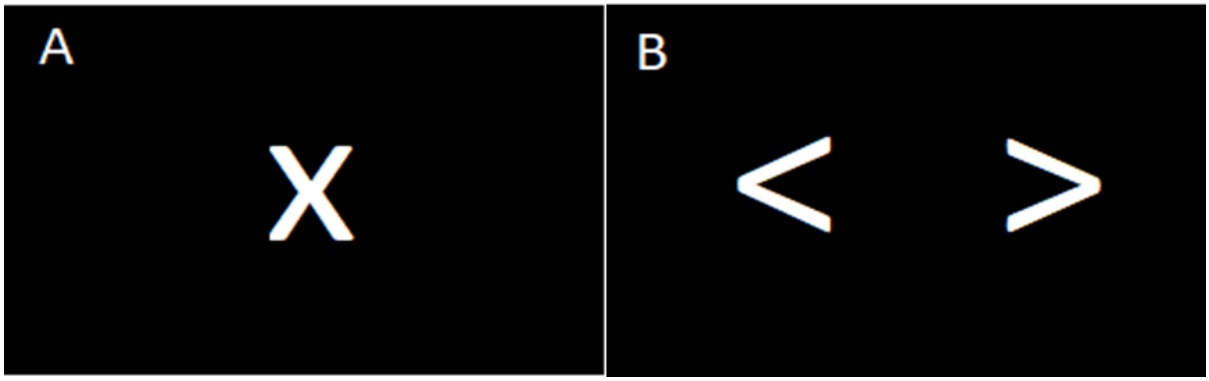

Figure 5. 1 Visual stimuli presented in the (A) simple reaction time and (B) choice reaction time tasks.

Continuous performance task

The continuous performance task is at test of sustained and selective attention. Sustained attention is the ability to maintain concentration over time on a given task while selective attention refers to the ability to focus on relevant stimuli in a distracting environment. In the continuous performance task assessment, one response button is pressed when a target letter 'X' appears on the laptop screen but only when the target letter is preceded by the letter 'A'. If the letter 'X' is preceded by any other letter of the alphabet, the participant is instructed not to press the response button.

Line angle discrimination testing

The angle discrimination task is a task of visuospatial function. In this test, participants are presented with an angled line relative to a horizontal base line in the top box and had to identify which of the lines in two lower boxes best matched the target angle. The test difficulty depends on the participant's response. Patients with DLB perform worse than those subjects with AD [390].

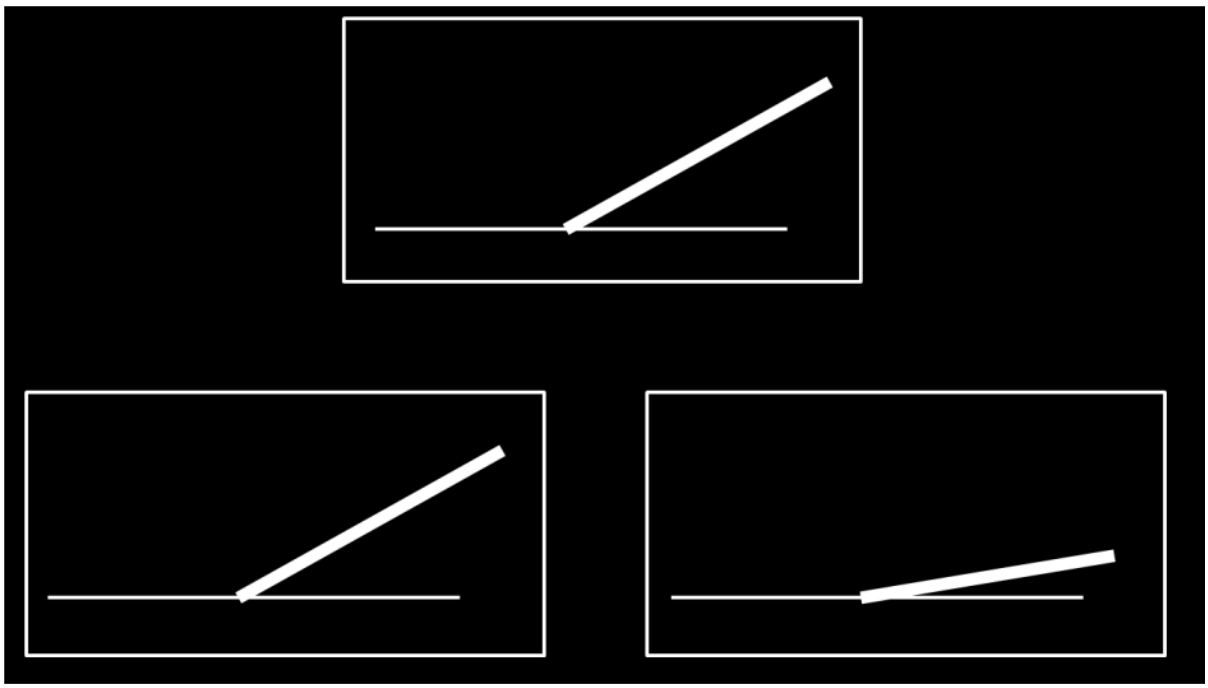

Figure 5. 2 The Line Angle Discrimination Testing. Subjects choose which of the lower angles matched the angle at the top of the screen.

Corsi Block-Tapping Test:

The Corsi Block-Tapping test is a visuospatial version of the digit span test. Participants see squares on a laptop screen lit up and the participant follows the sequence of squares in order of which they lit up. The computerised version –Psychology Experiment Building Language (PEBL) of the Corsi was used in this study (see http://pebl.sourceforge.net/battery.html). A flashing sequence of coloured squares is presented on-screen and the participant is required to replicate the pattern by touching the squares on the touch screen. The initial sequence begins with three squares and increases by one after each correct sequence. Participants are allowed only one incorrect attempt on each number of 'blocks'. If two incorrect attempts are made for the same number of blocks, the test ceases. Total score is used for analyses.

Visual Pattern Test

The visual pattern test is conducted by Neurobehavioural System visual pattern test. Participants see a checkerboard-like grid on a laptop screen, with the squares in the grid each randomly coloured (in one of two possible colours). They are then shown a blank grid and must reproduce the pattern.

The visual pattern test is a test of visual recall and thought to be a more direct measure of spatial working memory.

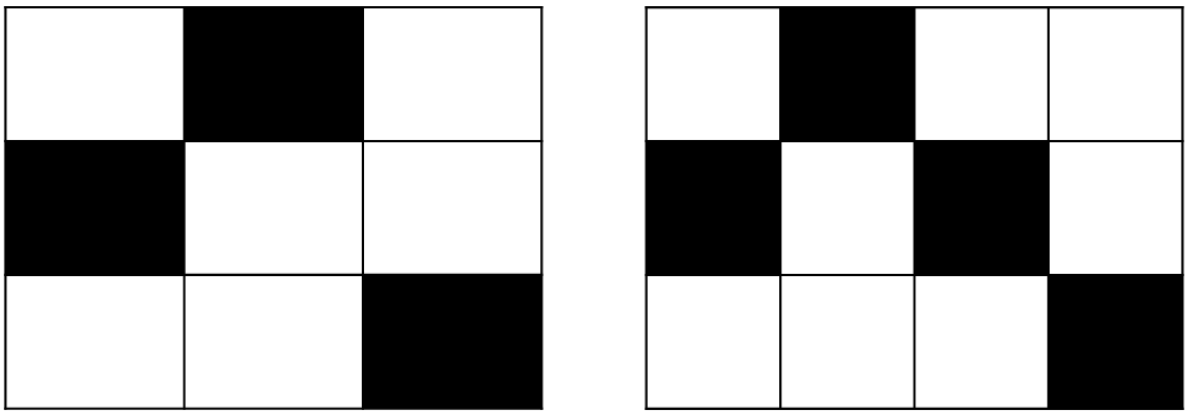

Example A: 3x3 grid with three boxes filled in

Example B: 4x3 grid with four boxes filled in

Figure 5. 3 Visual Pattern Test. Subjects are shown a checkerboard like grid pattern coloured in and then asked to reproduce the pattern on a subsequent blank checkerboard like grid.

5.2.9 Definitions of core and suggestive symptoms of Lewy body disease.

A consensus panel rated the presence or absence of each of the four core clinical LB symptoms characteristic of DLB in the fourth consensus report of the DLB consortium [cognitive fluctuations, complex visual hallucinations, clinical parkinsonism, clinical probable RBD] [7]. The clinical information recorded at interview by the study doctor was used alongside scales to determine the presence or absence of core clinical LB symptoms. The definitions used and the scales that informed the decision are outlined in Table 5.1.

Core Features	Definition	Scales used
Fluctuations	Spontaneous pronounced variations in cognition, attention and arousal.	CAF DCFS
Visual Hallucinations	Recurrent, complex visual hallucinations which are well-formed, featuring people, children, or animals etc.	NEVHI
Parkinsonism	At least one spontaneous features of parkinsonism: rest tremor, rigidity, bradykinesia.	MDS-UPDRS Part III
REM sleep behaviour Disorder	Recurrent dream enactment behaviour that mimics movement of dream content – being chased or attacked, vocalising, failing limbs.	MSQ
Suggestive Features		
Neuroleptic Sensitivity	Severe reaction to neuroleptic medication e.g. acute onset or exacerbation of parkinsonism, and impaired consciousness.	NA
Hyposmia	Olfactory dysfunction	Sniffin' sticks odor identification test kit
Excessive daytime Scale	Persistent sleepiness and fatigue during the daytime despite adequate nightime sleep	Epworth Sleep Scale

Autonomic Symptoms	Autonomic dysfunction include symptoms such as orthostatic hypotension, reduced heart rate variability, supine hypertension, constipation, faecal incontinence, urinary, and sexual dysfunction.	COMPASS 31 LBSQ Valsalva manoeuvre Active Standing Heart Rate Variability
Abbreviations: CAF= Clinician Assessment of Fluctuation; DCFS= Dementia Cognitive Fluctuation Scale; NEVHI= North-East Visual Hallucinations Interview; MDS-UPDRS= Movement Disorder Society- Unified Parkinson's Disease Rating Scale; MSQ= Mayo Sleep Questionnaire; NA= Not applicable; COMPASS 31= Composite Autonomic Symptom Scale-31; LBSQ= Comprehensive Lewy body dementia symptom checklist.		

Table 5. 1 Definitions of core and suggestive symptoms of Lewy body disease.

5.2.10 ^{123}I-FP-CIT SPECT imaging acquisition

Subjects were given 85mg potassium iodate thyroid protection 1 hour prior to the intravenous injection of 185MBq ^{123}I-2h-carbomethoxy-3h-(4-iodophenyl)-N-(3-fluoropropyl)-N-nortropane (^{123}I-FP-CIT) (DaTSCAN, GE Healthcare, UK). Participants were scanned 3-6 h following a bolus intravenous injection of 185 MBq of ^{123}I-FP-CIT (DaTSCAN, GE Healthcare, UK) using a dual-headed gamma camera (Siemens Symbia S or Siemens Intevo) fitted with low-energy high-resolution parallel hole collimators. One hundred and twenty 25s views over a 360° orbit (60 views per detector) were acquired on a 128 x 128 matrix with a zoom of 1.23 x giving a pixel size 3.9 mm x 3.9 mm. Overall image acquisition time was 25 min.

5.2.11 Repeat ^{123}I-FP-CIT SPECT imaging

All participants on the SUPErB study had the option to volunteer to undergo one repeat ^{123} I-FP-CIT SPECT between 1-year and 2-year post recruitment to the study. A further subset of volunteers with MCI who originally participated in the LewyPro study had undergone ^{123}I-FP-CIT SPECT imaging in that study prior to consenting to take part in SUPErB study and these ^{123}I-FP-CIT SPECT images were available for analyses. Another subset of subjects on the SUPErB study also had a clinical ^{123}I-FP-CIT SPECT before consenting to the SUPErB study. Therefore, a significant proportion of participants in the study had three ^{123}I-FP-CIT SPECTs' at varying time points.

5.2.12 Visual rating of ^{123}I-FP-CIT SPECT images

Visual assessment of all scans was undertaken blind to clinical diagnosis by five raters': a consultant radiologist, a consultant medical physicist and qualified medical physicist experienced in nuclear medicine reporting, and two certified old age psychiatrists (GP, JL, GR, AT, PD).

Scans were rated independently blind to clinical information on coded images by each panel member using a modified version of the Benamer scale based on a six-category ^{123}I-FP-CIT SPECT visual rating procedure [210]. Briefly: grade 0 (bilateral tracer uptake in caudate and putamen are largely symmetric); grade 1 (asymmetric uptake with normal or almost normal putamen activity in one hemisphere with more marked reduction in the contralateral putamen); grade 2 (significant bilateral reduction in putamen uptake with activity confined to the caudate); grade 3 (virtually absent uptake bilaterally affecting both putamen and caudate nuclei); grade 4 (very mild or equivocal global striatal reduction in uptake); grade 5 (significant global striatal reduction in uptake) and grade 6 (other abnormal pattern of uptake). After rating all scans, any scan where there was no complete agreement between all raters' was then subsequently reviewed by all five raters' together at a consensus meeting where a consensus rating was agreed. For the purposes of diagnosis, all scans were rated as normal (grade 0) or abnormal (graded as 1-5). In addition to primary visual reading, all scans underwent semi-quantitative analysis as described below and raters' had access to combined visual and semi-quantification to individual rater and panel decisions.

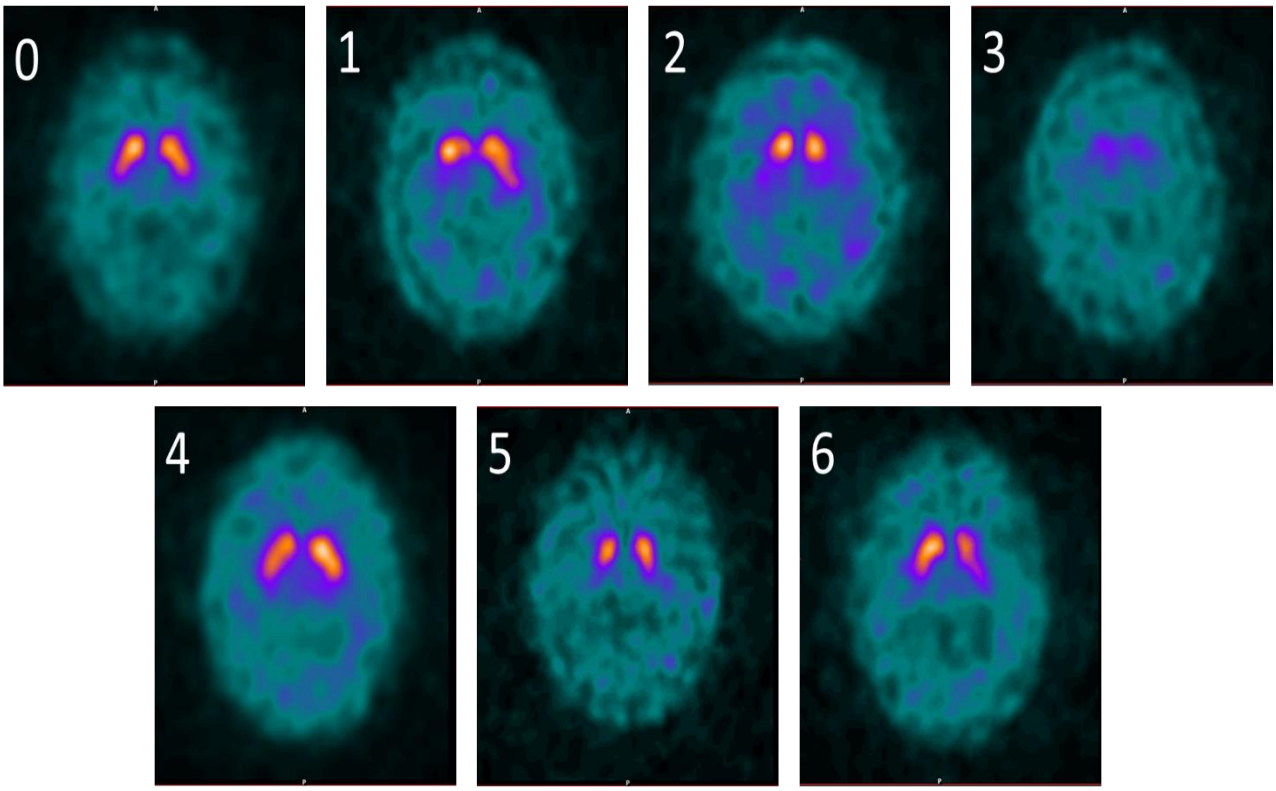

Figure 5. 4 Visual assessment of ^{123}I-FP-CIT SPECT using modified Benamer scale.

Grade 0 – Normal. Bilateral tracer uptake in caudate and putamen are largely symmetric;

Grade 1 – Asymmetric uptake with normal or almost normal putamen activity in one hemisphere with more marked reduction in the contralateral hemisphere.

Grade 2 – Significant bilateral reduction in putamen uptake with activity confined to the caudate

Grade 3 – Virtually absent uptake bilaterally affecting both putamen and caudate nuclei

Grade 4 – Very mild or equivocal global striatal reduction in uptake

Grade 5 – Significant global striatal reduction in uptake

Grade 6 – Other abnormal pattern of Uptake

5.2.13 Semi-quantification of ^{123}I-FP-CIT SPECT images

Semi-quantitative analysis was performed on both a Hermes workstation (Hermes Medical Solutions, Stockholm, Sweden) with Hybrid Viewer BRASS v2.5 and using DaTQUANT (v1.01 standalone software, GE Healthcare, Little Chalfont UK). Striatal volumes of interest and occipital lobe (background) volumes were established from a template derived from imaging (^{123}I-FP-CIT SPECT) of HC. Automated image registration is performed by both software packages where the study image is loaded on top of the template image to automatically place the regions. Both

software packages are capable of providing results for the whole striatum or striatal sub-regions such as the putamen or caudate.

A database of our study age-matched HC scans was constructed specially in DaTQUANT to create a set of age-corrected Z scores for the left and right striatum and compare these with the MCI cohort. The raw ^{123}I-FP-CIT SPECT data were imported into DaTQUANT and reconstructed within the program using OSEM iterative reconstruction with the default parameters used for the normal database (two iterations and ten subsets with a Butterworth filter of cut-off 0.6 cycles per cm and power 10), with attenuation or scatter correction.

5.2.14 MIBG cardiac scintigraphy

All participants were administered 111 ± 10% MBq ^{123}I-MIBG via slow intravenous injection. Potassium iodate tablets (170mg) were given before and after injection to minimize uptake of free iodine by the thyroid. Images were acquired on a dual headed Siemens Symbia Intevo or Siemens Symbia T series gamma camera (Siemens Healthcare, Munich, Germany) with medium energy low penetration collimators with energy window of 159 keV ± 10%, matrix size 128 x 128 and no zoom applied.

Images were processed on a Hermes workstation (Hermes Medical Ltd, Stockholm). Cardiac MIBG uptake was quantified using the heart-to-mediastinum count ratio (HMR) as a diagnostic indicator using a 6cm circular ROI placed over the left ventricle and 4 X 3 cm rectangular ROI between the lungs in the mediastinum, as described previously [391]. Images were processed by two medical physics experts (JJL and GR), both without access to any clinical information, and the mean value recorded. Normal HMR values depend on both technical factors and the patient population, as detailed in previous work [392]. A local HMR cut-off value was therefore derived from the control images, and set as two standard deviations below the mean HMR value.

5.2.15 MRI acquisition and T1-weighted sequence protocol

All participants underwent T1-weighted volumetric imaging on a Philips Achieva 3T scanner (Philips Medical Systems, Best, Netherlands) at the Newcastle University Magnetic Resonance Centre.

An eight-channel receiver head coil was used and foam pads were placed around the head to improve head position and comfort. Participants were asked to minimise any body movement during the scan. The sequence was a standard sagittal T1-weighted volumetric sequence covering the whole brain using a magnetization prepared rapid gradient echo (MP-RAGE) sequence with the following parameters: echo time (TE) of 4.6 ms; repetition time (TR) of 8.3ms; flip angle= 8°, SENSE factor=2. The in-plane field of view was 216 x 240 mm with a slice thickness of 1.0 mm, yielding a voxel size of 1.0 x 1.0 x 1.0 mm. Scan time=4 minutes 30 seconds.

5.2.16 Statistical analyses

Descriptive analyses of group demographics, clinical and cognitive variables was conducted using the Statistical Package for Social Sciences software (SPSS version 25, http://www-01.ibm.com/software/analytics/spss/).

Baseline cross-sectional demographic and clinical variable analysis

Continuous variables were assessed for normality by using visual inspection of the histograms, Shapiro-Wilk test and Levene's test. Differences in demographics and clinical data were assessed using either Student's t-test or one-way analysis of variance (ANOVA) as appropriate for continuous variables and chi-square test (χ^2) for categorical data. Where *post-hoc* analysis was required to test for group differences following ANOVA, a Bonferroni correction for multiple comparisons was applied to control for Type 1 errors. A probability value of <0.05 was regarded as a significant difference for each test statistic.

Details of specific statistical analysis pertaining to cross-sectional MRI data and serial ^{123}I-FP-CIT SPECT analysis are outlined in greater detail in the relevant chapters of this thesis.

Chapter 6. Serial nigrostriatal dopaminergic imaging in MCI-LB

6.1 Aims

The aim of this analysis was to examine if repeated dopamine transporter imaging could detect differential changes in striatal tracer uptake between MCI-LB and MCI-AD compared with HC.

6.2 Hypotheses

6.2.1 Primary hypotheses

1. Serial ^{123}I-FP-CIT SPECT in possible and probable MCI-LB participants would show a progressive decline in striatal DAT availability in excess of that observed in age-matched HC and MCI-AD.
2. Serial ^{123}I-FP-CIT SPECT in probable MCI-LB with baseline visually normal striatal uptake would demonstrate striatal uptake loss in excess of probable MCI-LB with a baseline visually abnormal striatal uptake.

6.3 Methods

6.3.1 Participants

All subjects were >60 years old and consisted of aged-matched HC and MCI subjects. All participants on the SUPErB study had the option to volunteer to undergo one repeat ^{123}I-FP-CIT SPECT between 1-year and 2-year post recruitment to the study. A further subset of volunteers with MCI who originally participated in the LewyPro study had undergone ^{123}I-FP-CIT SPECT imaging in that study prior to consenting to taking part in the SUPErB study and these ^{123}I-FP-CIT SPECT images were available for analysis. The LewyPro study was a pilot study which led to the funding for the SUPErB study. The inclusion and exclusion criteria for LewyPro are the same as for the SUPERB study but the SUPERB study had a more detailed set of assessments. Another subset of subjects on the SUPErB study also had a clinical ^{123}I-FP-CIT SPECT before consenting to the SUPErB study. Therefore, a significant proportion of participants in the study had three ^{123}I-FP-CIT SPECTs'. All participants gave informed consent before recruitment into the SUPErB or LewyPro study and separately consented to undertake a repeat ^{123}I-FP-CIT SPECT imaging.

A total of 90 subjects (HC, MCI-AD, possible MCI-LB and probable MCI-LB) underwent repeat ^{123}I-FP-CIT SPECT imaging in the SUPErB study, of which 5 were excluded due to atypical/static MCI by consensus panel opinion (n=3) and cerebral infarcts on MRI brain (n=2). Therefore, a total of 85 subjects were included in this analysis, with 73/85 subjects undergoing the first repeat between 12-18 months after the baseline imaging and 12/85 undergoing the first repeat ^{123}I-FP-CIT SPECT between 19-36 months after the baseline scan. A further, 22 participants underwent a second repeat ^{123}I-FP-CIT SPECT between 12-20 months after the first repeat ^{123}I-FP-CIT SPECT (Table 6.1). Table 6.2 shows the timeframes for repeat ^{123}I-FP-CIT SPECT per diagnostic classification.

	1st Repeat Scan	**2nd Repeat Scan**
Control	29	0
Possible MCI-LB	10	5
Probable MCI-LB	27	13
MCI-AD	19	4
Total	85	22

Table 6. 1 Numbers of participants undergoing 1st and 2nd repeat ^{123}I-FP-CIT imaging per diagnostic grouping.

	Time from baseline to 1st Repeat Scan		***Time from 1st Repeat to 2nd Repeat scan***
	12-18 months	**19-36 months**	**12-20 months**
Control	29	0	0
Possible MCI-LB	7	3	5
Probable MCI-LB	20	7	13
MCI-AD	17	2	4
Total	73	12	22

Table 6. 2 Timeframe between 1st and 2nd repeat ^{123}I-FP-CIT imaging and numbers of participants per diagnostic grouping in each timeframe.

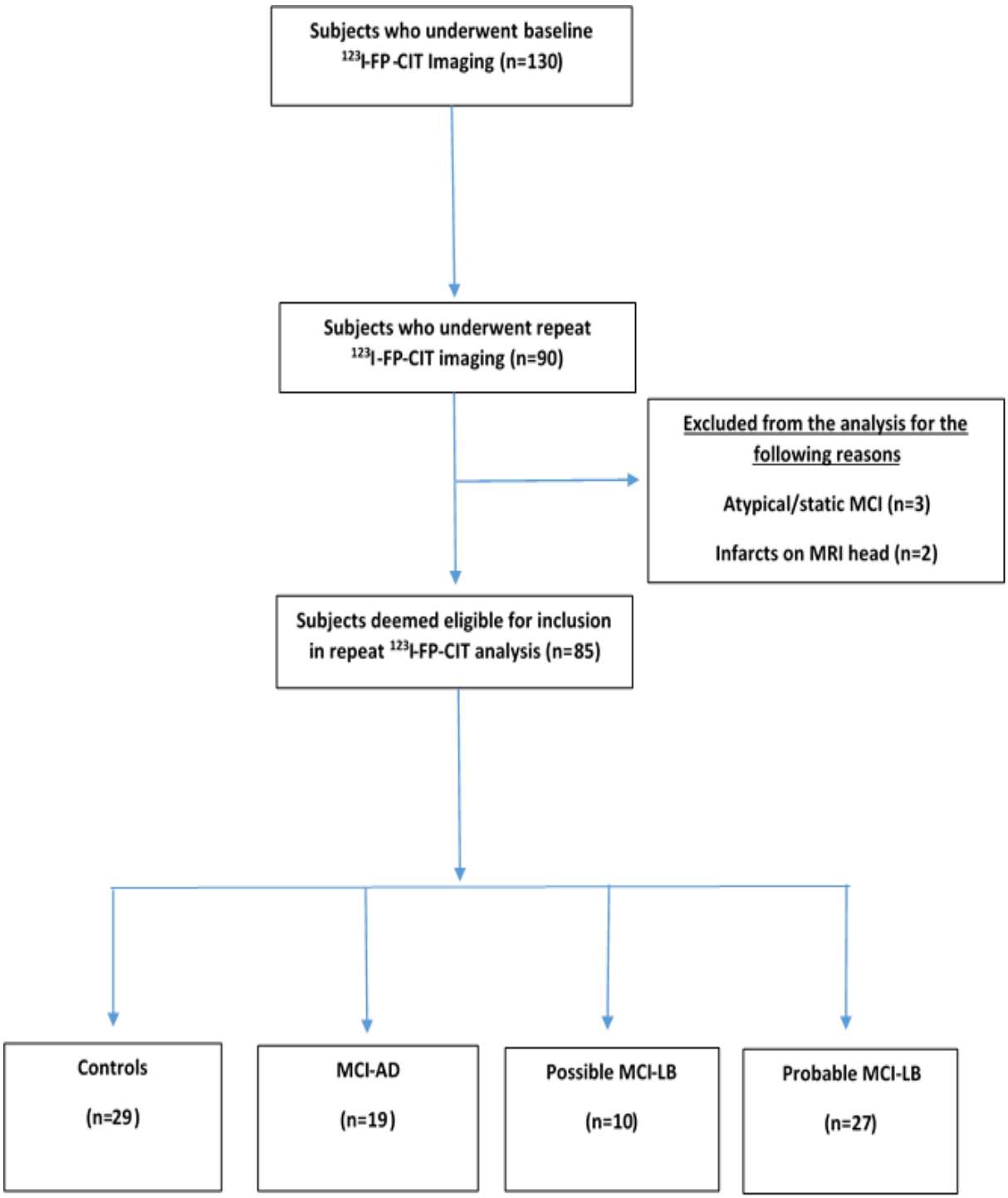

Figure 6. 1 Flowchart for inclusion into repeat ^{123}I-FP-CIT SPECT imaging analysis.

6.3.2 Diagnostic classification

Subjects were allocated to one of four clinical diagnoses: HC (cognitively normal individual with no core symptoms of DLB), possible MCI-LB (MCI plus one core symptom of DLB or MCI with none of the four core symptoms of DLB but having an abnormal cardiac MIBG), probable MCI-LB (MCI plus two or more of the four core symptoms of DLB or MCI plus once core symptom of DLB and an

abnormal cardiac MIBG), MCI-AD (MCI with none of the four core symptoms of DLB and a normal cardiac MIBG).

6.3.3 Imaging analysis of ^{123}I-FP-CIT SPECT

Visual assessment

Visual assessment of all scans was undertaken blind to clinical diagnosis by five raters': a consultant radiologist, a consultant medical physicist and qualified medical physicist experienced in nuclear medicine reporting, and two certified old age psychiatrists (GP, JL, GR, AT, PD). The details of the visual assessment are discussed in more detail in chapter 5 of this thesis.

Semi-quantification of 123I-FP-CIT SPECT images

Semi-quantitative calculations of SBR were performed using DaTQUANT software v1.01 (GE healthcare, Little Chalfont, England, UK). The raw SPECT images were imported into DaTQUANT and subsequently reconstructed using OSEM iterative reconstruction, with no attenuation or scatter correction. DaTQUANT automatically places a volume of interest (VOI) over the striatum (also its sub-regions such as the caudate and the putamen) and over the occipital lobe. The template for the VOI is obtained from the SPECT images of HC. The SBR is derived for the striatum, caudate and putamen by dividing the mean count per pixel in these regions by the mean count per pixel in the occipital lobe VOI. The respective VOI is shown in Figure 6.3.

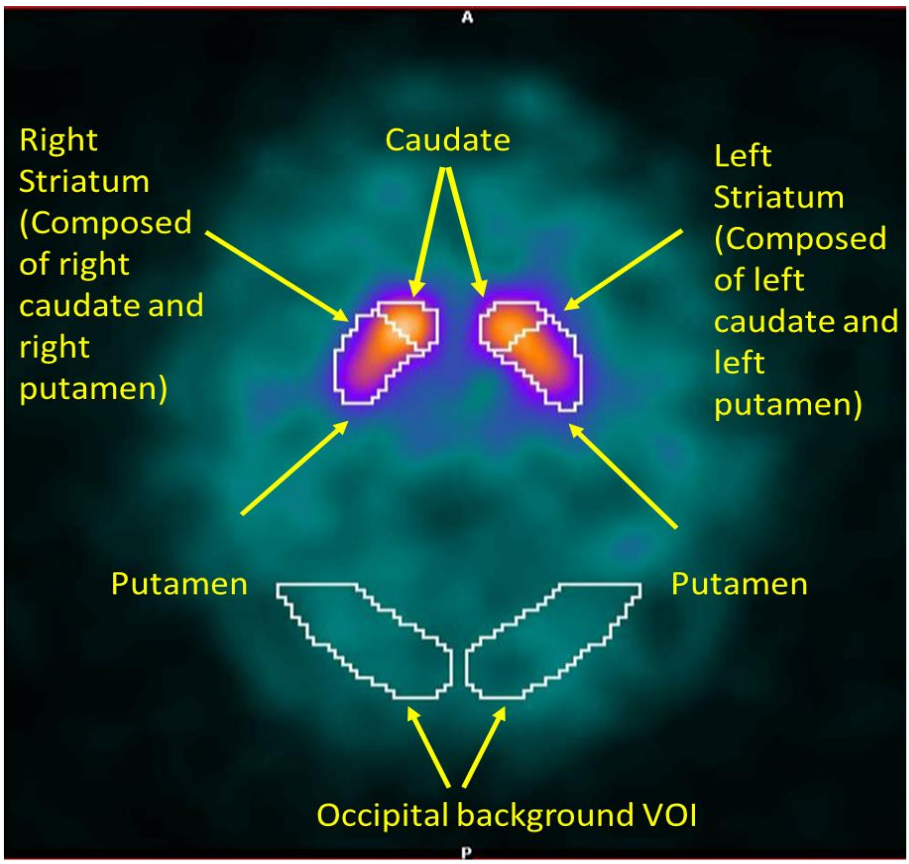

Figure 6. 2 DaTQUANT VOIs imposed on a ^{123}I-FP-CIT SPECT image. The VOI displayed are the caudate, putamen, entire striatum and occipital lobe.

6.3.4 Statistical analysis

Longitudinal statistical analysis

Mixed effects models were used to investigate changes in ^{123}I-FP-CIT uptake in the striatum primarily, and the caudate and putamen secondarily, for each diagnostic group compared to HC, and whether ^{123}I-FP-CIT uptake differed with time (diagnosis x time interaction included where indicated by improved model fit). This longitudinal analysis was conducted using the lme4 package [393] for R statistical software (Version 3.5.2; R Foundation for Statistical Computing, Vienna, Austria). Fixed effects included were age, time in years from baseline imaging, gender, side (left vs right as reported previously [84]), diagnostic group (HC, MCI-AD, possible MCI-LB and probable MCI-LB). Random intercept and slopes were included at the subject level, allowing for correlation between these. Each individual model used SBRs derived from DaTQUANT for the striatum, caudate and putamen as outcome variable. Reference groups for categorical variables were HC diagnosis, female gender, and left brain side. Age was centred on 60. Improvements in model fit were assessed

with likelihood ratio tests. A significance level of $p < 0.05$ was used to indicate a significant improvement in model fit for parameter inclusion.

Calculation of annual percentage change in ^{123}I-FP-CIT striatal binding ratios

In order to make direct comparisons with previously published data, the annual percentage change in SBR was also calculated for each participant. The percentage change in SBR in each striatal region was calculated as the difference between the last ^{123}I-FP-CIT SPECT and baseline ^{123}I-FP-CIT SPECT, divided by the baseline scan and the result multiplied by 100. Subsequently, the annual rate of change in SBR for the striatum, caudate and putamen and their 95% confidence level was derived from linear interpolation for each diagnostic group.

Percentage baseline ^{123}I-FP-CIT uptake in the whole striatum, caudate and putamen was calculated for MCI-AD, possible MCI-LB and probable MCI-LB group, as a percentage of the mean value for age-matched HC.

6.4 Results

6.4.1 Demographics and clinical characteristics

Clinical characteristics, neuropsychological tests and demographic data are shown in Table 6.3. The core clinical features and indicative biomarker abnormalities for all diagnostic groups are shown in Table 6.4.

There were no significant difference between MCI groups and HC with respect to age. There were significantly more males in the probable MCI-LB group compared to HC, MCI-AD, and possible MCI-LB ($\chi^2(3)=8.02$, $p=0.045$). HC had a significantly longer duration of education than possible MCI-LB but there were no differences between MCI groups ($F(3,80)= 3.45$, $p=0.02$). There were no significant differences between MCI groups with regard to cognitive scores (MMSE, ACE-R, AVLT, FAS, Graded naming score) but HC had significantly higher cognitive scores than MCI groups, (Table 6.3). The mean Geriatric depression scores were significantly higher for the MCI-AD and probable MCI-LB groups compared to HC group ($F(3, 81)= 10.33$, $p<0.0001$). The mean CIR-G scores were higher in possible MCI-LB and probable MCI-LB groups than in HC ($F(3,78)= 6.57$, $p=0.01$).

.

In terms of indicative biomarkers, abnormal ^{123}I-FP-CIT SPECT (6.9% (n=2)) and cardiac MIBG (3.4% (n=1)) results occurred in the HC group and abnormal ^{123}I-FP-CIT SPECT (5.3% (n=1)) results occurred in the MCI-AD group, see Table 6.4.

Characteristic	HC (n= 29)	MCI-AD (n=19)	Possible MCI-LB (n=10)	Probable MCI-LB (n= 27)	Group Comparisons
Mean age (years)	73.45 (7.0)	74.5 (7.9)	73.0 (7.2)	73.1 (6.6)	F(3, 81) = 0.19 , p=0.90
M:F (%)	21:8 (72% / 28%)	10:9 (53% / 47%)	6:4 (60%/40%)	24:3 (89% / 11%)	**$\chi^2(3)=8.02$, p=0.045** [e,g,l]
Mean years of education	14.6 (4.0)	13.3 (3.3)	11.0 (1.6)	12.4 (3.2)	**F(3,80)= 3.45, p=0.02** [a]
Duration of memory compliant (months)	NA	57.4 (64.5)	76.0 (72.3)	55.6 (41.5)	F(2,51) = 0.48, p=0.63
IADL	NA	6.9 (1.4)	6.4 (1.1)	6.3 (1.4)	F(2,48) = 0.84, p=0.44
GDS (Max 15)	1.1 (1.8)	3.9 (2.8)	2.6 (2.1)	5.4 (4.0)	**F(3, 81)= 10.33, p<0.0001** [h,g]
CIRS-G	5.2 (3.0)	7.2 (2.8)	10.3 (4.6)	8.5 (4.1)	**F(3,78)= 6.57, p=0.01** [f,g]
Mean CDR	NA	0.5 (0)	0.5 (0)	0.5 (0.16)	F(2,53)= 1.72, p=0.19
Mean MMSE score (Max 30)	28.4 (1.2)	26.7 (2.2)	26.2 (2.9)	26.9 (2.1)	**F(3,81)= 5.11, p=0.003** [a,b,c]
Mean ACE-R score (Max 100)	92.6 (4.3)	83.4 (9.3)	81.8 (8.0)	83.2 (9.5)	**F(3,81)= 9.42, p<0.001** [a,b,c]
Rey total trials 1-5 (max 75)	44.5 (11.5)	31.8 (10.0)	31.8 (11.7)	30.9 (8.4)	**F(3,81)=10.50, p<0.001** [a,b,c]
Rey delayed recall (max 15)	8.3 (3.6)	4.3 (4.1)	5.0 (3.2)	4.6 (3.4)	**F(3,81)= 6.93, p<0.0001** [b,c]
FAS	43.3 (9.9)	37.6 (13.5)	26.9 (10.6)	33.8 (15.1)	**F(3,81)= 5.15, p=0.003** [a,b]
ESS	4.8 (3.0)	5.4 (5.0)	5.9 (5.3)	8.1 (4.5)	**F(3,81)=3.13, P=0.03** [g]
Graded Naming	23.7 (4.1)	20.7 (4.5)	22.0 (4.4)	20.4 (5.0)	**F(3,81)=2.94, p=0.038** [b]
MDS-UPDRS III	NA	16.5 (10.4)	19.7 (11.3)	22.2 (14.8)	F(2,53)=1.04, p=0.36
Hoehn and Yahr Stage	NA	NA	0.2 (0.6)	0.7 (1.0)	t(25.7)= -1.68, p=0.11
NPI total	NA	13.0 (11.8)	11.5 (12.8)	16.5 (11.2)	F(2,48)=0.79, p=0.46
NPI distress	NA	6.0 (4.4)	7.1 (7.1)	9.8 (8.8)	F(2,48)=1.45, p=0.24

Values are expressed as mean ± standard deviation (SD).
Bold underlined characters indicate significant results.
Abbreviations: HC=Healthy controls; MCI-AD=Mild cognitive impairment due to Alzheimer's disease; MCI-LB= Mild cognitive impairment due to Lewy bodies disease; IADl= Instrumental activities of daily living; GDS= Geriatric depression score; CIRS-G = Cumulative Illness Rating Scale-Geriatric; CDR = Clinical dementia rating; MMSE=Mini-Mental State Examination; Rey= Rey Auditory Verbal Learning test; FAS= Verbal fluency measure; ESS= Epworth Sleep Scale; MDS-UPDRS III = Movement Disorder Society-Unified Parkinson's Disease Rating Scale (MDS-UPDRS); NPI= Neuropsychiatric Inventory; ACE-R= Addenbrooke's Cognitive Examination-Revised.
[a] Possible MCI-LB < Control

[b] **Probable MCI-LB < Control**
[c] **MCI-AD < Control**
[d] **MCI-AD < Possible MCI-LB**
[e] **MCI-AD < Probable MCI-LB**
[f] **Possible MCI-LB > Control**
[g] **Probable MCI-LB > Control**
[h] **MCI-AD > Control**
[I] **Possible MCI-LB < MCI-AD**
[j] **Probable MCI-LB <MCI-AD**
[k] **Probable MCI-LB < Possible MCI-LB**
[l] **Possible MCI-LB < Probable MCI-LB**

Table 6. 3 Demographics and group characteristics.

Clinical Features	**HC (n=29) Present N (%)**	**MCI-AD (n=19) Present N (%)**	**Possible MCI-LB (n=10) Present N (%)**	**Probable MCI-LB (n=27) Present N (%)**
Core Features				
Cognitive Fluctuations	0 (0%)	0 (0%)	1 (10%)	16 (59.3%)
Recurrent Visual Hallucinations	0 (0%)	0 (0%)	0 (0%)	5 (18.5%)
Spontaneous Motor Parkinsonism	0 (0%)	0 (0%)	1 (10%)	10 (37.0%)
REM sleep behaviour disorder	0 (0%)	0 (0%)	3 (30%)	23 (85.2%)
Indicative Biomarkers				
Abnormal ^{123}I-FP-CIT SPECT (visual assessment)	2 (6.9%)	1 (5.3%)	3 (30%)	15 (55.5%)
Abnormal MIBG	1 (3.4%)	0 (0%)	5 (50%)	19 (70.3%)

Table 6. 4 Percentage of core clinical features and indicative biomarker's abnormalities for all diagnostic groups.

6.4.2 Visual assessment of ^{123}I-FP-CIT SPECT images

Table 6.5 outlines the visual classification of ^{123}I-FP-CIT SPECT into normal and abnormal based on diagnostic grouping at baseline, 1st repeat and 2nd repeat ^{123}I-FP-CIT SPECT. At baseline, 6.9% (n=2) of controls had a visually abnormal ^{123}I-FP-CIT SPECT but both these were reported normal by the consensus panel upon their 1st repeat scan.

Among the possible MCI-LB group, 30% (n=3) had abnormal baseline visual imaging, while one subject with an abnormal baseline ^{123}I-FP-CIT (and abnormal MIBG) was subsequently reported as normal on subsequent imaging. Among the possible MCI-LB subjects who had normal ^{123}I- FP-CIT imaging at baseline (n=7), only 1/7 (14.3%) subsequently developed visually abnormal repeat ^{123}I-FP-CIT imaging.

In the probable MCI-LB group, the percentage of those subjects with a visually abnormal ^{123}I-FP-CIT SPECT at baseline remained relatively constant through baseline, 1st repeat and 2nd repeat, ranging from 56% to 54%. Among the probable MCI-LB group with a visually normal baseline ^{123}I-FP-CIT SPECT (n=12), 3/12 (25%) developed an abnormal ^{123}I-FP-CIT on repeat imaging. Among the probable MCI-LB group with a visually abnormal baseline ^{123}I-FP-CIT SPECT (15/27), all had a visually abnormal ^{123}I-FP-CIT SPECT upon 1st repeat, 6 of these subjects went on to have a second repeat ^{123}I-FP-CIT SPECT and 1/6 (16.7%) had a normal scan.

At baseline, 18/19 MCI-AD subjects (94.7%) had visually normal ^{123}I-FP-CIT SPECT with only 1/19 having an abnormal ^{123}I-FP-CIT SPECT. On 1st repeat 4/19 (21.1%) had abnormal ^{123}I-FP-CIT imaging, this consisted of 3 individuals with normal imaging at baseline developing an abnormal scan on 1st repeat and the subject with an abnormal scan a baseline remaining abnormal upon repeat. Notably only 1/4 (25%) who had an abnormal ^{123}I-FP-CIT on 1st repeat imaging had a 2nd repeat and this was reported as normal.

	Baseline		**1st Repeat Scan**		**2nd Repeat Scan**	
	Normal	**Abnormal**	**Normal**	**Abnormal**	**Normal**	**Abnormal**
HC	27 (93.1%)	2 (6.9%)	29 (100%)	0	NA	NA
Possible MCI-LB	7 (70%)	3 (30%)	7 (70%)	3 (30%)	3 (60%)	2 (40%)
Probable MCI-LB	12 (44.4%)	15 (55.6%)	11 (40.7%)	16 (59.3%)	6 (46.2%)	7 (53.8%)
MCI-AD	18 (94.7%)	1 (5.3%)	15 (78.9%)	4 (21.1%)	4 (100%)	0

Table 6. 5 Visual assessment classification of ^{123}I-FP-CIT imaging into normal and abnormal as per diagnostic grouping at baseline, 1st repeat and 2nd repeat imaging.

6.4.3 Mixed effects models used to investigate changes in ^{123}I-FP-CIT uptake in the striatum for each diagnostic group compared with HC.

A quadratic term was assessed but did not improve model fit. Therefore, a linear mixed effects model was utilised to assess the association between changing ^{123}I-FP-CIT striatal uptake over time and diagnostic group. A basic model was constructed, consisting of; age, gender, time in years and side (left and right striatum). The addition of diagnostic group to the model significantly improved the model fit ($p<0.001$). Finally, the interaction of diagnostic group and time significantly improved the model fit ($p=0.038$).

Significant predictors of longitudinal decline in striatal uptake are shown in Table 6.6. Probable MCI-LB was associated with a lower striatal uptake at baseline ($p=0.0001$) and more significant longitudinal decline over time in the striatum compared to HC ($p=0.022$). The longitudinal decline over time in the probable MCI-LB group was related to significant reduction in the putamen uptake ($p=0.009$) while the decline in caudate uptake was non-significant compared to HC ($p=0.08$). The possible MCI-LB group did not differ from HC in baseline striatal uptake or decline in striatal uptake over time ($p=0.058$) compared to HC. Longitudinal decline in striatal sub-regions in the possible MCI-LB group was significant in the putamen ($p=0.02$) but not the caudate ($p=0.20$). MCI-AD was not associated with lower striatal uptake at baseline ($p=0.59$) and there no difference in longitudinal striatal decline compared to HC ($p=0.915$) or any of the striatal sub-regions (putamen; $p=0.38$ and caudate; $p=0.74$).

	Striatum	Caudate	Putamen
Basic model			
Intercept[a]	**2.12 (0.10), p <0.001**	**2.27 (0.12), <0.001**	**2.04 (0.10), p<0.001**
Time: in years	0.005 (0.02), p=0.82	0.02 (0.02), p=0.44	-0.003 (0.02), p=0.88
Side: Right	0.002 (0.01), p=0.89	-0.016 (0.02), p=0.32	0.02 (0.01), p=0.12
Gender: Male	**-0.22 (0.08), p=0.008**	-0.14 (0.09), p=0.13	**-0.24 (0.08), p=0.002**
Age: years > 60	**-0.02 (0.005), p=0.001**	**-0.015 (0.005), p=0.001**	**-0.02 (0.004), p<0.001**
Basic Model + Diagnosis vs control			
MCI-AD	0.05 (0.09), p=0.59	0.03 (0.10), p=0.81	0.05 (0.09), p=0.59
Possible MCI-LB	-0.19 (0.12), p=0.10	-0.20 (0.13), p=0.14	-0.19 (0.12), p=0.11
Probable MCI-LB	**-0.35 (0.09), p=0.0001**	**-0.32 (0.09), p=0.0152**	**-0.36 (0.09), p<0.001**
Time change (Diagnosis x time)			
MCI-AD	-0.006 (0.06), p=0.915	-0.02 (0.08), p=0.74	-0.06 (0.06), p=0.38
Possible MCI-LB	**-0.14 (0.07), p=0.058**	-0.13 (0.10), p=0.20	**-0.17 (0.07), p=0.02**
Probable MCI-LB	**-0.13 (0.05), p=0.022**	-0.14 (0.08), p=0.08	**-0.15 (0.05), p=0.009**

Table 6. 6 Predictors of longitudinal change in ^{123}I-FP-CIT uptake in the striatum and striatal sub-regions using linear mixed effects model (including diagnostic group interacting with time).

[a]Estimate (SE); p value; bold underlined values indicate significant results

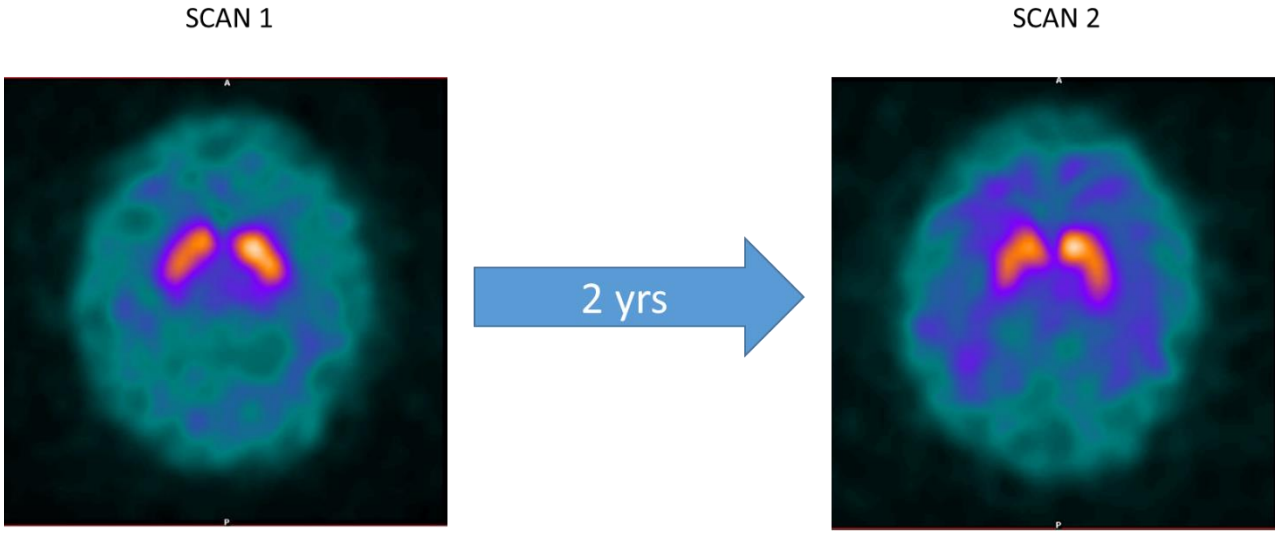

Figure 6. 3 Progressive loss of striatal ^{123}I-FP-CIT uptake in a patient with probable MCI-LB with a baseline visually normal scan and an abnormal follow up scan 2 years later. Axial sections at the level of the striatum. Asymmetrical loss of right putamen uptake in scan 2.

6.4.4 Baseline and annual percentage change in ^{123}I-FP-CIT uptake

Baseline ^{123}I-FP-CIT uptake in the striatum, caudate and putamen for each diagnostic group is displayed in Table 6.7. The probable MCI-LB group had reduced ^{123}I-FP-CIT uptake throughout the whole striatum (-19.43% ± 27.2) as a percentage of mean age-matched HC values but was more marked in the putamen (-21.26% ± 30.5) than the caudate (-15.93% ± 23.6). The possible MCI-LB group also had reduced ^{123}I-FP-CIT uptake thorough the striatum (whole striatum: -5.47% ± 16.8, caudate: -6.90% ± 15.9, putamen: -4.63% ± 19.5) as a percentage of mean HC values. There was no percentage reduction in ^{123}I-FP-CIT uptake in the whole striatum or striatal sub-regions in the MCI-AD group relative to HC.

Determination of annual percentage change in ^{123}I-FP-CIT uptake using linear interpolation for the four diagnostic groups (HC, MCI-AD, possible MCI-LB and probable MCI-LB) is shown in Table 6.8. A mean annual decline in striatal ^{123}I-FP-CIT uptake was found in both the possible MCI-LB -5.5% (95% CI: -12.6 to 1.6) and probable MCI-LB group -6.0% (95% CI: -9.1 to -2.8). In contrast, minor increases in annual percentage ^{123}I-FP-CIT striatal uptake was noted in both HC 3.8% (95% CI: -2.1 to 9.9) and MCI-AD groups 2.9% (95% CI: -4.5 to 10.4).

	HC (n= 29)	**MCI-AD (n= 19)**	**Possible MCI-LB (n= 10)**	**Probable MCI-LB (n= 27)**
Striatal uptake	1.72 ± 0.21	1.78 ± 0.38	1.63 ± 0.29	1.39 ± 0.47
Caudate Uptake	1.95 ± 0.25	1.96 ± 0.42	1.82 ± 0.31	1.64 ± 0.46
Putamen uptake	1.61 ± 0.20	1.70 ± 0.37	1.54 ± 0.31	1.27 ± 0.49
Striatum % of normal value	NA	3.64% ± 22.2	-5.47% ± 16.8	-19.43% ± 27.2
Caudate % of normal value	NA	0.46% ± 21.7	-6.90% ± 15.9	-15.93% ± 23.6
Putamen % of normal value	NA	5.50% ± 23.1	-4.63% ± 19.5	-21.26% ± 30.5
Data are displayed as mean ± standard deviation. NA = not applicable				

Table 6. 7 Baseline ^{123}I-FP-CIT striatal binding ratios per diagnostic group

	HC (n= 29)	MCI-AD (n= 19)	Possible MCI-LB (n= 10)	Probable MCI-LB (n= 27)
Striatum	3.8% (-2.1 to 9.9)	2.9% (-4.5 to 10.4)	-5.5% (-12.6 to 1.6)	-6.0% (-9.1 to -2.8)
Caudate	3.8% (-2.7 to 10.3)	8.0% (-1.7 to 17.8)	-2.4% (-8.4 to 3.5)	-3.7% (-8.2 to 0.8)
Putamen	4.1% (-2.3 to 10.5)	0.29% (-7.2 to 7.8)	-6.6% (-15.6 to 2.4)	-7.4% (-11.4 to -3.5)
Data are mean (95% confidence interval), annual percentage (%) changes in ^{123}I-FP-CIT uptake were performed after adjusting for % change from baseline and last ^{123}I-FP-CIT imaging and dividing by the annual time difference between the scans. MCI-AD,				

Table 6. 8 Annual percentage change in ^{123}I-FP-CIT uptake in HC, MCI-AD, possible MCI-LB and probable MCI-LB.

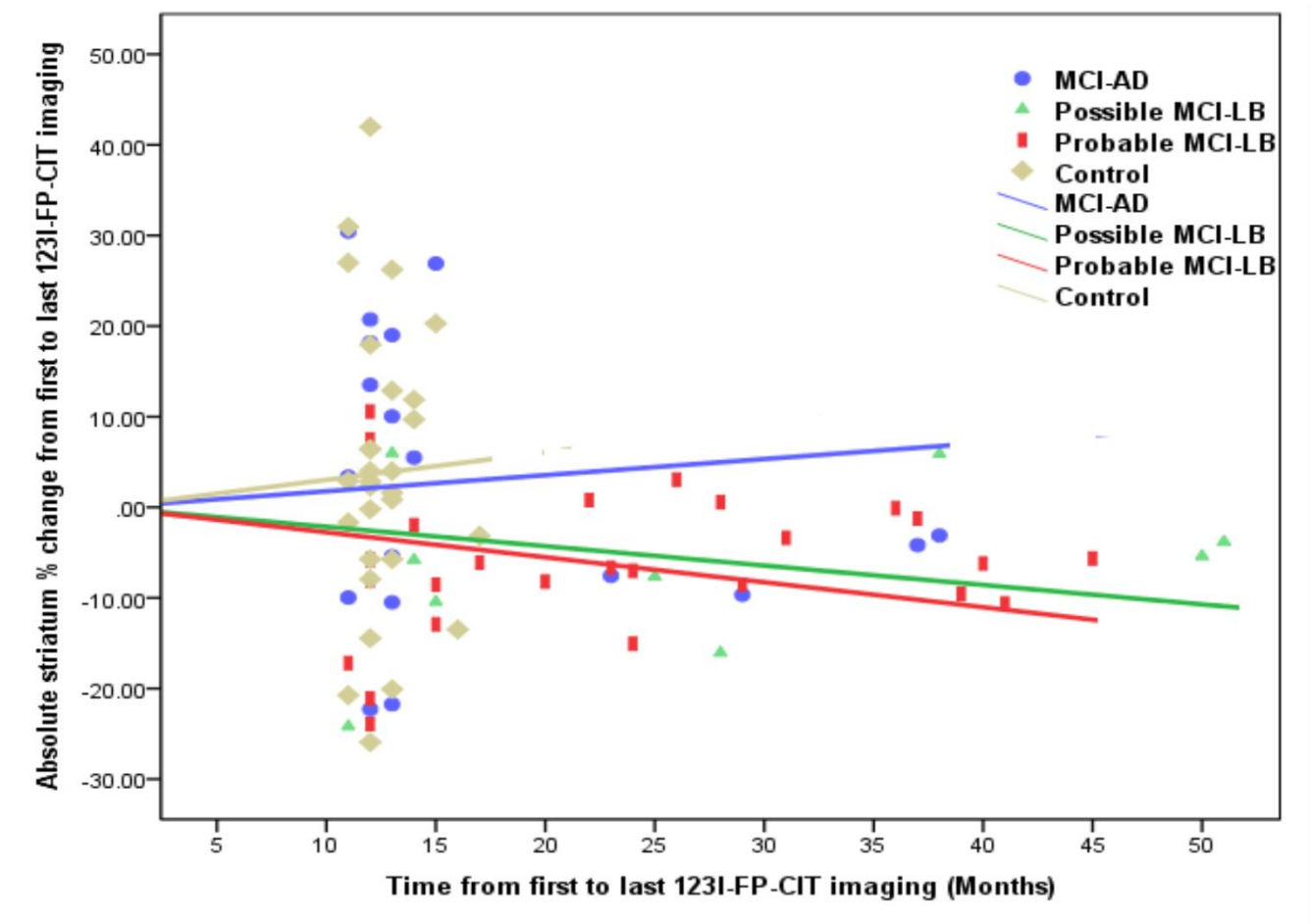

Figure 6. 4 Percentage difference in striatal ^{123}I-FP-CIT uptake between first and last follow-up 123I-FP-CIT scan for possible, probable MCI-LB, MCI-AD and HC.

6.4.5 Assessment of differential decline over time of striatal uptake between probable MCI-LB subjects with a visually normal versus a visually abnormal baseline ^{123}I-FP-CIT SPECT

A further linear mixed effects model was constructed to assess if there was a differential change in ^{123}I-FP-CIT striatal uptake over time between those probable MCI-LB with a visually normal versus a visually abnormal baseline ^{123}I-FP-CIT SPECT. Again, a basic model was constructed, consisting of; age, gender, time in years and side (left and right striatum). The addition of the subdivided probable MCI-LB group (visually normal vs abnormal rated baseline SPECT) to the model significantly improved the model fit ($p<0.001$). However, the interaction of diagnostic group (visually normal vs abnormal rated baseline SPECT) over time did not significantly improved the model fit ($p=0.23$), indicating there was no significant difference in striatal uptake decline overtime between the ^{123}I-FP-CIT SPECT rated visually normal vs those rated visually abnormal in the probable MCI-LB group.

6.5 Discussion

In this chapter, we investigated serial changes in nigrostriatal dopaminergic innervation using ^{123}I-FP-CIT SPECT in HC, MCI-AD, possible MCI-LB and probable MCI-LB. As the data consisted of follow-up imaging conducted at varying time intervals from baseline imaging for each subject, a mixed effects statistical model accounting for time from baseline imaging was used to analyse the data. This study demonstrates that the rate of decline in the striatum was significantly greater in the probable MCI-LB group, was non-significant in the possible MCI-LB and the MCI-AD group when compared with aged-matched HC. Furthermore, the nigrostriatal loss predominantly affected the putamen and significant loss in this striatal sub-region was demonstrated in both the MCI-LB groups (probable and possible). Moreover, whole striatal as well as caudate and putamen ^{123}I-FP-CIT uptake, was significantly lower in the probable MCI-LB group at baseline compared with HC, while striatal values for the MCI-AD and possible MCI-LB ^{123}I-FP-CIT uptake were not significantly lower than HC. To the best of our knowledge, this is the first study to demonstrate progressive loss of striatal dopaminergic innervation using a MCI cohort with suspected LB disease.

Sequential nigrostriatal presynaptic DAT imaging with either SPECT or PET is a relatively understudied topic in LB disease. Using a linear mixed effects model assessing rates of decline of ^{123}I-FP-CIT uptake derived from semi-quantitative SBRs, we found a significant striatal decline of DAT

availability in the probable MCI-LB group over time (p=0.02) but no significant striatal decline in the possible MCI-LB group over time (p=0.058) compared to HC. In fact, the estimate of effect size was slightly greater in the possible MCI-LB group (-0.14) than the probable MCI-LB group (-0.13). However, there was a larger standard error for the decline of the possible MCI-LB group (0.07) than the probable MCI-LB group (0.05) which ultimately was responsible for the non- significant result obtained in the possible MCI group. The larger standard error was due to two factors; (1) the smaller subject numbers (n=10) in the possible MCI-LB group; (2) the diagnostic clinical uncertainty within the possible MCI-LB group is larger based on experience obtained from studies in possible DLB whereby a significant proportion within this subgroup will likely turn out to have alternative diagnosis besides LB disease for their cognitive impairment. Notably, examination of the rate of decline in the striatal sub-region found significant decline only in the putamen uptake over time in both MCI-LB groups but not the caudate. Reassuringly, the MCI-AD group did not have any significant decline in the whole striatum or its sub-regions compared to controls which would be consistent with the lack of involvement of the nigrostriatal pathway in AD pathology.

In order to compare this study with prior published literature, estimates for mean annual percentage decline in striatal ^{123}I-FP-CIT uptake were derived as relatively few studies have examined annual percentage change in either DLB or prodromal DLB phenotypes. This study found a mean reduction in the striatum of -6% in the probable MCI-LB and -5.5% in the possible MCI-LB groups. In both MCI-LB groups, the mean loss in the striatum was predominately due to loss in the putamen (-7.4% and -6.6%) rather than the caudate (-3.4% and -2.4%). Therefore, our study demonstrates a preserved rostro-caudal (caudate-to-putamen) gradient of dopaminergic loss in prodromal DLB in contrast to flatter rostro-caudal gradient, with a reduced caudate-to putamen ratio in early DLB [75, 211, 212, 219]. Only one study in DLB has been undertaken which examined annual percentage loss in striatal ^{123}I-FP-CIT uptake and this showed a more uniform loss throughout the striatum and a loss far in excess of values in our study, with annual decline in caudate uptake of -12.7% and -13.0% in the putamen [68]. The findings from our study are more akin to annual percentage declines reported in IRBD and PD studies which found greater loss in the putamen than the caudate. In IRBD, the annual rate of decline in the putamen was -5.8% and in the caudate was -3.0% [240]. Studies in PD have shown similar declines in the caudate (-4.6% to 11.0%) and in the putamen (-6.0% to 10.0%) [236-238]. There is some evidence to suggest that the decline in striatal uptake is not linear but becomes more rapid around the time of clinical conversion to dementia

from MCI and as the clinical deterioration in DLB is more rapid it would account for the more rapid decline in annual striatal uptake. In the IRBD study, those who converted to PD had a more rapid decline in the putamen of approximately 10% per year [240]. Eventually, dopaminergic nigrostriatal denervation progresses and comes to involve both putamina and with time head of caudate involvement leads to a decline in the rostro-caudal gradient. In contrast, if there is a dopaminergic deficit present at the early stages in DLB, it tends to be more symmetrical and have a flatter rostro-caudal gradient, with a reduced caudate-to putamen ratio [75, 211, 212, 219].

The levels of striatal dopaminergic loss at baseline in both the probable MCI-LB and possible MCI-LB group compared to controls were substantial in the probable MCI-B, with mean losses of -19.4% and milder in the possible MCI-LB, with a mean loss of -5.5%. On visual assessment, 55% of the probable MCI-LB and 30% of the possible MCI-LB cohort had an abnormal ^{123}I-FP-CIT SPECT. Evidence of an early dopaminergic deficit in a cohort of MCI participants with suspected LB disease, is consistent with findings from other prodromal α-synucleinopathies studies (e.g. IRBD, prodromal Parkinson's disease and MCI-LB) [142] [27, 240]. A previous study reported that an abnormal ^{123}I-FP-CIT SPECT was present in 60% of the probable MCI-LB and 40% of possible MCI-LB subjects [27]. This represented a high specificity (89%) but a low sensitivity (54.2%) for the detection of LB disease at the MCI stage [27], especially when compared to a sensitivity 78% and specificity 90% at the dementia stage [200]. A possible explanation for the difference in sensitivity at the prodromal DLB stage versus the dementia stage is that nigrostriatal degeneration is less severe in earlier stage. Similar to the findings in our cohort, other prodromal DLB phenotypes such as IRBD have shown an abnormal ^{123}I-FP-CIT SPECT in 59% of subjects [149]. Moreover, the extent of baseline dopaminergic deficit in IRBD predicts future conversion to either DLB or PD. A baseline reduction of ^{123}I-FP-CIT uptake in putamen greater than 25% from the mean of normal HC values predicting those who developed a α-synucleinopathy after 3 years of follow-up [149]. Unfortunately, we are presently unable to comment on whether the extent of baseline dopaminergic deficit in our MCI-LB subjects predicts more rapid progression to DLB, as too few of the cohort has reached 3 years of follow-up. The longitudinal follow-up of our cohort should allow for a better understanding of whether the extent of initial dopaminergic deficit on baseline ^{123}I-FP-CIT imaging predicts time to conversion to DLB.

Interestingly, the visual assessment of ^{123}I-FP-CIT SPECT showed a relatively static proportion of individuals within the probable and possible MCI-LB cohort having an abnormal ^{123}I-FP-CIT SPECT over time and an increase in the proportion of MCI-AD subjects having an abnormal ^{123}I-FP-CIT SPECT over time. However, care must be taken with visual interpretation of ^{123}I-FP-CIT SPECT results as false positives and negatives are frequent. Notably, in the MCI-AD group, 5.3% (n=1) of subjects had a visually abnormal ^{123}I-FP-CIT at baseline and this proportion increased to 21.1% (n=4) with a visually abnormal ^{123}I-FP-CIT SPECT at the time of first repeat. There are two explanations to account for why this might have been the case. Firstly, these cases may be false positive results in the interpretation of ^{123}I-FP-CIT SPECT imaging. False-positive results have been noted to occur in approximately 10-15% of cases [28, 248]. In order to minimise false-positives due to cerebrovascular disease, all subjects had their MRI reviewed by a clinician to check for evidence of cerebral infarcts prior to inclusion in the study. Secondly, it could be that that a significant proportion of the MCI-AD have mixed pathology, with underlying LB pathology being subclinical and only being detectable with the aid of a biomarker. Only analysis of the quantitative data demonstrated a decline over time on repeat imaging of our MCI-LB groups, visual assessments failing to demonstrate a significant change in the proportion of those ^{123}I-FP-CIT SPECT images which became abnormal on repeat imaging. The rationale for repeat ^{123}I-FP-CIT SPECT imaging is based on the observation that 10% of DLB patients have only neocortical LB pathology sparing the midbrain and therefore will have an initial negative ^{123}I-FP-CIT [28] . However, as time progresses spread of the LB pathology from “top-to-bottom” may occur resulting in midbrain involvement and an eventual positive ^{123}I-FP-CIT SPECT. A previous study in probable DLB patients has demonstrated the benefit of repeat ^{123}I-FP-CIT SPECT imaging as those with an initial visually normal scan eventually developed an abnormal ^{123}I-FP-CIT SPECT with time [71]. The median time between scans in that study was 18 months [71]. Therefore, visual assessment of scans in the early stage of DLB may lack sensitivity. The findings from our study would be consistent with the aforementioned study. Only the application of semi-quantitative uptake values detected the significant decline over time in the MCI-LB groups indicating the relatively mild loss in dopaminergic neurons at the earliest stage of LB disease. In fact, nigrostriatal dopaminergic neuron loss was approximately half in our study compare with that reported in prior work in DLB [68] and a loss of dopaminergic neurons became detectable in our study by semi-quantitative measures at a mean time between scans of 17 months.

There was a mis-match between baseline biomarker abnormalities and the presence of clinical parkinsonism, 55% of probable MCI-LB subjects had a visually abnormal ^{123}I-FP-CIT SPECT while clinical parkinsonism was only detectable in 37% of these subjects. It is unsurprising that clinical parkinsonism is undetectable in our cohort based on the relatively mild striatal dopaminergic loss outlined above in semi-quantitative analysis, particularly given that the evidence indicates that parkinsonism only becomes detectable when 30-60% of terminals are lost [206]. In PD, abnormalities in ^{123}I-FP-CIT SPECT may be detectable in advance of clinical manifestations, with striatal uptake being reduced by a lesser extent in the sided contralateral to unilateral symptom onset [257]. Therefore, biomarkers such as ^{123}I-FP-CIT SPECT and MIBG have an important role to play in the early diagnosis of LB disease which tends to be subclinical in its earliest manifestations.

This study has several strengths: (1) a prospective longitudinal design in a cohort of patients with MCI-LB, using serial functional imaging at various time points; (2) the inclusion of matched HC to establish whether the process of ageing alone could account for the decline in striatal 123I-FP-CIT uptake; (3) the confirmation of clinical core features of LB disease by consensus panel blinded to the imaging results; (4) the construction of diagnostic groups incorporating imaging biomarkers.

Some limitations of the study should be acknowledged. Some of the cohort may have diagnostic misattribution, especially as many are early in their disease trajectory and future pathological examination may lead to diagnostic re-assignment. However, much effort was done to minimise this problem with the incorporation of cardiac MIBG into to the diagnostic process. Another limitation of this study is that follow-up was relatively short, with a variable time between baseline and repeat ^{123}I-FP-CIT imaging.

In conclusion, the results of this study confirm that ^{123}I-FP-CIT SPECT can be abnormal at the prodromal stage of DLB. Furthermore, we found that there was progressive decline over time in striatal binding, predominately in the putamen, in patients with MCI-LB compared with aged-matched HC. Serial dopaminergic imaging with ^{123}I-FP-CIT SPECT is a sensitive marker of nigrostriatal neurodegeneration in LB disease and differences in the rates of decline between patient groups may have the potential to differentiate between MCI-LB from MCI-AD. Follow up DAT imaging may be of value in patients with MCI-LB and a normal baseline scan.

Chapter 7. Structural MRI changes in MCI-LB: cortical thickness, cortical, subcortical and brainstem volume analysis

7.1 Aims

The primary aim of this chapter was to investigate cortical thickness patterns and cortical, subcortical and brainstem volumes in subjects with MCI-LB to determine if these structural MRI measures may aid in the differential diagnosis of MCI-LB from MCI-AD.

7.2 Hypotheses

7.2.1 Primary hypotheses

1. Cortical thinning in MCI-LB will be intermediate between HC and MCI-AD.
2. Atrophy in subcortical structures in MCI-LB will be intermediate between HC and MCI-AD. Specifically, the limbic structures in MCI-AD will have more pronounced atrophy relative to MCI-LB.
3. Atrophy in brainstem structures, particularly the midbrain, will be more pronounced in MCI-LB compared with HC and MCI-AD.

7.3 Methods

7.3.1 Participants

One hundred and eighteen subjects completed ^{123}I-FP-CIT SPECT, MIBG and structural MRI imaging as well as clinical assessments. Two subjects had contraindications to MRI scans. Six scans had significant pial and WM surface errors which were not amendable to manual correction and hence were excluded from the analysis. Consistent with prior published MRI analysis, the possible MCI-LB group (n=18) was excluded from the analysis and the probable MCI-LB group is referred to as the MCI-LB group in this chapter. Therefore, ninety four subjects were included in this analysis, consisting of; HC (n=31), MCI-AD (n=29), MCI-LB (n=34).

7.3.2 Diagnostic Classification

Subjects were allocated to one of four clinical diagnoses: HC (cognitively normal individual with no core symptoms of DLB), possible MCI-LB (MCI plus one core symptom of DLB or MCI with none of the four core symptoms of DLB but having either an abnormal cardiac MIBG or ^{123}I-FP-CIT SPECT), probable MCI-LB (MCI plus two or more of the four core symptoms of DLB or MCI plus once core symptom of DLB and either an abnormal cardiac MIBG or ^{123}I-FP-CIT SPECT), MCI-AD (MCI with none of the core four symptoms of DLB and both a normal cardiac MIBG and ^{123}I-FP-CIT SPECT).

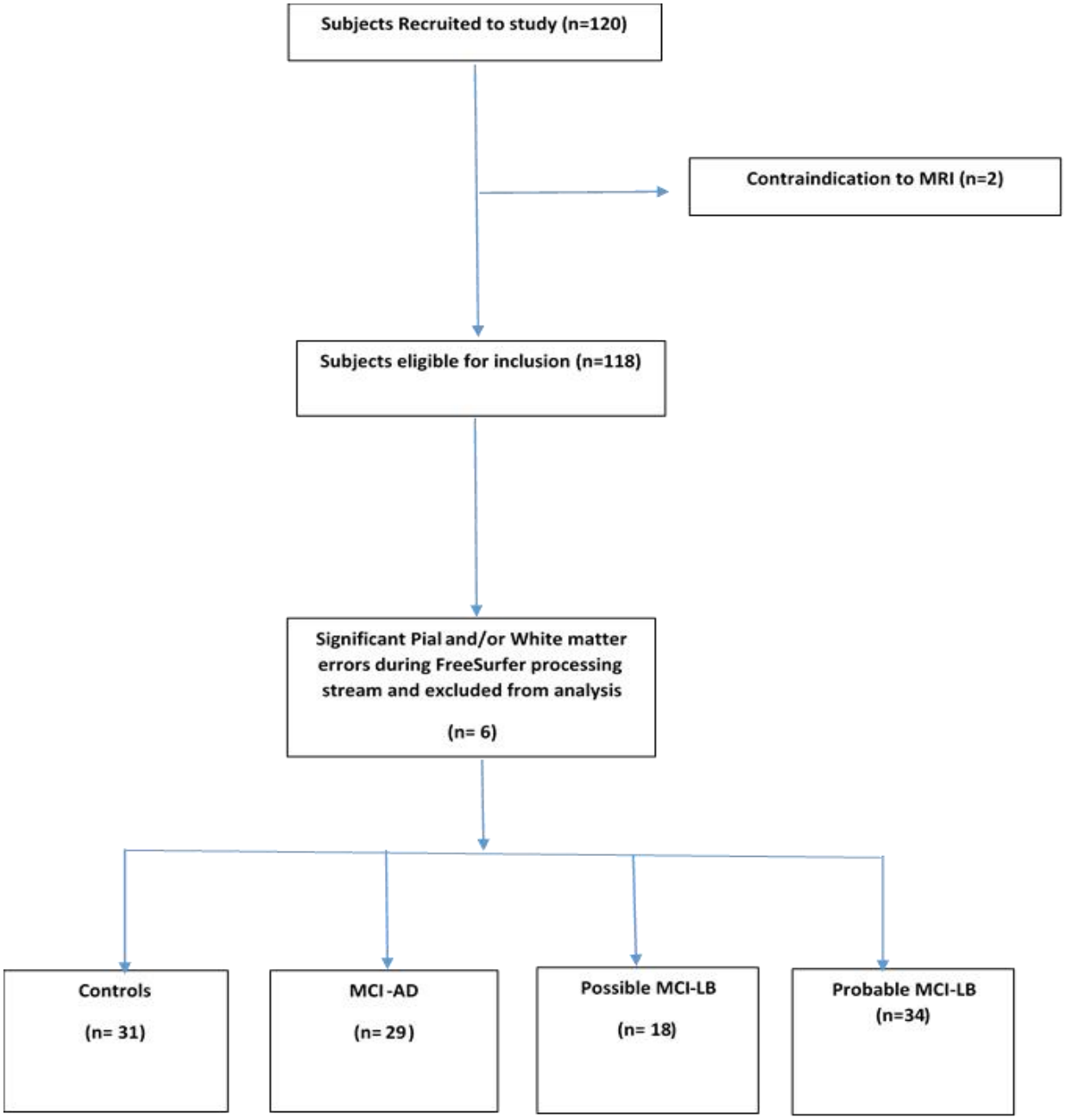

Figure 7. 1 Flowchart for inclusion in cortical thickness and cortical, subcortical and brainstem volume analysis.

7.3.3 Image processing for cortical thickness analysis

Cortical thickness analysis was performed from a three-dimensional model of cortical surface reconstructions computed from T1 weighted images using the FreeSurfer software package (v. 6.0, http://surfer.nmr.mgh.harvard.edu/). The technical aspects and details of the procedure have been previously described in other publications [394, 395]. In brief, the processing pipeline procedure involves intensity non-uniformity correction, automated Talairach space transformation of each subject's native brain, removal of non-brain tissue (skull stripping), segmentation of the GM-WM volumetric structures, tessellation of the GM-WM and GM-cerebrospinal fluid borders. Parcellation of the cerebral cortex into units based on gyral and sulcal structure allows for representations of cortical thickness [396, 397]. The cortical thickness was then calculated as the shortest distance between the cortical surface and the GM-WM boundary (Figure 7.2). A cortical map was generated by calculating the average thickness of each cortex. All images were aligned to a common surface template and smoothing with a Gaussian kernel of 20mm full-width half maximum (FWHM) was performed on the cortical maps of each subject for the entire cortex analysis.

Following completion of the automated FreeSurfer pipeline, visual inspection was undertaken to assess the quality of skull stripping and ensure that cortical surfaces followed the GM and WM boundaries. Manual corrections were performed as appropriate to correct errors in skull stripping, GM or WM boundaries before regenerating the pial or WM surfaces or both.

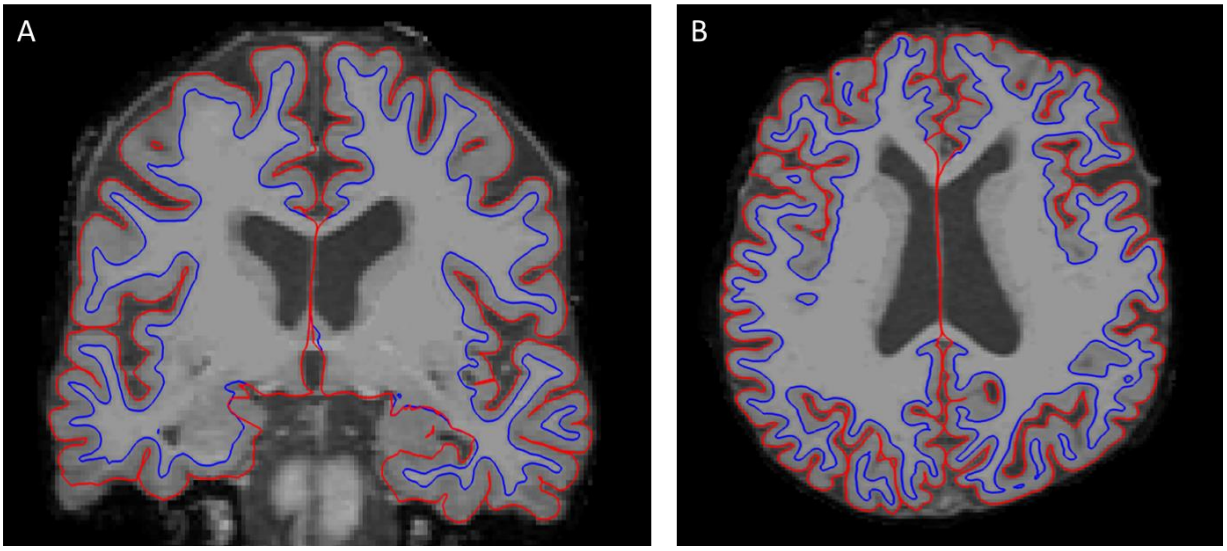

Figure 7. 2 Coronal (A) and Axial (B) images of GM and WM structures, with grey/white (blue) and pial surfaces (red) overlaid.

7.3.4 Image processing for subcortical and brainstem volume analysis

Subcortical volumes were measured automatically using the FreeSurfer procedure for volumetric measures. In brief, this involves an automated subcortical parcellation in FreeSurfer to detect the subcortical structures based on a probabilistic atlas. The probabilistic atlas, obtained from a manually labelled training set [398], was mapped into Talairach space in which all participants images were registered, and the value for each voxel was measured and assigned one of 40 labels [398]. The six subcortical labels that were used for analysis were; putamen, caudate, thalamus, amygdala, pallidum and nucleus accumbens. The total intracranial volume (TIV) was also calculated using FreeSurfer, as previously described [399].

The automated volumetric brainstem volume segmentation was implemented in FreeSurfer using the "recon-all" command line followed by "brainstem-substructures" option. The automated segmentation of brainstem volumes was based on a probabilistic atlas of the brainstem structures delineated manually from 49 scans [400]. The five brainstem structures segmented according to this algorithm include; medulla, pons, superior cerebellar peduncle, midbrain and whole brainstem volume.

7.3.5 Statistical analyses

For analysing cortical, subcortical and brainstem MRI volume data, between-group differences were tested using analysis of covariance (ANCOVA), controlling for age and TIV and adjusting for multiple comparisons by *post-hoc* Bonferroni correction.

7.3.6 Cortical thickness

Cortical thickness difference between-groups was measured on a vertex wise basis using the general linear model (GLM) and was conducted using the QDEC software (http://surfer.nmr.mgh.havard.edu/fswiki/Qdec). Pair-wise comparisons between groups were conducted to determine the cortical thickness differences between HC, MCI-AD and MCI-LB groups. Cortical thickness was modelled as a function of the group controlling for the effects of age and gender as nuisance covariates. For all statistical analyses, a false discovery rate (FDR) correction was applied.

7.4 Results

7.4.1 Demographics and clinical characteristics

Clinical characteristics, neuropsychological tests and demographic data are shown in Table 7.1 and the core features of MCI-LB group are shown in Table 7.2. The patient groups and HC group did not differ significantly with respect to age. The duration of memory complaints did not differ between MCI-AD and the MCI-LB group (P=0.51). Mean years of education was significantly higher among HC than MCI-LB ($F(2,88)=3.85$, $p=0.03$) but there was no difference between MCI-AD and MCI-LB. There was a significant difference between-groups in terms of gender ($X^2(2)=18.26$, $P<0.001$), with significantly fewer females in the MCI-LB ($\chi^2(1)=4.4$, $p=0.04$) and MCI-AD ($\chi^2(1)=5.34$, $P=0.02$) groups compared to controls. ACE-R scores were significantly lower in the probable MCI-LB and MCI-AD groups ($F(2,91)=14.59$, $P<0.001$) compared to control participants but there was no difference between MCI groups (p=1.0). There were significant differences between groups in terms of FAS score, graded naming test, ESS, GDS and NPI score.

Characteristic	HC (n= 31)	MCI-AD (n= 29)	MCI-LB (n= 34)	Group Comparisons
Mean age (years)	73.71 ± 7.32	75.38 ± 7.70	74.68 ± 6.69	F(2,91)=0.41, P=0.67
M:F (%)	22/9 (71%/29%)	12/17 (41.4%/58.6%)	31/3 (91.2%/8.8%)	**$X^2(2)=18.26$, P<0.001[a,f]**
Mean years of education	14.67 ± 4.0	12.81 ± 3.78	12.24 ± 2.95	**F(2,88)= 3.85, P=0.03 [a]**
Duration of memory compliant (months)	NA	44.23 ± 56.244	53.00 ± 44.65	t(57)= -0.67, P=0.51
IADL	NA	7.4 ± 1.0	6.5 ± 1.4	**t(52)=2.68, p=0.01**
GDS (Max 15)	1.26 ± 1.83	3.53 ± 2.59	4.64 ± 3.88	**F(2,91)=11.03, P<0.001[a,b]**
CIRS-G	5.27 3.3	6.11 3.3	8.1 4.1	**F(2,86)=4.91, p=0.01[d]**
Mean CDR	0	0.5 ± 0	0.5 ± 0.15	t(60)=1.62, P=0.11
Mean MMSE score (Max 30)	28.45 ± 1.12	27.14 ± 2.18	26.62 ± 2.41	**F(2,91)=7.11, P=0.001[a,b]**
Mean ACE-R score (Max 100)	92.68 ± 4.24	83.55 ± 8.40	84.06 ± 8.84	**F(2,91)=14.59, P<0.001[a,b]**
Rey total trials 1-5 (Max 75)	44.5 ± 11.1	33.1 ± 1.9	32.4 ± 7.6	**F(2,91)=15.68, P<0.001[a,b]**
Rey delayed recall (Max 15)	8.42 ± 3.5	3.71 ± 4.3	5.00 ± 3.4	**F(2,89)=12.74, P<0.001[a,b]**
FAS	43.06 ± 9.83	37.55 ± 11.69	32.44 ± 7.58	**F(2,91)=5.31, P=0.007[a]**
ESS	4.74 ± 2.90	5.62 ± 4.37	8.97 ± 4.32	**F(2,91)=10.55, P<0.001[c.d]**
Graded Naming	23.71 ± 3.96	19.55 ± 4.98	20.79 ± 4.12	**F(2,91)=7.30, P=0.001[a,b]**
MDS-UPDRS III	NA	15.62 ± 14.89	22.65 ± 14.65	t(61)= -1.88, P=0.06
Hoehn and Yahr Stage	NA	0	0.73 ± 1.0	**t(59)= -3.57, p=0.001**
NPI total	NA	8.74 ± 10	16.06 ± 12.99	**t(52)=-2.25, P=0.03**
NPI distress	NA	3.57 ± 3.48	8.87 ± 8.48	**t(52)=-3.15 , p=0.03**

Values are expressed as mean ± standard deviation (SD).
Bold underlined characters indicate significant results.

Abbreviations: HC= Healthy controls, MCI-AD=Mild cognitive impairment due to Alzheimer's disease; MCI-LB= Mild cognitive impairment due to Lewy bodies disease; IADl= Instrumental activities of daily living; GDS= Geriatric depression score; CIRS-G = Cumulative Illness Rating Scale-Geriatric; CDR = Clinical dementia rating; MMSE=Mini-Mental State Examination; Rey= Rey Auditory Verbal Learning test; FAS= Verbal fluency measure; ESS= Epworth Sleep Scale; MDS-UPDRS III = Movement Disorder Society-Unified Parkinson's Disease Rating Scale (MDS-UPDRS); NPI= Neuropsychiatric Inventory; ACE-R= Addenbrooke's Cognitive Examination-Revised.

[a]**MCI-LB < Control**
[b]**MCI-AD < Control**
[c]**MCI-AD < MCI-LB**
[d]**MCI-LB > Control**
[e]**MCI-AD > Control**
[f]**MCI-LB < MCI-AD**

Table 7. 1 Demographics and group characteristics.

Clinical Features	**Present N (%)**
Core Features	
Cognitive Fluctuations	21 (61.8%)
Recurrent Visual Hallucinations	6 (17.6%)
Spontaneous Motor Parkinsonism	12 (35.3%)
REM sleep behaviour disorder	27 (79.4%)
Indicative Biomarkers	
Abnormal FP-CIT SPECT	22(64.7%)
Abnormal MIBG	24 (70.6%)

Table 7. 2 Percentage of core clinical features and indicative biomarker's abnormalities for MCI-LB participants.

7.4.2 Cortical thickness analysis

Analysis of cortical thickness in both the left ($F(2,88)=3.82$, $p=0.08$) and right hemisphere ($F(2.88)=2.32$, $p=0.10$) did not show any significant difference between HC, MCI-LB and MCI-AD (Table 7.3). The vertex-wise comparisons with correction for multiple comparisons of cortical thickness found no differences between; HC vs MCI-AD; or HC vs MCI-LB; or MCI-AD vs MCI-LB. At a more liberal threshold of $p<0.001$ (uncorrected), two clusters of cortical thinning in MCI-AD compared to HC were noted in the right hemisphere: right parahippocampal and right insula. At the threshold $p<0.001$ (uncorrected), there was no difference in cortical thinning between: HC vs MCI-LB; or MCI-LB vs MCI-AD.

Cortical thickness (mm)	HC (n= 31)	MCI-AD (n= 29)	MCI-LB (n= 34)	ANCOVA[a]
Left hemisphere (mm)	2.29 ± 0.22	2.37 ± 0.16	2.34 ± 0.15	F(2,88)=3.82, p=0.08, η_p^2=0.056
Right hemisphere (mm)	2.28 ± 0.23	2.36 ± 0.16	2.33 ± 0.16	F(2.88)=2.32, p=0.10, η_p^2=0.05
Frontal (mm)	2.37 ± 0.22	2.45 ± 0.17	2.41 ± 0.16	F(2,88)=2.30, p=0.11, η_p^2=0.05
Parietal (mm)	2.17 ± 0.19	2.34 ± 0.16	2.22 ± 0.12	F(2,88)=2.18, p=0.12, η_p^2=0.047
Temporal (mm)	2.63 ± 0.33	2.69 ± 0.21	2.68 ± 0.23	F(2,88)=0.81, p=0.45, η_p^2=0.018,
Occipital (mm)	1.82 ± 0.19	1.90 ± 0.12	1.86 ± 0.15	F(2.88)=2.98, p=0.06, η_p^2=0.063
Cingulate (mm)	2.31 ± 0.30	2.42 ± 0.18	2.37 ± 0.22	F(2,88)=2.31, p=0.11, - η_p^2=0.05
Insula (mm)	2.55 ± 0.32	2.65 ± 0.21	2.64 ± 0.23	F(2,88)=2.17, p=0.12, η_p^2 =0.047

Units of measurement are mm
Values are expressed as mean ± standard deviation (SD).
Bold underlined characters indicate significant results.
Abbreviations: HC= Healthy controls, MCI-AD=Mild cognitive impairment due to Alzheimer's disease; ANCOVA= analysis of covariance; MCI-LB= Mild cognitive impairment due to Lewy body disease;
[a]ANCOVA followed by Bonferroni correction was carried out to test the difference among groups

Table 7. 3 Cortical thickness values for HC, MCI-AD and MCI-LB.

7.4.3 Gross brain volumes

Average total cerebral cortex volume, cerebral WM volume, total GM volume, total subcortical GM volume and lateral ventricles volume were estimated for each group and presented in Table 7.4. After controlling for age and TIV, there was no significant difference between-groups in terms of gross brain volumes. Lateral ventricle volume was increased in MCI-LB as compared to HC ($p<0.01$) but was not significantly different to MCI-AD ($p=0.15$).

	HC (n= 31)	MCI-AD (n= 29)	MCI-LB (n= 34)	Group Comparisons
Cerebral Cortex volume (cm^3)	432 ± 39	416 ± 49	425 ± 43	F(2,89)=1.09, P=0.34, η_p^2 =0.024
Cerebral WM volume (cm^3)	473 ± 91	421 ± 69	466 ± 98	F(2,89)=2.73, p=0.07, η_p^2=0.058
Total GM volume (cm^3)	594 ± 48	578 ± 59	585 ± 55	F(2,89)=1.77, P=0.18, η_p^2=0.038
Total Subcortical GM (cm^3)	54 ± 4	52 ± 5	53 ± 4	F(2,89)=1.99 P=0.14, η_p^2=0.043
Lateral ventricles volume (cm^3)	36 ± 15	45 ± 22	53 ± 24	**F(2,89)=6.02, P<0.01,** η_p^2=**0.12**
TIV (cm3)	1626 ± 121	1605 ± 166	1674 ± 187	F(2,90)=1.44, P=0.24 η_p^2 = 0.031

Units of measurement cm^3
Values are expressed as mean ± standard deviation (SD).
Bold underlined characters indicate significant results.
Abbreviations: HC= Healthy controls, MCI-AD=Mild cognitive impairment due to Alzheimer's disease; MCI-LB= Mild cognitive impairment due to Lewy bodies disease; TIV= Total intracranial volume; GM= Grey matter; WM= White matter

Table 7. 4 Comparison of difference in mean values for cerebral cortex, cerebral WM and lateral ventricle volumes between groups.

7.4.4 Subcortical grey matter volume

Mean subcortical GM volumes were estimated for each group and are shown in Table 7.5. Volumetric analysis showed that MCI-LB had intermediate mean values of subcortical volumes between HC and MCI-AD (MCI-AD < MCI-LB < HC), with the exception of thalamic volumes which were lowest in MCI-LB. After controlling for age and TIV, thalamic volumes were significantly lower in the MCI-LB group compared to HC (p=0.032) and MCI-AD (p=0.035). There was also a significant difference noted between groups in terms of amygdala volume (F(2,89)=6.87, P=0.002), with *post-hoc* comparisons showed reduced amygdala volume in MCI-AD compared to HC (p=0.001). No difference between groups were noted in terms of caudate, putamen, pallidum or nucleus accumbens volume.

Subcortical structure	HC (n= 31)	MCI-AD (n= 29)	MCI-LB (n= 34)	ANCOVA[a]	Bonferroni pairwise post hoc		
					MCI-LB vs HC	MCI-AD vs HC	MCI-LB vs MCI-AD
Amygdala (mm^3)	3040. ± 448	2601 ± 492	2872 ± 468	**F(2,89)=6.87, P=0.002, η_p^2 =0.132**	0.09	**0.001**	0.35
Thalamus (mm^3)	13919 ± 1414	13616 ± 1430	13552 ± 1545	**F(2,89)=3.16, P=0.047, η_p^2 =0.066**	**0.035**	0.93	**0.032**
Caudate (mm^3)	6787 ± 873	6676 ± 1426	6742 ± 1137	F(2,89)=0.23, p=0.80, η_p^2 = 0.005	NA	NA	NA
Putamen (mm^3)	8503 ± 855	8428 ± 1156	8445 ± 1484	F(2,91)=0.41, P=0.66, η_p^2 =0.009	NA	NA	NA
Pallidum (mm^3)	3662 ± 502	3514 ± 398	3646 ± 645	F(2,89)=0.20, P=0.82, ηp2=0.004	NA	NA	NA
Accumbens (mm^3)	823 ± 123	737 ± 157	773 ± 140	**F(2,89)=3.20, p=0.045, η_p^2 =0.067**	0.11	0.09	1.0

Units of measurement mm^3
Values are expressed as mean ± standard deviation (SD).
Bold underlined characters indicate significant results.
Abbreviations: HC= Healthy controls, MCI-AD=Mild cognitive impairment due to Alzheimer's disease; MCI-LB= Mild cognitive impairment due to Lewy body disease

Table 7. 5 Subcortical volumes in HC, MCI-AD and MCI-LB.

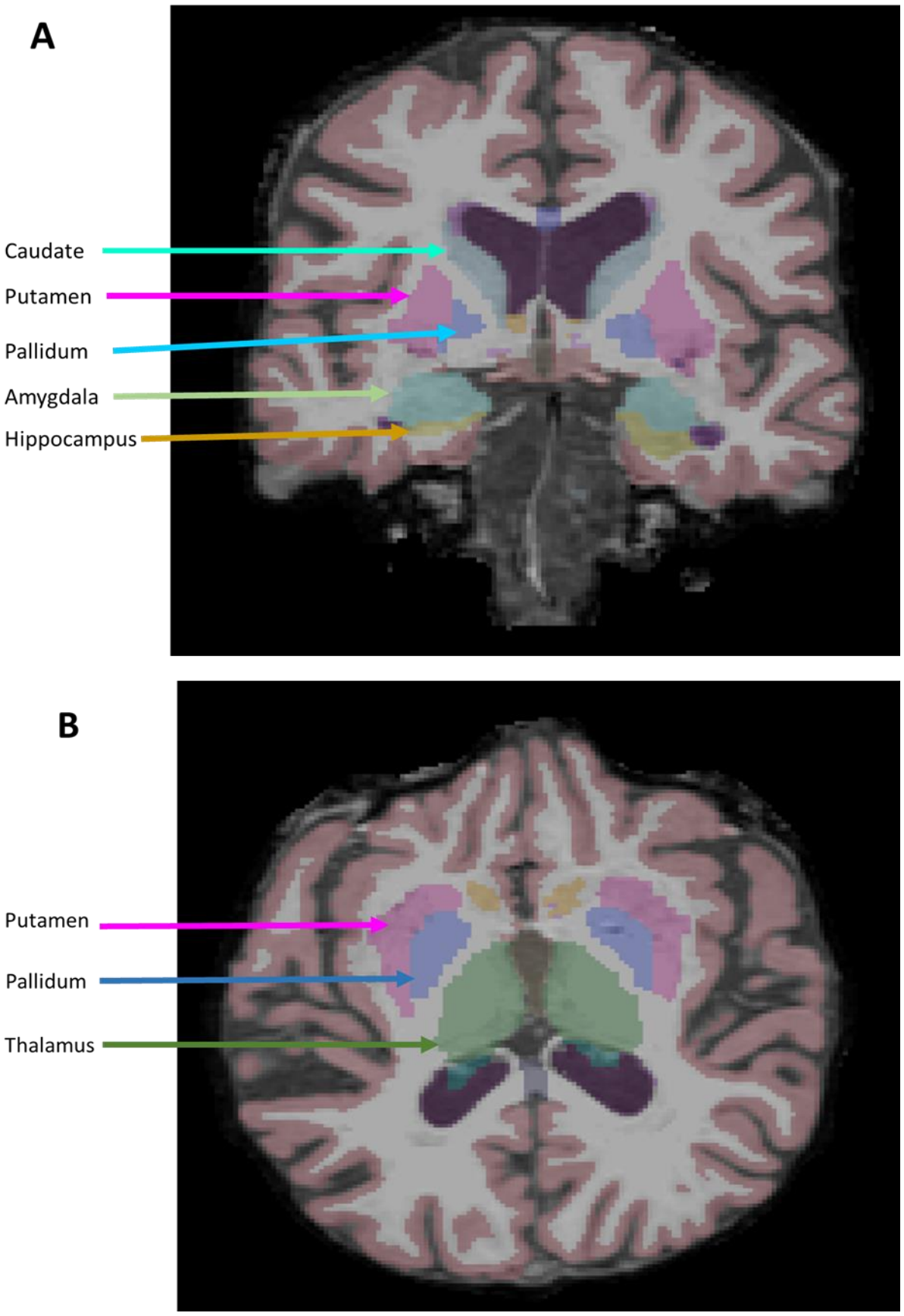

Figure 7. 3 Segmentation of subcortical structures by FreeSurfer (A) Coronal section (B) Axial.

7.4.5 Brainstem volume

Brainstem substructures volume were estimated and are presented in Table 7.6. For all brainstem substructures the lowest mean value was found in MCI-AD, but after controlling for age and TIV no statistical difference in volume was found between all three groups.

Brainstem structure	HC (n= 31)	MCI-AD (n= 29)	MCI-LB (n= 34)	Group comparison
Medulla (mm^3)	4677 ± 508	4472 ± 590	4609 ± 609	F(2,88)=0.51, p=0.61, η_p^2 0.011
Pons (mm^3)	14947 ± 1708	13926 ± 1658	14555 ± 2185	F(2,88)=1.64, p=0.20, η_p^2 =0.036
Superior cerebellar peduncle (mm^3)	281 ± 46	272 ± 64	291 ± 73	F(2,88)=0.52, p=0.59, η_p^2 =0.012
Midbrain (mm^3)	6044 ± 641	5688 ± 531	5838 ± 726	F(2,88)=1.93, p=0.15 η_p^2 =0.042
Whole brainstem volume (mm^3)	25950 ± 2768	24359 ± 2670	25293 ± 3423	F(2,88)=1.59, p=0.21, η_p^2 =0.035
Units of measurement mm^3 Values are expressed as mean ± standard deviation (SD). Bold underlined characters indicate significant results. Abbreviations: HC= healthy controls, MCI-AD=Mild cognitive impairment due to Alzheimer's disease; MCI-LB= Mild cognitive impairment due to Lewy body disease				

Table 7. 6 Brainstem substructure volumes in HC, MCI-AD and MCI-LB.

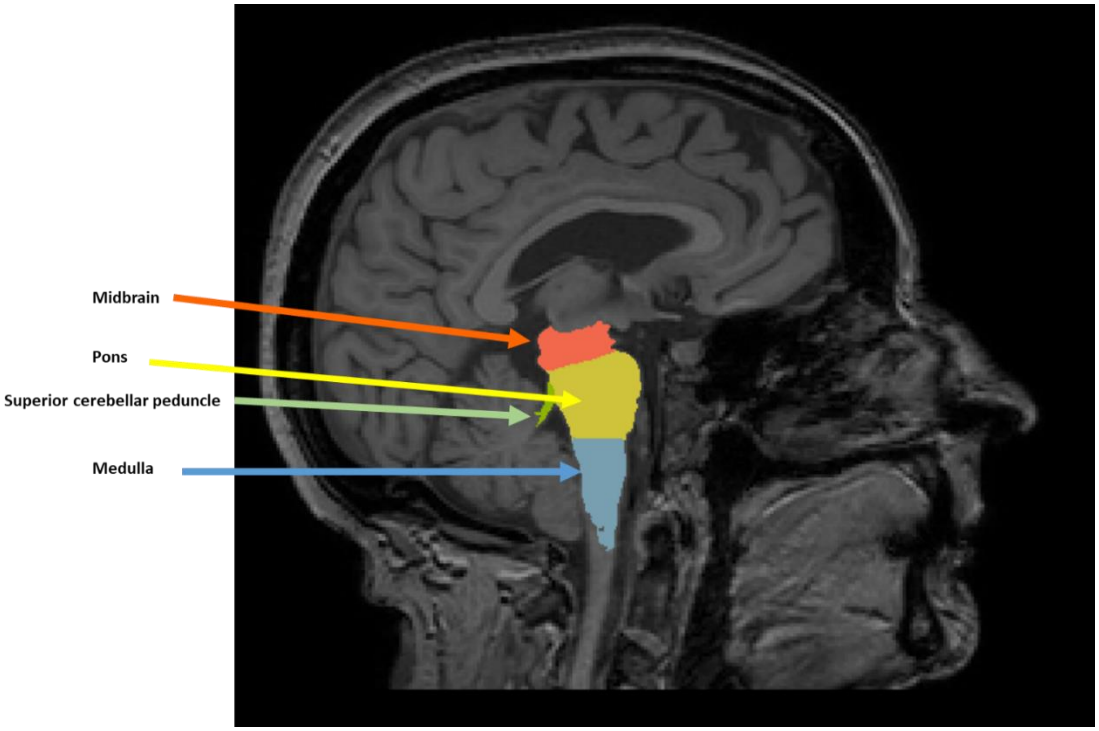

Figure 7. 4 Sagittal view of brainstem structure segmentation in FreeSurfer.

7.5 Discussion

The pattern of cortical thinning associated with MCI-LB, MCI-AD and HC was investigated in this study. After controlling for age and gender as well as correcting for multiple comparisons, no difference in cortical thickness was detected between any of the three groups. Relaxing the statistical criteria to a $p < 0.001$ (uncorrected) showed that only MCI-AD as compared with HC had cortical thinning in the right parahippocampal and right insula regions. Meanwhile, MCI-LB showed no evidence of cortical thinning or increased cortical thickness relative to HC or MCI-AD. A largely similar pattern of preserved brainstem volumes was apparent between the three diagnostic groups. However, subcortical volumes differences were found with smaller thalamic volume in MCI-LB and MCI-AD having reduced amygdala volume.

An absence of cortical thinning was noted in the MCI-LB group relative to both HC and MCI-AD. This would indicate that cortical thinning at least at the MCI-LB stage is mild. This finding would accord with the results from the one prior prodromal DLB study investigating the extent of cortical thinning among a prodromal DLB cohort compared with HC and prodromal AD cohort [173]. This study also failed to find any significant difference in cortical thinning between HC and a prodromal DLB cohort after correcting for multiple comparisons. In contrast to our findings, a significant difference in cortical thickness was reported between the prodromal DLB cohort and the prodromal AD cohort, with less thinning in the prodromal DLB cohort and the most significant areas of thinning occurring in prodromal AD in the left hemisphere, mainly in the parietal lobes and left parahippocampal gyri [173]. Meanwhile the prodromal DLB cohort had more cortical thinning in the right insula and pars opercularis relative to the prodromal AD cohort. A number of factors may account for the differing results in this study from our study, namely the difference in age as these prodromal cohorts were significant younger (prodromal DLB: 67.5 years, prodromal AD: 69.3 years) than our participants (MCI-LB: 74.7 yrs, MCI-AD: 75.4 yrs). Secondly, there was significantly higher prevalence of core features in their prodromal DLB cohort compared to our cohort (hallucinations 60.7%, cognitive fluctuations 92.9%) indicating that our cohort may have had a milder degree of clinical neurodegeneration.

Interestingly, at the dementia stage, most studies have reported regional cortical thinning in DLB affecting the posterior cingulate, temporo-occipital, orbitofrontal and occipital cortices [173, 307, 308]. However, there have been studies which did not show a significant difference in cortical

thickness between DLB and AD [309]. The lack of atrophic change in our study would suggest that other mechanisms besides neuronal loss are likely to be responsible for the cognitive dysfunction and core features in early LB disease such as alterations effecting metabolic, cerebral blood perfusion and neurotransmitter/synaptic dysfunction.

Total brain matter volumes were examined to determine if there were any global differences between the three diagnostic groups. In terms of global subcortical GM volume and total GM volume, neither MCI-LB nor MCI-LB significantly differed from HC or each other. Although, the occurrence of subcortical GM atrophy in DLB has been previously described [278, 303]. It is unsurprising that we were unable to find differences in global subcortical GM volume as previous studies have suggested vulnerability of specific subcortical structures rather than a more generalised atrophic process [401] [278].

The amygdala, a limbic structure, was significantly reduced in volume in MCI-AD compared to HC but was relatively preserved in MCI-LB compared to HC. Volume loss of limbic structures has been reported in a number of studies, with AD demonstrating substantially greater atrophy in these structures' than DLB [313]. While amygdala volume was lower in MCI-AD, there was no significant difference in amygdala volume between MCI-AD and MCI-LB suggesting the differences between groups are small and therefore utilising this structure as a reliable biomarker to differentiate between MCI groups may not be feasible.

Thalamic volume was found to be significantly reduced in MCI-LB compared with HC and MCI-AD. The thalamus plays a role in maintaining consciousness, arousal [335, 402], as well as being involved in motor, sensory and cognitive function [403]. It is a structure particularly vulnerable to LB pathology [72]. A number of MRI studies have demonstrated that atrophy, abnormal functional connectivity, perfusion deficits and metabolic abnormalities preferentially occurs in the thalamus of DLB subjects relative to HC and AD [359, 402, 404-407]. Thalamic atrophy in DLB has been associated with attentional dysfunction and cognitive fluctuations [335], as thalamic cholinergic denervation has been shown to be present in α-synucleinopathies but not in AD [408]. There was no difference between groups in the remaining subcortical structures: caudate; putamen; pallidum and nucleus accumbens. One explanation for differences found between groups with respect to thalamic volume

but no differences found between groups for other subcortical structures might be related to measurements errors. In comparison with other subcortical structures, the thalamus is the largest structures measured and therefore might be less prone to measurement errors than the other subcortical structures.

Brainstem substructures volumes were examined in this study. The rationale for this approach was that LB pathology allegedly spreads in a caudal-to-cranial manner according to the Braak hypothesis [72]. Therefore, neuronal loss with subsequent volume loss would likely affect the brainstem initially before spreading to the limbic structures and onwards towards cortical structures. There was no difference in midbrain, pons, superior cerebellar peduncle or medulla volume between groups. While neuropathology studies have shown severe neuronal loss in the midbrain in DLB [409], to the best of our knowledge, no prior imaging study has reported brainstem substructure volumes in DLB.

In conclusion, there was no difference in cortical thickness between MCI-LB compared to controls and MCI-AD. Structural MRI elucidated distinct patterns of subcortical structural change in MCI-LB and MCI-AD which could be used to potentially differentiate the two conditions. MCI-LB had a relative loss of thalamic volume compared to controls and MCI-AD. Also, MCI-AD had more atrophic change in the amygdala compared to controls but it was not significantly different from MCI-LB. Overall, the results of this study indicate that in early disease cortical structure is relatively spared and only at the subcortical level could differences between MCI groups be revealed.

Chapter 8. Patterns of grey matter atrophy in MCI-LB: a VBM-DARTEL study.

8.1 Aims

The aim of this study was to use 3T MRI to elucidate structural changes in a MCI-LB cohort, and to compare the findings with age-matched HC and a MCI-AD cohort. Additionally, we explored the relationship between GM loss and clinical symptoms. The intention of this research was to better understand the earliest *in vivo* structural brain changes caused by the differing neuropathological processes, such knowledge could potentially lead to earlier and more accurate differential diagnosis of LB disease at the MCI stage, and also a means to monitor disease progression.

8.2 Hypotheses

8.2.1 Primary hypotheses

1. The MCI-LB cohort will have minimal global cortical GM atrophy compared to HC as assessed using voxel-based morphometry. If GM differences exist between the MCI-LB cohort and HC, it will be regional GM losses with a posterior (parieto-occipital) and subcortical atrophy pattern predominating in the MCI-LB cohort.
2. The MCI-LB cohort will have less global cortical GM atrophy and less regional atrophy, as assessed using VBM, compared with the MCI-AD cohort. In particular, the MCI-AD cohort will have more global GM atrophy with prominent temporo-parietal GM loss.
3. MCI-LB cohort will have less GM atrophy affecting the MTL structures compared with the MCI-AD cohort.

8.3 Methods

8.3.1 Participants

One hundred and twenty subjects completed both ^{123}I-FP-CIT SPECT and MIBG imaging. Of the 120 subjects, two subjects had contraindications to MRI scans. Therefore, 118 of these participants completed structural MRI neuroimaging. The details of subjects diagnostic classification have previously been outlined in “Chapter 7: Structural MRI changes in MCI-LB: cortical thickness, cortical, subcortical and brainstem volume analysis”. Consistent with prior published MRI analysis comparing DLB to AD, the possible MCI-LB group (n=21) was excluded from the analysis and the

probable MCI-LB group is referred to as the MCI-LB group in this chapter. Therefore, 97 subjects were included in this analysis, consisting of; HC (n=31), MCI-AD (n=32), MCI-LB (n=34).

8.3.2 Voxel-based morphometry

Structural MRI data pre-processing was performed in SPM12 v6906 (Statistical Parametric Mapping, Welcome Trust Centre for Neuroimaging, http://www.fil.ion.ucl.ac.uk), running on MATLAB R2017a (Mathworks, Natick, MA, USA). The first step in pre-processing was segmenting MR images in to GM, WM, and cerebrospinal fluid components using the unified segmentation model [410]. Secondly, the GM images were subjected to spatial normalisation into standard Montreal Neurological Institute (MNI) space (http://www.mni.mcgill.ca/) using the diffeomorphic anatomical registration through exponentiated lie algebra (DARTEL) technique [277]. Thirdly, after an initial affine registration of the GM DARTEL templates to the tissue probability MNI space, non-linear warping of GM images was performed to the DARTEL GM template in MNI space. Then, the individual images were modulated to ensure the relative volumes of GM were preserved following the spatial normalisation procedure. Finally, the images were smoothed using an 8-mm FWHM Gaussian isotropic kernel. This was done to improve the normality of distribution and thus increase signal to noise ratio of the images. The smoothed, modulated, DARTEL-warped and normalised GM datasets were used for statistical analysis. The TIV was calculated by summing the total GM, WM and cerebrospinal fluid from the probability maps generated from the initial segmentation.

8.3.3 Statistical analysis

For analysing MRI brain volume data, between-group differences were tested using ANCOVA, controlling for age and TIV and adjusting for multiple comparisons by *post-hoc* Bonferroni correction.

VBM-DARTEL analysis

Group differences in regional volume were assessed using the General Linear Model in SPM12 based on random Gaussian field theory [411]. An absolute threshold mask of 0.05 was used for GM analysis. Age and TIV (SPM12) were included in the design matrix as nuisance variables. The TIV was calculated as the sum of the GM, WM and CSF volumes. Multiple regression (correlation) analyses were also performed to investigate effects of GM loss on cognitive scores (total ACE-R score,

memory, language, fluency, attention/orientation and visuospatial domains) as wells as the effects of GM loss on MDS-UPDRS III in subjects with MCI-LB and MCI-AD, separately.

Significant clusters were defined using a cluster-wise uncorrected threshold of $p<0.001$ and clusters were only regarded as significant if they were larger than 100 voxels. A family-wise error (FWE) threshold of $P_{FWR}<0.05$ was applied to correct for multiple comparisons. Both cluster level and voxel-level significance were considered. The anatomical location was then determined using Talairach daemon (http://www.talairach.org/).

8.4 Results

8.4.1 Demographics and clinical characteristics

Clinical characteristics, neuropsychological tests and demographic data are shown in Table 8.1. The core clinical features and indicative biomarker abnormalities for the MCI-B group are shown in Table 8.2. The patient groups and HC group did not differ significantly with respect to age. The duration of memory complaints did not differ between MCI-AD and the MCI-LB groups ($P=0.51$). There is a significant difference between-groups in terms of gender between groups ($\chi2(2)=18.26$, $P<0.001$), with significantly fewer females in the MCI-LB ($\chi2\ (1)=4.4$, $p=0.04$) and significantly more females in the MCI-AD ($\chi2(1)=5.34$, $P=0.02$) groups compared to HC.

In terms of cognitive testing, compared to HC participants, ACE-R, AVLT and graded naming scores were significantly lower in the MCI-LB and MCI-AD groups but there was no difference between the MCI groups ($p=1.0$).

As expected, there was significantly more motor impairment in the in the MCI-LB group compared to MCI-AD group ($t(64)=-2.1$, $p=0.04$). There were also more neuropsychiatric symptoms reported on the NPI in the MCI-LB compared to MCI-AD ($t(54)= -2.3$, $P=0.03$). The MCI-LB group had a greater ESS score than MCI-AD and HC ($F(2,94)=11.43$, $P<0.001$).

Characteristic	HC (n= 31)	MCI-AD (n= 32)	MCI-LB (n= 34)	Group Comparisons
Mean age (years)	73.7 ± 7.3	75.5 ± 7.9	74.7 ± 6.7	F(2,94)=0.49, P=0.61
M:F (%)	22/9 (71%/29%)	12/20 (37%/63%)	31/3 (91.2%/8.8%)	**$X^2(2)=21.81$, P<0.001** [a,f]
Mean years of education	14.7 ± 4.0	13.2 ± 3.5	12.2 ± 3.0	**F(2,91)= 3.88, P=0.02**[a]
Duration of memory compliant (months)	NA	43.2 ± 53.4	53.00 ± 44.7	t(57)= -0.67 P=0.51
IADL	NA	7.4 ± 0.9	6.5 ± 1.4	**t(54)=2.8, p=0.007**
GDS (Max 15)	1.3 ± 1.8	3.3 ± 2.6	4.6 ± 3.9	**F(2,94)=11.00, P<0.001**[c,d,e]
CIRS-G	5.3 ± 3.3	6.0 ± 3.3	8.1 ± 4.1	**F(2,94)=5.13, p=0.008**[d]
Mean CDR	NA	0.5 ± 0	0.5 ± 0.15	t(63)=1.7, p=0.09
Mean MMSE score (Max 30)	28.5 ± 1.1	27.0 ± 2.1	26.6 ± 2.4	**F(2,94)=7.49, P=0.001**[a,b]
Mean ACE-R score (Max 100)	92.7 ± 4.2	83.1 ± 8.5	84.1 ± 8.8	**F(2,94)=15.50, P<0.001**[a,b]
Rey total trials 1-5 (max 75)	44.5 ± 11.1	32.5 ± 9.8	32.4 ± 7.6	**F(2,94)=17, P<0.001**[a.b]
Rey delayed recall (max 15)	8.4 ± 3.5	3.4 ± 4.2	5.0 ± 3.4	**F(2,94)=13.2, p<0.001**[a,b]
FAS	43.1 ± 9.8	37.9 ± 11.2	32.4 ± 7.6	**F(2,94)=5.45, P=0.006**[a]
ESS	4.7 ± 2.9	5.2 ± 4.4	8.9 ± 4.3	**F(2,94)=11.43, P<0.001**[c,d]
Graded Naming	23.7 ± 4.0	19.3 ± 5.0	20.8 ± 4.1	**F(2,94)=8.36, P=0.001**[a,b]
MDS-UPDRS III	NA	15.3 ± 14.2	22.7 ± 14.7	**t(64)=-2.1, p=0.04**
Hoehn and Yahr Stage	NA	0	0.73 ± 1.0	**t(62)= -3.8, p<0.001**
NPI total	NA	8.9 ± 9.70	16.1 ± 13.0	**t(54)= -2.3, P=0.03**
NPI distress	NA	3.7 ± 3.5	8.9 ± 8.5	**t(54)= -2.85, p=0.006**

Values are expressed as mean ± standard deviation (SD).

Bold underlined characters indicate significant results.

Abbreviations: MCI-AD=Mild cognitive impairment due to Alzheimer's disease; MCI-LB= Mild cognitive impairment due to Lewy bodies disease; IADl= Instrumental activities of daily living; GDS= Geriatric depression score; CIRS-G = Cumulative Illness Rating Scale-Geriatric; CDR = Clinical dementia rating; MMSE=Mini-Mental State Examination; Rey= Rey Auditory Verbal Learning test; FAS= Verbal fluency measure; ESS= Epworth Sleep Scale; MDS-UPDRS III =

Movement Disorder Society-Unified Parkinson's Disease Rating Scale (MDS-UPDRS); NPI= Neuropsychiatric Inventory; ACE-R= Addenbrooke's Cognitive Examination-Revised.
[a]**MCI-LB < Control**
[b]**MCI-AD < Control**
[c]**MCI-AD < MCI-LB**
[d]**MCI-LB > Control**
[e]**MCI-AD > Control**
[f]**MCI-LB < MCI-AD**

Table 8. 1 Demographics and group characteristics.

Clinical Features	**Present N (%)**
Core Features	
Cognitive Fluctuations	21 (61.8%)
Recurrent Visual Hallucinations	6 (17.6%)
Spontaneous Motor Parkinsonism	12 (35.3%)
REM sleep behaviour disorder	27 (79.4%)
Indicative Biomarkers	
Abnormal FP-CIT SPECT	22(64.7%)
Abnormal MIBG	24 (70.6%)

Table 8. 2 Percentage of core clinical features and indicative biomarker's abnormalities for MCI-LB participants.

8.4.2 Brain volume measurement

Brain volume measurements are shown in Table 8.3. After controlling for the effects of age, total GM volume was significantly lower in the MCI-LB group compared with HC (p=0.005). There was no difference in total GM volume between MCI-LB and MCI-AD (p=0.45), or MCI-AD and HC (p=0.25). After controlling for the effect of age, TIV was significantly greater in the MCI-LB group compared to MCI-AD (p=0.03). Global GM/TIV is significantly lower in the MCI-LB group compared to HC (P=0.005) after controlling for age differences. There was no difference in global GM/ICV between the MCI-LB and MCI-AD groups (p=0.12).

Tissue	HC (n= 31)	MCI-AD (n= 32)	MCI-LB (n= 34)	ANCOVA	Bonferroni pairwise post hoc		
					MCI-LB vs HC	MCI-AD vs HC	MCI-LB vs MCI-AD
GM(cm^3)	573 ± 65	535 ± 67	546 ± 53	**F(2,92)=5.36, P=0.006, η^2=0.10**	**P=0.005**	P=0.25	P=0.45
WM (cm^3)	437 ± 58	405 ± 67	434 ± 66	F(2,92)=0.76, P=0.47, η^2=0.02	P=0.82	P=0.92	P=1.0
Cerebrospinal fluid (cm^3)	514 ± 92	536 ± 89	582 ± 112	**F(2,92)=4.59, P=0.01, η^2=0.09**	**P=0.01**	P=0.18	P=0.94
TIV (cm^3)	1525 ± 107	1476 ± 128	1562 ± 159	**F(2, 93)= 3.35, P=0.04, η^2=0.07**	P=0.83	P=0.46	**P=0.03**
Global GM/TIV	0.376 ± 0.040	0.363 ± 0.040	0.351 ± 0.027	**F(2,93)=5.42, P=0.006, η^2=0.10**	**P=0.005**	P=0.75	P=0.12

Units of measurement cm^3
Values are expressed as mean ± standard deviation (SD).
Bold underlined characters indicate significant results.
Abbreviations: MCI-AD=Mild cognitive impairment due to Alzheimer's disease; MCI-LB= Mild cognitive impairment due to Lewy body disease; ANCOVA= analysis of covariance; TIV= Total intracranial volume; GM= Grey matter; WM= White matter

Table 8. 3 GM, WM and TIV in HC, MCI-AD and MCI-LB.

8.4.3 Differences in grey matter volume between MCI-LB and HC

Compared with HC, MCI-LB had reduced GM density in the left middle frontal gyrus, right middle temporal gyrus, and left inferior temporal gyrus ($p < 0.001$ and cluster size >100 voxels, uncorrected). After correcting for multiple comparisons ($P_{FWE\text{-}corr} < 0.05$), three regions remained significant at the cluster level of analysis; left middle frontal gyrus, right middle temporal gyrus and left inferior temporal gyrus (Figure 8.1, Table 8.4). HC did not show any atrophy which exceeded that in MCI-LB.

Cluster-Level ($P_{FEW-corr}$)	Cluster-Level (P_{uncorr})	Voxel-Level ($P_{FWE-Corr}$)	Voxel-Level (P_{uncorr})	EXTENT (K)	t,Z	MNI COORDINATES (x,y,z) (mm)	Anatomical REGION
HC vs MCI-LB							
0.026	**0.004**	**0.066**	**<0.001**	**1020**	**4.98, 4.54**	**-36, 42, 20**	**Left middle frontal gyrus**
<0.001	**<0.001**	**0.108**	**<0.001**	**3876**	**4.81, 4.41**	**59, -33, -2**	**Right middle temporal gyrus**
<0.001	**<0.001**	**0.507**	**<0.001**	**2271**	**4.18, 3.91**	**-54, -56, -27**	**Left inferior temporal gyrus**

Bold underlined characters indicate significant cluster results surviving correction by multiple comparison

$P_{FWE-Corr}$=probability value, family wise error corrected; P_{uncorr}= probability value; MNI= Montreal Neurological Institute; HC= Healthy controls; MCI-LB = Mild cognitive impairment with Lewy bodies.

Table 8. 4 Localisation of significant GM volume difference between MCI-LB and HC.

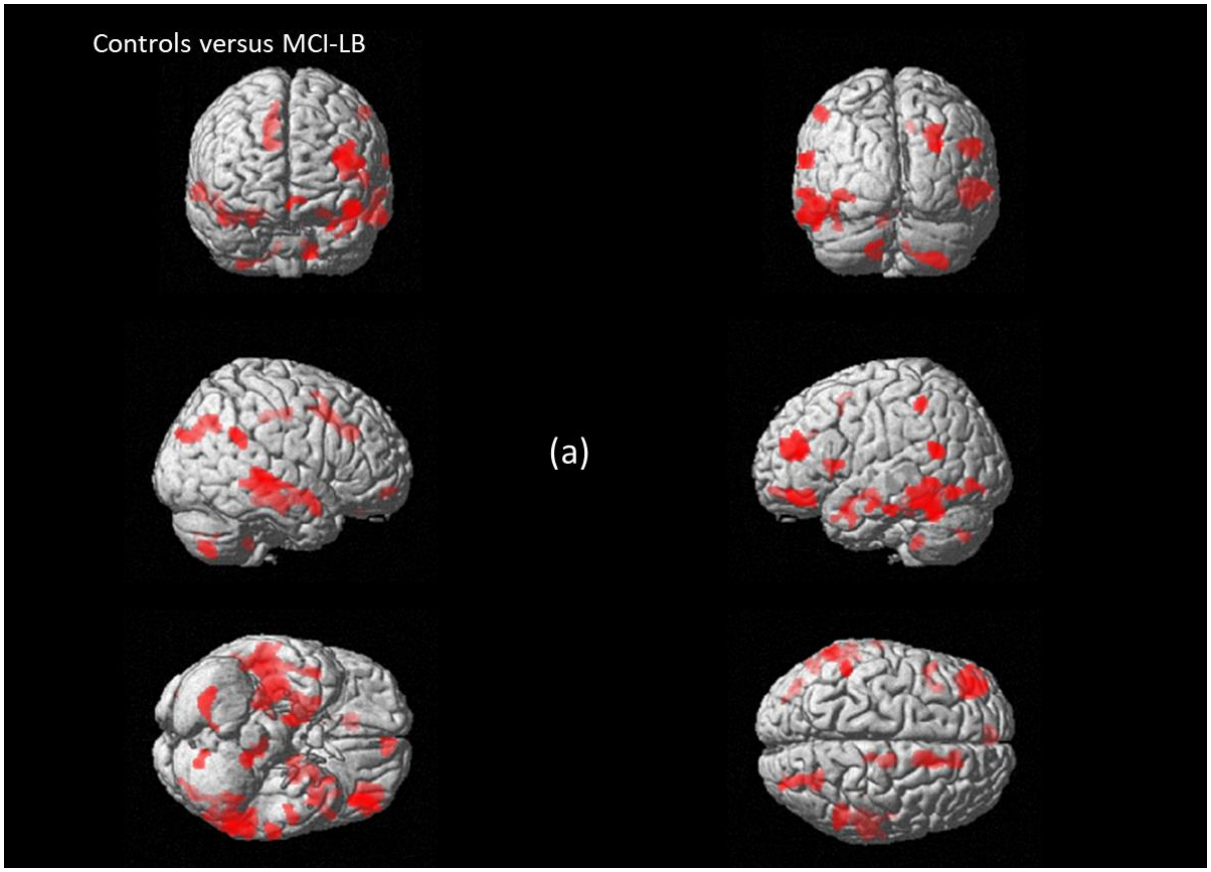

Figure 8. 1 Three-dimensional surface renders showing the areas of GM loss (red) in MCI-LB compared to HC. All results are represented at p<0.001 uncorrected.

8.4.4 Differences in grey matter volume between MCI-AD and HC

Compared with HC, MCI-AD had reduced GM density in the right & left hippocampus, left & right inferior temporal gyrus, left temporal pole, right fusiform gyrus ($p < 0.001$ and cluster size >100 voxels, uncorrected). After correcting for multiple comparisons ($P_{FWE\text{-}corr} < 0.05$), the right & left hippocampus and left temporal pole remained significant at the cluster level (Figure 8.2, Table 8.5). HC did not show any atrophy which exceeded that in MCI-AD.

Cluster-Level ($P_{FEW\text{-}corr}$)	Cluster-Level (P_{uncorr})	Voxel-Level ($P_{FWE\text{-}Corr}$)	Voxel-Level (P_{uncorr})	EXTENT (K)	t,Z	MNI COORDINATES (x,y,z) (mm)	Anatomical REGION
HC vs MCI-AD							
<0.001	**<0.001**	**0.281**	**<0.001**	**2585**	**4.44,4.11**	**18, -6, -15**	**Right Hippocampus**
0.043	**0.006**	**0.291**	**<0.001**	**927**	**4.43, 410**	**-33.-27, -11**	**Left hippocampus**
0.059	**0.009**	**0.694**	**<0.001**	**836**	**3.97, 3.72**	**-35, 6, -23**	**Left temporal pole**

Bold underlined characters indicate significant cluster results surviving correction by multiple comparison
$P_{FWE\text{-}Corr}$=probability value, family wise error corrected; P_{uncorr}= probability value, uncorrected; MNI= Montreal Neurological Institute; HC= Healthy controls; MCI-AD= Mild cognitive impairment due to Alzheimer's disease

Table 8. 5 Localisation of significant GM volume differences between MCI-AD and HC.

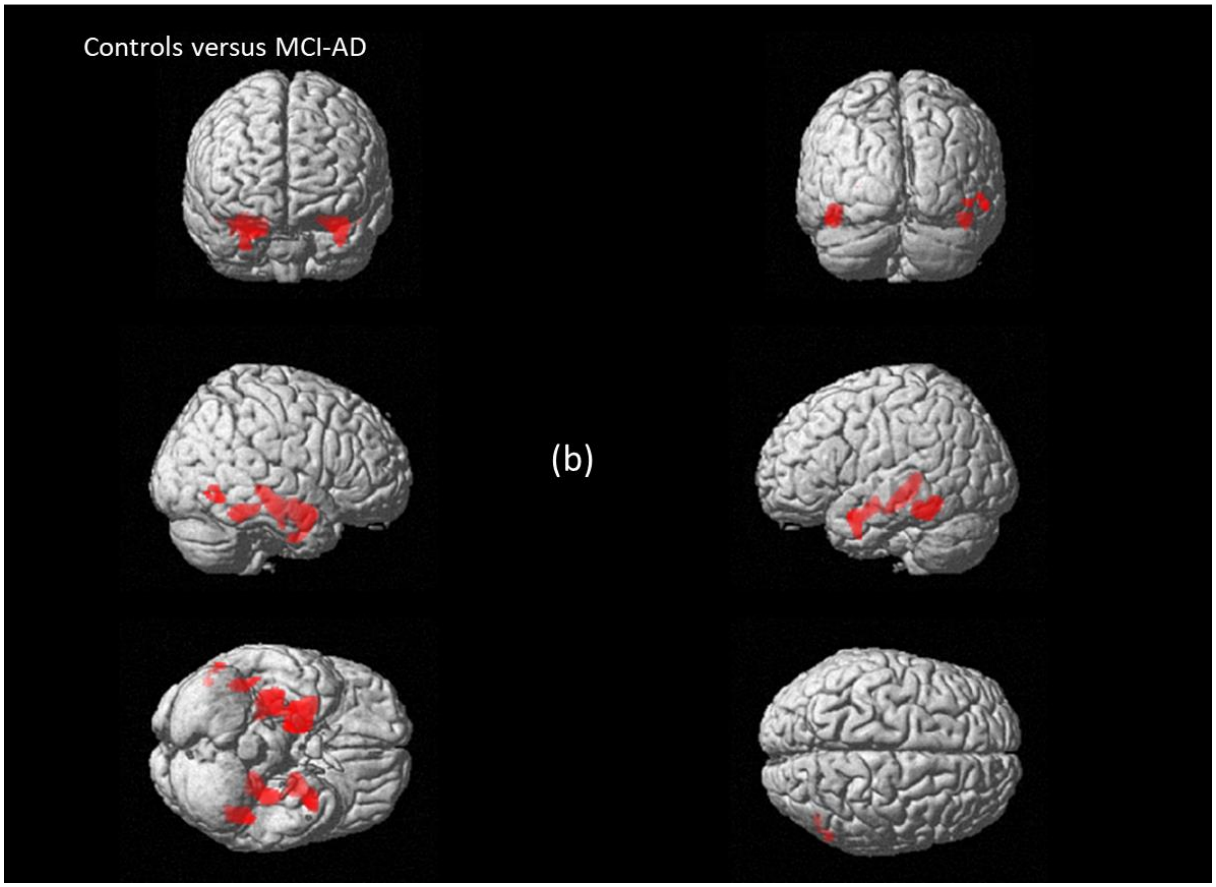

Figure 8. 2 Three-dimensional surface renders showing the areas of GM loss (red) in MCI-AD compared to HC. All results are represented at p<0.001 uncorrected.

.

8.4.5 Differences in grey matter volume between MCI-AD and MCI-LB

Compared with MCI-LB, there were no significant clusters of GM volume loss in the MCI-AD patient group ($p < 0.001$ and cluster size >100 voxels, uncorrected). The reverse contrast revealed 3 clusters ($p < 0.001$ and cluster size >100 voxels, uncorrected) of reduced GM volume in the MCI-LB compared to MCI-AD group; left cerebellum exterior, right cerebellum exterior and left middle occipital gyrus (Figure 8.3; Table 8.6). Only two of these survived correction for multiple comparison ($P_{FWE\text{-}corr} <0.05$); left cerebellum exterior, right cerebellum exterior (Figure 8.3, Table 8.6).

Cluster-Level ($P_{FEW-corr}$)	Cluster-Level (P_{uncorr})	Voxel-Level ($P_{FWE-Corr}$)	Voxel-Level (P_{uncorr})	EXTENT (K)	t,Z	MNI COORDINATES (x,y,z) (mm)	Anatomical REGION
MCI-AD vs MCI-LB							
<0.001	**<0.001**	**0.083**	**<0.001**	**3629**	**4.88, 4.47**	**6, -65, -42**	**Right cerebellum exterior**
0.048	**0.007**	**0.644**	**<0.001**	**877**	**4.02, 3.77**	**-21, -80, -36**	**Left cerebellum exterior**

Bold underlined characters indicate significant cluster results surviving correction by multiple comparison
$P_{FWE-Corr}$=probability value, family wise error corrected; P_{uncorr}= probability value, uncorrected; MNI= Montreal Neurological Institute; MCI-AD= Mild cognitive impairment due to Alzheimer's disease; MCI-LB = Mild cognitive impairment with Lewy bodies.

Table 8. 6 Localisation of significant GM volume differences between MCI-AD and MCI-LB.

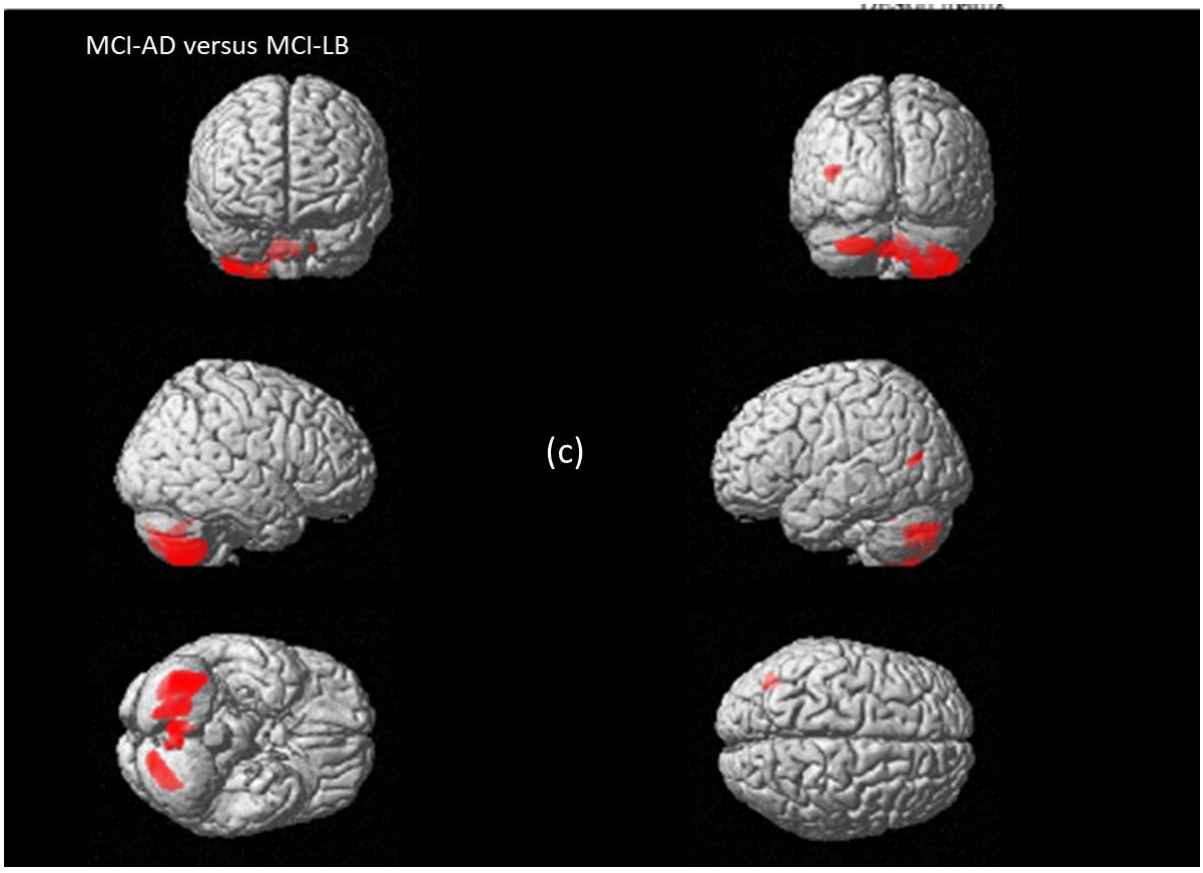

Figure 8. 3 Three-dimensional surface renders showing the areas of GM loss (red) in MCI-LB compared to MCI-AD. All results are represented at p<0.001 uncorrected.

8.4.6 Correlations between grey matter atrophy and cognitive/clinical scores in MCI-AD and MCI-LB

Significant correlations between GM atrophy and cognitive scores (total ACE-R score, memory, language, fluency, attention/orientation and visuospatial domains) and clinical scores (MDS-UPDRS III) in the MCI-LB and MCI-AD groups are shown in Table 8.7 and Table 8.8. A positive correlation was observed between total ACE score and regions of GM atrophy in MTL structures in both MCI-LB and MCI-AD groups. The memory domain of the ACE-R in the MCI-AD group was strongly positively correlated with MTL atrophy but in the MCI-LB group the memory domain was not correlated with medical temporal lobe atrophy but correlated more weakly with cerebellar structures. An opposing pattern of correlation was seen between groups in their relationship to GM atrophy and the ACE-R visuospatial domain. A positive correlation was observed in the MCI-LB group between ACE-R visuospatial domain scores with GM atrophy in the occipital lobe, thalamus and temporal lobe. Meanwhile, a positive correlation was observed in the MCI-AD group between ACE-R visuospatial domain scores with GM atrophy in the frontal lobe and putamen. Neither language, fluency, attention/orientation domains or MDS-UPDRS part III was correlated with GM atrophy.

Cluster-Level ($P_{FEW-corr}$)	Cluster-Level (P_{uncorr})	Voxel-Level ($P_{FWE-Corr}$)	Voxel-Level (P_{uncorr})	EXTENT (K)	t,Z	MNI COORDINATES (x,y,z) (mm)	Anatomical REGION
Positive correlation between GM atrophy and Total ACE-R Score							
0.006	**<0.001**	**0.258**	**<0.001**	**1294**	**5.47, 4.52**	**-23 -30 -14**	**Left hippocampus**
Positive correlation between GM atrophy and ACE-R memory domain							
0.04	**0.002**	**0.658**	**<0.001**	**876**	**4.90, 4.17**	**-8 -77 -45**	**Left Cerebellum Exterior**
Positive correlation between GM atrophy and ACE-R language domain							
0.040	**0.002**	**0.974**	**<0.001**	**873**	**4.34, 3.79**	**44 -62 -44**	**Right Cerebellum Exterior**
Positive correlation between GM atrophy and ACE-R visuospatial domain							
0.001	**<0.001**	**0.015**	**<0.001**	**1674**	**6.77, 5.23**	**27 -69 -9**	**Right Occipital Fusiform gyrus**
0.038	**0.002**	**0.107**	**<0.001**	**877**	**5.90, 4.77**	**21 -29 -3**	**Right Thalamus**
0.015	**0.001**	**0.239**	**<0.001**	**1076**	**5.51, 4.55**	**-18 -30 -5**	**Left Thalamus**
0.009	**<0.001**	**0.680**	**<0.001**	**1189**	**4.88, 4.15**	**45 -18 -12**	**Right middle temporal gyrus**

Bold underlined characters indicate significant cluster results surviving correction by multiple comparison

$P_{FWE-Corr}$=probability value, family wise error corrected; MNI= Montreal Neurological Institute; MCI-AD= Mild cognitive impairment due to Alzheimer's disease; probable MCI-LB = Mild cognitive impairment with Lewy bodies; GM= Grey matter

Table 8. 7 Relationship between GM atrophy and clinical/cognitive measures in MCI-LB.

Cluster-Level ($P_{FEW-corr}$)	Cluster-Level (P_{uncorr})	Voxel-Level ($P_{FWE-Corr}$)	Voxel-Level (P_{uncorr})	EXTENT (K)	t,Z	MNI COORDINATES (x,y,z) (mm)	Anatomical REGION
Positive correlation between GM atrophy and Total ACE-R Score							
0.008	**<0.001**	**0.024**	**<0.001**	**1271**	**6.68, 5.12**	**-12 -39 -11**	**Left parahippocampal gyrus**
Positive correlation between GM atrophy and ACE-R memory domain							
<0.001	**<0.001**	**0.116**	**<0.001**	**5060**	**5.94, 4.74**	**-18 -36 -8**	**Left parahippocampal gyrus**
<0.001	**<0.001**	**0.879**	**<0.001**	**2274**	**4.63, 3.96**	**26 -20 -26**	**Right parahippocampal gyrus**
Positive correlation between GM atrophy and ACE-R language domain							
0.040	**0.002**	**0.974**	**<0.001**	**873**	**4.34, 3.79**	**44 -62 -44**	**Right Cerebellum Exterior**
Positive correlation between GM atrophy and ACE-R visuospatial domain							
<0.001	**<0.001**	**0.033**	**<0.001**	**5018**	**6.54, 5.05**	**32 -66 17**	**Right middle frontal gyrus**
<0.001	**<0.001**	**0.081**	**<0.001**	**6236**	**6.11, 4.83**	**-23 18 3**	**Left putamen**
<0.001	**<0.001**	**0.339**	**<0.001**	**1343**	**5.85, 4.69**	**24 21 -5**	**Right putamen**

Bold underlined characters indicate significant cluster results surviving correction by multiple comparison
$P_{FWE-Corr}$=probability value, family wise error corrected; MNI= Montreal Neurological Institute; MCI-AD= Mild cognitive impairment due to Alzheimer's disease; probable MCI-LB = Mild cognitive impairment with Lewy bodies; GM= Grey matter

Table 8. 8 Relationship between GM atrophy and clinical/cognitive measures in MCI-AD.

8.5 Discussion

In this chapter, a VBM-DARTEL algorithm was utilised to compare the pattern of GM atrophy between HC, MCI-LB and MCI-AD. The findings demonstrated: (1) MCI-LB had GM atrophy predominantly in the frontal and temporal lobes compared to HC; (2) MCI-AD had bilateral hippocampal atrophy compared to HC; (3) MCI-LB had bilateral cerebellar atrophy compared to MCI-AD but no reduction in MTL volume was shown in MCI-AD compared to MCI-LB.

A distinct pattern of GM atrophy was found in the MCI-LB cohort compared with HC which showed volumetric loss in the frontal (left middle frontal gyrus) and temporal lobe (right middle temporal

gyrus and left inferior temporal gyrus). The frontal cortex has been associated with executive dysfunction in dementia [412]. In keeping with the relative preservation of the hippocampi and relative absence of NFT in DLB, no significant atrophy was noted in hippocampi relative to controls. The result is partially consistent with a prior VBM-DARTEL study in prodromal DLB which showed atrophy in the right medial frontal gyrus, bilateral insula and right claustrum relative to controls [367]. No difference in the insula and right claustrum was found in this study between MCI-LB and HC which might be due to methodological difference in the diagnosis of prodromal DLB between the two studies. In our study, diagnosis of prodromal DLB was based on a combination of core symptoms and imaging biomarkers (^{123}I-FP-CIT SPECT and MIBG), while in Roquet et al. diagnosis of prodromal DLB was based on symptoms alone without imaging biomarkers [367]. In DLB, frontal changes have been noted on prior VBM studies and decreased GM volume in the middle frontal gyrus in DLB has been associated with visual hallucinations [413]. Neuropathological studies, have reported high concentrations of LB in hallucinating patients, mainly in temporal and frontal regions [65, 414, 415]. Furthermore, reduced frontal cortical thickness in other α-synucleinopathies has been shown to predict conversion from PD-MCI to PDD [416].

In agreement with evidence from MRI studies in AD and MCI-AD outlined in chapter 4, the MCI-AD group in this study had more pronounced GM atrophy than HC in the MTLs, with evidence of bilateral reduction in hippocampal volume. There is an asymmetric component to the hippocampal atrophy with the right being more affected than the left. Notably, Roquet et al. in their prodromal DLB study showed that their prodromal AD group had no significant difference in atrophy compared with HC but had a tendency towards GM loss in right hippocampus [367]. In AD, numerous studies have reported smaller hippocampal volume compared with aged-matched HC [417] and atrophy in the MTL is included in the current diagnostic criteria for AD [112, 115]. At the MCI stage, consistent with the findings in our study, there is bilateral hippocampal volume loss in MCI and the extent of atrophy is less than that in AD dementia and an asymmetric component with the right hippocampal volume being lower than the left [417]. In fact, right hippocampal changes can occur up to 10 years before the clinical onset of AD [418].

In comparisons between prodromal groups (MCI-AD and MCI-LB) bilateral reduction in volume in both cerebellums was found in MCI-LB. Functionally, the role of cerebellum is to co-ordinate movement and balance [419]. However, it may also be involved in cognitive tasks such as language,

executive functions and spatial cognition [419]. Only one previous study has shown DLB having a distinct pattern of cerebellar GM loss compared to HC [328]. Pathological evidence of cerebellar atrophy in other neurodegenerative conditions exists, especially in α-synucleinopathies such as in PD [420], MSA and IRBD [421]. In DLB, cerebellar α-synuclein deposition affecting both purkinje and glial cells [422] has been reported and more recently, functional metabolic and perfusion imaging changes have suggested that cerebellar uptake along with uptake in other motor areas may be associated with cognitive and attentional fluctuations [423] as well as visual hallucinations [424].

In contrast to our hypothesis, comparisons between MCI-AD and MCI-LB did not demonstrate a significantly greater reduction of GM volume in the MTL in MCI-AD and no other cerebral structures had more pronounced atrophy relative to MCI-LB. In the only other VBM-DARTEL study in prodromal DLB, comparison between the prodromal DLB and prodromal AD groups did not reveal any significant difference in GM volume at all [367]. One plausible explanation for the absence of difference in MTL atrophy at the prodromal stage is that even at the dementia stage, the regional patterns of GM atrophy overlap in DLB and AD [425, 426]. The degree of GM loss in DLB being much less than in AD [425, 426]. Notably, there was a trend towards loss of GM in the left hippocampus in the MCI-LB compared to HC at the less robust statistical level (uncorrected $p < 0.001$) which did not survive correction for multiple comparisons.

Relatively few studies have explored the relationship between cognitive scores and GM atrophy in DLB. Previous studies in this area have demonstrated a relationship between MTL atrophy and memory sub-scores [292, 330].A positive relationship was found in the above study between MTL structures and total ACE-R cognitive scores in both MCI-LB and MCI-AD, while memory sub-scores were significantly more positively correlated with MTL structure atrophy in MCI-AD rather than in MCI-LB. Interestingly, in a study by Watson et al. comparing DLB to AD, no relationship was found between MTL atrophy and memory subscale scores in AD [292]. The authors speculated that the reason for this may be due to a floor effect, making it difficult to detect these correlations at the dementia stage. The results from our study would support such a notion. Furthermore, a positive correlation between visuospatial sub-scores and GM atrophy in the occipital lobe in the MCI-LB group, as demonstrated in our study, would be consistent with an early neurodegenerative LB disease process. The MCI-LB group also had a positive correlation between GM atrophy in the right cerebellum and the language domain of the ACE-R score. The poorer language performance may be

a product of slowed language production which may occur in some patients with cerebellar damage. However, there are studies in non-dementia populations indicating that cerebellar damage can lead to impairment on tests of verbal fluency [427].

In conclusion, a pattern of GM loss was demonstrated affecting the temporal and frontal lobe structures in MCI-LB. In particular, relatively preserved MTLs were shown in the MCI-LB group compared to controls, with the MCI-AD group showing the contrary pattern having more atrophy bilaterally in the hippocampi. Bilateral cerebellar GM loss was noted in the MCI-LB group compared with MCI-AD but conversely there was no degree of GM loss in the MCI-AD group compared with MCI-LB. These changes have important implications with regards to understanding the earliest *in vivo* structural changes due the neuropathological alterations and how they affect key manifestations of clinical and cognitive features of Lewy body disease.

Chapter 9. Whole hippocampal volume, hippocampal subfields and extra-hippocampal structures volume in MCI-LB and MCI-AD.

9.1 Aims

The main aim of this study was to use 3T MRI to investigate whether whole hippocampal volume and differing hippocampal subfield atrophy patterns, could be used as surrogate biomarkers of AD pathology, thereby allowing for earlier and better differential diagnosis of MCI-LB from MCI-AD.

9.2 Hypotheses

9.2.1 Primary hypotheses

1. Whole hippocampal volume would demonstrate greater atrophy in the MCI-AD than in MCI-LB but both groups would have greater hippocampal atrophy than HC.
2. Hippocampal subfields would be differentially altered in MCI-LB compared to MCI-AD and would discriminate between MCI-AD and MCI-LB better than whole hippocampal volume. Specifically, the cornu ammonis and subiculum hippocampal subfields will be more affected in MCI-AD but preferentially preserved in MCI-LB.
3. The MCI-LB group would demonstrate a reduced volume in adjacent MTL structures compared with HC but less marked than in MCI-AD.
4. Measures of cognition in the MCI groups (MCI-LB and MCI-AD) would be associated with whole hippocampal volumes.

9.3 Methods

9.3.1 Participants

The details of subjects enrolled in this study and diagnostic classification have previously been outlined in “Chapter 7: Structural MRI changes in MCI-LB: cortical thickness, cortical, subcortical and brainstem volume analysis”. Consistent with prior published MRI analysis, the possible MCI-LB group (n=18) was excluded from the analysis and the probable MCI-LB group is referred to as the MCI-LB group in this chapter. Therefore, ninety four subjects were included in this analysis, consisting of; HC (n=31), MCI-AD (n=29), MCI-LB (n=34).

9.3.2 MRI morphometry

Structural T1-weighted MRI images were processed using FreeSurfer V.6.0 (http://surfer.nmr.mgh.harvard.edu/). Cortical thickness and volumetric segmentation was performed using recon-all command line, automated reconstruction was performed and labelling of cortical and subcortical regions (classified by using the Desikan-Killiany Atlas). The technical aspects of these methods have been published elsewhere [394, 395, 428] and the processing stream in FreeSurfer has been outlined in Chapter 7 of this thesis. Regional volume of specific MTL structures (parahippocampal gyrus, entorhinal cortex and temporal pole), alongside the total hippocampal volumes and the TIV were calculated by using this FreeSurfer V.6.0 processing pipeline.

The automated volumetric hippocampal subfields segmentation was implemented in FreeSurfer using the "recon-all" command line followed by "hippocampal-subfields-T1" option. The automated segmentation tool is based on a probabilistic statistical atlas built on ultra-high resolution ex vivo MRI data from autopsy brains – technical details have been previously described [429]. In brief, a Bayesian inference approach was used to segment the hippocampal subfields, and a probabilistic atlas of the hippocampal formations based on manual delineations of subfields into 12 subfields: the granule cell and molecular layer of the dentate gyrus (GC-ML-DG); cornu ammonis (CA) areas of CA1, CA3, CA4; subiculum; presubiculum; parasubiculum; molecular layer of hippocampus proper (ML-HP); fimbria; hippocampal tail; hippocampal fissure; and hippocampal-amygdala transition area (HATA). Visual inspection of each subject's hippocampal subfield segmentation and corresponding T1 images was performed to assess alignment of subfield masks with processed T1 images and ensure there was no errors. Representative images of the hippocampal subfields are shown in Figure 9.1.

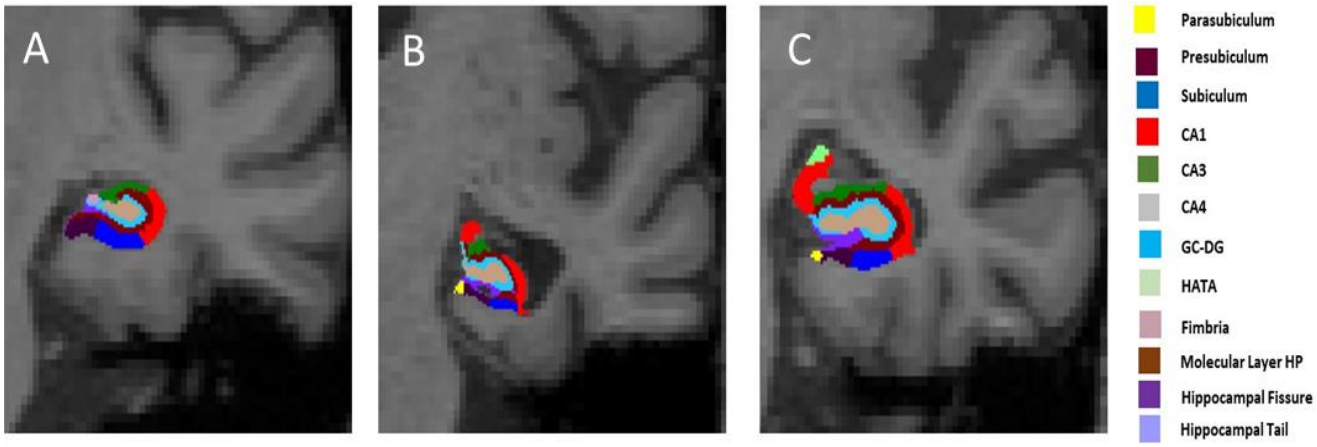

Figure 9. 1 Segmented hippocampal subfields from each representative subjective in all three diagnostic groups; (A) HC (B) MCI-AD (C) MCI-LB.

9.3.3 Statistical analysis

For analysing MRI data, between-group differences were tested using ANCOVA, controlling for age and TIV and adjusting for multiple comparisons by *post-hoc* Bonferroni correction (p=0.017).

To investigate whether total hippocampal volume and subfields were associated with cognitive scores, simple linear models were constructed with the inclusion of age and TIV as covariates.

9.4 Results

9.4.1 Demographics and clinical characteristics

As previous outlined in "chapter 7: Structural MRI changes in MCI-LB: cortical thickness, cortical, subcortical and brainstem volume analysis". Clinical characteristics, neuropsychological tests and demographic data of the cohort are shown in Table 7.1 of chapter 7.

9.4.2 Quantitative total hippocampal volumetry

After controlling for age and TIV and correcting for multiple comparisons using a Bonferroni correction, the total hippocampus volume was significantly smaller in the MCI-AD group compared with HC ($p<0.001$). There was no significant difference in total hippocampal volumes between HC and MCI-LB (p=0.11). After controlling for age and TIV, no significant difference between MCI-LB and the MCI-AD group was observed in total hippocampal volume (P=0.12) (Figure 9.2, Table 9.1).

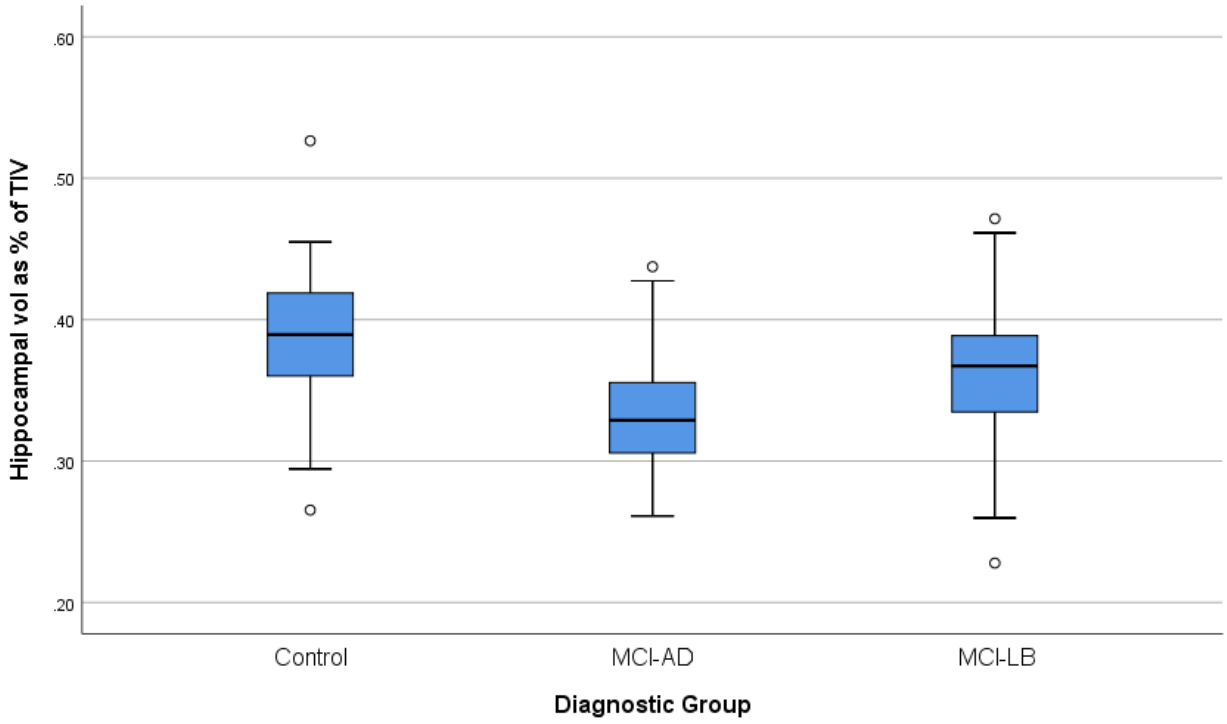

Figure 9. 2 Boxplot of hippocampal volumes as a percentage of total hippocampal volume for each diagnostic group.

Abbreviations: MCI-AD= Mild cognitive impairment due to Alzheimer's disease; MCI-LB= Mild cognitive impairment with Lewy bodies; TIV= Total intracranial volume; Vol= volume.

9.4.3 Quantitative hippocampal subfields

For the majority of hippocampal subfields, MCI-AD group showed a strong and highly significant difference from HC; hippocampal tail ($p<0.001$), subiculum ($p=0.001$), CA1 ($p=0.002$), presubiculum ($p=0.04$), CA3 ($p=0.002$), CA4 ($p=0.002$), HATA ($p=0.03$), molecular layer of HP ($p<0.001$), GC ML DG ($p=0.002$). Comparison between HC and MCI-LB showed no significant difference in any hippocampal subfield but there was trend towards lower volumes in the following subfields; CA4 ($p=0.07$), molecular layer of HP ($p=0.07$), GC ML DG ($p=0.05$). Comparison between the MCI-LB and the MCI-AD groups showed no significant difference in hippocampal subfields, with the exception of the hippocampal tail being significantly smaller in MCI-AD compared to MCI-LB ($P=0.04$).

Hippocampal subfields (mm^3)	HC (n= 31)	MCI-AD (n= 29)	MCI-LB (n= 34)	ANCOVA[a]	Bonferroni pairwise post hoc		
					MCI-LB vs HC	MCI-AD vs HC	MCI-LB vs MCI-AD
Total Hippocampal volume	6355 ± 962	5407 ± 882	6025 ± 961	**F(2,89)=8.40, P<0.001, η_p^2=0.16**	P=0.11	**P<0.001**	P=0.12
Hippocampal tail	947 ± 170	771 ± 131	893 ± 176	**F(2,89)=8.62, p<0.001, η_p^2=0.16**	P=0.28	**P<0.001**	**P=0.04**
Subiculum	817 ± 133	692 ± 137	780 ± 135	**F(2,89)=6.67, p=0.002, η_p^2 =0.13**	P=0.33	**P=0.001**	P=0.11
CA1	1218 ± 216	1034 ± 159	1160 ± 206	**F(2,89)=6.43, p=0.002, η_p^2=0.13**	P=0.19	**P=0.002**	P=0.19
Fissure	372 ± 57	360 ± 59	384 ± 88	F(2.89)=0.29, P=0.75, η_p^2=0.006	P=1.0	P=1.0	P=1.0
Presubiculum	552 ± 86	482 ± 105	528 ± 99	**F(2,89)=3.30, P=0.04, η_p^2=0.07**	P=0.62	**P=0.04**	P=0.52
Parasubiculum	109 ± 17	107 ± 28	111 ± 26	F(2,89)=0.20, P=0.98, η_p^2 =0.00	P=1.0	P=1.0	P=1.0
CA3	408 ± 65	349 ± 62	386 ± 67	**F(2,89)=6.07, p=0.003, η_p^2=0.12**	P=0.19	**P=0.002**	P=0.29
CA4	480 ± 67	417 ± 64	453 ± 74	**F(2,89)=6.57, p=0.002, η_p^2=0.13**	P=0.07	**P=0.002**	P=0.56
Fimbria	123 ± 40	108 ± 46	113 ± 38	F(2,89)=0.66, P=0.52, η_p^2=0.02	P=1.0	P=0.93	P=1.0
HATA	111 ± 22	96 ± 20	107 ± 19	**F(2,89)=3.61, p=0.03, η_p^2=0.08**	P=0.59	**P=0.03**	P=0.44
Molecular Layer HP	1047 ± 166	885 ± 154	984 ± 160	**F(2.89)=8.65, p<0.001, η_p^2=0.16**	P=0.07	**P<0.001**	P=0.17
GC ML DG	543 ± 86	468 ± 76	509 ± 86	**F(2,89)=6.64, p=0.002, η_p^2=0.13**	P=0.05	**P=0.002**	P=0.63

Values are expressed as mean ± standard deviation (SD).
Bold underlined characters indicate significant results.
Abbreviations: HC= Healthy controls; MCI-AD=Mild cognitive impairment due to Alzheimer's disease; ANCOVA= analysis of covariance; MCI-LB= Mild cognitive impairment due to Lewy bodies disease; the granule cell and molecular layer of the dentate gyrus= GC-ML-DG; CA = cornu ammonis; HP=hippocampus proper; HATA= hippocampal-amygdala transition area
[a]ANCOVA followed by Bonferroni correction was carried out to test the difference among groups

Table 9. 1 Total hippocampal and hippocampal subfields volumes in MCI-AD, MCI-LB and HC.

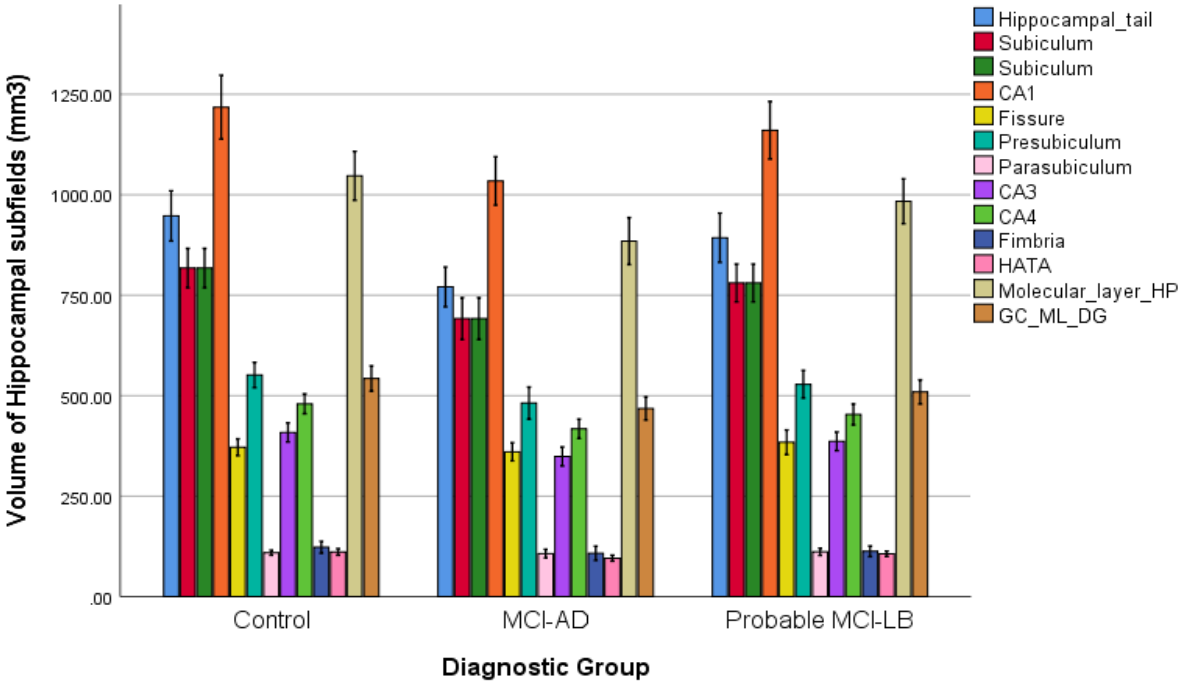

Figure 9. 3 Comparison of hippocampal subfields in HC (n=31), MCI-AD (n=29) and probable MCI-LB (n=34). The bars in the figure represent standard error bars.

Abbreviations: MCI-AD= Mild cognitive impairment due to Alzheimer's disease; MCI-LB= Mild cognitive impairment with Lewy bodies; CA=Cornus ammonis; GC-ML-DG= the granule cell and molecular layer of the dentate gyrus; HATA= Hippocampus-amygdala-transition-area; HP= Hippocampus proper.

9.4.4 Comparison of extra-hippocampal structural volumes.

Table 9.2 show measurements of extra-hippocampal structural volumes. No significant difference was observed between the three groups in the measurement of cortical volumes in the following

extra-hippocampal structures; parahippocampal gyrus (p=0.29), entrorhinal area (p=0.55), temporal pole (p=0.77).

Medial temporal sub-regions (mm^3)	**HC (n= 31)**	**MCI-AD (n= 29)**	**MCI-LB (n= 34)**	**ANCOVA[a]**	**Bonferroni pairwise post hoc**		
					MCI-LB vs HC	**MCI-AD vs HC**	**MCI-LB vs MCI-AD**
Left parahippocampal volume (mm^3)	1851 ± 314	1698 ± 347	1745 ± 321	F(2,88)=1.17, P=0.32, ηp2=0.03	P=0.72	P=0.46	P=1.0
Right parahippocampal volume (mm^3)	1704 ± 207	1631 ± 268	1629 ± 254	F(2,88)=0.93, p=0.40, ηp2=0.02	P=0.56	p=1.0	p=1.0
Left entorhinal volume (mm^3)	1898 ± 456	1802 ± 467	1869 ± 386	F(2,88)=0.11, p=0.90, ηp2=0.002	P=1.0	P=1.0	P=1.0
Right entorhinal volume (mm^3)	1803 ± 380	1601 ± 451	1695 ± 453	F(2,88)=1.05, P=0.36, ηp2=0.023	P=1.0	P=0.46	P=1.0
Left temporal pole volume (mm^3)	2396 ± 434	2315 ± 400	2403 ± 372	F(2,88)=0.31, p=0.74, ηp2=0.007	p=1.0	p=1.0	P=1.0
Right temporal pole volume (mm^3)	2334 ± 454	2352 ± 475	2407 ± 397	F(2,88)=0.43, p=0.65, ηp2=0.01	P=1.0	P=1.0	P=1.0
Total parahippocampal volume (mm^3)	3555 ± 441	3329 ± 582	3374 ± 521	F(2,88)=1.23, P=0.29, ηp2=0.028	P=0.50	P=0.53	P=1.0
Total entorhinal volume (mm^3)	3701 ± 726	3403 ± 763	3564 ± 777	F(2,88)= 0.6, p=0.55, ηp2=0.013	P=1.0	P=0.83	P=1.0
Total temporal volume (mm^3)	4730 ± 755	4668 ± 791	4810 ± 659	F(2,88)=0.26, p=0.77, ηp2=0.06,	P=1.0	P=1.0	P=1.0

Values are expressed as mean ± standard deviation (SD).
Bold underlined characters indicate significant results.
Abbreviations: HC= Healthy controls; MCI-AD=Mild cognitive impairment due to Alzheimer's disease; ANCOVA= analysis of covariance; MCI-LB= Mild cognitive impairment due to Lewy bodies disease;
[a]ANCOVA followed by Bonferroni correction was carried out to test the difference among groups

Table 9. 2 Comparison of volumes in the medial temporal sub-regions in MCI-LB, MCI-AD and HC.

9.4.5 Correlations with memory functions and hippocampal volume

Tables 9.3 and 9.4 summarise the association between cognitive, clinical scores and hippocampal volumes in MCI-LB and MCI-AD, respectively. In the MCI-LB group, there was significant association with total ACE-R score and hippocampal volume (p=0.005). This was predominately due to the association with the visuospatial domain (p=0.04), language domain (p=0.002) and fluency (p=0.02) with total hippocampal volume. A different pattern of association was observed in the MCI-AD group between total ACE-R score and total hippocampal volume, while there was a trend towards a positive association between ACE-R and hippocampal volume, this was of borderline significance (p=0.051). Moreover, the memory domain (p=0.02) and attention and orientation domain (p=0.02) had a significant association with hippocampal volume in the MCI-AD group. Unlike in the MCI-LB group, there was no association between hippocampal volume and visuospatial/language/ fluency domains in the MCI-AD group. As expected, MDS-UPDRS part III did not correlate with hippocampal volume loss in either the MCI-AD or MCI-LB group.

	R^2	F	B	SE B	β	t	P
MDS-UPDRS III score	0.062	8.00	15.93	9.59	0.24	1.66	0.11
ACE_R (Total)	0.145	11.66	41.59	13.56	0.38	3.07	**0.005**
ACE-R orientation	0.009	6.72	64.05	99.51	0.09	0.64	0.53
ACE-R memory	0.064	8.40	52.68	28.23	0.25	1.87	0.07
ACE-R fluency	0.105	9.93	122.32	48.86	0.33	2.50	**0.02**
ACE-R language	0.169	12.86	241.36	70.90	0.41	3.40	**0.002**
ACE-R visusospatial	0.084	9.11	150.98	69.11	0.29	2.19	**0.04**
Bold underlined characters indicate significant results.							

Table 9. 3 The association between total hippocampal volume and MCI-LB.

	R^2	F	B	SE B	β	t	P
MDS-UPDRS III score	0	7.044	-1.24	9.86	-0.21	-0.13	0.90
ACE-R (Total)	0.54	9.62	35.31	17.20	0.34	2.05	0.05
ACE-R orientation	0.107	10.82	208.76	84.18	0.33	2.48	**0.02**
ACE-R memory	0.107	10.83	72.38	29.09	0.40	2.49	**0.02**
ACE-R fluency	0.014	7.45	40.78	49.60	0.12	0.82	0.42
ACE-R language	0.005	7.18	-31.14	63.93	-0.079	-0.49	0.63
ACE-R visusospatial	0.001	7.06	15.98	74.63	0.33	0.21	0.83
Bold underlined characters indicate significant results.							

Table 9. 4 The association between total hippocampal volume and MCI-AD.

9.5 Discussion

In a large cohort of well-characterised MCI-AD, MCI-LB and HC, this chapter examined if medial temporal lobe preservation on MRI could be used as a biomarker to distinguish between MCI-AD and MCI-LB. An automated segmentation method was applied to extract whole hippocampal volume and hippocampal subfield volume. The main findings in relation to our hypotheses are as follow: (i) MCI-LB has preserved whole hippocampal volumes and global hippocampal subfields as compared to HC (ii) MCI-AD showed significantly reduced whole hippocampal volumes and widespread reduction in hippocampal subfields relative to HC (iii) neither whole hippocampal volumes nor hippocampal subfields volumes discriminated MCI-LB from MCI-AD (iv) there were no differences between the HC, MCI-AD and MCI-LB in relation to adjacent MTL structures.

- ***Volumetric comparison of patterns of hippocampal atrophy with HC***

In agreement with the literature on prior imaging and neuropathological studies [285, 430, 431], whole hippocampal atrophy and widespread subfield losses were found in MCI-AD as compared to HC, in particular the following subfields: CA1; subiculum; CA3; CA4; molecular layer HP; GC-ML-DG. Hippocampal atrophy at the MCI stage is associated with higher risk of progression to AD dementia [432] and structural MRI neuroimaging is among the most established biomarkers for AD and is now used for the diagnosis of prodromal AD [116]. Hippocampal atrophy strongly correlates with AD

pathology and neuropathological studies have shown differential vulnerability of hippocampal subfields to AD pathology, with stronger and earlier changes to the CA1 and subiculum in terms of neurofibrillary tangles (NFT) accumulation and neuronal loss. Subsequently, the AD pathology propagates anteriorly from the CA1 and subiculum regions to the CA2 and CA3 subfields. In contrast to MCI-AD findings in this chapter, MCI-LB exhibited hippocampal preservation compared to HC across the subfields.

- ***Volumetric comparison of patterns of hippocampal atrophy between MCI-LB and MCI-AD.***

In terms of whole hippocampal volume, MCI-AD had lower absolute mean volume than MCI-LB but hippocampal volume were not significantly different on post-hoc pairwise comparison between MCI-LB and MCI-AD. At the dementia stage, preserved MTL volume on MRI is listed as a supportive biomarker of DLB and as a potential biomarker for MCI-LB in the research criteria [7, 9]. Conversely, atrophy in the MTL is included in the current diagnostic criteria for AD [112, 115]. However, even in more advanced neurodegeneration, MTL atrophy discriminates between AD and DLB with a relatively low sensitivity 64.4% and specificity 64.9% and overall diagnostic accuracy 64.7% [433]. Therefore, MTL atrophy does occur in DLB and it may be indicative of substantial co-existent AD neuropathology and may predict a more rapid clinical course. However, contrary to the findings of this study, a retrospective study by Kantarci et al. showed preserved hippocampal volumes at the MCI stage predicted progression to DLB after accounting for the competing risk for progression to AD dementia [368].There are some notable methodological difference between the Kantarci et al. study and our study which may account for the differing results [368]. Firstly, the Kantarci et al. study was retrospective and participants were specifically chosen for inclusion based on whether they converted to DLB or AD which may have introduced ascertainment biases into the study, while our study is cross-sectional with patients being followed up prospectively. The assignment of a DLB diagnosis in the Kantarci et al. study was based on clinical diagnosis alone without the incorporation of biomarkers unlike our study which utilised two imaging biomarkers alongside clinical features to assign MCI-LB diagnosis. Therefore, the absence of a LB biomarker assessment in the Kantarci et al. study may have resulted in the inclusion of AD subjects with underlying mixed AD/LB pathology (i.e. the study would have had low sensitivity for the detection of LB pathology) whereas these mixed pathology cases would not been included in the MCI-AD group in our study. Furthermore, the exact method of determining normal from abnormal hippocampal volume in the Kantarci et al. study remains opaque. Hippocampal atrophy appears to have been determined based on the volume

range of a separate cohort of clinically diagnosed patients with AD dementia. This method is unusual and different from the approach in our study above and other published work [285, 286].

At the sub-regional level, absolute hippocampal subfield volumes were all lower in the MCI-AD group than in the MCI-LB. However, the magnitude of the differences were small and resulted in the inability to show any statistical difference between the groups, with the exception of the hippocampal tail volume, thus precluding the ability of standard volumetric hippocampal subfield assessments to readily distinguish between MCI-AD and MCI-LB. While in this study all the hippocampal subfield volumes were as expected lower in the MCI-AD group the magnitude of difference was modest compared with MCI-LB and the mean volumes were not significantly different between MCI-LB and MCI-AD. To the best of our knowledge, this is the first cross-sectional study to examine the utility of hippocampal subfields in discriminating between MCI-AD and MCI-LB.

To date, at the dementia stage only a few studies have compared atrophy patterns of the hippocampal subfields between DLB and AD. The results of these studies are conflicting which may be in part due to methodological differences; subfield volumetric difference [285, 286, 294], radial-distance mapping [288], and analyses of shape deformations [280]. Some studies showed sparing of the CA1 and subiculum in DLB compared to AD [285, 286], while others showed no preservation of the CA1 [280, 288]. Histopathological evidence in DLB would indicate neuronal loss and LN are confined to the presubiculum and CA2-3, with sparing of the CA1 and subiculum regions [431]. The CA1 neurons have a higher vulnerability to NFT pathology and the CA1 subfield is the first hippocampal area to be affected by NFT [283, 284]. While this study did show CA1 sparing in the MCI-LB cohort relative to HC, no such sparing was shown relative to MCI-AD. Although absolute CA1 volumes were lower in MCI-AD than MCI-LB, they were not significantly lower which may be due mixed pathology in the MCI-LB with some of the participants having concomitant AD and LB pathology.

As the cohort is early in the disease trajectory, longitudinal follow-up and repeat imaging of the CA1 and subiculum could conceivably become more pronounced with time in the MCI-AD cohort and allow their differentiation from MCI-LB. Other plausible explanations exist for the inability of MTL

structures to differentiate MCI-AD from MCI-LB in this study. Firstly, the MCI-AD cohort recruited to this study were not typical MCI-AD subjects as many were recruited on the premise of having symptoms suggestive of Lewy body disease. Longitudinal follow-up with post-mortem verification may result in an amended diagnosis. Secondly, neuropathological studies have shown that DLB is a heterogeneous disorder with the majority of subjects having co-existent AD/ LB pathology. Moreover, hippocampal atrophy is frequently seen in mixed AD/LB disease, with severity of NFT pathology similar to that seen in AD.

- ***Quantitative analysis of adjacent extra-hippocampal structures***

This study also assessed other regions of the MTL adjacent to the hippocampus; specifically the parahippocampus, entorhinal cortex and temporal pole. No significant difference was found between HC, MCI-AD and MCI-LB in terms of volumes of these three regions of the MTL listed above. No prior study has explored alterations in volumes of specific structures in the MTL adjacent to the hippocampus at the MCI-LB stage to determine if any these structures were preferentially preserved in MCI-LB relative to MCI-AD. However, two prior studies in DLB have examined thinning of these areas. Elder et al. showed that there was a significant difference between parahippocampus, entorhinal cortex and temporal pole thickness in DLB intermediate between controls and AD [295]. A study by Delli Pizzi et al. showed that the right parahippocampus gyrus and right entorhinal cortex thickness was reduced in DLB compared with controls but preserved in AD [286]. The parahippocampus gyrus has been associated with a variety of cognitive process, including visuospatial processing [434]. In chapter 7 of this thesis, no difference in cortical thinning was found between: HC vs MCI-LB; or MCI-LB vs MCI-AD.

In conclusion, in this study of a well-characterised cohort of MCI-AD, MCI-LB and HC, we did not find that volume of hippocampal subfields were superior to whole hippocampal volumes in distinguishing MCI-LB from MCI-AD. Furthermore, hippocampal subfields and adjacent extra-hippocampal structures were similarly atrophied in MCI-LB and in MCI-AD. Future work focussing on hippocampal subfield morphometry, particularly utilising longitudinal data is an important unmet need.

Chapter 10. Conclusions and future directions

10.1 Chapter overview

The studies in this thesis focused on two widely available clinical imaging modalities to investigate whether cross-sectional structural MRI alterations or longitudinal dopaminergic pathway deficits identified using ^{123}I-FP-CIT SPECT could be utilised as biomarkers to differentiate MCI-LB from MCI-AD and the association between clinical features and imaging biomarker findings. A better understanding of the *in vivo* evolution of the neurodegenerative process which begins with MCI before subsequently progressing to different dementia subtypes will facilitate the development of accurate biomarkers for the underlying pathological substrate at an earlier time point where neurodegeneration is much less pronounced and functional deficits are minimal. The development of such biomarkers will have an invaluable role in improving the accuracy of diagnosis of neurodegenerative conditions, monitoring *in vivo* rate of progression and assessing disease-modifying ability of potential therapeutic agents.

This chapter presents an overview of the main findings in this thesis and the novelty of the findings in the context of the field. It also highlights the strengths and limitations of the studies in this thesis, future work with our research cohort and how this will supplement the work in this thesis.

10.2 Summary of main findings

10.2.1 Longitudinal changes in ^{123}I-FP-CIT uptake in MCI-LB

In chapter 6, striatal uptake was investigated using sequential ^{123}I-FP-CIT SPECT imaging in four groups; HC, MCI-AD, possible MCI-LB and probable MCI-LB. The age-matched HC group with normal cognition was used as the comparator group as previous imaging analysis has suggested that striatal uptake may vary with age [216], although this has not been a universal finding in the literature [84]. This is the first longitudinal study to show that there is progressive dopaminergic loss in the striatum in both the probable MCI-LB and possible MCI-LB group, and while the decline in striatal uptake was significant in the probable MCI-LB group, the striatal decline was of non-significant in the possible MCI-LB group. The non-significant decline in the possible MCI-LB group is reflective of the larger standard error in this group despite having a slightly larger effect size than the probable MCI-LB group. This finding in the possible MCI-LB group is likely due to heterogeneity of the cases in this

cohort, with some having true LB disease and hence experiencing a more rapid striatal decline while others potentially being mis-attributed to this diagnostic group and having another aetiology for their cognitive decline. Even at the DLB stage, possible DLB is a heterogeneous cohort whose cognitive decline may be due to another aetiology besides LB pathology as only 40% of possible DLB subjects will retain that label at 12 months follow-up [222]. Analysis at a striatal sub-regional level demonstrated that significant decline occurred in the putamen of both the probable and possible MCI-LB groups. No significant decline in the striatum as a whole or striatal sub-regions was noted in the MCI-AD group.

This is the first study to investigate sequential ^{123}I-FP-CIT imaging in a MCI-LB cohort. It found a mean annual percentage decline in striatal uptake, as determined by linear interpolation, of around 6% per year in the MCI-LB cohorts. Moreover, the decline in striatal uptake was predominantly due to a decline in putaminal uptake (-7.4% to -6.6% annually in the probable and possible MCI-LB groups, respectively) rather than caudate uptake (-3.7% to -2.4% annually in the probable and possible MCI-LB groups, respectively). The results of this study accord favourably with the findings from the only other study using repeat ^{123}I-FP-CT SPECT in other prodromal phenotypes of DLB (IRBD) [240]. Serial ^{123}I-FP-CIT SPECT imaging in IRBD demonstrated a more rapid decline in the putamen compared to the caudate and average annual decline was -5.8% [240]. The results also extend on the observations in the only study on repeat ^{123}I-FP-CIT SPECT imaging in DLB by Colloby et al. [68] which showed that at the dementia stage dopaminergic loss was relatively uniform and the rate of annual decline in putamen was approximately double that in our study.

10.2.2 Structural MRI changes in MCI-LB: cortical thickness, cortical, subcortical and brainstem volume analysis

Cortical thickness analysis, cortical, subcortical and brainstem volumes were computed from T1-weighted images using the FreeSurfer software package. It was hypothesised that the MCI-LB group would have cortical thinning intermediate between HC and MCI-AD. Instead, a relative absence of cortical thinning was found in the MCI-LB group compared with HC and MCI-AD. It was also hypothesised that subcortical volumes would be relatively preserved in the MCI-LB group compared to MCI-AD and HC, while brainstem structures such as the midbrain would be more atrophied in MCI-LB compared to MCI-AD and HC. However, the results found a distinct pattern of subcortical volume loss between MCI-LB and MCI-AD which was not entirely in keeping with our hypothesis.

The amygdala, a limbic structure, was not significantly preserved in MCI-LB compared to MCI-AD. Meanwhile, thalamic volumes were significantly reduced in MCI-LB compared to controls and MCI-AD. In terms of the other subcortical structures and brainstem structures, no significant difference between groups was found in the following volumes: caudate; putamen; pallidum, nucleus accumbens, midbrain, pons and medulla.

The overall results from Chapter 7 would indicate that cortical structures are relatively spared at the MCI stage but LB pathology affects a distinct pattern of subcortical atrophy which appears to be different to MCI-AD and involves thalamic volume loss in MCI-LB.

10.2.3 Structural MRI changes in MCI-LB: VBM-DARTEL analysis

In chapter 8, using conventional T1-weighted structural MRI with VBM-DARTEL analysis, differences in patterns of regional or global GM atrophy were examined between MCI-LB, MCI-AD and HC. The MCI-LB cohort were found to have GM atrophy in the frontal and temporal lobes and the MCI-AD cohort were found to have bilateral hippocampal atrophy when compared to HC. In direct comparison between MCI-LB and MCI-AD, MCI-LB had significantly more bilateral cerebellar atrophy than MCI-AD but contrary to our hypothesis there was no relative preservation of the hippocampi in MCI-LB compared to MCI-AD. On correlation analysis, a positive relationship between MTL structures and total ACE-R cognitive scores in both MCI-LB and MCI-AD were found, while memory sub-scores were significantly more positively correlated with MTL structure atrophy in MCI-AD rather than in MCI-LB. In contrast to our hypothesis, we did not find any regional GM loss in the parietal-occipital pattern or a subcortical pattern of GM atrophy.

This is only the second study to explore structural MRI alterations in a prodromal DLB cohort using VBM-DARTEL but the first to incorporate biomarkers (^{123}I-FP-CIT SPECT and MIBG) as part of the diagnostic work-up. The results of this chapter are partially consistent with the prior VBM-DARTEL study in prodromal DLB which showed atrophy in the right medial frontal gyrus but in contrast to the prior VBM-DARTEL study, there was no atrophy found in the MCI-LB cohort in the insula or right claustrum relative to HC [367]. The reason for this might be related to the methodological difference in the diagnosis of prodromal DLB between the two studies, with the prior VBM-DARTEL study

lacking LB imaging biomarkers. In contrast, LB imaging biomarkers were utilised (^{123}I-FP-CIT SPECT and MIBG) alongside core clinical features to determine the diagnostic grouping in chapter 8.

In chapter 7 and chapter 8 of this thesis, two different automated approaches (Freesufer and VBM-DARTEL) were utilised to quantify structural brain changes in HC, MCI-LB and MCI-AD. Both MRI structural analysis techniques assesses changes in grey matter using T1-weighted images. Both techniques had consistent findings in terms of no difference in cortical structures between MCI-LB and MCI-AD, as well as MCI-AD having more hippocampal volume loss compared to controls. However, there were some inconsistent findings identified between the two MRI structural analysis techniques. Firstly, VBM-DARTEL demonstrated MCI-LB had reduced frontal and temporal GM volume compared with HC, a finding which was not demonstrated using FreeSurfer. Secondly, FreeSurfer showed reduced thalamic volume in MCI-LB compared to HC and MCI-AD, a finding not demonstrated using VBM-DARTEL. In the case where structural MRI findings are inconsistent between these two methodological approaches, it is likely that these are spurious results and not reflective of true underlying structural MRI differences between groups. Prior studies have found differences in findings between VBM-DARTEL and FreeSurfer and have attributed these findings to methodological difference in the algorithm underpinning each technique [435].

10.2.4 Structural MRI changes in MCI-LB: whole hippocampal volumes, hippocampal subfield volumes and adjacent extra-hippocampal structures.

In chapter 9, we examined whether structural changes in whole hippocampal volume, hippocampal subfield volume or adjacent extra-hippocampal structures could be utilised to differentiate between MCI-LB and MCI-AD. This was the first prospective study in prodromal DLB to examine this question and built on a retrospective study which found that preserved hippocampal volumes at the MCI stage predicted progression to DLB [368]. In this chapter, it was found that while the absolute hippocampal volumes were lower in MCI-AD than in MCI-LB, the difference was small between the two groups and not significantly different after controlling for age and TIV. This is an unsurprising result given that it would be expected that atrophy would be mild at the MCI stage in both MCI-LB and MCI-AD. Furthermore, it is highly likely that a substantial proportion of the MCI-LB subjects will have co-existent AD neuropathology and this could be responsible for some MTL atrophy in these subjects. This chapter also assessed other regions of the MTL which were adjacent to the hippocampus, specifically the parahippocampus, entorhinal cortex and temporal pole. No significant

difference was found between HC, MCI-AD and MCI-LB in terms of cortical thickness and cortical volume in relation to these three regions of the MTL listed above

Regarding hippocampal subfield volumes, it was observed that absolute hippocampal subfield volumes were all lower in MCI-AD compared to MCI-LB. However, the magnitude of the differences were small and therefore hippocampal subfield volumes were not significantly different between MCI-LB and MCI-AD, with the exception of hippocampal tail volume which was significantly lower in the MCI-AD group. There have been no prior reports in the literature examining the difference in hippocampal subfields between MCI-LB and MCI-AD. Therefore, this is the first cross-sectional study to examine the utility of hippocampal subfields in these groups. However, contrary to the findings of our study, a retrospective study by Kantarci et al. showed that preserved hippocampal volumes at the MCI predicted progression to DLB after accounting for the competing risk for progression to AD dementia [368].

10.3 Study strengths and limitations.

There are several key strengths of this study. The study benefitted from having a prospective longitudinal design and a well-characterised MCI cohort with age-matched HC. The latest follow-up data was used to confirm the diagnosis with the majority of cohort having completed at least one year follow-up at this stage. All participants underwent extensive clinical and neuropsychological assessment using validated rating scales. The presence of diagnostic core symptoms of LB disease was determined by a consensus panel blinded to imaging data ratings for both ^{123}I-FP-CIT SPECT and MIBG. The final construction of diagnostic groups was based on incorporating imaging biomarkers alongside clinical features. This methodology is consistent with the recently published research diagnostic criteria for MCI-LB [9]. Furthermore, it is the largest cohort of MCI-LB subjects recruited to date from a single geographical site, with imaging undertaken on the same structural 3T MRI and nuclear medicine department.

Another key strength of the study was the robust rating methodology of ^{123}I-FP-CIT SPECT images which was the independently assessed by five experts familiar with interpretation of nuclear medicine images and who were blinded to the clinical diagnosis. Disagreement between the five

raters' was resolved by discussion and consensus majority opinion. Moreover, raters' had access to data from ^{123}I-FP-CIT SPECT quantification software packages to improve diagnostic certainty.

In terms of the MRI data analysis chapters, possible MCI-LB participants were excluded from the analysis in order to limit diagnostic mis-attribution. These were MCI subjects with only one core clinical feature of LB or positive biomarker in the absence of LB core features. This approach is consistent with prior published MRI analysis in prodromal DLB and DLB [173, 292]. In terms of ^{123}I-FP-CIT SPECT chapter analysis, ^{123}I-FP-CIT SPECT imaging ratings were not used to construct the final diagnostic groupings in order to avoid circular reasoning. However, unlike the MRI analysis, possible MCI-LB subjects were included in the data analysis as the outcomes of these subjects are clinically pertinent as there is much uncertainty about the benefit of repeat ^{123}I-FP-CIT SPECT imaging in this cohort of patients.

Some limitations are inherent in our study. Firstly, the assignment of a diagnosis of MCI-LB, either possible or probable, was based on published research criteria but the sensitivity and specificity of these criteria to detect LB at its earliest stage remain to be fully determined. Ultimately, these participants will need to be followed-up longitudinally with neuropathological confirmation of the underlying pathological substrate responsible for participants' cognitive impairment. The incorporation of biomarkers into the diagnostic algorithm consistent with a LB disease diagnosis, such as MIBG and ^{123}I-FP-CIT SPECT, will hopefully improve the ante-mortem sensitivity and specificity of the diagnosis and facilitate for a good correlation between clinical diagnosis with future neuropathological diagnosis. Similarly, at present there is a deficit in the ability to detect underlying AD pathology which can co-exist with LB pathology as there was originally no amyloid or tau PET scanning available to this study. While all subjects were offered the opportunity of undergoing a lumbar puncture for CSF analysis to detect AD pathology only 10% of the cohort consented to this measure. Despite the lack of AD pathology biomarkers in our study, our approach is consistent with NIA-AA framework which does not require the detection of AD pathology in-vivo but the exclusion of other potential causes of cognitive impairment [10]. Although, we accept that our MCI-AD subjects may not be representative of the wider MCI-AD population as subjects recruited to this study all had some features suggestive of LB disease at recruitment they nonetheless fulfilled NIA-AA criteria. Several participants have consented to brain donation and data based on pathological diagnosis will emerge in the coming years.

In terms of other limitations of the study, it is notable that a substantial proportion of the MCI-LB participants, approximately 30%, were receiving either cholinesterase inhibitors or memantine. This is a marker of clinician's confidence to use medications at MCI stage when they are confident there is an underlying neurodegenerative condition. Notably, this confidence is probably bolstered by the fact that 80% of MCI-LB cohort have RBD which is high indicative of underlying neurodegenerative condition [39, 178]. There was a substantial sex imbalance in our MCI-LB cohort compared with MCI-AD and HC. The MCI-LB group is imbalanced towards males but it notable that DLB is more common in males than females [5].

In terms of imaging analysis, the MRI data is limited by the fact it is cross-sectional in nature especially with respect to the cortical thinning and VBM-DARTEL data. Longitudinal studies will be necessary to track atrophic change which would be expected to be minor this early in the disease trajectory especially given that in MCI-AD and early AD rates of 1.5% global atrophy per year have been reported in the literature [301]. Regarding the repeat ^{123}I-FP-CIT SPECT data analysis, the majority of subjects had repeat imaging between 12-18 months from baseline scanning. However, little is known about the optimal timing to repeat imaging in MCI-LB. There is a plan to have a second repeat ^{123}I-FP-CIT SPECT for a larger number of MCI-LB subjects to determine the optimal time for repeat imaging in prodromal DLB and to better determine the annual decline in striatal uptake by reducing within subject/group variability.

10.4 Future work

Longitudinal follow-up of subjects in the SUPErB study is still ongoing but baseline recruitment of participants finished in September 2019. While the majority of baseline structural MRI imaging data was considered in this thesis, approximately 14 subjects were recruited subsequent to the data cut-off for my thesis analysis. Moreover, funding and ethical approval has been secured for further repeat ^{123}I-FP-CIT SPECT imaging in the SUPErB cohort and recruitment to undergo this further imaging is currently ongoing at present. We plan to publish much of the work outlined in this thesis after future re-analysis with the complete dataset.

The diagnostic accuracy of our approach to identifying prodromal DLB will require participants to be followed-up over a number of years to determine how the clinical phenotype evolves with time. Ultimately, the diagnosis will require neuropathology confirmation and a number of participants have consented to brain donation already.

The pathological underpinning of DLB is the presence of LB but how it progresses through the peripheral and central nervous system is a matter of considerable debate. Furthermore, a substantial proportion of dementia patients have mixed LB/AD pathology at autopsy. The complicated correlation between clinical phenotype and pathological findings means even at the dementia stage diagnosis may be reliant on imaging biomarker. Therefore, it is unlikely that a single imaging biomarker will be sufficiently sensitive or specific by itself to detect prodromal DLB and a multimodal imaging approach will be required. In order to better delineate out the underlying pathological contributions to cognitive impairment in our cohort, a subset of participants will be requested to undergo future amyloid PET imaging. This approach should shed more light on the interaction between co-pathologies *in vivo*.

In summary, this thesis offers at present an incomplete data analysis of some of the imaging modalities in the SUPErB study. By incorporating a longitudinal design and multimodal assessment process, the SUPErB study offers the exciting potential to identify biomarkers for the progression of MCI-LB.

10.5 Conclusion

In conclusion, the results of this thesis shows promise for the ability of imaging biomarkers to identify the earliest *in vivo* structural and functional brain alternations to differentiate MCI-LB from MCI-AD and HC. Sequential ^{123}I-FP-CIT SPECT imaging is a promising biomarker to detect progressive dopaminergic loss in MCI-LB subjects in excess of age-matched HC which is not detected in MCI-AD subjects. Similarly, structural MRI methods may have a valuable role, as part of a multimodal imaging approach. The main findings from the structural MRI data suggest: (1) a distinct pattern of GM volume loss in the frontal and temporal lobes among the MCI-LB cohort compared to HC, (2) bilateral reduction in both cerebellum in the MCI-LB compared to MCI-AD groups, (3) there was no relative preservation of the medial temporal lobe at the MCI-LB stage compared to MCI-AD, (4)

there was no cortical thickness difference between MCI-LB and MCI-AD or HC (5) subcortical volume differences were noted, with more pronounced thalamic volume loss and relative preservation of the amygdala in MCI-LB compared to MCI-AD. These results suggest that structural MRI changes may be present early in MCI-LB but are not that pronounced on cross-sectional analysis. Future longitudinal repeat structural MRI data analysis may be able to delineate a distinct pattern of GM atrophy associated with MCI-LB.

References

1. Brodaty, H. and M. Donkin, *Family caregivers of people with dementia.* Dialogues Clin Neurosci, 2009. **11**(2): p. 217-28.
2. Donegan, K., et al., *Trends in diagnosis and treatment for people with dementia in the UK from 2005 to 2015: a longitudinal retrospective cohort study.* Lancet Public Health, 2017. **2**(3): p. e149-e156.
3. Ford, E., et al., *Predicting dementia from primary care records: A systematic review and meta-analysis.* PLoS One, 2018. **13**(3): p. e0194735.
4. Prince, M., et al., *The global prevalence of dementia: a systematic review and metaanalysis.* Alzheimers Dement, 2013. **9**(1): p. 63-75.e2.
5. Kane, J.P.M., et al., *Clinical prevalence of Lewy body dementia.* Alzheimers Res Ther, 2018. **10**(1): p. 19.
6. Vann Jones, S.A. and J.T. O'Brien, *The prevalence and incidence of dementia with Lewy bodies: a systematic review of population and clinical studies.* Psychol Med, 2014. **44**(4): p. 673-83.
7. McKeith, I.G., et al., *Diagnosis and management of dementia with Lewy bodies: Fourth consensus report of the DLB Consortium.* Neurology, 2017. **89**(1): p. 88-100.
8. Thomas, A.J., et al., *Improving the identification of dementia with Lewy bodies in the context of an Alzheimer's-type dementia.* Alzheimers Res Ther, 2018. **10**(1): p. 27.
9. McKeith, I.G., et al., *Research criteria for the diagnosis of prodromal dementia with Lewy bodies.* Neurology, 2020.
10. Albert, M.S., et al., *The diagnosis of mild cognitive impairment due to Alzheimer's disease: recommendations from the National Institute on Aging-Alzheimer's Association workgroups on diagnostic guidelines for Alzheimer's disease.* Alzheimers Dement, 2011. **7**(3): p. 270-9.
11. Donaghy, P.C., et al., *Neuropsychiatric symptoms and cognitive profile in mild cognitive impairment with Lewy bodies.* Psychol Med, 2018. **48**(14): p. 2384-2390.
12. Geser, F., et al., *How to diagnose dementia with Lewy bodies: state of the art.* Mov Disord, 2005. **20 Suppl 12**: p. S11-20.
13. Zupancic, M., A. Mahajan, and K. Handa, *Dementia with lewy bodies: diagnosis and management for primary care providers.* Prim Care Companion CNS Disord, 2011. **13**(5).
14. Wakisaka, Y., et al., *Age-associated prevalence and risk factors of Lewy body pathology in a general population: the Hisayama study.* Acta Neuropathol, 2003. **106**(4): p. 374-82.
15. Hogan, D.B., et al., *The Prevalence and Incidence of Dementia with Lewy Bodies: a Systematic Review.* Can J Neurol Sci, 2016. **43 Suppl 1**: p. S83-95.
16. Palmqvist, S., et al., *Practical suggestions on how to differentiate dementia with Lewy bodies from Alzheimer's disease with common cognitive tests.* Int J Geriatr Psychiatry, 2009. **24**(12): p. 1405-12.
17. Oinas, M., et al., *Neuropathologic findings of dementia with lewy bodies (DLB) in a population-based Vantaa 85+ study.* J Alzheimers Dis, 2009. **18**(3): p. 677-89.
18. Schneider, J.A., et al., *The neuropathology of older persons with and without dementia from community versus clinic cohorts.* J Alzheimers Dis, 2009. **18**(3): p. 691-701.
19. Metzler-Baddeley, C., *A review of cognitive impairments in dementia with Lewy bodies relative to Alzheimer's disease and Parkinson's disease with dementia.* Cortex, 2007. **43**(5): p. 583-600.
20. Fernandez, H.H., et al., *Quetiapine for psychosis in Parkinson's disease versus dementia with Lewy bodies.* J Clin Psychiatry, 2002. **63**(6): p. 513-5.
21. Hickey, C., et al., *Differentiating the dementias. Revisiting synucleinopathies and tauopathies.* Curr Alzheimer Res, 2008. **5**(1): p. 52-60.
22. Weisman, D. and I. McKeith, *Dementia with Lewy bodies.* Semin Neurol, 2007. **27**(1): p. 42-7.
23. Gomperts, S.N., *Lewy Body Dementias: Dementia With Lewy Bodies and Parkinson Disease Dementia.* Continuum (Minneap Minn), 2016. **22**(2 Dementia): p. 435-63.
24. Ballard, C., et al., *Psychiatric morbidity in dementia with Lewy bodies: a prospective clinical and neuropathological comparative study with Alzheimer's disease.* Am J Psychiatry, 1999. **156**(7): p. 1039-45.

25. Donaghy, P.C., J.T. O'Brien, and A.J. Thomas, *Prodromal dementia with Lewy bodies.* Psychol Med, 2015. **45**(2): p. 259-68.
26. Donaghy, P.C., et al., *Mild cognitive impairment with Lewy bodies: neuropsychiatric supportive symptoms and cognitive profile.* Psychol Med, 2020: p. 1-9.
27. Thomas, A.J., et al., *Diagnostic accuracy of dopaminergic imaging in prodromal dementia with Lewy bodies.* Psychol Med, 2019. **49**(3): p. 396-402.
28. Thomas, A.J., et al., *Autopsy validation of 123I-FP-CIT dopaminergic neuroimaging for the diagnosis of DLB.* Neurology, 2017. **88**(3): p. 276-283.
29. Aarsland, D., et al., *Comparison of extrapyramidal signs in dementia with Lewy bodies and Parkinson's disease.* J Neuropsychiatry Clin Neurosci, 2001. **13**(3): p. 374-9.
30. Postuma, R.B., et al., *MDS clinical diagnostic criteria for Parkinson's disease.* Mov Disord, 2015. **30**(12): p. 1591-601.
31. Burn, D.J., et al., *Motor subtype and cognitive decline in Parkinson's disease, Parkinson's disease with dementia, and dementia with Lewy bodies.* J Neurol Neurosurg Psychiatry, 2006. **77**(5): p. 585-9.
32. Allan, L.M., et al., *Incidence and prediction of falls in dementia: a prospective study in older people.* PLoS One, 2009. **4**(5): p. e5521.
33. Goldman, J.G., et al., *Effects of dopaminergic medications on psychosis and motor function in dementia with Lewy bodies.* Mov Disord, 2008. **23**(15): p. 2248-50.
34. Jellinger, K.A., *Dementia with Lewy bodies and Parkinson's disease-dementia: current concepts and controversies.* J Neural Transm (Vienna), 2018. **125**(4): p. 615-650.
35. Taylor, J.P., et al., *New evidence on the management of Lewy body dementia.* Lancet Neurol, 2020. **19**(2): p. 157-169.
36. McKeith, I., et al., *Neuroleptic sensitivity in patients with senile dementia of Lewy body type.* Bmj, 1992. **305**(6855): p. 673-8.
37. Walker, Z., et al., *Evolution of clinical features in possible DLB depending on FP-CIT SPECT result.* Neurology, 2016. **87**(10): p. 1045-51.
38. McKeith, I.G., et al., *Diagnosis and management of dementia with Lewy bodies: third report of the DLB Consortium.* Neurology, 2005. **65**(12): p. 1863-72.
39. Iranzo, A., et al., *Neurodegenerative disease status and post-mortem pathology in idiopathic rapid-eye-movement sleep behaviour disorder: an observational cohort study.* Lancet Neurol, 2013. **12**(5): p. 443-53.
40. Schenck, C.H., et al., *Rapid eye movement sleep behavior disorder: devising controlled active treatment studies for symptomatic and neuroprotective therapy--a consensus statement from the International Rapid Eye Movement Sleep Behavior Disorder Study Group.* Sleep Med, 2013. **14**(8): p. 795-806.
41. Boeve, B.F., et al., *Validation of the Mayo Sleep Questionnaire to screen for REM sleep behavior disorder in an aging and dementia cohort.* Sleep Med, 2011. **12**(5): p. 445-53.
42. Dugger, B.N., et al., *Rapid eye movement sleep behavior disorder and subtypes in autopsy-confirmed dementia with Lewy bodies.* Mov Disord, 2012. **27**(1): p. 72-8.
43. Allan, L.M., et al., *Autonomic dysfunction in dementia.* J Neurol Neurosurg Psychiatry, 2007. **78**(7): p. 671-7.
44. Karantzoulis, S. and J.E. Galvin, *UPDATE ON DEMENTIA WITH LEWY BODIES.* Current translational geriatrics and experimental gerontology reports, 2013. **2**(3): p. 196-204.
45. Mueller, C., et al., *The prognosis of dementia with Lewy bodies.* Lancet Neurol, 2017. **16**(5): p. 390-398.
46. Price, A., et al., *Mortality in dementia with Lewy bodies compared with Alzheimer's dementia: a retrospective naturalistic cohort study.* BMJ Open, 2017. **7**(11): p. e017504.
47. Rongve, A., et al., *Cognitive decline in dementia with Lewy bodies: a 5-year prospective cohort study.* BMJ Open, 2016. **6**(2): p. e010357.
48. Lee, D.R., et al., *Examining carer stress in dementia: the role of subtype diagnosis and neuropsychiatric symptoms.* Int J Geriatr Psychiatry, 2013. **28**(2): p. 135-41.
49. Morfis, L. and D.J. Cordato, *Dementia with Lewy bodies in an elderly Greek male due to alpha-synuclein gene mutation.* J Clin Neurosci, 2006. **13**(9): p. 942-4.

50. Zarranz, J.J., et al., *The new mutation, E46K, of alpha-synuclein causes Parkinson and Lewy body dementia.* Ann Neurol, 2004. **55**(2): p. 164-73.
51. Ross, O.A., et al., *Lrrk2 and Lewy body disease.* Ann Neurol, 2006. **59**(2): p. 388-93.
52. Nalls, M.A., et al., *A multicenter study of glucocerebrosidase mutations in dementia with Lewy bodies.* JAMA Neurol, 2013. **70**(6): p. 727-35.
53. Guyant-Marechal, I., et al., *Intrafamilial diversity of phenotype associated with app duplication.* Neurology, 2008. **71**(23): p. 1925-6.
54. Kobayashi, S., et al., *Apolipoprotein E4 frequencies in a Japanese population with Alzheimer's disease and dementia with Lewy bodies.* PLoS One, 2011. **6**(4): p. e18569.
55. Labbe, C., et al., *MAPT haplotype H1G is associated with increased risk of dementia with Lewy bodies.* Alzheimers Dement, 2016. **12**(12): p. 1297-1304.
56. Braak, H. and K. Del Tredici, *Neuropathological Staging of Brain Pathology in Sporadic Parkinson's disease: Separating the Wheat from the Chaff.* J Parkinsons Dis, 2017. **7**(s1): p. S71-s85.
57. Alafuzoff, I., et al., *Assessment of alpha-synuclein pathology: a study of the BrainNet Europe Consortium.* J Neuropathol Exp Neurol, 2008. **67**(2): p. 125-43.
58. Montine, T.J., et al., *National Institute on Aging-Alzheimer's Association guidelines for the neuropathologic assessment of Alzheimer's disease: a practical approach.* Acta Neuropathol, 2012. **123**(1): p. 1-11.
59. Jellinger, K.A. and J. Attems, *Prevalence and pathology of dementia with Lewy bodies in the oldest old: a comparison with other dementing disorders.* Dement Geriatr Cogn Disord, 2011. **31**(4): p. 309-16.
60. White, L.R., et al., *Neuropathologic comorbidity and cognitive impairment in the Nun and Honolulu-Asia Aging Studies.* Neurology, 2016. **86**(11): p. 1000-8.
61. Toledo, J.B., et al., *Clinical and multimodal biomarker correlates of ADNI neuropathological findings.* Acta Neuropathol Commun, 2013. **1**: p. 65.
62. Clinton, L.K., et al., *Synergistic Interactions between Abeta, tau, and alpha-synuclein: acceleration of neuropathology and cognitive decline.* J Neurosci, 2010. **30**(21): p. 7281-9.
63. Frigerio, R., et al., *Incidental Lewy body disease: do some cases represent a preclinical stage of dementia with Lewy bodies?* Neurobiol Aging, 2011. **32**(5): p. 857-63.
64. Parkkinen, L., T. Pirttila, and I. Alafuzoff, *Applicability of current staging/categorization of alpha-synuclein pathology and their clinical relevance.* Acta Neuropathol, 2008. **115**(4): p. 399-407.
65. Harding, A.J., G.A. Broe, and G.M. Halliday, *Visual hallucinations in Lewy body disease relate to Lewy bodies in the temporal lobe.* Brain, 2002. **125**(Pt 2): p. 391-403.
66. Ross, G.W., et al., *Parkinsonian signs and substantia nigra neuron density in decendents elders without PD.* Ann Neurol, 2004. **56**(4): p. 532-9.
67. Lang, A.E. and A.M. Lozano, *Parkinson's disease. First of two parts.* N Engl J Med, 1998. **339**(15): p. 1044-53.
68. Colloby, S.J., et al., *Progression of dopaminergic degeneration in dementia with Lewy bodies and Parkinson's disease with and without dementia assessed using 123I-FP-CIT SPECT.* Eur J Nucl Med Mol Imaging, 2005. **32**(10): p. 1176-85.
69. O'Brien, J.T., et al., *Is ioflupane I123 injection diagnostically effective in patients with movement disorders and dementia? Pooled analysis of four clinical trials.* BMJ Open, 2014. **4**(7): p. e005122.
70. Walker, Z., et al., *Clinical usefulness of dopamine transporter SPECT imaging with 123I-FP-CIT in patients with possible dementia with Lewy bodies: randomised study.* Br J Psychiatry, 2015. **206**(2): p. 145-52.
71. van der Zande, J.J., et al., *[(123)]FP-CIT SPECT scans initially rated as normal became abnormal over time in patients with probable dementia with Lewy bodies.* Eur J Nucl Med Mol Imaging, 2016. **43**(6): p. 1060-6.
72. Braak, H., et al., *Staging of brain pathology related to sporadic Parkinson's disease.* Neurobiol Aging, 2003. **24**(2): p. 197-211.
73. Roselli, F., et al., *Severity of neuropsychiatric symptoms and dopamine transporter levels in dementia with Lewy bodies: a 123I-FP-CIT SPECT study.* Mov Disord, 2009. **24**(14): p. 2097-103.
74. Lamotte, G., et al., *Influence of education on cognitive performance and dopamine transporter binding in dementia with Lewy bodies.* Clin Neurol Neurosurg, 2016. **146**: p. 138-43.

75. Ziebell, M., et al., *Striatal dopamine transporter binding does not correlate with clinical severity in dementia with Lewy bodies.* J Nucl Med, 2013. **54**(7): p. 1072-6.
76. Kasanuki, K., et al., *123I-FP-CIT SPECT findings and its clinical relevance in prodromal dementia with Lewy bodies.* Eur J Nucl Med Mol Imaging, 2017. **44**(3): p. 358-365.
77. David, R., et al., *Striatal dopamine transporter levels correlate with apathy in neurodegenerative diseases A SPECT study with partial volume effect correction.* Clin Neurol Neurosurg, 2008. **110**(1): p. 19-24.
78. Orimo, S., et al., *Cardiac sympathetic denervation precedes neuronal loss in the sympathetic ganglia in Lewy body disease.* Acta Neuropathol, 2005. **109**(6): p. 583-8.
79. Kane, J.P.M., et al., *(123)I-MIBG scintigraphy utility and cut-off value in a clinically representative dementia cohort.* Parkinsonism Relat Disord, 2019.
80. Komatsu, J., et al., *(123)I-MIBG myocardial scintigraphy for the diagnosis of DLB: a multicentre 3-year follow-up study.* J Neurol Neurosurg Psychiatry, 2018. **89**(11): p. 1167-1173.
81. Treglia, G. and E. Cason, *Diagnostic performance of myocardial innervation imaging using MIBG scintigraphy in differential diagnosis between dementia with lewy bodies and other dementias: a systematic review and a meta-analysis.* J Neuroimaging, 2012. **22**(2): p. 111-7.
82. Tiraboschi, P., et al., *(123) I-2beta-carbomethoxy-3beta-(4-iodophenyl)-N-(3-fluoropropyl) nortropane single photon emission computed tomography and (123) I-metaiodobenzylguanidine myocardial scintigraphy in differentiating dementia with lewy bodies from other dementias: A comparative study.* Ann Neurol, 2016. **80**(3): p. 368-78.
83. Treglia, G., et al., *Iodine-123 metaiodobenzylguanidine scintigraphy and iodine-123 ioflupane single photon emission computed tomography in Lewy body diseases: complementary or alternative techniques?* J Neuroimaging, 2014. **24**(2): p. 149-54.
84. Roberts, G., et al., *(123)I-FP-CIT striatal binding ratios do not decrease significantly with age in older adults.* Ann Nucl Med, 2019. **33**(6): p. 434-443.
85. Marsh, S.E. and M. Blurton-Jones, *Examining the mechanisms that link β-amyloid and α-synuclein pathologies.* Alzheimer's Research & Therapy, 2012. **4**(2): p. 11-11.
86. Ishizawa, T., et al., *Colocalization of tau and alpha-synuclein epitopes in Lewy bodies.* J Neuropathol Exp Neurol, 2003. **62**(4): p. 389-97.
87. Colom-Cadena, M., et al., *Confluence of alpha-synuclein, tau, and beta-amyloid pathologies in dementia with Lewy bodies.* J Neuropathol Exp Neurol, 2013. **72**(12): p. 1203-12.
88. Donaghy, P., A.J. Thomas, and J.T. O'Brien, *Amyloid PET Imaging in Lewy body disorders.* Am J Geriatr Psychiatry, 2015. **23**(1): p. 23-37.
89. Donaghy, P.C., et al., *Clinical and imaging correlates of amyloid deposition in dementia with Lewy bodies.* Mov Disord, 2018. **33**(7): p. 1130-1138.
90. Mak, E., et al., *Beta amyloid deposition maps onto hippocampal and subiculum atrophy in dementia with Lewy bodies.* Neurobiol Aging, 2019. **73**: p. 74-81.
91. Barber, P.A., et al., *The electroencephalogram in dementia with Lewy bodies.* Acta Neurol Scand, 2000. **101**(1): p. 53-6.
92. Walker, M.P., et al., *Quantification and characterization of fluctuating cognition in dementia with Lewy bodies and Alzheimer's disease.* Dement Geriatr Cogn Disord, 2000. **11**(6): p. 327-35.
93. Bonanni, L., et al., *EEG comparisons in early Alzheimer's disease, dementia with Lewy bodies and Parkinson's disease with dementia patients with a 2-year follow-up.* Brain, 2008. **131**(Pt 3): p. 690-705.
94. Schumacher, J., et al., *Dysfunctional brain dynamics and their origin in Lewy body dementia.* Brain, 2019. **142**(6): p. 1767-1782.
95. Mollenhauer, B., et al., *A user's guide for alpha-synuclein biomarker studies in biological fluids: Perianalytical considerations.* Mov Disord, 2017. **32**(8): p. 1117-1130.
96. Forland, M.G., et al., *The value of cerebrospinal fluid alpha-synuclein and the tau/alpha-synuclein ratio for diagnosis of neurodegenerative disorders with Lewy pathology.* Eur J Neurol, 2020. **27**(1): p. 43-50.
97. Bousiges, O. and F. Blanc, *Diagnostic value of cerebro-spinal fluid biomarkers in dementia with lewy bodies.* Clin Chim Acta, 2019. **490**: p. 222-228.

98. Mollenhauer, B., et al., *Follow-up investigations in cerebrospinal fluid of patients with dementia with Lewy bodies and Alzheimer's disease.* J Neural Transm (Vienna), 2005. **112**(7): p. 933-48.
99. Mollenhauer, B., et al., *Total tau protein, phosphorylated tau (181p) protein, beta-amyloid(1-42), and beta-amyloid(1-40) in cerebrospinal fluid of patients with dementia with Lewy bodies.* Clin Chem Lab Med, 2006. **44**(2): p. 192-5.
100. Lippa, C.F., T.W. Smith, and E. Perry, *Dementia with Lewy bodies: choline acetyltransferase parallels nucleus basalis pathology.* J Neural Transm (Vienna), 1999. **106**(5-6): p. 525-35.
101. McKeith, I., et al., *Efficacy of rivastigmine in dementia with Lewy bodies: a randomised, double-blind, placebo-controlled international study.* Lancet, 2000. **356**(9247): p. 2031-6.
102. Mori, E., M. Ikeda, and K. Kosaka, *Donepezil for dementia with Lewy bodies: a randomized, placebo-controlled trial.* Ann Neurol, 2012. **72**(1): p. 41-52.
103. Ikeda, M., et al., *Donepezil for dementia with Lewy bodies: a randomized, placebo-controlled, confirmatory phase III trial.* Alzheimers Res Ther, 2015. **7**(1): p. 4.
104. Shea, C., C. MacKnight, and K. Rockwood, *Donepezil for treatment of dementia with Lewy bodies: a case series of nine patients.* Int Psychogeriatr, 1998. **10**(3): p. 229-38.
105. Samuel, W., et al., *Better cognitive and psychopathologic response to donepezil in patients prospectively diagnosed as dementia with Lewy bodies: a preliminary study.* Int J Geriatr Psychiatry, 2000. **15**(9): p. 794-802.
106. Lanctot, K.L. and N. Herrmann, *Donepezil for behavioural disorders associated with Lewy bodies: a case series.* Int J Geriatr Psychiatry, 2000. **15**(4): p. 338-45.
107. Grace, J., et al., *Long-Term use of rivastigmine in patients with dementia with Lewy bodies: an open-label trial.* Int Psychogeriatr, 2001. **13**(2): p. 199-205.
108. Maclean, L.E., C.C. Collins, and E.J. Byrne, *Dementia with Lewy bodies treated with rivastigmine: effects on cognition, neuropsychiatric symptoms, and sleep.* Int Psychogeriatr, 2001. **13**(3): p. 277-88.
109. Connolly, B.S. and A.E. Lang, *Pharmacological treatment of Parkinson disease: a review.* Jama, 2014. **311**(16): p. 1670-83.
110. Reitz, C. and R. Mayeux, *Alzheimer disease: epidemiology, diagnostic criteria, risk factors and biomarkers.* Biochem Pharmacol, 2014. **88**(4): p. 640-51.
111. Lane, C.A., J. Hardy, and J.M. Schott, *Alzheimer's disease.* Eur J Neurol, 2018. **25**(1): p. 59-70.
112. McKhann, G.M., et al., *The diagnosis of dementia due to Alzheimer's disease: recommendations from the National Institute on Aging-Alzheimer's Association workgroups on diagnostic guidelines for Alzheimer's disease.* Alzheimers Dement, 2011. **7**(3): p. 263-9.
113. Rowe, C.C., et al., *Amyloid imaging results from the Australian Imaging, Biomarkers and Lifestyle (AIBL) study of aging.* Neurobiol Aging, 2010. **31**(8): p. 1275-83.
114. Bransby, L., et al., *Sensitivity of a Preclinical Alzheimer's Cognitive Composite (PACC) to amyloid beta load in preclinical Alzheimer's disease.* J Clin Exp Neuropsychol, 2019. **41**(6): p. 591-600.
115. Dubois, B., et al., *Advancing research diagnostic criteria for Alzheimer's disease: the IWG-2 criteria.* Lancet Neurol, 2014. **13**(6): p. 614-29.
116. Dubois, B., et al., *Preclinical Alzheimer's disease: Definition, natural history, and diagnostic criteria.* Alzheimers Dement, 2016. **12**(3): p. 292-323.
117. Sperling, R.A., et al., *Toward defining the preclinical stages of Alzheimer's disease: recommendations from the National Institute on Aging-Alzheimer's Association workgroups on diagnostic guidelines for Alzheimer's disease.* Alzheimers Dement, 2011. **7**(3): p. 280-92.
118. Goldman, J.S. and V.M. Van Deerlin, *Alzheimer's Disease and Frontotemporal Dementia: The Current State of Genetics and Genetic Testing Since the Advent of Next-Generation Sequencing.* Mol Diagn Ther, 2018. **22**(5): p. 505-513.
119. Goldman, J.G., et al., *The spectrum of cognitive impairment in Lewy body diseases.* Mov Disord, 2014. **29**(5): p. 608-21.
120. Hyman, B.T., et al., *National Institute on Aging-Alzheimer's Association guidelines for the neuropathologic assessment of Alzheimer's disease.* Alzheimers Dement, 2012. **8**(1): p. 1-13.
121. Takeda, S., *Progression of Alzheimer's disease, tau propagation, and its modifiable risk factors.* Neurosci Res, 2018.

122. Braak, H. and E. Braak, *Neuropathological stageing of Alzheimer-related changes.* Acta Neuropathol, 1991. **82**(4): p. 239-59.
123. Thal, D.R., et al., *Phases of A beta-deposition in the human brain and its relevance for the development of AD.* Neurology, 2002. **58**(12): p. 1791-800.
124. Mirra, S.S., et al., *The Consortium to Establish a Registry for Alzheimer's Disease (CERAD). Part II. Standardization of the neuropathologic assessment of Alzheimer's disease.* Neurology, 1991. **41**(4): p. 479-86.
125. Geddes, J.W., et al., *Comparison of neuropathologic criteria for the diagnosis of Alzheimer's disease.* Neurobiol Aging, 1997. **18**(4 Suppl): p. S99-105.
126. Jack, C.R., Jr., et al., *A/T/N: An unbiased descriptive classification scheme for Alzheimer disease biomarkers.* Neurology, 2016. **87**(5): p. 539-47.
127. Risacher, S.L., et al., *Longitudinal MRI atrophy biomarkers: relationship to conversion in the ADNI cohort.* Neurobiol Aging, 2010. **31**(8): p. 1401-18.
128. Grundman, M., et al., *Brain MRI hippocampal volume and prediction of clinical status in a mild cognitive impairment trial.* J Mol Neurosci, 2002. **19**(1-2): p. 23-7.
129. Braskie, M.N. and P.M. Thompson, *A focus on structural brain imaging in the Alzheimer's disease neuroimaging initiative.* Biol Psychiatry, 2014. **75**(7): p. 527-33.
130. Leuzy, A., et al., *In vivo Detection of Alzheimer's Disease.* Yale J Biol Med, 2018. **91**(3): p. 291-300.
131. Silverman, D.H., et al., *Positron emission tomography in evaluation of dementia: Regional brain metabolism and long-term outcome.* Jama, 2001. **286**(17): p. 2120-7.
132. Caminiti, S.P., et al., *FDG-PET and CSF biomarker accuracy in prediction of conversion to different dementias in a large multicentre MCI cohort.* Neuroimage Clin, 2018. **18**: p. 167-177.
133. Sabri, O., et al., *Florbetaben PET imaging to detect amyloid beta plaques in Alzheimer's disease: phase 3 study.* Alzheimers Dement, 2015. **11**(8): p. 964-74.
134. Clark, C.M., et al., *Use of florbetapir-PET for imaging beta-amyloid pathology.* Jama, 2011. **305**(3): p. 275-83.
135. Vanderstichele, H., et al., *Standardization of preanalytical aspects of cerebrospinal fluid biomarker testing for Alzheimer's disease diagnosis: a consensus paper from the Alzheimer's Biomarkers Standardization Initiative.* Alzheimers Dement, 2012. **8**(1): p. 65-73.
136. Olsson, B., et al., *CSF and blood biomarkers for the diagnosis of Alzheimer's disease: a systematic review and meta-analysis.* Lancet Neurol, 2016. **15**(7): p. 673-684.
137. Ferreira, D., et al., *Meta-Review of CSF Core Biomarkers in Alzheimer's Disease: The State-of-the-Art after the New Revised Diagnostic Criteria.* Front Aging Neurosci, 2014. **6**: p. 47.
138. Forlenza, O.V., et al., *Cerebrospinal fluid biomarkers in Alzheimer's disease: Diagnostic accuracy and prediction of dementia.* Alzheimers Dement (Amst), 2015. **1**(4): p. 455-63.
139. *National Institute for Health and Care Excellence: Dementia: assessment, management and support for people living with dementia and their carers (NICE Guideline No. 97). Retrieved from https://www.nice.org.uk/guidance/ng97.* 2018.
140. Rai, H., L. Yates, and M. Orrell, *Cognitive Stimulation Therapy for Dementia.* Clin Geriatr Med, 2018. **34**(4): p. 653-665.
141. Birks, J.S. and R.J. Harvey, *Donepezil for dementia due to Alzheimer's disease.* Cochrane Database Syst Rev, 2018. **6**(6): p. Cd001190.
142. Berg, D., et al., *MDS research criteria for prodromal Parkinson's disease.* Mov Disord, 2015. **30**(12): p. 1600-11.
143. Donaghy, P.C. and I.G. McKeith, *The clinical characteristics of dementia with Lewy bodies and a consideration of prodromal diagnosis.* Alzheimers Res Ther, 2014. **6**(4): p. 46.
144. Chiba, Y., et al., *Retrospective survey of prodromal symptoms in dementia with Lewy bodies: comparison with Alzheimer's disease.* Dement Geriatr Cogn Disord, 2012. **33**(4): p. 273-81.
145. Fujishiro, H., et al., *Dementia with Lewy bodies: early diagnostic challenges.* Psychogeriatrics, 2013. **13**(2): p. 128-38.
146. Boeve, B.F., et al., *Clinicopathologic correlations in 172 cases of rapid eye movement sleep behavior disorder with or without a coexisting neurologic disorder.* Sleep Med, 2013. **14**(8): p. 754-62.
147. Boeve, B.F., et al., *Insights into REM sleep behavior disorder pathophysiology in brainstem-predominant Lewy body disease.* Sleep Med, 2007. **8**(1): p. 60-4.

148. Iranzo, A., et al., *Neurodegenerative disorder risk in idiopathic REM sleep behavior disorder: study in 174 patients.* PLoS One, 2014. **9**(2): p. e89741.
149. Iranzo, A., et al., *Dopamine transporter imaging deficit predicts early transition to synucleinopathy in idiopathic rapid eye movement sleep behavior disorder.* Ann Neurol, 2017. **82**(3): p. 419-428.
150. Beach, T.G., et al., *Unified staging system for Lewy body disorders: correlation with nigrostriatal degeneration, cognitive impairment and motor dysfunction.* Acta Neuropathol, 2009. **117**(6): p. 613-34.
151. Kane, J.P.M., et al., *(123)I-MIBG scintigraphy utility and cut-off value in a clinically representative dementia cohort.* Parkinsonism Relat Disord, 2019. **62**: p. 79-84.
152. Jellinger, K.A., *Lewy body-related alpha-synucleinopathy in the aged human brain.* J Neural Transm (Vienna), 2004. **111**(10-11): p. 1219-35.
153. Ballard, C., et al., *Differences in neuropathologic characteristics across the Lewy body dementia spectrum.* Neurology, 2006. **67**(11): p. 1931-4.
154. Marui, W., et al., *Progression and staging of Lewy pathology in brains from patients with dementia with Lewy bodies.* J Neurol Sci, 2002. **195**(2): p. 153-9.
155. Petersen, R.C., et al., *Mild cognitive impairment: clinical characterization and outcome.* Arch Neurol, 1999. **56**(3): p. 303-8.
156. Petersen, R.C., *Mild cognitive impairment as a diagnostic entity.* J Intern Med, 2004. **256**(3): p. 183-94.
157. Cagnin, A., et al., *Clinical and Cognitive Phenotype of Mild Cognitive Impairment Evolving to Dementia with Lewy Bodies.* Dement Geriatr Cogn Dis Extra, 2015. **5**(3): p. 442-9.
158. Petersen, R.C., et al., *Mild cognitive impairment: ten years later.* Arch Neurol, 2009. **66**(12): p. 1447-55.
159. Ferman, T.J., et al., *Nonamnestic mild cognitive impairment progresses to dementia with Lewy bodies.* Neurology, 2013. **81**(23): p. 2032-8.
160. *American Psychiatric Association. Diagnostic and Statistical Manual of Mental Disorders: DSM-5. Washington D.C.:.* American Psychiatric Association, 2013.
161. Winblad, B., et al., *Mild cognitive impairment--beyond controversies, towards a consensus: report of the International Working Group on Mild Cognitive Impairment.* J Intern Med, 2004. **256**(3): p. 240-6.
162. Boeve, B.F., *Mild cognitive impairment associated with underlying Alzheimer's disease versus Lewy body disease.* Parkinsonism Relat Disord, 2012. **18 Suppl 1**: p. S41-4.
163. Ciafone, J., et al., *The Neuropsychological Profile of Mild Cognitive Impairment in Lewy Body Dementias.* J Int Neuropsychol Soc, 2020. **26**(2): p. 210-225.
164. Kemp, J., et al., *Cognitive profile in prodromal dementia with Lewy bodies.* Alzheimers Res Ther, 2017. **9**(1): p. 19.
165. Kondo, D., et al., *Characteristics of mild cognitive impairment tending to convert into Alzheimer's disease or dementia with Lewy bodies: A follow-up study in a memory clinic.* J Neurol Sci, 2016. **369**: p. 102-108.
166. Sakakibara, R., et al., *Amnestic mild cognitive impairment with low myocardial metaiodobenzylguanidine uptake.* Am J Neurodegener Dis, 2012. **1**(2): p. 146-51.
167. Fujishiro, H., et al., *Diffuse occipital hypometabolism on [18 F]-FDG PET scans in patients with idiopathic REM sleep behavior disorder: prodromal dementia with Lewy bodies?* Psychogeriatrics, 2010. **10**(3): p. 144-52.
168. Fujishiro, H., et al., *Early detection of dementia with Lewy bodies in patients with amnestic mild cognitive impairment using 123I-MIBG cardiac scintigraphy.* J Neurol Sci, 2012. **315**(1-2): p. 115-9.
169. Pao, W.C., et al., *Polysomnographic findings in dementia with Lewy bodies.* Neurologist, 2013. **19**(1): p. 1-6.
170. McCarter, S.J., et al., *REM sleep muscle activity in idiopathic REM sleep behavior disorder predicts phenoconversion.* Neurology, 2019. **93**(12): p. e1171-e1179.
171. Bonanni, L., et al., *Quantitative electroencephalogram utility in predicting conversion of mild cognitive impairment to dementia with Lewy bodies.* Neurobiol Aging, 2015. **36**(1): p. 434-45.
172. Blanc, F., et al., *Grey matter atrophy in prodromal stage of dementia with Lewy bodies and Alzheimer's disease.* Alzheimers Res Ther, 2016. **8**: p. 31.

173. Blanc, F., et al., *Cortical Thickness in Dementia with Lewy Bodies and Alzheimer's Disease: A Comparison of Prodromal and Dementia Stages.* PLoS One, 2015. **10**(6): p. e0127396.
174. Gore, R.L., E.R. Vardy, and J.T. O'Brien, *Delirium and dementia with Lewy bodies: distinct diagnoses or part of the same spectrum?* J Neurol Neurosurg Psychiatry, 2015. **86**(1): p. 50-9.
175. Sunwoo, M.K., et al., *alpha-Synuclein pathology is related to postoperative delirium in patients undergoing gastrectomy.* Neurology, 2013. **80**(9): p. 810-3.
176. Vardy, E., et al., *History of a suspected delirium is more common in dementia with Lewy bodies than Alzheimer's disease: a retrospective study.* Int J Geriatr Psychiatry, 2014. **29**(2): p. 178-81.
177. Iranzo, A., J. Santamaria, and E. Tolosa, *Idiopathic rapid eye movement sleep behaviour disorder: diagnosis, management, and the need for neuroprotective interventions.* Lancet Neurol, 2016. **15**(4): p. 405-19.
178. Ferman, T.J., et al., *Inclusion of RBD improves the diagnostic classification of dementia with Lewy bodies.* Neurology, 2011. **77**(9): p. 875-82.
179. Postuma, R.B., et al., *Risk and predictors of dementia and parkinsonism in idiopathic REM sleep behaviour disorder: a multicentre study.* Brain, 2019. **142**(3): p. 744-759.
180. Gagnon, J.F., et al., *Mild cognitive impairment in rapid eye movement sleep behavior disorder and Parkinson's disease.* Ann Neurol, 2009. **66**(1): p. 39-47.
181. Genier Marchand, D., et al., *Detecting the Cognitive Prodrome of Dementia with Lewy Bodies: A Prospective Study of REM Sleep Behavior Disorder.* Sleep, 2017. **40**(1).
182. Terzaghi, M., et al., *Cognitive performance in REM sleep behaviour disorder: a possible early marker of neurodegenerative disease?* Sleep Med, 2008. **9**(4): p. 343-51.
183. Postuma, R.B., et al., *How does parkinsonism start? Prodromal parkinsonism motor changes in idiopathic REM sleep behaviour disorder.* Brain, 2012. **135**(Pt 6): p. 1860-70.
184. Postuma, R.B., et al., *Prodromal autonomic symptoms and signs in Parkinson's disease and dementia with Lewy bodies.* Mov Disord, 2013. **28**(5): p. 597-604.
185. Kim, M.S., J.H. Yoon, and J.M. Hong, *Early differentiation of dementia with Lewy bodies and Alzheimer's disease: Heart rate variability at mild cognitive impairment stage.* Clin Neurophysiol, 2018. **129**(8): p. 1570-1578.
186. Sadiq, D., et al., *Prodromal Dementia with Lewy Bodies and Prodromal Alzheimer's Disease: A Comparison of the Cognitive and Clinical Profiles.* J Alzheimers Dis, 2017. **58**(2): p. 463-470.
187. Yoon, J.H., et al., *Olfactory function and neuropsychological profile to differentiate dementia with Lewy bodies from Alzheimer's disease in patients with mild cognitive impairment: A 5-year follow-up study.* J Neurol Sci, 2015. **355**(1-2): p. 174-9.
188. Donaghy, P.C., et al., *Symptoms associated with Lewy body disease in mild cognitive impairment.* Int J Geriatr Psychiatry, 2017. **32**(11): p. 1163-1171.
189. Jicha, G.A., et al., *Prodromal clinical manifestations of neuropathologically confirmed Lewy body disease.* Neurobiol Aging, 2010. **31**(10): p. 1805-13.
190. Molano, J., et al., *Mild cognitive impairment associated with limbic and neocortical Lewy body disease: a clinicopathological study.* Brain, 2010. **133**(Pt 2): p. 540-56.
191. Ferman, T.J., et al., *Pathology and temporal onset of visual hallucinations, misperceptions and family misidentification distinguishes dementia with Lewy bodies from Alzheimer's disease.* Parkinsonism Relat Disord, 2013. **19**(2): p. 227-31.
192. Belden, C.M., et al., *Clinical characterization of mild cognitive impairment as a prodrome to dementia with Lewy bodies.* Am J Alzheimers Dis Other Demen, 2015. **30**(2): p. 173-7.
193. Cormack, F., et al., *Pentagon drawing and neuropsychological performance in Dementia with Lewy Bodies, Alzheimer's disease, Parkinson's disease and Parkinson's disease with dementia.* Int J Geriatr Psychiatry, 2004. **19**(4): p. 371-7.
194. Cagnin, A., et al., *High specificity of MMSE pentagon scoring for diagnosis of prodromal dementia with Lewy bodies.* Parkinsonism Relat Disord, 2015. **21**(3): p. 303-5.
195. O'Dowd, S., et al., *Fluctuating cognition in the Lewy body dementias.* Brain, 2019. **142**(11): p. 3338-3350.
196. Erskine, D., et al., *Pathological Changes to the Subcortical Visual System and its Relationship to Visual Hallucinations in Dementia with Lewy Bodies.* Neurosci Bull, 2019. **35**(2): p. 295-300.

197. Toledo, J.B., et al., *Pathological alpha-synuclein distribution in subjects with coincident Alzheimer's and Lewy body pathology.* Acta Neuropathol, 2016. **131**(3): p. 393-409.
198. Tiraboschi, P., et al., *Clinicians' ability to diagnose dementia with Lewy bodies is not affected by beta-amyloid load.* Neurology, 2015. **84**(5): p. 496-9.
199. *Biomarkers and surrogate endpoints: preferred definitions and conceptual framework.* Clin Pharmacol Ther, 2001. **69**(3): p. 89-95.
200. McKeith, I., et al., *Sensitivity and specificity of dopamine transporter imaging with 123I-FP-CIT SPECT in dementia with Lewy bodies: a phase III, multicentre study.* Lancet Neurol, 2007. **6**(4): p. 305-13.
201. McCleery, J., et al., *Dopamine transporter imaging for the diagnosis of dementia with Lewy bodies.* Cochrane Database Syst Rev, 2015. **1**: p. Cd010633.
202. Nirenberg, M.J., et al., *The dopamine transporter is localized to dendritic and axonal plasma membranes of nigrostriatal dopaminergic neurons.* J Neurosci, 1996. **16**(2): p. 436-47.
203. Varrone, A. and C. Halldin, *Molecular imaging of the dopamine transporter.* J Nucl Med, 2010. **51**(9): p. 1331-4.
204. Fusar-Poli, P. and A. Meyer-Lindenberg, *Striatal presynaptic dopamine in schizophrenia, Part I: meta-analysis of dopamine active transporter (DAT) density.* Schizophr Bull, 2013. **39**(1): p. 22-32.
205. Ba, F. and W.R. Martin, *Dopamine transporter imaging as a diagnostic tool for parkinsonism and related disorders in clinical practice.* Parkinsonism Relat Disord, 2015. **21**(2): p. 87-94.
206. Cheng, H.C., C.M. Ulane, and R.E. Burke, *Clinical progression in Parkinson disease and the neurobiology of axons.* Ann Neurol, 2010. **67**(6): p. 715-25.
207. Iranzo, A., et al., *Decreased striatal dopamine transporter uptake and substantia nigra hyperechogenicity as risk markers of synucleinopathy in patients with idiopathic rapid-eye-movement sleep behaviour disorder: a prospective study [corrected].* Lancet Neurol, 2010. **9**(11): p. 1070-7.
208. Brooks, D.J., *Imaging approaches to Parkinson disease.* J Nucl Med, 2010. **51**(4): p. 596-609.
209. Booij, J., et al., *The clinical benefit of imaging striatal dopamine transporters with [123I]FP-CIT SPET in differentiating patients with presynaptic parkinsonism from those with other forms of parkinsonism.* Eur J Nucl Med, 2001. **28**(3): p. 266-72.
210. Benamer, T.S., et al., *Accurate differentiation of parkinsonism and essential tremor using visual assessment of [123I]-FP-CIT SPECT imaging: the [123I]-FP-CIT study group.* Mov Disord, 2000. **15**(3): p. 503-10.
211. Walker, Z., et al., *Striatal dopamine transporter in dementia with Lewy bodies and Parkinson disease: a comparison.* Neurology, 2004. **62**(9): p. 1568-72.
212. O'Brien, J.T., et al., *Dopamine transporter loss visualized with FP-CIT SPECT in the differential diagnosis of dementia with Lewy bodies.* Arch Neurol, 2004. **61**(6): p. 919-25.
213. Lloyd, J.J., et al., *A new visual rating scale for Ioflupane imaging in Lewy body disease.* NeuroImage: Clinical, 2018. **20**: p. 823-829.
214. Badiavas, K., et al., *SPECT imaging evaluation in movement disorders: far beyond visual assessment.* Eur J Nucl Med Mol Imaging, 2011. **38**(4): p. 764-73.
215. Darcourt, J., et al., *EANM procedure guidelines for brain neurotransmission SPECT using (123)I-labelled dopamine transporter ligands, version 2.* Eur J Nucl Med Mol Imaging, 2010. **37**(2): p. 443-50.
216. Karrer, T.M., et al., *Reduced dopamine receptors and transporters but not synthesis capacity in normal aging adults: a meta-analysis.* Neurobiol Aging, 2017. **57**: p. 36-46.
217. Pencharz, D.R., et al., *Automated quantification with BRASS reduces equivocal reporting of DaTSCAN (123I-FP-CIT) SPECT studies.* Nucl Med Rev Cent East Eur, 2014. **17**(2): p. 65-9.
218. Ueda, J., et al., *Combined visual and semi-quantitative assessment of (123)I-FP-CIT SPECT for the diagnosis of dopaminergic neurodegenerative diseases.* Neurol Sci, 2017. **38**(7): p. 1187-1191.
219. Ziebell, M., et al., *Predictive value of dopamine transporter SPECT imaging with [(1)(2)(3)I]PE2I in patients with subtle parkinsonian symptoms.* Eur J Nucl Med Mol Imaging, 2012. **39**(2): p. 242-50.
220. Ransmayr, G., et al., *Striatal dopamine transporter function in dementia with Lewy bodies and Parkinson's disease.* Eur J Nucl Med, 2001. **28**(10): p. 1523-8.

221. Siepel, F.J., et al., *(123I)FP-CIT SPECT in suspected dementia with Lewy bodies: a longitudinal case study.* BMJ Open, 2013. **3**(4).
222. O'Brien, J.T., et al., *Diagnostic accuracy of 123I-FP-CIT SPECT in possible dementia with Lewy bodies.* Br J Psychiatry, 2009. **194**(1): p. 34-9.
223. Ponsen, M.M., et al., *Idiopathic hyposmia as a preclinical sign of Parkinson's disease.* Ann Neurol, 2004. **56**(2): p. 173-81.
224. Fearnley, J.M. and A.J. Lees, *Ageing and Parkinson's disease: substantia nigra regional selectivity.* Brain, 1991. **114 (Pt 5)**: p. 2283-301.
225. van Dyck, C.H., et al., *Age-related decline in dopamine transporters: analysis of striatal subregions, nonlinear effects, and hemispheric asymmetries.* Am J Geriatr Psychiatry, 2002. **10**(1): p. 36-43.
226. Matsuda, H., et al., *Japanese multicenter database of healthy controls for [(123)I]FP-CIT SPECT.* Eur J Nucl Med Mol Imaging, 2018. **45**(8): p. 1405-1416.
227. Varrone, A., et al., *European multicentre database of healthy controls for [123I]FP-CIT SPECT (ENC-DAT): age-related effects, gender differences and evaluation of different methods of analysis.* Eur J Nucl Med Mol Imaging, 2013. **40**(2): p. 213-27.
228. Nobili, F., et al., *Automatic semi-quantification of [123I]FP-CIT SPECT scans in healthy volunteers using BasGan version 2: results from the ENC-DAT database.* Eur J Nucl Med Mol Imaging, 2013. **40**(4): p. 565-73.
229. Koch, W., et al., *Extended studies of the striatal uptake of 99mTc-NC100697 in healthy volunteers.* J Nucl Med, 2007. **48**(1): p. 27-34.
230. Morrish, P.K., et al., *Measuring the rate of progression and estimating the preclinical period of Parkinson's disease with [18F]dopa PET.* J Neurol Neurosurg Psychiatry, 1998. **64**(3): p. 314-9.
231. Nurmi, E., et al., *Progression of dopaminergic hypofunction in striatal subregions in Parkinson's disease using [18F]CFT PET.* Synapse, 2003. **48**(3): p. 109-15.
232. Nurmi, E., et al., *Progression in Parkinson's disease: a positron emission tomography study with a dopamine transporter ligand [18F]CFT.* Ann Neurol, 2000. **47**(6): p. 804-8.
233. Nurmi, E., et al., *Rate of progression in Parkinson's disease: a 6-[18F]fluoro-L-dopa PET study.* Mov Disord, 2001. **16**(4): p. 608-15.
234. Fahn, S., et al., *Levodopa and the progression of Parkinson's disease.* N Engl J Med, 2004. **351**(24): p. 2498-508.
235. Jeong, E.H., M.K. Sunwoo, and Y.S. Song, *Serial I-123-FP-CIT SPECT Image Findings of Parkinson's Disease Patients With Levodopa-Induced Dyskinesia.* Front Neurol, 2018. **9**: p. 1133.
236. *Dopamine transporter brain imaging to assess the effects of pramipexole vs levodopa on Parkinson disease progression.* Jama, 2002. **287**(13): p. 1653-61.
237. Pirker, W., et al., *Progression of dopaminergic degeneration in Parkinson's disease and atypical parkinsonism: a longitudinal beta-CIT SPECT study.* Mov Disord, 2002. **17**(1): p. 45-53.
238. Pirker, W., et al., *Measuring the rate of progression of Parkinson's disease over a 5-year period with beta-CIT SPECT.* Mov Disord, 2003. **18**(11): p. 1266-72.
239. Li, Y., et al., *Predictive markers for early conversion of iRBD to neurodegenerative synucleinopathy diseases.* Neurology, 2017. **88**(16): p. 1493-1500.
240. Iranzo, A., et al., *Serial dopamine transporter imaging of nigrostriatal function in patients with idiopathic rapid-eye-movement sleep behaviour disorder: a prospective study.* Lancet Neurol, 2011. **10**(9): p. 797-805.
241. Jennings, D., et al., *Conversion to Parkinson Disease in the PARS Hyposmic and Dopamine Transporter-Deficit Prodromal Cohort.* JAMA Neurol, 2017. **74**(8): p. 933-940.
242. Chouker, M., et al., *Striatal dopamine transporter binding in early to moderately advanced Parkinson's disease: monitoring of disease progression over 2 years.* Nucl Med Commun, 2001. **22**(6): p. 721-5.
243. Marek, K., et al., *[123I]beta-CIT SPECT imaging assessment of the rate of Parkinson's disease progression.* Neurology, 2001. **57**(11): p. 2089-94.
244. Staffen, W., et al., *Measuring the progression of idiopathic Parkinson's disease with [123I] beta-CIT SPECT.* J Neural Transm (Vienna), 2000. **107**(5): p. 543-52.

245. Winogrodzka, A., et al., *[(123)I]beta-CIT SPECT is a useful method for monitoring dopaminergic degeneration in early stage Parkinson's disease.* J Neurol Neurosurg Psychiatry, 2003. **74**(3): p. 294-8.
246. Jung, Y., et al., *Clinicopathological and (123)I-FP-CIT SPECT correlations in patients with dementia.* Ann Clin Transl Neurol, 2018. **5**(3): p. 376-381.
247. Colloby, S.J., et al., *Neuropathological correlates of dopaminergic imaging in Alzheimer's disease and Lewy body dementias.* Brain, 2012. **135**(Pt 9): p. 2798-808.
248. Walker, Z., et al., *Dementia with Lewy bodies: a comparison of clinical diagnosis, FP-CIT single photon emission computed tomography imaging and autopsy.* J Neurol Neurosurg Psychiatry, 2007. **78**(11): p. 1176-81.
249. Litvan, I., et al., *Movement Disorders Society Scientific Issues Committee report: SIC Task Force appraisal of clinical diagnostic criteria for Parkinsonian disorders.* Mov Disord, 2003. **18**(5): p. 467-86.
250. Verghese, J., et al., *Validity of clinical criteria for the diagnosis of dementia with Lewy bodies.* Neurology, 1999. **53**(9): p. 1974-82.
251. Ceravolo, R., et al., *Dopaminergic degeneration and perfusional impairment in Lewy body dementia and Alzheimer's disease.* Neurol Sci, 2003. **24**(3): p. 162-3.
252. Kemp, P.M., K. Clyde, and C. Holmes, *Impact of 123I-FP-CIT (DaTSCAN) SPECT on the diagnosis and management of patients with dementia with Lewy bodies: a retrospective study.* Nucl Med Commun, 2011. **32**(4): p. 298-302.
253. Spehl, T.S., et al., *Role of semiquantitative assessment of regional binding potential in 123I-FP-CIT SPECT for the differentiation of frontotemporal dementia, dementia with Lewy bodies, and Alzheimer's dementia.* Clin Nucl Med, 2015. **40**(1): p. e27-33.
254. Walker, R.W. and Z. Walker, *Dopamine transporter single photon emission computerized tomography in the diagnosis of dementia with Lewy bodies.* Mov Disord, 2009. **24 Suppl 2**: p. S754-9.
255. Papathanasiou, N.D., et al., *Diagnostic accuracy of (1)(2)(3)I-FP-CIT (DaTSCAN) in dementia with Lewy bodies: a meta-analysis of published studies.* Parkinsonism Relat Disord, 2012. **18**(3): p. 225-9.
256. Marek, K., et al., *Longitudinal follow-up of SWEDD subjects in the PRECEPT Study.* Neurology, 2014. **82**(20): p. 1791-7.
257. Marek, K.L., et al., *[123I] beta-CIT/SPECT imaging demonstrates bilateral loss of dopamine transporters in hemi-Parkinson's disease.* Neurology, 1996. **46**(1): p. 231-7.
258. Donnemiller, E., et al., *Brain perfusion scintigraphy with 99mTc-HMPAO or 99mTc-ECD and 123I-beta-CIT single-photon emission tomography in dementia of the Alzheimer-type and diffuse Lewy body disease.* Eur J Nucl Med, 1997. **24**(3): p. 320-5.
259. Walker, Z., et al., *Differentiation of dementia with Lewy bodies from Alzheimer's disease using a dopaminergic presynaptic ligand.* J Neurol Neurosurg Psychiatry, 2002. **73**(2): p. 134-40.
260. Ceravolo, R., et al., *Presynaptic nigro-striatal function in a group of Alzheimer's disease patients with parkinsonism: evidence from a dopamine transporter imaging study.* J Neural Transm (Vienna), 2004. **111**(8): p. 1065-73.
261. Colloby, S.J., et al., *A comparison of 99mTc-exametazime and 123I-FP-CIT SPECT imaging in the differential diagnosis of Alzheimer's disease and dementia with Lewy bodies.* Int Psychogeriatr, 2008. **20**(6): p. 1124-40.
262. Morgan, S., et al., *Differentiation of frontotemporal dementia from dementia with Lewy bodies using FP-CIT SPECT.* J Neurol Neurosurg Psychiatry, 2012. **83**(11): p. 1063-70.
263. Shimizu, S., et al., *Correlation between clinical symptoms and striatal DAT uptake in patients with DLB.* Ann Nucl Med, 2017. **31**(5): p. 390-398.
264. Siepel, F.J., et al., *Loss of Dopamine Transporter Binding and Clinical Symptoms in Dementia With Lewy Bodies.* Mov Disord, 2016. **31**(1): p. 118-25.
265. Shimizu, S., et al., *Utility of the combination of DAT SPECT and MIBG myocardial scintigraphy in differentiating dementia with Lewy bodies from Alzheimer's disease.* Eur J Nucl Med Mol Imaging, 2016. **43**(1): p. 184-92.
266. Thomas, A.J., et al., *Diagnostic accuracy of dopaminergic imaging in prodromal dementia with Lewy bodies.* Psychol Med, 2018: p. 1-7.

267. Albin, R.L., et al., *Assessing mild cognitive impairment with amyloid and dopamine terminal molecular imaging.* J Nucl Med, 2013. **54**(6): p. 887-93.
268. Meles, S.K., et al., *FDG PET, dopamine transporter SPECT, and olfaction: Combining biomarkers in REM sleep behavior disorder.* Mov Disord, 2017.
269. Iranzo, A., et al., *Five-year follow-up of substantia nigra echogenicity in idiopathic REM sleep behavior disorder.* Mov Disord, 2014. **29**(14): p. 1774-80.
270. Zaccai, J., et al., *Patterns and stages of alpha-synucleinopathy: Relevance in a population-based cohort.* Neurology, 2008. **70**(13): p. 1042-8.
271. Dewey, M., T. Schink, and C.F. Dewey, *Claustrophobia during magnetic resonance imaging: cohort study in over 55,000 patients.* J Magn Reson Imaging, 2007. **26**(5): p. 1322-7.
272. Eshed, I., et al., *Claustrophobia and premature termination of magnetic resonance imaging examinations.* J Magn Reson Imaging, 2007. **26**(2): p. 401-4.
273. Scheltens, P., et al., *Visual assessment of medial temporal lobe atrophy on magnetic resonance imaging: interobserver reliability.* J Neurol, 1995. **242**(9): p. 557-60.
274. Koedam, E.L., et al., *Visual assessment of posterior atrophy development of a MRI rating scale.* Eur Radiol, 2011. **21**(12): p. 2618-25.
275. Pasquier, F., et al., *Inter- and intraobserver reproducibility of cerebral atrophy assessment on MRI scans with hemispheric infarcts.* Eur Neurol, 1996. **36**(5): p. 268-72.
276. Fazekas, F., et al., *Pathologic correlates of incidental MRI white matter signal hyperintensities.* Neurology, 1993. **43**(9): p. 1683-9.
277. Ashburner, J., *A fast diffeomorphic image registration algorithm.* Neuroimage, 2007. **38**(1): p. 95-113.
278. Whitwell, J.L., et al., *Focal atrophy in dementia with Lewy bodies on MRI: a distinct pattern from Alzheimer's disease.* Brain, 2007. **130**(Pt 3): p. 708-19.
279. Kantarci, K., et al., *Multimodality imaging characteristics of dementia with Lewy bodies.* Neurobiol Aging, 2012. **33**(9): p. 2091-105.
280. Sabattoli, F., et al., *Hippocampal shape differences in dementia with Lewy bodies.* Neuroimage, 2008. **41**(3): p. 699-705.
281. Burton, E.J., et al., *Medial temporal lobe atrophy on MRI differentiates Alzheimer's disease from dementia with Lewy bodies and vascular cognitive impairment: a prospective study with pathological verification of diagnosis.* Brain, 2009. **132**(Pt 1): p. 195-203.
282. Harper, L., et al., *MRI visual rating scales in the diagnosis of dementia: evaluation in 184 post-mortem confirmed cases.* Brain, 2016. **139**(Pt 4): p. 1211-25.
283. Bobinski, M., et al., *Neuronal and volume loss in CA1 of the hippocampal formation uniquely predicts duration and severity of Alzheimer disease.* Brain Res, 1998. **805**(1-2): p. 267-9.
284. Hayashi, H., et al., *Application of the VSRAD, a specific and sensitive voxel-based morphometry, to comparison of entorhinal cortex atrophy between dementia with Lewy bodies and Alzheimer's disease.* Dement Geriatr Cogn Disord, 2012. **34**(5-6): p. 328-31.
285. Mak, E., et al., *Differential Atrophy of Hippocampal Subfields: A Comparative Study of Dementia with Lewy Bodies and Alzheimer Disease.* Am J Geriatr Psychiatry, 2016. **24**(2): p. 136-43.
286. Delli Pizzi, S., et al., *Atrophy of hippocampal subfields and adjacent extrahippocampal structures in dementia with Lewy bodies and Alzheimer's disease.* Neurobiol Aging, 2016. **40**: p. 103-109.
287. Firbank, M.J., et al., *High resolution imaging of the medial temporal lobe in Alzheimer's disease and dementia with Lewy bodies.* J Alzheimers Dis, 2010. **21**(4): p. 1129-40.
288. Chow, N., et al., *Comparing hippocampal atrophy in Alzheimer's dementia and dementia with lewy bodies.* Dement Geriatr Cogn Disord, 2012. **34**(1): p. 44-50.
289. Barber, R., et al., *Volumetric MRI study of the caudate nucleus in patients with dementia with Lewy bodies, Alzheimer's disease, and vascular dementia.* J Neurol Neurosurg Psychiatry, 2002. **72**(3): p. 406-7.
290. Almeida, O.P., et al., *MRI study of caudate nucleus volume in Parkinson's disease with and without dementia with Lewy bodies and Alzheimer's disease.* Dement Geriatr Cogn Disord, 2003. **16**(2): p. 57-63.

291. Goto, H., et al., *Differential diagnosis of dementia with Lewy Bodies and Alzheimer Disease using combined MR imaging and brain perfusion single-photon emission tomography.* AJNR Am J Neuroradiol, 2010. **31**(4): p. 720-5.
292. Watson, R., et al., *Patterns of gray matter atrophy in dementia with Lewy bodies: a voxel-based morphometry study.* Int Psychogeriatr, 2012. **24**(4): p. 532-40.
293. Mak, E., et al., *Progressive cortical thinning and subcortical atrophy in dementia with Lewy bodies and Alzheimer's disease.* Neurobiol Aging, 2015. **36**(4): p. 1743-1750.
294. Mak, E., et al., *Multi-modal MRI investigation of volumetric and microstructural changes in the hippocampus and its subfields in mild cognitive impairment, Alzheimer's disease, and dementia with Lewy bodies.* Int Psychogeriatr, 2017. **29**(4): p. 545-555.
295. Elder, G.J., et al., *The influence of hippocampal atrophy on the cognitive phenotype of dementia with Lewy bodies.* Int J Geriatr Psychiatry, 2017. **32**(11): p. 1182-1189.
296. Shimizu, S., et al., *Neuroimaging for diagnosing dementia with Lewy bodies: What is the best neuroimaging technique in discriminating dementia with Lewy bodies from Alzheimer's disease?* Geriatr Gerontol Int, 2017. **17**(5): p. 819-824.
297. Fox, N.C., et al., *Imaging of onset and progression of Alzheimer's disease with voxel-compression mapping of serial magnetic resonance images.* Lancet, 2001. **358**(9277): p. 201-5.
298. Bradley, K.M., et al., *Serial brain MRI at 3-6 month intervals as a surrogate marker for Alzheimer's disease.* Br J Radiol, 2002. **75**(894): p. 506-13.
299. Schott, J.M., et al., *Measuring atrophy in Alzheimer disease: a serial MRI study over 6 and 12 months.* Neurology, 2005. **65**(1): p. 119-24.
300. Mak, E., et al., *Longitudinal assessment of global and regional atrophy rates in Alzheimer's disease and dementia with Lewy bodies.* Neuroimage Clin, 2015. **7**: p. 456-62.
301. Evans, M.C., et al., *Volume changes in Alzheimer's disease and mild cognitive impairment: cognitive associations.* Eur Radiol, 2010. **20**(3): p. 674-82.
302. Whitwell, J.L., et al., *Rates of cerebral atrophy differ in different degenerative pathologies.* Brain, 2007. **130**(Pt 4): p. 1148-58.
303. Watson, R., et al., *Subcortical volume changes in dementia with Lewy bodies and Alzheimer's disease. A comparison with healthy aging.* Int Psychogeriatr, 2016. **28**(4): p. 529-36.
304. O'Brien, J.T., et al., *Progressive brain atrophy on serial MRI in dementia with Lewy bodies, AD, and vascular dementia.* Neurology, 2001. **56**(10): p. 1386-8.
305. Nedelska, Z., et al., *Pattern of brain atrophy rates in autopsy-confirmed dementia with Lewy bodies.* Neurobiol Aging, 2015. **36**(1): p. 452-61.
306. Dickerson, B.C., et al., *The cortical signature of Alzheimer's disease: regionally specific cortical thinning relates to symptom severity in very mild to mild AD dementia and is detectable in asymptomatic amyloid-positive individuals.* Cereb Cortex, 2009. **19**(3): p. 497-510.
307. Watson, R., et al., *Assessment of regional gray matter loss in dementia with Lewy bodies: a surface-based MRI analysis.* Am J Geriatr Psychiatry, 2015. **23**(1): p. 38-46.
308. Lebedev, A.V., et al., *Multivariate classification of patients with Alzheimer's and dementia with Lewy bodies using high-dimensional cortical thickness measurements: an MRI surface-based morphometric study.* J Neurol, 2013. **260**(4): p. 1104-15.
309. van der Zande, J.J., et al., *Gray matter atrophy in dementia with Lewy bodies with and without concomitant Alzheimer's disease pathology.* Neurobiol Aging, 2018. **71**: p. 171-178.
310. Lee, Y.G., et al., *Amyloid-beta-related and unrelated cortical thinning in dementia with Lewy bodies.* Neurobiol Aging, 2018. **72**: p. 32-39.
311. Shimada, H., et al., *beta-Amyloid in Lewy body disease is related to Alzheimer's disease-like atrophy.* Mov Disord, 2013. **28**(2): p. 169-75.
312. Yousaf, T., et al., *Neuroimaging in Lewy body dementia.* J Neurol, 2019. **266**(1): p. 1-26.
313. Burton, E.J., et al., *Cerebral atrophy in Parkinson's disease with and without dementia: a comparison with Alzheimer's disease, dementia with Lewy bodies and controls.* Brain, 2004. **127**(Pt 4): p. 791-800.
314. Beyer, M.K., J.P. Larsen, and D. Aarsland, *Gray matter atrophy in Parkinson disease with dementia and dementia with Lewy bodies.* Neurology, 2007. **69**(8): p. 747-54.

315. Lee, J.E., et al., *A comparison of gray and white matter density in patients with Parkinson's disease dementia and dementia with Lewy bodies using voxel-based morphometry.* Mov Disord, 2010. **25**(1): p. 28-34.
316. Tam, C.W., et al., *Temporal lobe atrophy on MRI in Parkinson disease with dementia: a comparison with Alzheimer disease and dementia with Lewy bodies.* Neurology, 2005. **64**(5): p. 861-5.
317. Joki, H., et al., *White matter hyperintensities on MRI in dementia with Lewy bodies, Parkinson's disease with dementia, and Alzheimer's disease.* J Neurol Sci, 2018. **385**: p. 99-104.
318. Barber, R., et al., *MRI volumetric correlates of white matter lesions in dementia with Lewy bodies and Alzheimer's disease.* Int J Geriatr Psychiatry, 2000. **15**(10): p. 911-6.
319. Burton, E.J., et al., *Patterns of cerebral atrophy in dementia with Lewy bodies using voxel-based morphometry.* Neuroimage, 2002. **17**(2): p. 618-30.
320. Ballmaier, M., et al., *Comparing gray matter loss profiles between dementia with Lewy bodies and Alzheimer's disease using cortical pattern matching: diagnosis and gender effects.* Neuroimage, 2004. **23**(1): p. 325-35.
321. Ishii, K., et al., *Comparison of regional brain volume and glucose metabolism between patients with mild dementia with lewy bodies and those with mild Alzheimer's disease.* J Nucl Med, 2007. **48**(5): p. 704-11.
322. Sanchez-Castaneda, C., et al., *Correlations between gray matter reductions and cognitive deficits in dementia with Lewy Bodies and Parkinson's disease with dementia.* Mov Disord, 2009. **24**(12): p. 1740-6.
323. Sanchez-Castaneda, C., et al., *Frontal and associative visual areas related to visual hallucinations in dementia with Lewy bodies and Parkinson's disease with dementia.* Mov Disord, 2010. **25**(5): p. 615-22.
324. Takahashi, R., et al., *Measurement of gray and white matter atrophy in dementia with Lewy bodies using diffeomorphic anatomic registration through exponentiated lie algebra: A comparison with conventional voxel-based morphometry.* AJNR Am J Neuroradiol, 2010. **31**(10): p. 1873-8.
325. Kim, H.J., et al., *Analysis of the substantia innominata volume in patients with Parkinson's disease with dementia, dementia with lewy bodies, and Alzheimer's disease.* J Mov Disord, 2011. **4**(2): p. 68-72.
326. Rodriguez, M.J., et al., *Cognitive and structural magnetic resonance imaging features of Lewy body dementia and Alzheimer's disease.* Alzheimers Dement, 2012. **8**(3): p. 211-8.
327. O'Donovan, J., et al., *Does posterior cortical atrophy on MRI discriminate between Alzheimer's disease, dementia with Lewy bodies, and normal aging?* Int Psychogeriatr, 2013. **25**(1): p. 111-9.
328. Colloby, S.J., J.T. O'Brien, and J.P. Taylor, *Patterns of cerebellar volume loss in dementia with Lewy bodies and Alzheimers disease: A VBM-DARTEL study.* Psychiatry Res, 2014. **223**(3): p. 187-91.
329. Grothe, M.J., et al., *Atrophy of the cholinergic basal forebrain in dementia with Lewy bodies and Alzheimer's disease dementia.* J Neurol, 2014. **261**(10): p. 1939-48.
330. Tagawa, R., et al., *The Relationship Between Medial Temporal Lobe Atrophy and Cognitive Impairment in Patients With Dementia With Lewy Bodies.* J Geriatr Psychiatry Neurol, 2015. **28**(4): p. 249-54.
331. Colloby, S.J., et al., *Multimodal EEG-MRI in the differential diagnosis of Alzheimer's disease and dementia with Lewy bodies.* J Psychiatr Res, 2016. **78**: p. 48-55.
332. Colloby, S.J., et al., *Structural grey matter changes in the substantia innominata in Alzheimer's disease and dementia with Lewy bodies: a DARTEL-VBM study.* Int J Geriatr Psychiatry, 2017. **32**(6): p. 615-623.
333. Gazzina, S., et al., *Subcortical matter in the alpha-synucleinopathies spectrum: an MRI pilot study.* J Neurol, 2016. **263**(8): p. 1575-82.
334. Sarro, L., et al., *Amyloid-beta deposition and regional grey matter atrophy rates in dementia with Lewy bodies.* Brain, 2016. **139**(Pt 10): p. 2740-2750.
335. Watson, R., et al., *Does attentional dysfunction and thalamic atrophy predict decline in dementia with Lewy bodies?* Parkinsonism Relat Disord, 2017. **45**: p. 69-74.
336. Wardlaw, J.M., et al., *Neuroimaging standards for research into small vessel disease and its contribution to ageing and neurodegeneration.* Lancet Neurol, 2013. **12**(8): p. 822-38.

337. McAleese, K.E., et al., *Parietal white matter lesions in Alzheimer's disease are associated with cortical neurodegenerative pathology, but not with small vessel disease.* Acta Neuropathol, 2017. **134**(3): p. 459-473.
338. Fazekas, F., et al., *MR signal abnormalities at 1.5 T in Alzheimer's dementia and normal aging.* AJR Am J Roentgenol, 1987. **149**(2): p. 351-6.
339. Wahlund, L.O., et al., *A new rating scale for age-related white matter changes applicable to MRI and CT.* Stroke, 2001. **32**(6): p. 1318-22.
340. Scheltens, P., et al., *A semiquantative rating scale for the assessment of signal hyperintensities on magnetic resonance imaging.* J Neurol Sci, 1993. **114**(1): p. 7-12.
341. Wardlaw, J.M., K.J. Ferguson, and C. Graham, *White matter hyperintensities and rating scales-observer reliability varies with lesion load.* J Neurol, 2004. **251**(5): p. 584-90.
342. van den Heuvel, D.M., et al., *Measuring longitudinal white matter changes: comparison of a visual rating scale with a volumetric measurement.* AJNR Am J Neuroradiol, 2006. **27**(4): p. 875-8.
343. Oppedal, K., et al., *White matter hyperintensities in mild lewy body dementia.* Dement Geriatr Cogn Dis Extra, 2012. **2**(1): p. 481-95.
344. Burton, E.J., et al., *Progression of white matter hyperintensities in Alzheimer disease, dementia with lewy bodies, and Parkinson disease dementia: a comparison with normal aging.* Am J Geriatr Psychiatry, 2006. **14**(10): p. 842-9.
345. van Straaten, E.C., et al., *Periventricular white matter hyperintensities increase the likelihood of progression from amnestic mild cognitive impairment to dementia.* J Neurol, 2008. **255**(9): p. 1302-8.
346. De Reuck, J., et al., *Post-mortem 7.0-tesla magnetic resonance study of cortical microinfarcts in neurodegenerative diseases and vascular dementia with neuropathological correlates.* J Neurol Sci, 2014. **346**(1-2): p. 85-9.
347. Ballard, C., et al., *Neurocardiovascular instability, hypotensive episodes, and MRI lesions in neurodegenerative dementia.* Ann N Y Acad Sci, 2000. **903**: p. 442-5.
348. Fukui, T., et al., *Prevalence and clinical implication of microbleeds in dementia with lewy bodies in comparison with microbleeds in Alzheimer's disease.* Dement Geriatr Cogn Dis Extra, 2013. **3**(1): p. 148-60.
349. Nakatsuka, T., et al., *Discrimination of dementia with Lewy bodies from Alzheimer's disease using voxel-based morphometry of white matter by statistical parametric mapping 8 plus diffeomorphic anatomic registration through exponentiated Lie algebra.* Neuroradiology, 2013. **55**(5): p. 559-66.
350. Park, H.E., et al., *Subcortical whiter matter hyperintensities within the cholinergic pathways of patients with dementia and parkinsonism.* J Neurol Sci, 2015. **353**(1-2): p. 44-8.
351. Gungor, I., et al., *Frequency and topography of cerebral microbleeds in dementia with Lewy bodies compared to Alzheimer's disease.* Parkinsonism Relat Disord, 2015. **21**(9): p. 1101-4.
352. Kim, S.W., et al., *Cerebral Microbleeds in Patients with Dementia with Lewy Bodies and Parkinson Disease Dementia.* AJNR Am J Neuroradiol, 2015. **36**(9): p. 1642-7.
353. Takemoto, M., et al., *Different Clinical and Neuroimaging Characteristics in Early Stage Parkinson's Disease with Dementia and Dementia with Lewy Bodies.* J Alzheimers Dis, 2016. **52**(1): p. 205-11.
354. Sarro, L., et al., *An investigation of cerebrovascular lesions in dementia with Lewy bodies compared to Alzheimer's disease.* Alzheimers Dement, 2017. **13**(3): p. 257-266.
355. Kantarci, K., et al., *Dementia with Lewy bodies and Alzheimer disease: neurodegenerative patterns characterized by DTI.* Neurology, 2010. **74**(22): p. 1814-21.
356. Bozzali, M., et al., *Brain tissue damage in dementia with Lewy bodies: an in vivo diffusion tensor MRI study.* Brain, 2005. **128**(Pt 7): p. 1595-604.
357. Lee, J.E., et al., *A comparative analysis of cognitive profiles and white-matter alterations using voxel-based diffusion tensor imaging between patients with Parkinson's disease dementia and dementia with Lewy bodies.* J Neurol Neurosurg Psychiatry, 2010. **81**(3): p. 320-6.
358. Ota, M., et al., *Degeneration of dementia with Lewy bodies measured by diffusion tensor imaging.* NMR Biomed, 2009. **22**(3): p. 280-4.
359. Watson, R., et al., *Characterizing dementia with Lewy bodies by means of diffusion tensor imaging.* Neurology, 2012. **79**(9): p. 906-14.

360. Barkhof, F., et al., *The significance of medial temporal lobe atrophy: a postmortem MRI study in the very old.* Neurology, 2007. **69**(15): p. 1521-7.
361. Petrou, M., et al., *Amyloid deposition in Parkinson's disease and cognitive impairment: a systematic review.* Mov Disord, 2015. **30**(7): p. 928-35.
362. Vemuri, P., et al., *Antemortem differential diagnosis of dementia pathology using structural MRI: Differential-STAND.* Neuroimage, 2011. **55**(2): p. 522-31.
363. Kantarci, K., et al., *Focal atrophy on MRI and neuropathologic classification of dementia with Lewy bodies.* Neurology, 2012. **79**(6): p. 553-60.
364. Burton, E.J., et al., *Neuropathological correlates of volumetric MRI in autopsy-confirmed Lewy body dementia.* Neurobiol Aging, 2012. **33**(7): p. 1228-36.
365. De Reuck, J.L., et al., *The significance of cortical cerebellar microbleeds and microinfarcts in neurodegenerative and cerebrovascular diseases. A post-mortem 7.0-tesla magnetic resonance study with neuropathological correlates.* Cerebrovasc Dis, 2015. **39**(2): p. 138-43.
366. Graff-Radford, J., et al., *Predicting Survival in Dementia With Lewy Bodies With Hippocampal Volumetry.* Mov Disord, 2016. **31**(7): p. 989-94.
367. Roquet, D., et al., *Insular atrophy at the prodromal stage of dementia with Lewy bodies: a VBM DARTEL study.* Sci Rep, 2017. **7**(1): p. 9437.
368. Kantarci, K., et al., *Hippocampal volumes predict risk of dementia with Lewy bodies in mild cognitive impairment.* Neurology, 2016. **87**(22): p. 2317-2323.
369. Honig, L.S., et al., *Trial of Solanezumab for Mild Dementia Due to Alzheimer's Disease.* N Engl J Med, 2018. **378**(4): p. 321-330.
370. Health, D.o., *Mental Health Clustering (v3.0).* London: Department of Health, 2013.
371. Miller, M.D., et al., *Rating chronic medical illness burden in geropsychiatric practice and research: application of the Cumulative Illness Rating Scale.* Psychiatry Res, 1992. **41**(3): p. 237-48.
372. Mosimann, U.P., et al., *A semi-structured interview to assess visual hallucinations in older people.* Int J Geriatr Psychiatry, 2008. **23**(7): p. 712-8.
373. Johns, M.W., *A new method for measuring daytime sleepiness: the Epworth sleepiness scale.* Sleep, 1991. **14**(6): p. 540-5.
374. D'Ath, P., et al., *Screening, detection and management of depression in elderly primary care attenders. I: The acceptability and performance of the 15 item Geriatric Depression Scale (GDS15) and the development of short versions.* Fam Pract, 1994. **11**(3): p. 260-6.
375. Almeida, O.P. and S.A. Almeida, *Short versions of the geriatric depression scale: a study of their validity for the diagnosis of a major depressive episode according to ICD-10 and DSM-IV.* Int J Geriatr Psychiatry, 1999. **14**(10): p. 858-65.
376. *Lewy Body Dementia Association: Comprehensive Lewy Body Dementia Symptom Checklist. Available at:*

www.lbda.org/sites/default/files/2013_comprehensive_lbd_symptom_checklist.pdf (Accessed: 23/10/2018). 2014.

377. Goetz, C.G., et al., *Movement Disorder Society-sponsored revision of the Unified Parkinson's Disease Rating Scale (MDS-UPDRS): scale presentation and clinimetric testing results.* Mov Disord, 2008. **23**(15): p. 2129-70.
378. Sletten, D.M., et al., *COMPASS 31: a refined and abbreviated Composite Autonomic Symptom Score.* Mayo Clin Proc, 2012. **87**(12): p. 1196-201.
379. Mioshi, E., et al., *The Addenbrooke's Cognitive Examination Revised (ACE-R): a brief cognitive test battery for dementia screening.* Int J Geriatr Psychiatry, 2006. **21**(11): p. 1078-85.
380. Barry, D., M.E. Bates, and E. Labouvie, *FAS and CFL forms of verbal fluency differ in difficulty: a meta-analytic study.* Appl Neuropsychol, 2008. **15**(2): p. 97-106.
381. Mckenna, P. and E.K. Warrington, *Graded naming test: object picture book. 2nd rev. edn Cambridge: Cambridge Cognition Ltd.* 2007.
382. Rey, A., *L'examen clinique en psychologie [the clinical psychological examination] Paris: Presses Universitaires de France.* 1964.
383. Folstein, M.F., L.N. Robins, and J.E. Helzer, *The Mini-Mental State Examination.* Arch Gen Psychiatry, 1983. **40**(7): p. 812.

384. Nelson, H.E., *National Adult Reading Test (NART): For the assessment of premorbid intelligence in patients with dementia: Test manual. Windsor: NFER-Nelson.* 1982.
385. Cummings, J.L., et al., *The Neuropsychiatric Inventory: comprehensive assessment of psychopathology in dementia.* Neurology, 1994. **44**(12): p. 2308-14.
386. Lee, D.R., et al., *The dementia cognitive fluctuation scale, a new psychometric test for clinicians to identify cognitive fluctuations in people with dementia.* Am J Geriatr Psychiatry, 2014. **22**(9): p. 926-35.
387. Walker, M.P., et al., *The Clinician Assessment of Fluctuation and the One Day Fluctuation Assessment Scale. Two methods to assess fluctuating confusion in dementia.* Br J Psychiatry, 2000. **177**: p. 252-6.
388. Graf, C., *The Lawton instrumental activities of daily living scale.* Am J Nurs, 2008. **108**(4): p. 52-62; quiz 62-3.
389. Hughes, C.P., et al., *A new clinical scale for the staging of dementia.* Br J Psychiatry, 1982. **140**: p. 566-72.
390. Wood, J.S., et al., *Testing visual perception in dementia with Lewy bodies and Alzheimer disease.* Am J Geriatr Psychiatry, 2013. **21**(6): p. 501-8.
391. Roberts, G., et al., *A comparison of visual and semiquantitative analysis methods for planar cardiac 123I-MIBG scintigraphy in dementia with Lewy bodies.* Nucl Med Commun, 2019. **40**(7): p. 734-743.
392. Roberts, G., et al., *Cardiac (123)I-MIBG normal uptake values are population-specific: Results from a cohort of controls over 60 years of age.* J Nucl Cardiol, 2019.
393. Bates, D., et al., *Fitting linear mixed-effects models using lme4.* Journal of Statistical Software, 2015. **67**(1): p. 1-48.
394. Dale, A.M., B. Fischl, and M.I. Sereno, *Cortical surface-based analysis. I. Segmentation and surface reconstruction.* Neuroimage, 1999. **9**(2): p. 179-94.
395. Fischl, B. and A.M. Dale, *Measuring the thickness of the human cerebral cortex from magnetic resonance images.* Proc Natl Acad Sci U S A, 2000. **97**(20): p. 11050-5.
396. Fischl, B., et al., *Automatically parcellating the human cerebral cortex.* Cereb Cortex, 2004. **14**(1): p. 11-22.
397. Desikan, R.S., et al., *An automated labeling system for subdividing the human cerebral cortex on MRI scans into gyral based regions of interest.* Neuroimage, 2006. **31**(3): p. 968-80.
398. Fischl, B., et al., *Whole brain segmentation: automated labeling of neuroanatomical structures in the human brain.* Neuron, 2002. **33**(3): p. 341-55.
399. Buckner, R.L., et al., *A unified approach for morphometric and functional data analysis in young, old, and demented adults using automated atlas-based head size normalization: reliability and validation against manual measurement of total intracranial volume.* Neuroimage, 2004. **23**(2): p. 724-38.
400. Iglesias, J.E., et al., *Bayesian segmentation of brainstem structures in MRI.* Neuroimage, 2015. **113**: p. 184-95.
401. Hanyu, H., et al., *MR features of the substantia innominata and therapeutic implications in dementias.* Neurobiol Aging, 2007. **28**(4): p. 548-54.
402. Delli Pizzi, S., et al., *Thalamic Involvement in Fluctuating Cognition in Dementia with Lewy Bodies: Magnetic Resonance Evidences.* Cereb Cortex, 2015. **25**(10): p. 3682-9.
403. Basso, M.A., D. Uhlrich, and M.E. Bickford, *Cortical function: a view from the thalamus.* Neuron, 2005. **45**(4): p. 485-8.
404. Chang, C.C., et al., *(99m)Tc-ethyl cysteinate dimer brain SPECT findings in early stage of dementia with Lewy bodies and Parkinson's disease patients: a correlation with neuropsychological tests.* Eur J Neurol, 2008. **15**(1): p. 61-5.
405. Shimizu, S., et al., *Value of analyzing deep gray matter and occipital lobe perfusion to differentiate dementia with Lewy bodies from Alzheimer's disease.* Ann Nucl Med, 2008. **22**(10): p. 911-6.
406. Su, L., et al., *Whole-brain patterns of (1)H-magnetic resonance spectroscopy imaging in Alzheimer's disease and dementia with Lewy bodies.* Transl Psychiatry, 2016. **6**(8): p. e877.
407. Kenny, E.R., et al., *Subcortical connectivity in dementia with Lewy bodies and Alzheimer's disease.* Br J Psychiatry, 2013. **203**(3): p. 209-14.

408. Kotagal, V., et al., *Thalamic cholinergic innervation is spared in Alzheimer disease compared to parkinsonian disorders.* Neurosci Lett, 2012. **514**(2): p. 169-72.
409. Seidel, K., et al., *The brainstem pathologies of Parkinson's disease and dementia with Lewy bodies.* Brain Pathol, 2015. **25**(2): p. 121-35.
410. Ashburner, J. and K.J. Friston, *Unified segmentation.* Neuroimage, 2005. **26**(3): p. 839-51.
411. Friston, K.J., Holmes, A.P., Worsley, K.J., Poline, J.P., Frith, C.D. and Frackowiak, R.S.J *Statistical parametric maps in functional imaging: a general linear approach.* Human Brain Mapping, 1995. **2**: p. 189-210.
412. Inoue, K., et al., *Impaired memory and executive function associated with decreased medial temporal and prefrontal blood flow in Clinical Dementia Rating 0.5 status: the Osaki-Tajiri project.* Psychogeriatrics, 2012. **12**(1): p. 27-33.
413. Pezzoli, S., et al., *Frontal and subcortical contribution to visual hallucinations in dementia with Lewy bodies and Parkinson's disease.* Postgrad Med, 2019. **131**(7): p. 509-522.
414. Gallagher, D.A., et al., *Testing an aetiological model of visual hallucinations in Parkinson's disease.* Brain, 2011. **134**(Pt 11): p. 3299-309.
415. Papapetropoulos, S., et al., *Cortical and amygdalar Lewy body burden in Parkinson's disease patients with visual hallucinations.* Parkinsonism Relat Disord, 2006. **12**(4): p. 253-6.
416. Chung, S.J., et al., *Frontal atrophy as a marker for dementia conversion in Parkinson's disease with mild cognitive impairment.* Hum Brain Mapp, 2019. **40**(13): p. 3784-3794.
417. Shi, F., et al., *Hippocampal volume and asymmetry in mild cognitive impairment and Alzheimer's disease: Meta-analyses of MRI studies.* Hippocampus, 2009. **19**(11): p. 1055-64.
418. Tondelli, M., et al., *Structural MRI changes detectable up to ten years before clinical Alzheimer's disease.* Neurobiol Aging, 2012. **33**(4): p. 825.e25-36.
419. Vogel, M., *The cerebellum.* Am J Psychiatry, 2005. **162**(7): p. 1253.
420. Pereira, J.B., et al., *Structural brain correlates of verbal fluency in Parkinson's disease.* Neuroreport, 2009. **20**(8): p. 741-4.
421. Schulz, J.B., et al., *Multiple system atrophy: natural history, MRI morphology, and dopamine receptor imaging with 123IBZM-SPECT.* J Neurol Neurosurg Psychiatry, 1994. **57**(9): p. 1047-56.
422. Mori, F., et al., *Alpha-synuclein accumulates in Purkinje cells in Lewy body disease but not in multiple system atrophy.* J Neuropathol Exp Neurol, 2003. **62**(8): p. 812-9.
423. Taylor, J.P., et al., *Covariant perfusion patterns provide clues to the origin of cognitive fluctuations and attentional dysfunction in dementia with Lewy bodies.* Int Psychogeriatr, 2013. **25**(12): p. 1917-28.
424. Miyazawa, N., et al., *Hypermetabolism in patients with dementia with Lewy bodies.* Clin Nucl Med, 2010. **35**(7): p. 490-3.
425. Hashimoto, M., et al., *Medial temporal and whole-brain atrophy in dementia with Lewy bodies: a volumetric MRI study.* Neurology, 1998. **51**(2): p. 357-62.
426. Barber, R., et al., *Medial temporal lobe atrophy on MRI in dementia with Lewy bodies.* Neurology, 1999. **52**(6): p. 1153-8.
427. Stoodley, C.J. and J.D. Schmahmann, *The cerebellum and language: evidence from patients with cerebellar degeneration.* Brain Lang, 2009. **110**(3): p. 149-53.
428. Fischl, B., M.I. Sereno, and A.M. Dale, *Cortical surface-based analysis. II: Inflation, flattening, and a surface-based coordinate system.* Neuroimage, 1999. **9**(2): p. 195-207.
429. Iglesias, J.E., et al., *A computational atlas of the hippocampal formation using ex vivo, ultra-high resolution MRI: Application to adaptive segmentation of in vivo MRI.* Neuroimage, 2015. **115**: p. 117-37.
430. Bobinski, M., et al., *Atrophy of hippocampal formation subdivisions correlates with stage and duration of Alzheimer disease.* Dementia, 1995. **6**(4): p. 205-10.
431. Harding, A.J., B. Lakay, and G.M. Halliday, *Selective hippocampal neuron loss in dementia with Lewy bodies.* Ann Neurol, 2002. **51**(1): p. 125-8.
432. Jack, C.R., Jr., et al., *Prediction of AD with MRI-based hippocampal volume in mild cognitive impairment.* Neurology, 1999. **52**(7): p. 1397-403.
433. Oppedal, K., et al., *A signature pattern of cortical atrophy in dementia with Lewy bodies: A study on 333 patients from the European DLB consortium.* Alzheimers Dement, 2019. **15**(3): p. 400-409.

434. Burgess, N., E.A. Maguire, and J. O'Keefe, *The human hippocampus and spatial and episodic memory.* Neuron, 2002. **35**(4): p. 625-41.
435. Rajagopalan, V. and E.P. Pioro, *Disparate voxel based morphometry (VBM) results between SPM and FSL softwares in ALS patients with frontotemporal dementia: which VBM results to consider?* BMC Neurology, 2015. **15**(1): p. 32.